THE UNIVERSITY OF QUEENSLAND

AUSTRALIA

Investigation of the surface species formed on enargite in electrochemically controlled oxidising environments and in the presence of flotation collectors

Chris Plackowski

BE Minerals Process Engineering (Hons)

A thesis submitted for the degree of Doctor of Philosophy at

The University of Queensland in 2014

School of Chemical Engineering

Abstract

Arsenic sulphides such as enargite and tennantite can represent significant penalty elements in base metals production. There are significant economic advantages to achieving a separation of arsenic bearing minerals at an early stage in processing, but to date no feasible widely applicable commercial method of flotation separation has been developed. A review of the existing literature on the selective flotation of enargite considered its surface properties and floatability. Special consideration was given to the various approaches in the study of enargite surface chemistry, and the implications for the flotation of enargite. Developments in these approaches were critically reviewed and discussed.

The surface oxidation and hydrophobicity of natural enargite (Cu_3AsS_4) and the formation of oxidation species at the mineral surface were examined by a novel experimental approach that combines electrochemical techniques and atomic force microscopy (AFM). Combined with ex situ cryo X-ray photoelectron spectroscopy (XPS), the surface speciation of oxidised enargite was obtained, and compared with the newly fractured natural enargite surface.

At pH 4, surface layer formations consisting of metal-deficient sulphide and elemental sulphur were identified, associated with a limited increase in root-mean-square (rms) roughness (1.228 to 3.143 nm) and an apparent heterogeneous distribution of surface products as demonstrated by AFM imaging. A mechanism of initial rapid dissolution of Cu followed by diffusion-limited surface layer deposition was identified.

At pH 10, a similar mechanism was identified although the differences between the initial and diffusion-limited phases were less definitive. Surface species were identified as copper sulphate and hydroxide. A significant increase in surface rms roughness was found (0.795 to 9.723 nm). Dynamic (receding) contact angle measurements obtained by a droplet evaporation method found no significant difference between the oxidised surface and a freshly polished surface. A significant difference was found between the polished surface and that oxidized at pH 4, with an increase in contact angle of about 13° (46° to 59°) after oxidation. Competing effects of hydrophilic and hydrophobic species on the mineral surface under oxidizing conditions at pH 4 and the change in surface roughness at pH 10 may contribute to the observed effects of electrochemically controlled oxidation on enargite hydrophobicity.

The effects of X-ray radiation on the surface after electrochemical oxidation were investigated using XPS. Surface species present on unoxidized enargite were compared with those present after oxidation at pH 10, and the effects of X-ray irradiation time as a

function of temperature were studied. XPS spectra characteristic of a copper (II) hydroxide surface layer reduced in intensity with increasing X-ray exposure time. Associated changes in the relative concentrations of surface oxygen species were also observed. Temperature was shown to significantly influence the rate of change. A two-stage mechanism involving the dehydration of $Cu(OH)_2$ to CuO, followed by photoreduction of CuO to Cu_2O was proposed, and sample cooling was found to reduce these effects.

Oxidation of natural enargite under potentiostatic control and the formation of oxidation species at the surface were investigated at potentials where oxidation was known to occur (+347, +516, +705, +869 and +1100 mV SHE, or Standard Hydrogen Electrode). XPS analysis found a progressively increasing level of oxidation as applied potential increased. Surface layer deposition was linked to potential, with limited evidence of oxidation after treatment at +347 and +516 mV, where no evidence of Cu(II) compounds was found, while a decrease in copper at the surface suggested dissolution as the primary reaction mechanism. At +705 mV, Cu(II) species identified as $CuSO_4$ and $Cu(OH)_2$ were found, although arsenic oxides or sulphides were not found.

After treatment at +869 and +1100 mV significant evidence of oxidation was found, with $CuSO_4$ and $Cu(OH)_2$ identified and additional sulphur and arsenic species (CuS and As_2O_3) identified. Comparison of these results with published reaction mechanisms for similar treatments showed that they did not account for all species identified in the XPS data. Analysis of buffer solutions post-treatment by ICP (Inductively Coupled Plasma spectroscopy) showed a pattern of change in concentrations of Cu, As and S characterized by a step-change increase in dissolution between the +516 and +705 mV treatment conditions, which correlates with the formation of Cu(II) on the mineral surface.

Investigation of the effects of applied potential on froth flotation collector adsorption was completed to better understand the potential for selective recovery of enargite. Electrochemical techniques and XPS were used to study the adsorption of sodium ethyl xanthate and dialkyl dithiophosphinate at pH 10. Cyclic voltammetry was used to investigate the effect of applied potential on enargite in sodium ethyl xanthate and dialkyl dithiophosphinate (3418A) solutions of different concentrations at pH 10 while surface speciation due to anodic and cathodic applied potentials was investigated by XPS. The flotation response of enargite at these potentials was determined using a micro-flotation cell after conditioning in the presence of xanthate for 5 minutes.

Declaration by author

This thesis is composed of my original work, and contains no material previously published or written by another person except where due reference has been made in the text. I have clearly stated the contribution by others to jointly-authored works that I have included in my thesis.

I have clearly stated the contribution of others to my thesis as a whole, including statistical assistance, survey design, data analysis, significant technical procedures, professional editorial advice, and any other original research work used or reported in my thesis. The content of my thesis is the result of work I have carried out since the commencement of my research higher degree candidature and does not include a substantial part of work that has been submitted to qualify for the award of any other degree or diploma in any university or other tertiary institution. I have clearly stated which parts of my thesis, if any, have been submitted to qualify for another award.

I acknowledge that an electronic copy of my thesis must be lodged with the University Library and, subject to the General Award Rules of The University of Queensland, immediately made available for research and study in accordance with the *Copyright Act 1968*.

I acknowledge that copyright of all material contained in my thesis resides with the copyright holder(s) of that material. Where appropriate I have obtained copyright permission from the copyright holder to reproduce material in this thesis.

Publications during candidature

Plackowski, C., Nguyen, A.V., Bruckard, W.J., A critical review of surface properties and selective flotation of enargite in sulphide systems. *Minerals Engineering*, 2012, 30, 1-11.

Chris Plackowski, Marc A. Hampton, Anh V. Nguyen, and Warren J. Bruckard, The effects of X-ray irradiation and temperature on the formation and stability of chemical species on enargite surfaces during XPS. *Minerals Engineering*, 2013, 45, 59-66.

Chris Plackowski, Marc A. Hampton, Anh V. Nguyen, and Warren J. Bruckard, Fundamental Studies of Electrochemically Controlled Surface Oxidation and Hydrophobicity of Natural Enargite, *Langmuir*, 2013, 29(7), 2371-2386.

Chris Plackowski, Marc A. Hampton, Anh V. Nguyen, and Warren J. Bruckard, An XPS Investigation of the Surface Species Formed by Electrochemically Induced Surface Oxidation of Enargite in the Oxidative Potential Range. *Minerals Engineering*, 2014, 55, 60-74.

Chris Plackowski, Anh V. Nguyen, and Warren J. Bruckard, Surface characterisation, collector adsorption and flotation response of enargite in a redox potential controlled environment. *Minerals Engineering*, Submitted Feb. 2014.

Publications included in this thesis

Plackowski, C., Nguyen, A.V., Bruckard, W.J., A critical review of surface properties and selective flotation of enargite in sulphide systems. *Minerals Engineering*, 2012, 30, 1-11. – incorporated as Chapter 2.

Contributor	Statement of contribution
Author Chris Plackowski (Candidate)	Wrote the paper (80%)
Author Anh V. Nguyen	Edited paper (10%)
Author Warren J. Bruckard	Edited paper (10%)

Chris Plackowski, Marc A. Hampton, Anh V. Nguyen, and Warren J. Bruckard, The effects of X-ray irradiation and temperature on the formation and stability of chemical species on enargite surfaces during XPS. *Minerals Engineering*, 2013, 45, 59-66. – incorporated as Chapter 3.

Contributor	Statement of contribution
Author Chris Plackowski (Candidate)	Designed experiments (70%) Wrote the paper (70%)
Author Marc A. Hampton	Designed experiments (30%) Wrote and edited paper (20%)
Author Anh V. Nguyen	Wrote and edited paper (5%)
Author Warren J. Bruckard	Wrote and edited paper (5%)

Chris Plackowski, Marc A. Hampton, Anh V. Nguyen, and Warren J. Bruckard, Fundamental Studies of Electrochemically Controlled Surface Oxidation and Hydrophobicity of Natural Enargite, *Langmuir*, 2013, 29(7), 2371-2386. – incorporated as Chapter 4.

Contributor	Statement of contribution
Author Chris Plackowski (Candidate)	Designed experiments (70%) Wrote the paper (70%)
Author Marc A. Hampton	Designed experiments (20%) Wrote and edited paper (10%)
Author Anh V. Nguyen	Designed experiments (10%) Wrote and edited paper (10%)
Author Warren J. Bruckard	Wrote and edited paper (10%)

Chris Plackowski, Marc A. Hampton, Anh V. Nguyen, and Warren J. Bruckard, An XPS Investigation of the Surface Species Formed by Electrochemically Induced Surface Oxidation of Enargite in the Oxidative Potential Range. *Minerals Engineering*, 2014, 55, 60-74. – incorporated as Chapter 5.

Contributor	Statement of contribution
Author Chris Plackowski (Candidate)	Designed experiments (80%) Wrote the paper (75%)
Author Marc A. Hampton	Designed experiments (20%) Wrote and edited paper (5%)
Author Anh V. Nguyen	Wrote and edited paper (10%)
Author Warren J. Bruckard	Wrote and edited paper (10%)

Chris Plackowski, Anh V. Nguyen, and Warren J. Bruckard, Surface characterisation, collector adsorption and flotation response of enargite in a redox potential controlled environment. *Minerals Engineering*, Submitted Feb. 2014. – incorporated as Chapter 6.

Contributor	Statement of contribution
Author Chris Plackowski (Candidate)	Designed experiments (100%) Wrote the paper (80%)
Author Anh V. Nguyen	Wrote and edited paper (10%)
Author Warren J. Bruckard	Wrote and edited paper (10%)

Contributions by others to the thesis

Dr. Barry J. Wood of the Australian Microscopy and Microanalysis Research Facility at the Centre for Microscopy and Microanalysis, The University of Queensland, for his considerable expertise in provision of the XPS analysis, as well as extensive advice and guidance in the processing, interpretation and presentation of the data acquired. Without his substantial contribution this thesis would not have been possible.

Statement of parts of the thesis submitted to qualify for the award of another degree

None.

Acknowledgements

I would like to express my appreciation to the following people:

- Prof. Anh V. Nguyen for offering me an APA scholarship that covered both tuition fee and living allowance.

- Mr. Warren J. Bruckard for financial support from the CSIRO, including living allowance top-up and a generous research expenses contribution.

- My supervisors Prof Anh V. Nguyen and Dr Marc A. Hampton as well as Mr Warren J. Bruckard (CSIRO Process Science and Engineering) for everything they did during the course of this work.

- Dr. Marc Hampton for his tireless assistance in experimental work including AFM, electrochemistry techniques and sample preparation, as well as many helpful discussions, and Mr Tuan Nguyen for his expert help in data processing and analysis for the contact angle work.

- Prof. D.J. Bradshaw for her great feedback and invaluable advice regarding presentation skills.

- Dr. Elaine Whightman and Ms. Jessica Gray for their valuable advice and essential contribution to sample preparation.

- Ms Siu-Bit Iball and all the staff of the School of Chemical Engineering for their kind assistance.

- All my friends and colleagues in the Chemical Engineering postgraduate community for their support and friendship throughout the course of my PhD.

- Last but not least, I would like to dedicate this work to my family, who have always been supportive throughout the course of this journey.

Keywords

Surface chemistry, enargite, sulphide mineral, flotation, oxidation, electrochemistry, hydrophobicity, XPS, atomic force microscopy, contact angle.

Australian and New Zealand Standard Research Classifications (ANZSRC)

ANZSRC code: 091404, Mineral Processing/Beneficiation, 50%
ANZSRC code: 091499, Resources Engineering and Extractive Metallurgy not elsewhere classified, 20%
ANZSRC code: 090499, Chemical Engineering not elsewhere classified, 30%

Fields of Research (FoR) Classification

FoR code: 0904, Chemical Engineering, 50%
FoR code: 0914, Resources Engineering and Extractive Metallurgy, 50%

Table of Contents

List of Figures

Chapter II

Chapter III

Chapter IV

Chapter V

Chapter VI

List of Tables

Chapter III

Chapter IV

Chapter V

Chapter VI

Chapter I

Introduction

1. Background to the Research

Enargite is a significant mineral for a number of reasons. It contains arsenic, which is a highly toxic inorganic pollutant responsible for serious environmental and human health problems in several parts of the world (Chatterjee et al., 1995). Although it does occur naturally, health and environmental regulations now require arsenic emissions from mining, processing and metal production processes such as smelting to be captured and rendered inert for safe disposal. This is expensive and in addition significant financial penalties are increasingly imposed by smelters to process concentrate containing typically more than 0.2 wt% arsenic (Wilson and Chanroux, 1993, Smith and Bruckard, 2007).

Depletion of more favourable and easy to process ore bodies means that new ways must be found to process deposits that in the past were considered uneconomic or unsuitable because of contaminants such as arsenic. Arsenic in final copper concentrates is also undesirable in copper metal production. For example, arsenic is known to be detrimental to properties of copper metal such as electrical conductivity and annealability, both of which are critical for electrical copper (Biswas and Davenport, 1994; Cordova et al., 1997).

There are significant economic advantages to achieving a separation of arsenic bearing minerals at an early stage in processing, but to date no feasible widely applicable commercial method of separation at the flotation stage has been developed. Compared to other sulphide mineral types, relatively limited research has been carried out on the selective flotation of enargite and methods of achieving an effective separation from non-arsenic copper sulphides.

Enargite is the main form of copper arsenic mineralisation in many deep epithermal copper-gold deposits (Filippou et al., 2007). It is commonly associated with copper sulphides such as chalcopyrite ($CuFeS_2$) and chalcocite (Cu_2S). All these minerals are significant in the formation of copper sulphide ore mineralisation and are economically important sources of copper.

The main difference between copper arsenic sulphides and other arsenic minerals is that the former can represent significant economic forms of copper mineralisation in their own right. Therefore, it is not just their separation from other copper sulphides that is important, but also their recovery for further processing to extract, where possible, the copper.

In copper sulphide systems, enargite is one of the most problematic arsenic minerals. It has surface properties suitable for air bubble attachment (Leja, 1982) and can be separated by froth flotation using air bubbles (Nguyen and Schulze, 2004). However, due to their similar flotation properties, enargite and most copper-bearing sulphides such as bornite, chalcocite and chalcopyrite are difficult to separate using conventional froth flotation processes. A better understanding of

surface electrochemistry of enargite is important if effective separation techniques using flotation are to be developed.

Previous research has shown that crude separation may be achieved using selective oxidation techniques (Guo and Yen, 2005), or through the use of pulp potential control (Senior et al., 2006, Fornasiero et al., 2001, Huch, 1994, Guo and Yen, 2005, Kantar, 2002, Smith and Bruckard, 2007). However, the fundamental mechanisms involved in these separations and the species present are not yet well understood. Oxidation and precipitation mechanisms have been proposed and argued. The present work seeks to contribute to a better understanding of the formation of oxidation products and the effects on the surface morphology of electrochemically controlled enargite at pH 10 and 4.

Although some promising studies have been completed (Senior et al., 2006, Bruckard et al., 2007, Smith and Bruckard, 2007, Bruckard et al., 2010), compared to other sulphide mineral types, relatively limited research has been carried out on the selective flotation of enargite and methods of achieving an effective separation from non-arsenic copper sulphides. An understanding of surface oxidation, the species formed and the nature of the surface layer also has implications for other approaches to arsenic reduction in the case of ores containing enargite. Hydrometallurgical approaches to removing arsenic, in particular leaching processes, have been shown to be effective (Balaz et al., 2000, Curreli et al., 2005). In addition the surface species and formation of a surface layer are important considerations in the leaching of enargite in acid environments (Fantauzzi et al., 2007) where the release of arsenic can have serious environmental consequences.

As will be shown in Chapter 2 of this thesis, the formation of different species including copper sulphate or hydroxide and elemental sulphur on the mineral surface could occur (Plackowski et al., 2012). However, disagreement exists about the nature of oxidation products formed and it is uncertain whether species such as copper hydroxide or oxide, or Cu^{2+} species associated with sulphate and chloride, are the main oxidation products.

Another review considered enargite oxidation both in the natural environment and laboratory setting (Lattanzi et al., 2008). Oxidation was found to be a slow process, as evidenced by the low current densities seen in electrochemical oxidation. At low pH it was found copper dissolution accompanied by formation of elemental sulphur predominates. At high pH, Cu^{2+} species are evident along with oxides of arsenic, and formation of polysulphides, sulphite and sulphate as a result of sulphur oxidation, as shown by XPS studies.

It was also found that, although some progress has been made, knowledge of the fundamental surface chemistry relating to enargite must be further developed before the mechanisms that enable a successful separation by froth flotation can be understood (Plackowski et al., 2012).

This thesis deals with experimental work using the copper arsenic sulphide mineral enargite (Cu_3AsS_4) as the focus of investigations into the nature of the chemical processes taking place at the surface under idealised conditions representative of aspects of the froth flotation environment. It is composed of published and draft papers beginning with a review of the literature concerned with current developments in the research into separation of enargite from other minerals in copper sulphide flotation systems. This includes characterisation of surface oxidation and various approaches to achieving selectivity in flotation of enargite and copper sulphide minerals.

In Chapter 3 the focus is on the effects of X-ray exposure and temperature during XPS analysis to alter the mineral surface, and the importance of developing a procedure to minimise these effects. Changes in the surface chemistry due to application of XPS were quantified and the mechanism of action described. A suitable technique using liquid nitrogen cooling was developed to minimise these changes and enable reliable XPS data to be obtained.

In the first of the experimental investigations of enargite surface chemistry, the electrochemical characteristics of enargite were studied using cyclic voltammetry (CV) and chronoamperometry (CA), and electrochemically induced surface oxidation by applied potential (+869 mV (SHE) at pH 10, and + 610 mV at pH 4) was investigated. The corresponding surface chemical changes were characterized by X-ray photoelectron spectroscopy (XPS), and morphological changes examined with atomic force microscopy (AFM). Contact angle measurements using a droplet evaporation technique are used to investigate surface hydrophobicity. Surface layer formation consisting of metal deficient sulphide and elemental sulphur was identified, and a mechanism of Cu dissolution and diffusion-limited surface layer deposition was proposed.

In this way this study seeks to develop some insight into the mechanisms underlying the enargite surface oxidation and hydrophobicity, and inform the future development of various approaches to achieving selectivity in the separation by flotation of enargite and copper sulphide minerals.

This work was further developed with the study of oxidation of the surface of natural enargite (Cu_3AsS_4) under potentiostatic control and the formation of oxidation species at the mineral surface at selected applied potentials in the oxidative range. In order to quantify surface chemical changes over a broad potential range, five anodic potentials, as identified by cyclic voltammetry studies, were selected to determine the progression of chemical changes induced at the enargite surface. The selected potentials were +347, +516, +705, +869 and +1100 mV SHE. XPS analysis combined with thermodynamic data was used to develop reaction mechanisms to explain the observed changes.

The final paper seeks to further develop our understanding of the flotation response of enargite as a function of pulp potential. Its purpose is to examine the enargite surface after treatment at oxidizing and reducing potentials (+516 and -400 mV SHE respectively) in the presence of flotation collector using XPS to identify the chemical species. In particular the aim was to determine what differences exist in collector adsorption after treatment at these applied potentials, and if there is a correlation with the flotation recovery of enargite in a simple single mineral microflotation system. The latter was investigated using the UCT microflotation cell as described by Bradshaw and O'Connor (1996) to determine if there is a difference in the flotation response of enargite as a result of treatment an oxidizing or reducing potential in the presence of flotation collector.

2. Research Aims and Objectives

Recent research activity by the CSIRO referred to in the previous section (Senior et al., 2006, Bruckard et al., 2007, Bruckard et al., 2010) demonstrated promising results showing that it is feasible to separate copper arsenic sulphides at laboratory scale, the principal species being enargite and to a lesser extent tennantite, from copper sulphides using controlled potential flotation. However it has been identified that fundamental knowledge in this area is lacking, and an understanding of the chemical mechanisms by which this separation can be achieved is incomplete. For this reason fundamental studies relating to the flotation of arsenic minerals in copper sulphide systems are needed to identify what surface species are present under oxidising and reducing conditions at a given pH in a controlled potential flotation environment.

The overall objective of this research program is to characterise the fundamental properties of enargite that enable selective flotation and separation from non-arsenic copper sulphides to be achieved.

The aim of this thesis is to investigate and characterise the fundamental mechanisms, in particular the surface chemistry, of arsenic mineral oxidation, both in isolation as well as controlled environments that replicate flotation conditions. By doing so a better understanding of the mechanisms by which selective flotation of arsenic minerals, such as enargite (Cu_3AsS_4) and tennantite ($Cu_{12}As_4S_{13}$), from common and economically significant copper sulphide and oxide minerals, can be achieved. The mineral enargite is the specific focus of this study as it is one of the more commonly occurring copper arsenic sulphides found in copper ore deposits.

The specific objectives are:

i. To identify the chemical species present at the mineral surface under controlled potential conditions and compare the findings with past research.
ii. To understand the mechanisms by which the observed chemical changes take place.

iii. To characterise the morphological changes at the mineral surface that correspond to chemical changes observed under controlled potential conditions.
iv. To characterise the effects of the presence of flotation collectors on the system.
v. To understand the effects of applied potential on the floatability of enargite.
vi. To evaluate the effect of applied potential on flotation of enargite in a single mineral system.

It is envisaged that the outcomes of this research will contribute to an understanding of the physical and chemical changes occurring at the enargite surface that are responsible for the observed flotation behaviour in a controlled potential flotation environment.

3. Hypotheses

Based on a review of the findings available in the current literature and the stated research objectives the following hypotheses are proposed.

i. Electrochemical products on the enargite surface significantly influence the floatability of enargite.

   It is known that electrochemical oxidation can produce a surface layer on sulphide minerals, and that this layer can affect collector adsorption and floatability. It is important to investigate the formation, composition and effects of this layer.

ii. An optimum range of applied potential exists over which enargite demonstrates good floatability.

   Previous studies have shown enargite floats strongly over a range of applied potential, while outside this range floatability is poor. However the upper limit has not been defined and must be investigated.

iii. Application of an electrical potential changes surface morphology, collector adsorption and contact angle at the mineral surface.

   These factors are important in determining floatability as they directly affect surface hydrophobicity. By measuring these characteristics the changes can be quantified.

iv. Flotation selectivity of enargite is influenced by changes in surface properties resulting from an applied electrical potential.

   Having measured changes in surface properties, their effects on selective floatability of enargite according to potential must then be investigated.

4. Statement of Originality

This thesis has not been submitted for a degree in any University, and does not contain material published by another person. The original contributions of this thesis are outlined briefly below:

• A novel approach incorporating in-situ AFM of the copper arsenic sulphide mineral enargite under potentiostatic control to investigate the effects of applied potential in the oxidative range on surface morphology, and ex-situ surface analysis using X-ray photoelectron spectroscopy to identify the chemical species produced on the surface as a result of oxidation in a controlled potential environment. Additionally, contact angle has been investigated using a droplet evaporation method to assess the combined effects of surface chemical and topographical changes on surface hydrophobicity. This approach, demonstrated for a model system, has shown its potential for use in quantifying changes in surface characteristics relevant to flotation.

• The effects of exposure of the oxidised enargite surface to the environment that exists in the analysis chamber during XPS measurement was demonstrated experimentally. It was shown that significant changes are induced in the surface composition by a combination of relatively high temperature, ultra-high vacuum and X-ray exposure. A method of limiting these effects using liquid nitrogen cooling was demonstrated. This is an issue which was not previously considered for enargite.

• The changes in surface chemistry of enargite as oxidising potential is progressively increased have been demonstrated for the oxidative potential range, which is relevant for flotation systems using Eh control to achieve a separation of enargite from other non-arsenic bearing copper sulphides.

• The effects of the presence of flotation collectors on the surface species formed on enargite under potentiostatic control in the oxidising and reducing potential range was demonstrated. This approach enables the experimental system to be more closely aligned with real flotation systems where Eh control is used to effect a separation of enargite from other copper sulphides by flotation. Floatability and therefore hydrophobicity was confirmed using microflotation test work.

5. Structure of the thesis

This thesis has been structured following the format of chapters comprised of published or submitted papers. Chapter 1 presents the background to the research, aims and hypotheses, statement of originality and structure of the thesis. Chapters 2 to 6 are the candidates own research

papers. Chapter 2 presents a literature review of current research developments into the separation of enargite (Cu_3AsS_4) from other minerals in copper sulphide flotation systems (Plackowski, C., Nguyen, A.V., Bruckard, W.J., A critical review of surface properties and selective flotation of enargite in sulphide systems. Minerals Engineering, 2012, 30, 1-11.). Chapter 3 presents an investigation of the effects of XPS analysis on the surface composition of electrochemically oxidised enargite (Plackowski, C., Hampton, M.A., Nguyen, A.V., Bruckard, W.J., The effects of X-ray irradiation and temperature on the formation and stability of chemical species on enargite surfaces during XPS. Minerals Engineering, 2013, **45**, 59-66.). Chapter 4 deals with the study of surface oxidation and hydrophobicity of natural enargite and formation of oxidation species at the mineral surface using a newly developed experimental approach combining atomic force microscopy (AFM) with in-situ electrochemical techniques (Plackowski, C., Hampton, M.A., Nguyen, A.V., Bruckard, W.J., Fundamental Studies of Electrochemically Controlled Surface Oxidation and Hydrophobicity of Natural Enargite. Langmuir, 2013, **29(7)**, 2371-2386.). Chapter 5 extends the work carried out in the previous paper, and comprises a detailed study of the surface changes induced on enargite by electrochemical oxidation (Plackowski, C., Hampton, M.A., Bruckard, W.J., Nguyen, A.V., An XPS investigation of surface species formed by electrochemically induced surface oxidation of enargite in the oxidative potential range. Minerals Engineering, 2014, **55**, 60-74.) Chapter 6 extends the work carried out previously by introducing flotation collector into the system to investigate the effects of applied potential on adsorption (Chris Plackowski, Anh V. Nguyen, and Warren J. Bruckard, Surface characterisation, collector adsorption and flotation response of enargite in a redox potential controlled environment. *Minerals Engineering*, Submitted Feb. 2014.). Chapter 7 comprises the concluding chapter and includes recommendations for future research.

References

Balaz, P., Achimovicova, M., Bastl, Z., Ohtani, T. & Sanchez, M. 2000. Influence of mechanical activation on the alkaline leaching of enargite concentrate. Hydrometallurgy, 54, 205-216.

Bradshaw, D. J. & O'connor, C. T. 1996. Measurement of the sub-process of bubble loading in flotation. Minerals Engineering, 9, 443-448.

Bruckard, W. J., Davey, K. J., Jorgensen, F. R. A., Wright, S., Brew, D. R. M., Haque, N. & Vance, E. R. 2010. Development and evaluation of an early removal process for the beneficiation of arsenic-bearing copper ores. Minerals Engineering, 23, 1167-1173.

Bruckard, W. J., Kyriakidis, I. & Woodcock, J. T. 2007. The flotation of metallic arsenic as a function of pH and pulp potential - A single mineral study. International Journal of Mineral Processing, 84, 25-32.

Chatterjee, A., Das, D., Mandal, B. K., Chowdhury, T. R., Samanta, G. & Chakraborti, D. 1995. Arsenic in ground-water in 6 districts of West-Bengal, India - The biggest arsenic calamity in the world .1. Arsenic Species in Drinking-Water and Urine of the Affected People. Analyst, 120, 643-650.

Curreli, L., Ghiani, M., Surracco, M. & Orru, G. 2005. Beneficiation of a gold bearing enargite ore by flotation and As leaching with Na hypochlorite. Miner. Eng., 18, 849-854.

Fantauzzi, M., Elsener, B., Atzei, D., Laftanzi, P. & Rossi, A. 2007. The surface of enargite after exposure to acidic ferric solutions: an XPS/XAES study. Surf. Interface Anal., 39, 908-915.

Fornasiero, D., Fullston, D., Li, C. & Ralston, J. 2001. Separation of enargite and tennantite from non-arsenic copper sulfide minerals by selective oxidation or dissolution. International Journal of Mineral Processing, 61, 109-119.

Guo, H. & Yen, W. T. 2005. Selective flotation of enargite from chalcopyrite by electrochemical control. Minerals Engineering, 18, 605-612.

Huch, R. O., 1994. Method for achieving enhanced copper-containing mineral concentrate grade by oxidation and flotation. United States patent application 07/878444.

Kantar, C. 2002. Solution and flotation chemistry of enargite. Colloids and Surfaces A: Physicochemical and Engineering Aspects, 210, 23-31.

Lattanzi, P., Da Pelo, S., Musu, E., Atzei, D., Elsener, B., Fantauzzi, M. & Rossi, A. 2008. Enargite oxidation: A review. Earth-Science Reviews, 86, 62-88.

Leja, J. 1982. Surface Chemistry of Froth Flotation, New York, NY, Plenum Press.

Nguyen, A. V. & Schulze, H. J. 2004. Colloidal science of flotation, New York, Marcel Dekker.

Plackowski, C., Nguyen, A. V. & Bruckard, W. J. 2012. A critical review of surface properties and selective flotation of enargite in sulphide systems. Minerals Engineering, 30, 1-11.

Senior, G. D., Guy, P. J. & Bruckard, W. J. 2006. The selective flotation of enargite from other copper minerals - a single mineral study in relation to beneficiation of the Tampakan deposit in the Philippines. International Journal of Mineral Processing, 81, 15-26.

Smith, L. K. & Bruckard, W. J. 2007. The separation of arsenic from copper in a Northparkes copper-gold ore using controlled-potential flotation. International Journal of Mineral Processing, 84, 15-24.

Wilson, P. C. & Chanroux, C. 1993. Revenue calculations and marketing; copper. In: Noakes, M. & Lanz, T. (eds.) Cost Estimation Handbook for the Australian Mining Industry. Parkville: The Australian Institute of Mining and Metallurgy.

Chapter II

A critical review of surface properties and selective flotation of enargite in sulphide systems

Chris Plackowski, Anh V. Nguyen1 and Warren Bruckard

Published in Minerals Engineering, 2012, 30, 1-11.

1. Abstract

Arsenic sulphides such as enargite, tennantite and arsenopyrite can present a significant penalty element in base metals production. There are significant economic advantages to achieving a separation of arsenic bearing minerals at an early stage in processing, but to date no feasible widely applicable commercial method of separation at the flotation stage has been developed. This review focuses on the current state of knowledge in the selective flotation of enargite, commonly found in association with non-arsenic copper sulphide mineralisation. Due to its similar flotation properties with many other copper sulphides, enargite is typically recovered together with the copper minerals, producing a high arsenic bulk concentrate which is costly and problematic to process. Special consideration is given to the various approaches used in the study of the surface chemistry of enargite in different environments, and the implications for the flotation of enargite. Developments in the various approaches in the selective flotation of enargite are critically reviewed and discussed.

Key words: enargite, arsenic, copper minerals, flotation

2. Introduction

Arsenic can occur naturally in elemental form, but more commonly as a compound in several mineral types which include copper arsenic sulphides such as enargite (Cu_3AsS_4) and tennantite ($Cu_{12}As_4S_{13}$), and associated arsenic-bearing minerals such as arsenopyrite (FeAsS). It is a highly toxic inorganic pollutant, responsible for serious environmental and human health problems in several parts of the world. Specifically, arsenic emissions from downstream processing such as smelting must be captured and rendered inert for safe disposal. Such treatments are expensive and significant financial penalties are increasingly imposed to process concentrate containing typically more than 0.2wt% arsenic. Arsenic in final copper concentrates is also undesirable in copper metal production. For example, arsenic is known to be detrimental to properties of copper metal such as electrical conductivity and annealability, both of which are critical for electrical copper (Biswas and Davenport, 1994; Cordova et al., 1997).

There are significant economic advantages to achieving a separation of arsenic bearing minerals at an early stage in processing, but to date no feasible widely applicable commercial method of separation at the flotation stage has been developed. Compared to other sulphide mineral types, relatively limited research has been carried out on the selective flotation of enargite and methods of achieving an effective separation from non-arsenic copper sulphides.

This review focuses on enargite, which is the main form of copper arsenic mineralisation in many deep epithermal copper-gold deposits (Filippou et al., 2007). It is commonly associated with copper sulphides such as chalcopyrite ($CuFeS_2$) and chalcocite (Cu_2S). All these minerals are significant in the formation of copper sulphide ore mineralisation and are economically important sources of copper.

The main difference between copper arsenic sulphides and other arsenic minerals is that the former can represent significant economic forms of copper mineralisation in their own right. Therefore, it is not just their separation from other copper sulphides that is important, but also their recovery for further processing to extract, where possible, the copper.

The purpose of this paper is to present a review of current developments in the research into separation of enargite from other minerals in copper sulphide flotation systems. This includes characterisation of surface oxidation and various approaches to achieving selectivity in flotation of enargite and copper sulphide minerals.

3. Surface properties and floatability of enargite

3.1. Surface potential

Castro and Honores (2000) used microelectrokinetic (zeta potential) measurements, rest potentials of enargite electrodes and Hallimond tube flotation tests to investigate the surface properties and floatability of enargite. Zeta potential was found to be negative (-21 mV to -47 mV) in the pH range 2.5-12.0 with no isoelectric point. Zeta Potential peaks were found at about pH 5.5 and 11.0 (Figure 1). They argued that these peaks could be due to the presence of arsenate ions (AsO_4^{3-}) dissolved from the mineral surface. This was tested by investigating the effect of adding sodium arsenate (Na_3AsO_4).

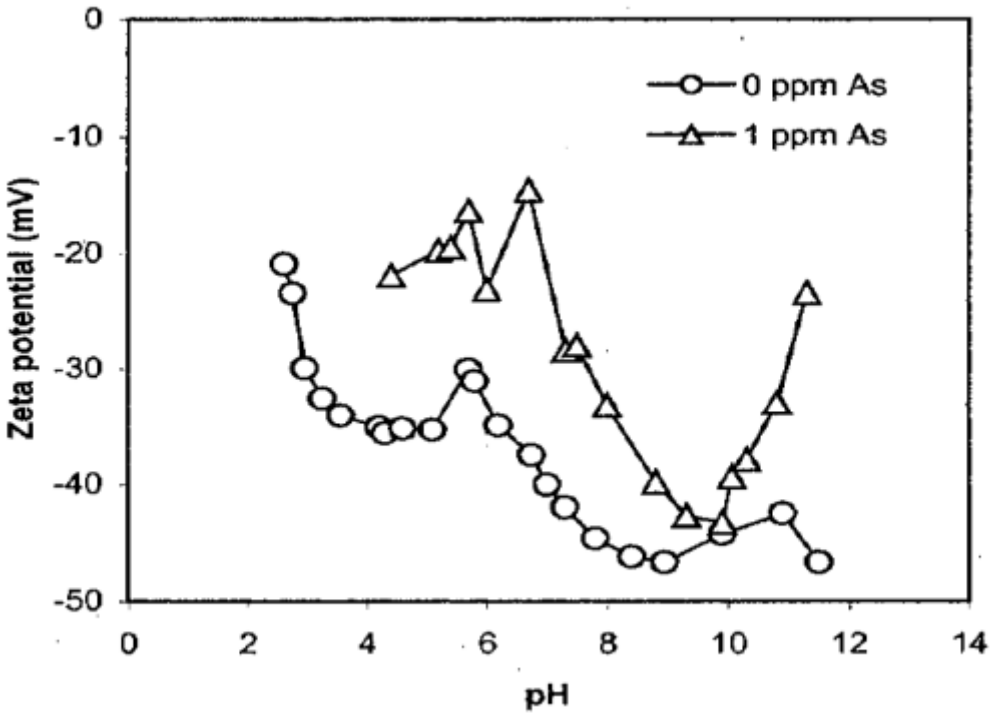

Figure 1. Zeta potential of enargite as a function of pH in the presence and absence of arsenate ions in 10^{-3}M $NaNO_3$ supporting electrolyte (Castro and Honores, 2000).

The presence of arsenate ions was found to make the zeta potential less negative across the pH range, but a new peak at pH 6.5 was seen. Comparing with data for the hydrolysis of arsenate and thio-arsenate ions reported in the literature (Schwedt and Rieckhoff, 1996) the potential peaks were found to correspond well with these pK values. From this study it was suggested that the negative zeta potential of enargite may be due to the presence of negatively charged thio-arsenate species formed from acids such as H_3AsO_4, H_3AsO_3S, $H_3AsO_2S_2$ and H_3AsOS_3.

By comparing rest potentials with the Eh-pH diagrams of the As-H_2O system and enargite (Figure 2) it was proposed that dissolution of enargite and formation of arsenate ions may occur in alkaline conditions, while in acidic conditions a surface layer of arsenic trioxide would be expected. This behaviour is the opposite of what is seen for copper sulphides, which form an oxide layer under alkaline conditions and undergo dissolution under acidic conditions.

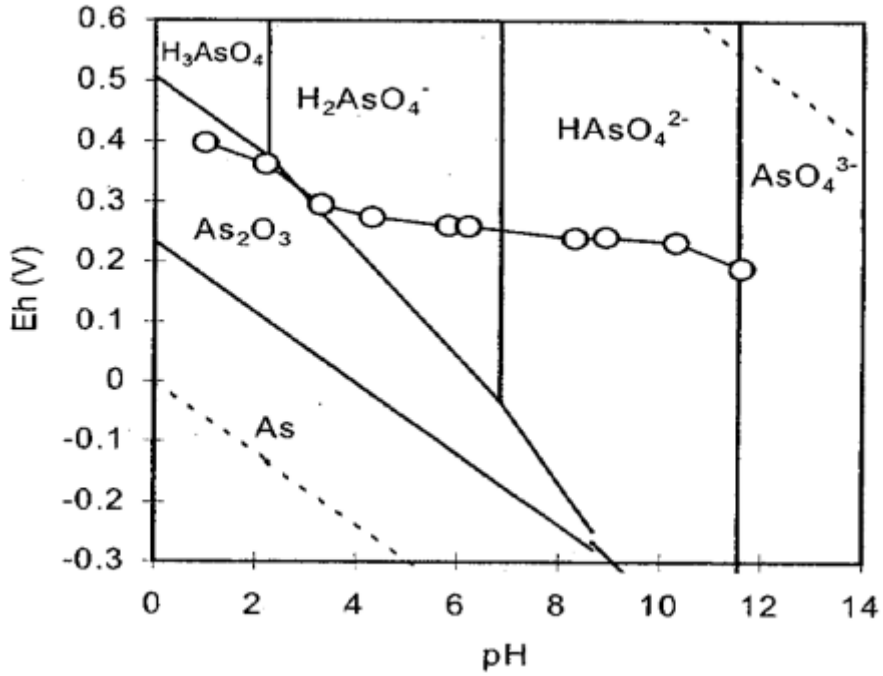

Figure 2. Rest potentials of the enargite electrode in aqueous solution as a function of pH, plotted on the thermodynamic equilibrium diagram for the As-H_2O system at 10^{-3} M As (25°C) (Castro and Honores, 2000).

Hallimond tube studies using isopropyl xanthate showed good floatability at pH 10.0 even at very low collector concentrations. Oxidation by pre-treatment with NaClO at pH 11.0 was found to have only a slight depressant effect. This was interpreted to mean that thio-arsenate groups at the surface contribute to the good floatability of enargite and increase in resistance to oxidation compared to other copper sulphides. The good flotation response at high pH was thought to occur because collector adsorption on active sites at the mineral surface was unaffected by the increasingly negative zeta potential seen with increasing pH. Dissolution and hydrolysis of thio-arsenate and arsenate ions followed by re-adsorption at the mineral surface was proposed as the mechanism for the formation of negative surface charge observed in the zeta potential measurements.

Fullston et al. (1999a) studied the surface oxidation of enargite and tennantite by investigating the dissolution of the minerals and changes in zeta potential under different oxidising conditions. Samples were conditioned at pH 11.0 either in the presence of nitrogen or oxygen gas prior to the zeta potential and dissolution measurements.

The mechanism of oxidation and formation of surface charge was proposed to be one of protonation or deprotonation of either metal sulphide surfaces

$$Mineral\left|\cdots MSH + H^{+} \rightleftarrows Mineral\right|\cdots MSH_{2}^{+} \quad [1]$$

$$Mineral\left|\cdots MSH \rightleftarrows Mineral\right|\cdots MS^{-} + H^{+} \quad [2]$$

or metal hydroxides

$$Mineral\left|\cdots MOH + H^{+} \rightleftarrows Mineral\right|\cdots MOH_{2}^{+} \quad [3]$$

$$Mineral\left|\cdots MOH \rightleftarrows Mineral\right|\cdots MO^{-} + H^{+} \quad [4]$$

at the mineral surface as illustrated by the reactions above. It was argued that changes in pH and redox conditions caused the formation of a surface oxide layer on a metal-deficient (hence sulphur-rich) mineral surface, resulting in the observed changes in zeta potential. The extent of copper dissolution and formation of oxidation products on the mineral surface was found to increase with more oxidising conditions. It was also found that the dissolution of copper was greater than that of arsenic.

The process of oxidation in a low pH environment was proposed to be as follows. Initially, dissolution of metal ions takes place leaving a metal-deficient or sulphur-rich mineral surface. With continuing oxidation the sulphide groups oxidise to form polysulphide or elemental sulphur. Under conditions of high pH in an oxygenated environment this process is one of metal hydrolysis on the mineral surface and in solution followed by precipitation of metal hydroxide on the metal-deficient surface.

The following reactions were proposed to occur on the enargite (and tennantite) surface.

Oxidation at pH 9.0:

$$Cu_3AsS_4 + x/2O_2 + x\ H_2O \rightarrow Cu_{3-x}AsS_4(Cu(OH)_2)_x \quad [5]$$

Dissolution of copper hydroxide during the acid titration:

$$Cu_{3-x}AsS_4\ (Cu(OH)_2)_x + 2xH^{+} \rightarrow Cu_{3-x}AsS_4 + xCu_2{+}{+} + 2xH_2O \quad [6]$$

Dissolution of copper from the mineral lattice at low pH values:

$$Cu_{3-x}AsS_4 + 2yH^{+} + y/2O_2 \rightarrow Cu_{3-x-y}AsS_4 + yCu_2{+} + yH_2O \quad [7]$$

Precipitation of copper hydroxide during the base titration:

$$Cu_{3-x-y}AsS_4 + (x + y)Cu^{2+} + 2(x + y)H_2O \rightarrow Cu_{3-x-y}AsS_4\ (Cu(OH)_2)_{(x+y)} + 2(x + y)H^{+} \quad [8]$$

In a follow-up study by Fullston et al. (Fullston et al., 1999b) the surface oxidation of enargite and tennantite was investigated using X-ray photoelectron spectroscopy (XPS), with the same conditioning methods as the previous study. After conditioning, the mineral surface was found to be

lightly oxidised, where the presence of a thin surface oxidation layer was shown by the detection, using XPS, of the non-oxidised mineral beneath. The main oxidation product was found to be a copper oxide/hydroxide layer, with an associated sulphur-rich phase comprised of a metal-deficient sulphide/polysulphide, and also arsenic oxide/hydroxide and sulphite species. From the XPS analysis arsenic sulphides, mainly As_4S_4 and As_2S_3, were found to be the major arsenic sulphide species at the enargite surface, but were minor species at the tennantite surface and also in the bulk of both minerals.

Castro and Baltierra (2005) used an experimental and thermodynamic approach to study the surface chemistry of enargite as a function of pH. Zeta potential measurements as a function of pH were conducted for two different electrolytes, 0.001 M KCl and 0.001 M $NaNO_3$. In both cases zeta potential was found to be negative across the pH range studied, with no isoelectric point found.

The magnitude of the zeta potential was found to become increasingly negative with increasing pH. These results were interpreted in terms of adsorption of the hydrolysis products of the As-Cu-S-H_2O system formed at the mineral surface. Potential valleys observed at pH 4.5 and 9.0 were interpreted as indicative of the adsorption of ions such as $H_2AsO_4^-$ and $HAsO_4^{2-}$. Peaks at pH 5.5 for both electrolytes, pH 11.0 for KCl and pH 9.5 for $NaNO_3$, were also observed. Zeta potential reversal observed in the presence of copper ions was explained in terms of the formation and adsorption of copper-hydroxyl complexes such as $Cu(OH)^+$ by hydrolysis, and precipitation of a surface layer of copper hydroxide.

Fullston et al. (1999c) investigated the zeta potential of several copper sulphide minerals as a function of pH and oxidising conditions. It was found that variation in zeta potential with changes in pH and extent of oxidising conditions were consistent with the formation of a copper hydroxide layer on a metal-deficient, sulphur-rich mineral surface. The extent of copper hydroxide layer formation was found to increase as the mineral was subject to more oxidising conditions.

The zeta potential measurements were interpreted to mean that dissolution of the copper hydroxide surface layer takes place as pH decreases below about pH 8.0, while increasing pH results in the precipitation of a copper hydroxide surface layer above pH 6.0. In the case of acid titration followed by base titration, hysteresis between the acid and base zeta potential titration curves is seen where the mineral was prepared under oxidising conditions, but not when reducing conditions were used. This is attributed to the precipitation of copper sulphide on the mineral surface. The hysteresis was explained as the result of greater copper hydroxide precipitation with increasing pH, with the additional copper coming from increased metal dissolution at low pH.

From this study the minerals were ranked for oxidation in order of high to low: chalcocite > tennantite > enargite > bornite > covellite > chalcopyrite. It was concluded that separation by flotation of enargite and tennantite from the other copper sulphides, by exploiting differences in their susceptibility to oxidisation, could be possible if chalcocite were not present.

3.2. Electrochemical investigations

Given that the industrial process of froth flotation of sulphide minerals is fundamentally electrochemical in nature, an understanding of the electrochemical properties of sulphide minerals is an essential part of an investigation of surface properties and behaviour in the flotation environment. Various authors have carried out investigations to characterise the surface properties of enargite using electrochemical methods.

As well as chemical oxidative pre-treatments, discussed in a later section, electrochemical oxidation is an important technique to investigate mineral surface reactivity under controlled conditions.

In an investigation of the electrochemical oxidation and reduction of natural enargite (Asbjornsson et al., 2004a), Asbjornsson et al. studied the surface reactivity of enargite in acid solution using cyclic voltammetry and chronoamperometry coupled with XPS, Raman spectroscopy and inductively coupled plasma-atomic emission spectrometry (ICP-AES).

The presence of Cu^{II} species associated with sulphate (SO_4^{2-}) and chloride (Cl^-) ions at the enargite surface, at potentials greater than +440 mV SHE, was reported. The ion concentration increased with increasing potential. Oxidation of arsenic to As^{III} at potentials less than +840 mV SHE was noted, as well as detection of small amounts of As^V above this range.

Interestingly, in the oxidative potential range an active-passive transition was reported at potentials around +540 mV SHE, believed to be the result of formation of elemental sulphur and sulphate, as well as Cu^{II} and As^{III}/As^V species. Formation of H_2S, arsine and elemental copper due to electrochemical reduction was also reported. The latter was demonstrated by the loss of an enargite Raman signal at increasingly negative potentials, a phenomenon attributed to the formation of elemental copper at the mineral surface.

Pauporté and Schuhmann (Pauporté and Schuhmann, 1996) used techniques including electrochemical impedance spectroscopy (EIS) and voltammetry to study the electrochemistry of natural enargite under alkaline conditions. It was concluded from the EIS data that in the potential range +140 to +440 mV SHE the observed variation in impedance was consistent with the formation and dissolution of a surface layer.

Voltammetric studies were used to compliment the EIS data. Scans were carried out in the potential range -360 to +640 mV SHE. The voltammetry results showed the formation of current peaks in the anodic scan direction that decreased in magnitude over three successive scans. A model was proposed to explain the observed behaviour. It was suggested that a two-step reaction was involved, with the formation of a surface product of copper involving the transfer of one or more electrons, followed by the formation of a soluble species. However the authors did not specify the compound or compounds represented by the surface product or soluble species. It was concluded that the EIS and voltametric behaviour resulted from the same processes.

In a study of enargite by electrochemical methods, Cordova et al. (Cordova et al., 1997; Cordova et al., 1996) used a number of techniques to understand the reactions at the enargite electrode surface in solutions of different pH values. These methods included open circuit potential, stationary polarisation, cyclic voltammetry and electrochemical impedance spectroscopy.

It was found that under anodic conditions (positive applied potential) Cu^{2+} ions are initially released into solution leaving a metal-deficient surface where arsenic and sulphur remain. It was suggested the surface is probably composed of AsS_4 or $Cu_{3-x}AsS_4$. As oxidation continues this surface gradually becomes a passivating layer, causing a decrease in the oxidation rate. This is similar to the mechanisms of oxidation proposed by Fullston et al. (1999a) in their zeta potential study.

Under cathodic conditions it was proposed that electro reduction produces S^{2-} species and the formation of a surface layer composed of As_2S_2 and Cu_2S species. At increasingly negative potentials As_2S_2 is partly reduced to metallic arsenic although it was reported that no metallic copper could be found.

Studies were also carried out under the same conditions but in the presence of 10^{-4}M xanthate. It was concluded that in the potential range where a surface film is not formed (-460 to +140 mV SHE) no collector was adsorbed. A mechanism was suggested where xanthate takes part in the formation of the surface film during oxidation and is incorporated in it.

Guo and Yen (Guo and Yen, 2008) investigated the electrochemical behaviour of natural and synthetic enargite using open circuit potential, stationary polarisation and cyclic voltammetry. Changes in solution pH, scan direction, scan rate and scan range were found to alter the electrochemical behaviour significantly. Interestingly, enargite was found to be insensitive to the presence of dissolved oxygen with little effect on the electrochemical behaviour observed.

The main effect of pH was observed to be an increase in the applied potential needed to oxidise enargite as pH is decreased. This was interpreted to mean enargite more readily forms a

passivation layer in neutral or alkaline pH. It was found to be most stable at neutral or alkaline pH at about 40 m V SHE. However, passivation of the surface may occur over the range -660 to +1070 mV SHE.

The main oxidation product formed on the mineral surface was found to be copper hydroxide ($Cu(OH)_2$) where the applied potential was less than +570 mV SHE. At potentials above +760 mV SHE elemental sulphur is also formed. At high rates of oxidation Cu_2O was found to be the main hydrophilic product formed, rather than $Cu(OH)_2$.

These findings are interesting in light of previous work (Asbjornsson et al., 2004a) discussed earlier, which reported the presence of Cu^{II} species, associated with sulphate and chloride, at the surface, at potentials greater than +440 mV SHE. No mention of copper hydroxide or oxide formation was made.

In a related study (Asbjornsson et al., 2004b) tennantite ($Cu_{12}As_4S_{13}$) was investigated using the same methods. In this case under oxidising potentials of +340 mV SHE formation of elemental sulphur, and +840 mV SHE formation of arsenic (III) and (V) oxides, was observed. This is similar behaviour to that observed by these authors for enargite.

Velásquez and co-workers (Velásquez et al., 2000b) used cyclic voltammetry (CV) to control the redox potential applied to a natural enargite surface in an alkaline solution. Surface composition under different applied potentials was analysed using XPS, SEM, EDX and EIS. A previous study by the same authors (Velasquez et al., 2000a) in which CV and XPS were used to characterise natural enargite, provides verification of the XPS results.

From the CV results two oxidation peaks in the positive sweep direction were observed, at +340 and +840 mV SHE. Surface composition analysis by XPS was reported to show a gradual decrease in Cu concentration with respect to As and S from +190 to +440 mV SHE. At +740 mV SHE complete oxidation of the mineral surface resulted in the formation of CuO, As_2O_3, As_2O_5, $CuSO_4$ and $Cu(OH)_2$.

This is an interesting finding in light of the more recent results discussed above (Asbjornsson et al., 2004a; Guo and Yen, 2008) where both $CuSO_4$ and $Cu(OH)_2$ are identified as oxidation products, but only at higher potentials (above +740 mV SHE). This contrasts with the findings of Guo and Yen (2008) where $Cu(OH)_2$ is found below +570 mV SHE and Cu_2O formation occurs at higher rates of oxidation. In addition Guo and Yen (2008) do not identify $CuSO_4$ formation. This suggests further work is needed to resolve these discrepancies, clarify the mechanism of oxidation and identify the surface species that are formed.

Subsequent cycling of the applied potential in the negative sweep direction (Velásquez et al., 2000b) over the range +840 to -610 mV SHE found oxide, hydroxide and sulphate species are no longer present as +440 mV SHE is reached. This would appear to be consistent with the observation of progressive dissolution of Cu at low but increasingly positive potentials, followed by precipitation of copper compounds above about +740 mV SHE. The authors contend that the oxidation species formed on the enargite surface are only stable at high applied potentials but do not specify a threshold potential at which this stability transformation takes place. Additionally they argue that the Cu concentration at the mineral surface is dependent only on applied potential, and not sweep direction (Velasquez et al., 2000a).

Further examination of the mineral surface was carried out using SEM and EDX (Velásquez et al., 2000b) to characterise morphology and composition. It was reported that at +740 mV SHE the surface is covered by a very thin heterogeneous oxidised layer. From this layer protrude surface structures formed from nucleation sites which are thought to be composed of oxide, hydroxide and sulphate material.

3.3. Chemical oxidation

One method that has been investigated for its effectiveness in achieving a separation of various copper sulphide minerals by flotation is that of oxidative pre-treatment to cause selective oxidation at the mineral surface. Fornasiero et al. (2001) investigated the selective oxidation of the mineral surfaces in solution, or oxidation followed by selective dissolution of the surface products formed, as a pre-treatment stage to achieve separation of enargite and tennantite from chalcopyrite, chalcocite and covellite. This will be discussed further in a later section.

Sasaki et al (2010) focussed on the effects of oxidative treatments at the mineral surface, comparing the physical and chemical response of enargite, tennantite and chalcopyrite. The procedure involved oxidising the minerals with H_2O_2 and oxygen gas at pH values of 2, 5 and 11. XPS was used to identify the species present at the mineral surface. These authors found in the case of enargite that elemental sulphur was formed by oxidative dissolution. The proposed reactions by which this occurs are shown below.

$$4\,Cu_3AsS_4 + 11\,O_2 + 5\,H_2O + 20\,H^+ = 12\,Cu^{2+} + 4\,H_2AsO_4^- + 16\,S \qquad [9]$$

$$2\,Cu_3AsS_4 + 11\,H_2O_2 + 10\,H^+ = 6\,Cu^{2+} + 2\,H_2AsO_4^- + 14\,H_2O + 8\,S \qquad [10]$$

The evidence for this was given as a significant increase after oxidation at pH 2.0 in the proportion of elemental sulphur relative to total sulphur, as was seen in the XPS results for the S2p spectrum. In another study, elemental sulphur was also found on the enargite surface by Raman spectroscopy after electrochemical oxidation at pH 1.0 (Asbjornsson et al., 2004a). In terms of

copper, the predominant species in un-oxidised enargite was of the Cu^{I} form, with evidence of formation of Cu^{II} compounds following oxidation at pH≥5.0 (Sasaki et al., 2010), most likely hydroxide rather than oxides or sulphate forms due to the high solubility of copper sulphates and oxides (Welham, 2001).

3.4. Contact angle

The preceding discussion indicates that much attention has been given to the nature of the surface species present under oxidising or reducing conditions produced by various methods. In order to better understand the potential effects of these treatments on the floatability of the mineral, the surface wettability has been studied directly by means of contact angle measurements.

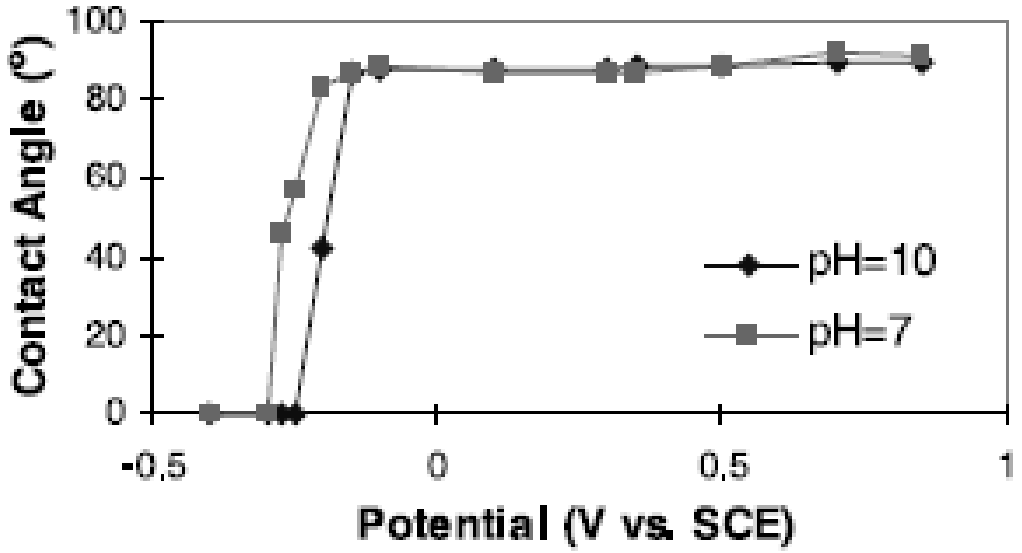

Figure 3. Effect of applied potential on contact angle of natural enargite at pH 10.0 and 7.0 (Guo and Yen, 2002).

Guo and Yen (2001) studied the effects of applied potential, pH, collector type and concentration on the wettability of enargite in the presence of collector under electrochemical control. Xanthate oxidation and dixanthogen reduction on the mineral surface were also studied.

Figure 3 shows the effect of applied potential for natural enargite. Below -250 mV SCE (-10 mV SHE) the contact angle was zero. The surface became hydrophobic above -200 mV SCE (+40 mV SHE) with a contact angle of 90° from -150 to +850 mV SCE (+90 to +1090 mV SHE). Changes in pH were found to have no significant effect on the contact angle magnitude. The net effect was to increase what Guo and Yen termed the "floatable potential range".

Where collector type was investigated, natural enargite was found to have a wider floatable potential range of about 125 mV using PAX (potassium amyl xanthate) compared to SIPX (sodium isopropyl xanthate). Increasing the collector concentration, in this case PAX, showed both an

increase in the floatable potential range width of about 70 mV, and an increase in contact angle of about 10° over the floatable potential range.

In addition Guo and Yen (2001) investigated xanthate oxidation and dixanthogen formation on the enargite surface, and reduction of dixanthogen to xanthate by cathodic polarisation. Dixanthogen formation was found to occur at similar potentials to those at which the surface became hydrophobic.

Guo and Yen (2002) extended the investigation of xanthate oxidation and dixanthogen formation carried out by Guo and Yen (2001). Ultraviolet (UV) spectroscopy applied to hexane extracts of the bulk solution and the solution surrounding the mineral surface confirmed the formation of dixanthogen on the mineral surface.

An important difference in these studies to those previously discussed is that the effects of the presence of flotation collectors in solution are investigated. In addition attempts were made to characterise the oxidation of xanthate and formation of dixanthogen on the enargite surface. From these findings it is possible to draw some correlations between applied potential and the transition of the mineral surface from hydrophilic to hydrophobic in the presence of a collector. The results of these studies indicate that a threshold potential exists where this transition takes place. Further evidence can be found in the work of Senior et al (2006) where such an effect was demonstrated for a number of sulphide mineral types.

However no published work has yet been found where a thorough review of the mineral surface chemistry has been carried out, using quantitative techniques such as XPS, to characterise the species formed at the mineral surface.

3.5. Single mineral flotation studies

Although arsenic more commonly occurs in mineral form, certain ore deposits are known to contain elemental arsenic. Bruckard et al. (2007) investigated the flotation of metallic (or elemental) arsenic, citing a lack of research in the area. A synthetic ore composed of 5% arsenic metal and 95% quartz was used in flotation tests carried out over a pH range of 5-12 and an Eh range of -500 to +500 mV SHE.

The flotation recovery was determined under two conditions. In the first selected pH values between pH 5 and 12 were used. Natural Eh ranged from +237 mV SHE at pH 5 to -45 mV SHE at pH 12. In the second, the flotation response was determined at selected Eh values between −500 and +500 mV SHE for pH values of 6 and 10.

Metallic arsenic was shown to have little floatability in the absence of collector. Using 40 g/t KEX, a typical flotation response of up to 95% recovery after 8 minutes, with about 5% quartz recovery was seen. Tests conducted over a range of pH values at natural Eh showed a flotation recovery of 95% to 85% in the pH range 5-10, then falling slowly to 53% at pH 12.

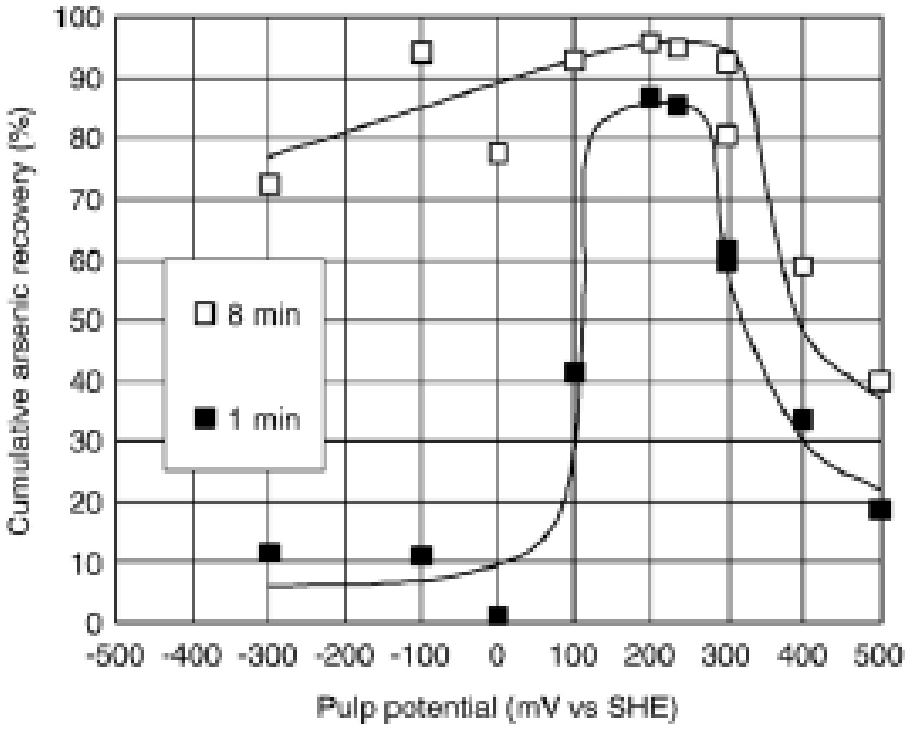

Figure 4. Cumulative arsenic metal recovery after 1 min and 8 min flotation with 40 g/t KEX as a function of pulp potential at pH 6 (Bruckard et al., 2007).

The effect of pulp potential was investigated by varying the pulp Eh at fixed pH values of 6 and 10. At pH 6 a strong flotation response was found in the Eh range +125 to +275 mV SHE, with a peak recovery of about 95%. In the Eh range +300 to + 400 mV SHE a transition from strong to poor floatability was observed, with an upper limiting potential, defined as the potential at which recovery is 50%, between +325 and +375 mV SHE. A typical pulp potential versus recovery curve is shown in Figure 4.

At pH 10 a strong flotation response at all Eh values tested between -300 and +225 mV SHE was found, with an upper limiting potential between +250 and +300 mV SHE. No lower limiting potential was found in the range tested.

Senior et al. (2006) investigated the flotation response of enargite using an artificial ore, composed of 10% natural enargite and 90% quartz, determined for a range of Eh values between -500 and +500 mV SHE and for pulp pH values of 8 and 11. Pulp potential was controlled by adding

dilute solutions (2.5% w/v) of laboratory grade sodium hypochlorite (NaClO) and sodium dithionite ($Na_2S_2O_4$).

To identify pulp pH and Eh conditions where effective separation of enargite could be achieved, the experimental flotation response of enargite was compared with data for chalcocite (Cu_2S), chalcopyrite ($CuFeS_2$) and cuprite (Cu_2O), sourced from the CSIRO Minerals databank on the pulp potential dependence of the flotation response for these minerals. A number of differences according to pulp potential conditions were identified that offered potential for exploitation.

The single mineral studies revealed a threshold potential for enargite below which it does not float and above which it does. For a pH of 8, this was found to be about -75 mV SHE and at pH 11 about -25 mV SHE. Threshold potential was defined as that at which recovery of the mineral of interest is 50%. Data for the effects of pulp potential on the flotation response of other copper mineral types was reported. For chalcocite, at pH 8 a lower threshold of about -155 mV SHE was found to exist, above which it floats, while no upper limiting potential was reported. However at pH 11 threshold potentials at about -155 and +270 mV SHE was reported, between which chalcocite floats strongly.

These results are in agreement with the findings of Heyes and Trahar (Heyes and Trahar, 1979) who reported that at pH 8 and 11 flotation of chalcocite was not observed below -200 mV SHE, there was a transition to complete floatability between -200 and -100 mV SHE, while at pH 8 no upper limiting potential was observed. However at pH 11 a second limiting potential between about +200 and +300 mV SHE was reported above which chalcocite does not float.

Chalcopyrite was similar (Senior et al., 2006) at pH 8 to chalcocite but the lower limiting threshold potential was about +160 mV SHE. No upper limiting potential was reported up to +360 mV SHE, which was the limit of the range studied. No data was reported for other pH values.

Cuprite was reported to differ from the other mineral types in that no lower limiting potential was observed and a strong flotation response in reducing conditions down to -400 mV SHE exists at pH 11. In addition an upper limiting potential of about +290 mV SHE was found. Based on these findings a number of possible separations that might be achieved by exploiting the observed differences in flotation response were proposed.

In the case of chalcopyrite, considered representative of the copper-iron sulphides, it was concluded (Senior et al., 2006) that separation from enargite is possible in the potential range -25 to +50 mV SHE at pH 8 where enargite floats strongly but chalcopyrite does not. Although no data was reported the authors concluded that the threshold potential would not be likely to change significantly with pH and so a similar separation could be possible at pH 11.

Where selective flotation of enargite from the copper sulphide minerals is concerned, represented in this study by chalcocite, it was concluded that the threshold potentials at pH 8 are not sufficiently different for an adequate separation to be achieved, but that this is not the case at pH 11. Under these conditions two possible Eh ranges were found to exist where separation might be achieved. The first is between about -150 and -75mV SHE where chalcocite floats, and the second is above about +270 mV SHE where enargite floats but chalcocite does not.

Where separation from copper oxides such as cuprite is concerned, it was found that selectivity is possible in two potential ranges. Cuprite was found to float at potentials below about -150 mV SHE while enargite does not. Conversely above about +290 mV SHE it was observed that enargite will float but cuprite does not.

Since the behaviour of cuprite is similar to chalcocite, where both minerals display a poor flotation response under oxidising conditions, it was concluded that separation of enargite from both these minerals should be possible in a single flotation step. It should be pointed out that these conclusions were based on data obtained from single mineral studies. No work was carried out to take into account the effects of interactions between different mineral types that might affect the flotation results in mixed mineral systems.

4. Selective flotation of enargite

4.1. Selective flotation reagents

Various studies have been carried out to investigate the potential for selective flotation of arsenic-bearing copper minerals using either chemical reagents that act as depressants, or use of oxidising and reducing agents to control electrochemical conditions of the flotation pulp, that is, pulp Eh control. By far most of the selective depressant work has focussed on arsenopyrite, but other mineral types have also been investigated. However, the number of studies involving the separation of copper arsenic sulphides, in particular enargite and tennantite, from non-arsenic copper sulphides, is limited.

Kydros et al. (1993) used sodium dithionite and sodium sulphite as arsenopyrite depressants in the treatment of a bulk auriferous concentrate in acidic media. It was reported that the use of sodium dithionite led to slight activation of pyrite, possibly due to the coverage of its surface with a sulphur-containing hydrophobic layer. Selective depression of arsenopyrite in the presence of sodium dithionite and sodium sulphite was found.

Tapley and Yan (2003) considered the effects of magnesium-ammonium mixture (MAA) with pH control, pre-aeration and potassium permanganate on pyrite-arsenopyrite separation, achieving successful depression of arsenopyrite. However no mechanism of action was proposed. Abeidu and

Almahdy (1980) reported the use of arsenic triiodide (AsI_3) followed by the addition of magnesia mixture to depress chalcopyrite and arsenopyrite for separation from pyrite in the manufacture of sulphuric acid. Magnesia mixture was prepared using $MgCl_2•6H_2O$, NH_4Cl and NH_4OH dissolved in distilled water. The proposed mechanism of depression was reported as based on the selective adsorption of arsenite ions (As^{3+}) onto the chalcopyrite surface to form insoluble copper arsenides (Cu_3As, Cu_3As_2). Since iron (Fe^{2+} and Fe^{3+}) does not form stable arsenides, pyrite was not affected. Since As^{3+} is readily oxidisable to As^{5+} it forms a stable complex anion $[AsO_4]^{3-}$ on the chalcopyrite surface which, along with the original arsenate sites on the arsenopyrite surface, react with the magnesia mixture to form strongly hydrophilic layers of the form $AsO_4NH_4Mg•6H_2O$. This surface layer inhibits collector adsorption on the chalcopyrite and arsenopyrite surfaces and facilitates the separation of pyrite.

Tajadod and Yen (1997a) investigated the surface properties and flotation characteristics of enargite and chalcopyrite in the presence of a xanthate collector, using sodium cyanide (NaCN) and potassium permanganate ($KMnO_4$) as depressants. Their effects on pre-adsorbed xanthate desorption from the mineral surfaces and the effects of sodium cyanide and potassium permanganate pre-conditioning on xanthate adsorption were investigated.

It was found that xanthate adsorption was more rapid on enargite than chalcopyrite. The effect of sodium cyanide on xanthate desorption was greatest for enargite, while the effect on chalcopyrite was minimal. Pre-conditioning with sodium cyanide followed by xanthate addition further reduced the final xanthate adsorption density. The effects of potassium permanganate on pre-adsorbed xanthate were found to be similar to those of sodium cyanide. After pre-conditioning with potassium permanganate followed by xanthate addition the adsorption density was found to be higher. Selective flotation by depression of enargite with sodium cyanide achieved no more than a partial separation, with about 70% of the arsenic rejected, but at the expense of about 45% of the copper.

Despite concluding that sodium cyanide is a suitable depressant for enargite and reducing arsenic content of copper concentrates, the high associated copper losses were recognised. Such high losses are not sustainable in industrial applications. In addition, no consideration is given to achieving a separation in the more complex multi-mineral systems that generally exist in practice.

In a related study (Tajadod and Yen, 1997b) a number of other methods to achieve a separation of enargite from chalcopyrite by flotation were investigated. This included the effects of sodium sulphide (Na_2S), oxidation by pulp aeration, and magnesium-ammonium mixture addition on xanthate adsorption density and mineral floatability.

Neither conditioning with sodium sulphide or pulp aeration was found to give sufficient difference in adsorption density to produce an effective separation. Flotation tests showed without any conditioning at pH 9, enargite and chalcopyrite showed similar floatability with recoveries of 71% and 81% respectively. Conditioning with Na_2S reduced the flotation recoveries to 58% and 26% for enargite and chalcopyrite. In comparison, after two hours conditioning by aeration only, recoveries were reported as 32% and 46% respectively. In contrast, conditioning with MAA reduced recoveries of enargite and chalcopyrite from 71% and 81% to 15% and 80% respectively, while aeration combined with MAA gave 12% and 79% respectively.

Sodium sulphide (Na_2S) conditioning and oxidation by pulp aeration were found to be ineffective in achieving a separation of enargite and chalcopyrite. Using MAA mixture and aeration as the conditioning step, xanthate adsorption on the enargite surface was significantly inhibited. A separation efficiency of arsenic from non-arsenic minerals of 50% was found to be possible. Where sodium sulphide was used as the chalcopyrite depressant a separation efficiency of 22.7% was found, while using aeration to oxidise the enargite gave a separation efficiency of less than 15%. Separation efficiency in this case was defined as the copper recovery minus the arsenic recovery.

The specificity of MAA for enargite was explained (Tajadod and Yen, 1997b) as the oxidation of the arsenic sites at the enargite surface to form a stable complex anion $[AsO_4]^{3-}$ which has a great affinity for the MAA. As a result the compound $AsO_4(NH_4)Mg.6H_20$ is formed, which is strongly hydrophilic and acts to block xanthate adsorption. As this compound formation is specific to the arsenic sites chalcopyrite is not affected and there is no inhibition of xanthate adsorption on its surface.

Based on these results it was concluded that it is possible to achieve a separation of enargite from chalcopyrite by froth flotation of a copper concentrate using MAA as an enargite depressant.

Yen and Tajadod (2000) compared two methods of separation of enargite from chalcopyrite by flotation, pulp potential control and depression of enargite by conditioning with MAA. At a potential of -10 mV SHE enargite could be recovered by flotation while chalcopyrite remained depressed. Enargite recovery was best in the range -145 to +14 mV SHE, while for chalcopyrite this range was -160 to +100 mV SHE.

Xanthate adsorption on enargite decreased with increasing MAA concentration with a reduction of 76% reported. No decrease for chalcopyrite was found at any MAA concentration. Flotation tests found that enargite recovery decreased with increased MAA concentration, falling below 15%, while chalcopyrite was not affected. In the pH range 7.0 – 9.0 enargite recovery was below 15% while chalcopyrite was unaffected at 80-82%. As the pH increased from 9 – 11, this

reduced to about 47%, with a further small decrease for enargite. In addition it was reported that if the minerals were aerated for 10 minutes prior to conditioning a further 2.3% decrease in enargite recovery was observed, while chalcopyrite was unaffected. It was concluded that selective flotation of enargite from chalcopyrite could be achieved using either pulp potential control or depression of enargite by conditioning with MAA prior to collector addition.

Castro et al. (2003) also investigated the depressant effects of MAA on enargite in the recleaner stage of copper ore flotation over a pH range of 7-10 and a MAA dosage range of 1.8 to 10.8 kg/t. A limited depressant effect was observed with the best result reported at pH 10 and a MAA dosage rate of 2.5 kg/t, resulting in an arsenic recovery of about 55%. However, when the dose rate was increased to 7 kg/t, no depression was observed. It was theorised that where a mineral surface is already coated by collector, adsorption of magnesium and ammonium ions to form a magnesium ammonium arsenate complex ($AsO_4NH_4Mg.6H_20$) at the mineral surface is limited. In this case the reported results contradict the findings of Yen and Tajadod (2000). Depression was not observed in the pH range 7–9 using 1.8 to 10.8 kg/t magnesia mixture. An important step appears to be pre-aeration of the pulp. According to Dai et al. (2005) in a study of the Garson Ni–Cu ore, magnesia mixture does not depress gersdorffite (NiAsS) without pre-aeration. Yen and Tajadod (2000) incorporated pre-aeration of the flotation pulp whereas this step was not used by Castro et al. (2003).

4.2. Selective oxidation

Fornasiero and co-workers (2001) investigated the separation of natural enargite and tennantite (Continental Minerals, USA) from natural chalcopyrite, chalcocite and covellite (Ward's Natural Science Establishment, USA) in mixed mineral systems using selective oxidation of the mineral surfaces in solution, or oxidation followed by selective dissolution of the surface products formed. Mixed mineral flotation tests were carried out using six two-mineral systems comprised of enargite and tennantite with each of the copper sulphide minerals. Conditioning was carried out under non-oxidising conditions with N_2 gas at pH 5.0 and 11.0, and under oxidising conditions with O_2 gas and hydrogen peroxide (H_2O_2) as an oxidising agent at pH 5.0 and 11.0. Collector was added at the end of conditioning. Ethylene diamine tetra-acetic acid (EDTA) addition at pH 11.0 was used to selectively remove surface oxidation products.

After conditioning with N_2 at pH 5.0 all minerals displayed a high flotation recovery without selectivity. However at pH 11.0, separation of chalcopyrite from tennantite, chalcopyrite from enargite and covellite from tennantite were significantly improved. Separation of chalcocite from enargite and chalcocite from tennantite were also improved but to a lesser extent. Separation of covellite from enargite was essentially unchanged from that seen at pH 5.0. Moreover, it was found

that for the covellite-tennantite system the arsenic bearing mineral was depressed, while for all other mineral pairs the reverse was true. Thus for this system covellite was recovered preferentially, whereas for the other three systems enargite and tennantite were recovered preferentially.

It was concluded from the variation observed in separation efficiency that in any real complex multi-mineral flotation system it would not be possible to achieve the desired result of an efficient separation of copper sulphides from copper arsenic sulphides.

Conditioning with O_2 at pH 5.0 resulted in higher recovery of non-arsenic minerals and so gave a good separation, particularly for the mineral systems containing enargite. Recoveries ranged from 47% to 82% for the non-arsenic minerals and from 40% to 53% for the arsenic minerals. At pH 11.0 depression of all minerals was reported with maximum recoveries lower than 20%.

Where EDTA was added after conditioning and before collector addition at pH 11.0, flotation recoveries and mineral separation was dependent on concentration. Without EDTA a thick layer of surface oxide species was present resulting in low flotation recoveries. In the chalcocite-tennantite system the optimum separation of arsenic and non-arsenic species was observed at an EDTA concentration of $2x10^{-5}$ mol dm^{-3}. At high EDTA concentrations surface oxidation products were removed from both mineral species resulting in high recoveries but little selectivity.

It was concluded that higher flotation recoveries of non-arsenic minerals resulted from greater collector adsorption and less surface oxide and hydroxide species than on enargite and tennantite, suggesting that the surface oxidation layer inhibited collector adsorption on the surface of enargite and tennantite. Thus, the observed results were due to a greater extent of surface oxidation of the arsenic minerals compared to the non-arsenic minerals. It is this surface oxidation layer that inhibits the adsorption of collector molecules onto the mineral surface resulting in decreased recovery of arsenic minerals. Arsenic oxides were found to be more stable than copper oxides at pH 5.0, and dissolve less than copper oxides when EDTA was added to the system at pH 11.0. The extent of oxide dissolution was found to be dependent on EDTA concentration and, when combined with the different rates of arsenic and copper oxide dissolution, control of arsenic and non-arsenic mineral recovery could be achieved by varying this concentration.

Huch (1994) developed and patented a method to separate chalcocite from enargite using froth flotation, whereby a pre-conditioning step incorporating an oxidising agent, preferably hydrogen peroxide, was used to treat a concentrate containing these minerals. An optimum pulp oxidation reduction potential of +50 to +200 mV (no reference standard given) was described. In this application it is considered that the mechanism of separation is the preferential oxidation and

depression of the more easily oxidised mineral, chalcocite, while enargite is recovered to concentrate.

In both cases the oxidation step was carried out before collector addition so that the formation of a surface oxide layer acts to prevent or reduce collector adsorption and increase flotation selectivity. The success of this approach therefore depends on two factors. First, sufficiently different rates of oxidation between the mineral types present for an oxide layer to form on one species and not another, and second, precise control of the oxidation to ensure only the target species is oxidised.

These findings provide a useful insight into the mechanisms by which the surface reactions of the mineral species studied can be controlled by altering the solution conditions under which flotation is carried out. It demonstrates that potential exists to achieve useful separations of arsenic and non-arsenic copper mineral species through an understanding of the behaviour of each of these minerals under different conditions. By controlling the formation and dissolution of surface oxidation species it has been shown that it is possible to alter the adsorption of collector molecules at the mineral surface and hence vary the flotation recovery that can be achieved. In this way selective mineral recovery was achieved in simple two mineral systems.

4.3. Pulp potential control

Pulp potential in the flotation of sulphide minerals is not a new concept and the use of Eh measurement and its interpretation has been practiced by researchers for more than thirty years. Despite the long-term research interest, its use in industrial flotation applications has been limited, according to Chander (2003). Woods (2003) concluded that in laboratory applications the monitoring and control of electrochemical potential has led to improvements in development of flotation strategies. In the separation of arsenic bearing copper sulphides from other copper sulphides control of Eh to achieve selectivity in flotation has shown promising results in recent years.

In a study of separation of enargite from chalcopyrite using pulp potential control, Guo and Yen (2005) investigated the surface oxidation and flotation response using cyclic polarisation, contact angle measurements and microflotation tests.

Chalcopyrite was found to oxidise more quickly at a lower potential than enargite, the difference possibly due to different electrical conductivity. Resistance of 1 cm^3 samples of chalcopyrite (2-3 Ω) and enargite (1000 Ω) was reported. Enargite was found to show formation of a passivation layer at potentials below +990 mV SHE, giving some resistance to oxidation. Contact angle varied with potential, as shown in Figure 5 for a $7x10^{-4}$ M PAX solution at pH 10.0.

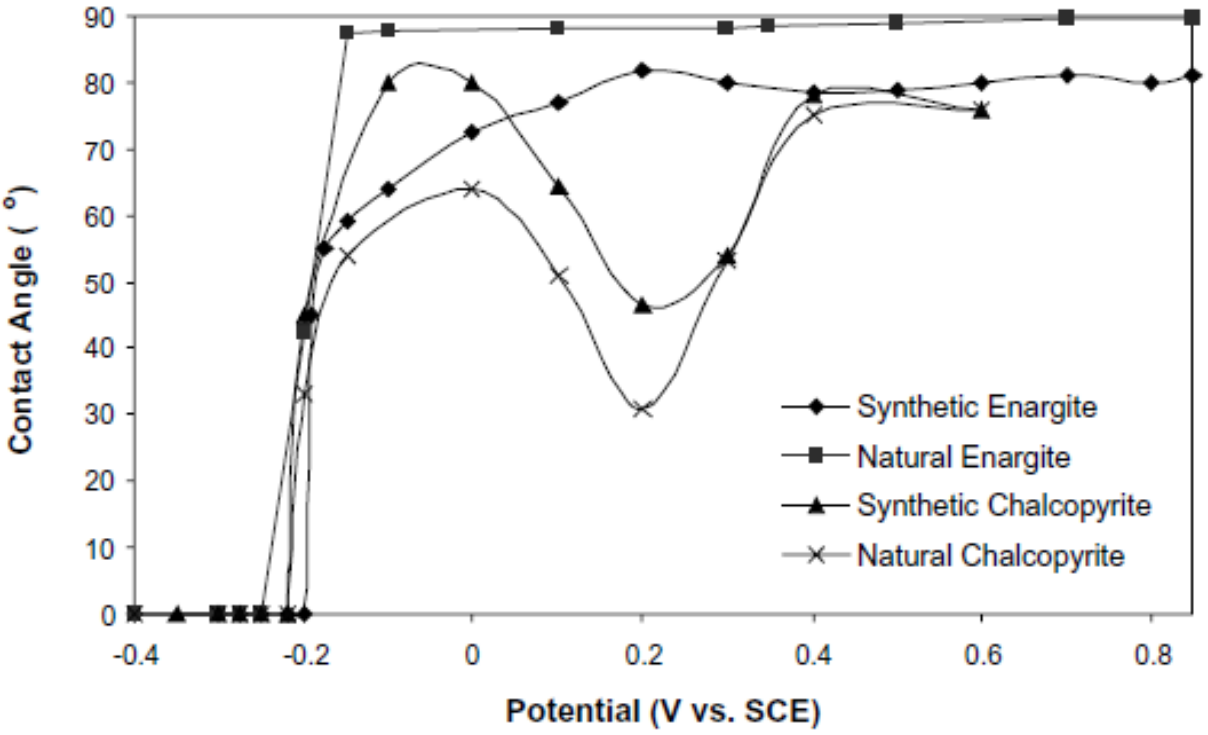

Figure 5. Effect of pulp potential on contact angle in $7x10^{-4}$M PAX at pH 10 (Guo and Yen, 2005).

The lower hydrophobicity (or smaller contact angle) observed for chalcopyrite was explained in terms of the surface oxidation products that form at different applied potentials. Hydrophobic species such as S^0 that form at low potentials (+140 to +340 mV SHE) become further oxidised to hydrophilic species such as SO_3^{2-} and SO_4^{2-} at potentials above +440 mV SHE. In contrast the hydrophobic oxidation products formed on the enargite surface persist up to a potential of +990 mV SHE.

Using a lower PAX concentration ($7x10^{-5}$ M PAX solution at pH 10.0) the contact angle for chalcopyrite was much smaller than for enargite and the difference between them was greater at potentials above +440 mV SHE, suggesting a more effective separation could be achieved under these conditions (Figure 6).

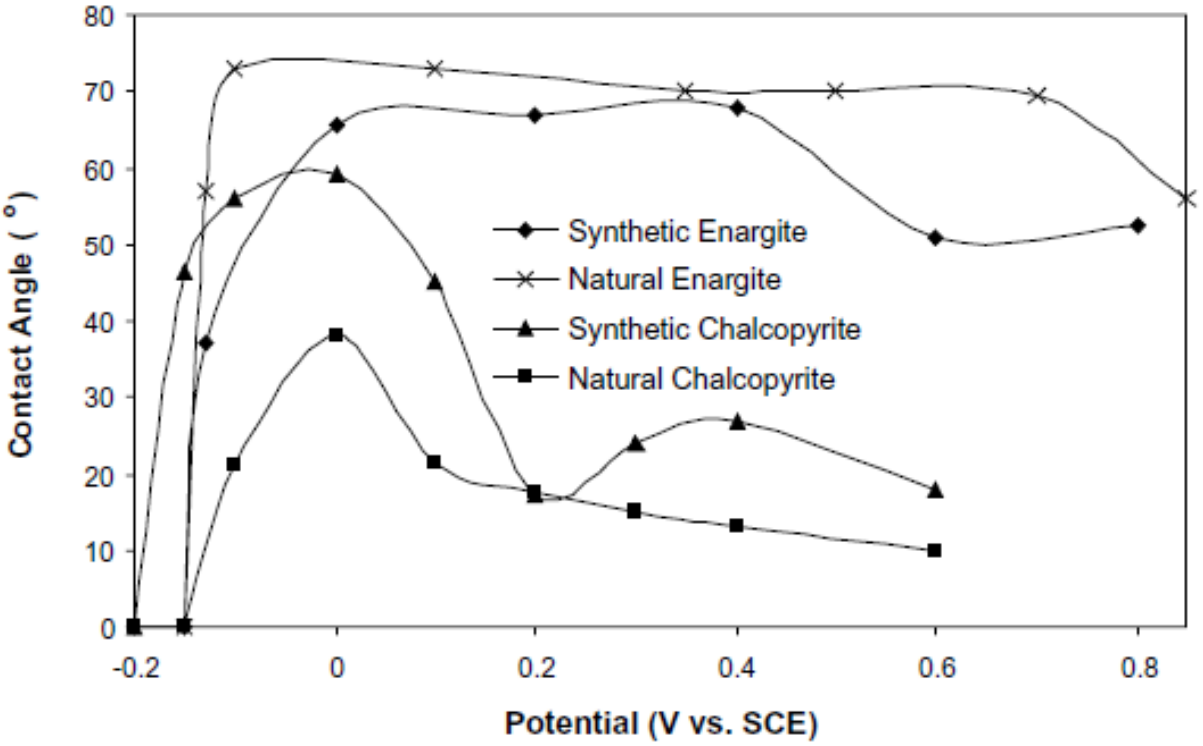

Figure 6. Effect of pulp potential on contact angle in $7x10^{-5}$M PAX at pH 10 (Guo and Yen, 2005).

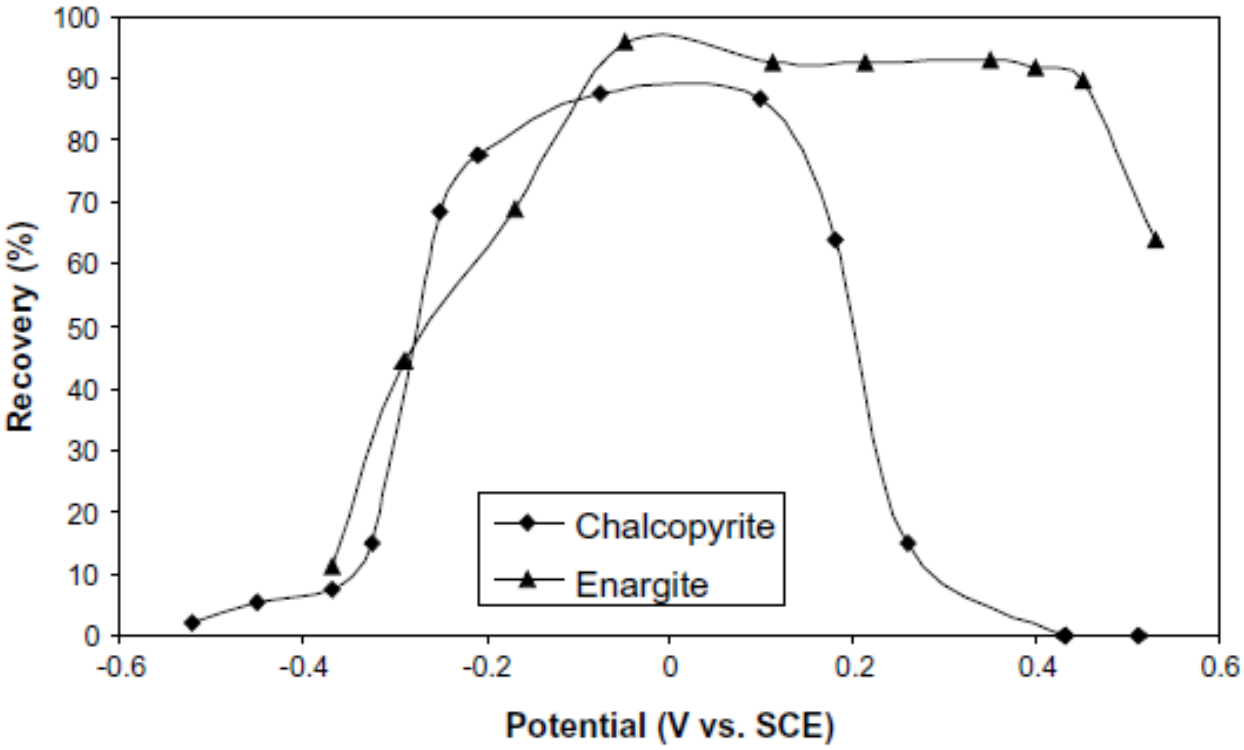

Figure 7. Effect of pulp potential on flotation recovery in $7x10^{-5}$M PAX solution at pH 10 (Guo and Yen, 2005).

Flotation tests showed the best selectivity was obtained with $7x10^{-5}$ M PAX solution at pH 10.0 at a potential of +740 mV SHE, with 93.4% enargite recovered to concentrate and 92.6% chalcopyrite recovered to tailings, as shown in Figure 7.

Kantar (2002) investigated the flotation characteristics of enargite using hydrogen peroxide and sodium sulphide to control the potential of the system. It was found that under oxidising conditions enargite was capable of collectorless flotation, due to the formation of elemental sulphur on the surface. In contrast under reducing conditions collectorless flo-tation was not possible, due to the formation of CuO. In the presence of xanthate, floatability was strongly dependent on the solution potential with maximum enargite recovery close to 100% at potentials between +150 and +270 mV SHE, and decreasing rapidly above or be-low this range.

Senior and co-workers (Senior et al., 2006) investigated the floatability of enargite as a function of pulp potential and pH to determine if its flotation behaviour was sufficiently different to other copper minerals for flotation separation to be achieved.

Single mineral flotation studies found a threshold potential of about -75 mV SHE at pH 8.0 and -25 mV SHE at pH 11.0 above which enargite floats and below which it does not. Threshold potential was defined as that potential at which the recovery after 1 minute is 50%. The transition from non-floatability to strongly floating took place over a range of about -150 to -50 mV SHE at pH 8.0. At pH 11.0 the threshold potential was found to be about -25mV SHE (Figure 8)

However the authors' state this difference may be due to scatter in the data and whether it is in fact a real difference is uncertain, although theoretically the threshold potential should change with pH, since it is related to the oxidation potential.

This transition is similar to that reported by Guo and Yen (2005) in the range of about -150 to +100 mV SHE at pH 10.0. Using the same definition as Senior et al, a threshold potential of about -10 mV SHE at pH 10.0 was found, which is in reasonable agreement with Senior et al. (2006), given the stated level of uncertainty.

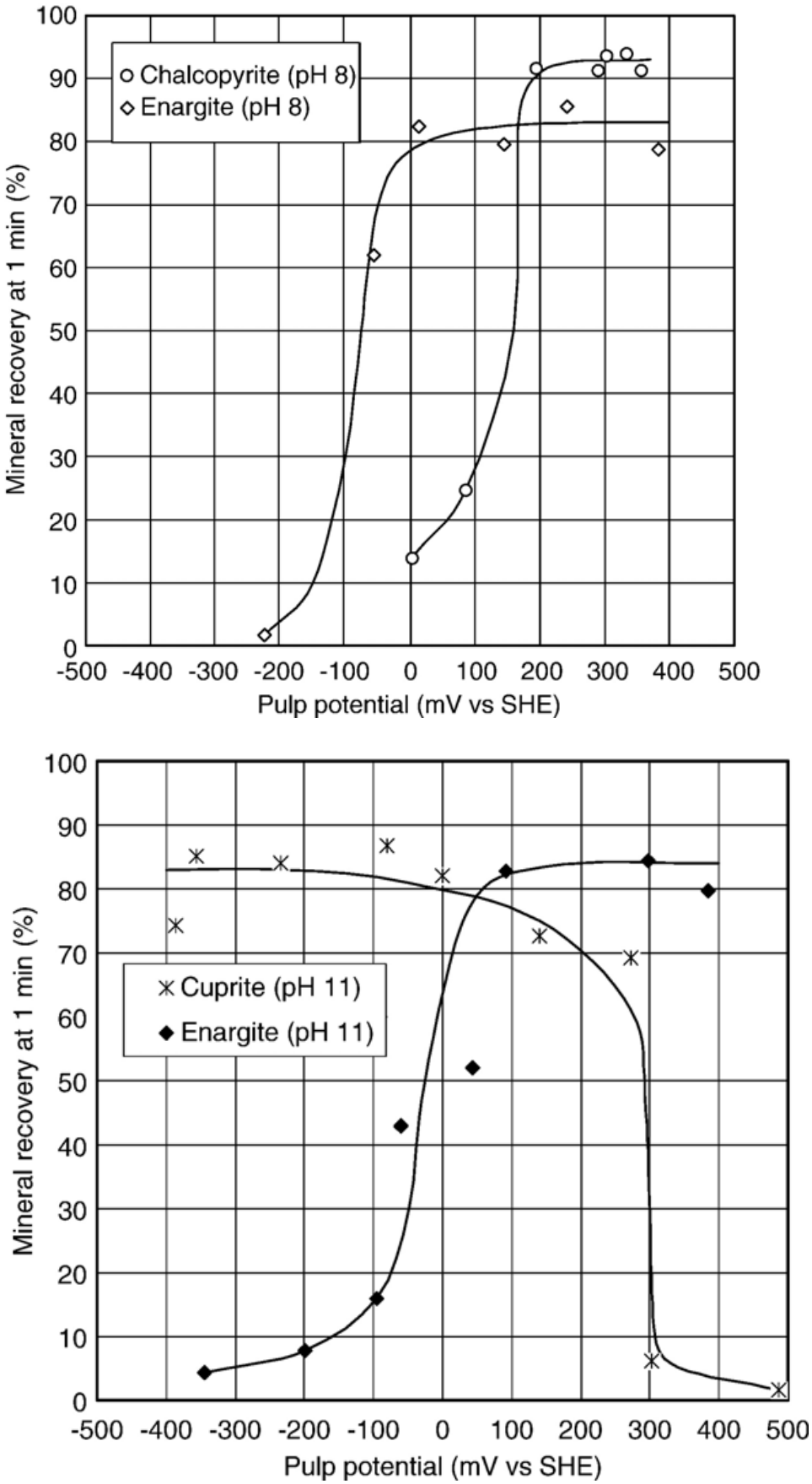

Figure 8. Enargite flotation recovery as a function of pulp potential at pH 11 and pH 8 (Senior et al., 2006).

Guo and Yen (2006) found good flotation of enargite in the potential range of +190 to +740 mV SHE in a 7×10^{-5} M PAX solution. Smith and Bruckard (2007) used controlled-potential flotation to separate tennantite from chalcopyrite and bornite. The separation was made on a bulk copper–arsenic concentrate after reducing the pulp potential to about -150 mV SHE at pH 12 and floating the tennantite from the other copper minerals.

The flotation behaviour of arsenic metal with ethyl xanthate as a function of pulp pH and pulp potential was studied by Bruckard et al. (2007). It was found that metallic arsenic has no natural floatability but floats readily (up to 95% recovery in 8 min) over a wide range of pH and Eh. In a detailed study of the electrochemical behaviour of enargite (Guo and Yen, 2008) a passivation layer was found to form over a broad potential range (-660 to +1070 mV SHE). The main oxidation product found on the mineral surface were copper hydroxide ($Cu(OH)_2$) below +570 mV SHE. At potentials above +760 mV SHE elemental sulphur was also formed.

Bruckard et al. (2010) investigated the feasibility of arsenic reduction using controlled potential flotation to produce both low-arsenic and high-arsenic concentrates. This was incorporated as a first treatment step in a proposed three-stage beneficiation process for arsenic-bearing copper ores. The second stage used low temperature roasting of the high-arsenic concentrate to produce a calcine for smelting. In the final stage the fume product is immobilised in a low temperature ceramic for disposal. It was shown that a net economic benefit can be achieved.

5. Summary

Zeta potential studies have been used to propose a mechanism of enargite oxidation at high pH involving dissolution and hydrolysis of thio-arsenate and arsenate ions followed by re-adsorption at the mineral surface and precipitation of metal hydroxides on the metal-deficient surface. At low pH dissolution of metal ions takes place leaving a metal-deficient or sulphur-rich mineral surface. With continuing oxidation the sulphide groups oxidise to form polysulphide or elemental sulphur. The differences between copper sulphides and copper arsenic sulphides suggest the potential for flotation separation taking place in alkaline environments by exploiting differences in their susceptibility to oxidisation.

Electrochemical techniques coupled with surface analysis have been used by a number of authors to investigate the chemical species formed on the enargite surface under oxidising (anodic) and reducing (cathodic) conditions. Under anodic conditions the formation of species including copper sulphate or hydroxide and elemental sulphur has been reported. Although there is broad agreement between these studies, some disagreement exists about the nature of oxidation product formed. It is not clear whether copper hydroxide or oxide species, or Cu^{II} species associated with

sulphate and chloride, are the main oxidation products. However, there seems to be good agreement that the main oxidation mechanism is one of progressive dissolution of Cu at low but increasingly positive potentials, followed by precipitation of copper compounds above about +740 mV SHE. An active-passive transition in the oxidative potential range was reported at potentials around +540 mV SHE, which correlates with the formation of an oxidative surface layer. This mechanism of surface layer formation also appears to be significant in the adsorption of xanthate collectors and in the application of controlled potential flotation of enargite. Chemical oxidation as a selective oxidative pre-treatment of the mineral surfaces produced similar results to electrochemical oxidation, with the formation of elemental sulphur and Cu^{II} compounds, most likely hydroxides.

Contact angle measurements further develop the idea of collector adsorption dependency on the formation of an oxide surface layer, and form a link between the fundamental studies of surface oxidation and flotation of enargite. It has been shown that there is a threshold potential range (of about -250 to -150 mV SHE) where contact angle sharply increases from zero to 90° as applied potential increases.

Single mineral studies provide further support for a threshold potential below which enargite does not float. It was shown that enargite will become floatable as pulp potential increases through about -75 mV SHE, depending on pH. This threshold is different from threshold potentials for flotation of non-arsenic copper sulphides, suggesting it is possible to achieve selective flotation of enargite by careful control of pulp potential.

Investigations of the selective flotation of As-minerals has focused on arsenopyrite and on enargite only in recent years. The main mechanisms of achieving enargite selectivity involve the use of selective flotation reagents, selective oxidation and control of pulp potential. Conditioning with reagents such as sodium cyanide and sodium sulphide has shown limited success, with generally poor separation efficiency and high copper losses. The use of MAA to depress enargite has shown mixed results, with some authors reporting good selectivity while other studies fail to give the same results. However methodological differences may explain these differences. Selective oxidation of the mineral surface to influence collector adsorption using a pre-conditioning step has been shown to be effective in separating enargite from non-arsenic copper sulphides. Typically, hydrogen peroxide or similar oxidising reagents are used and can be combined with pulp aeration using air or oxygen gas. Pulp potential control as a method for achieving selective flotation of arsenic minerals and in particular enargite has received increasing attention recently, and promising results have been reported. However, more work must be done both to understand the fundamental mechanisms that underpin a successful separation, and to further develop a process more readily applicable to industrial separation. In addition the use of other potentially more selective flotation

collectors, other than the traditional default standard of xanthates, has been neglected in the literature concerning enargite, and deserves investigation. In combination with a well developed method of pulp potential control, there is the potential for worthwhile developments towards the ultimate goal of achieving a robust industrial separation process.

Acknowledgments

The authors gratefully acknowledge the University of Queensland and CSIRO Process Science and Engineering for the postgraduate scholarships (CP) and financial supports.

References

Abeidu, A.M. and Almahdy, A.M., 1980. Magnesia mixture as a regulator in the separation of pyrite from chalcopyrite and arsenopyrite. Int. J. Miner. Process., 6(4): 285-302.

Asbjornsson, J. et al., 2004a. Electrochemical and surface analytical studies of enargite in acid solution. J. Electrochem. Soc., 151(7): E250-E256.

Asbjornsson, J. et al., 2004b. Electrochemical and surface analytical studies of tennantite in acid solution. J. Electroanal. Chem., 570(1): 145-152.

Biswas, A.K. and Davenport, W.G., 1994. Extractive metallurgy of copper. Pergamon, Oxford, 500 p pp.

Bruckard, W.J. et al., 2010. Development and evaluation of an early removal process for the beneficiation of arsenic-bearing copper ores. Minerals Engineering, 23(15): 1167-1173.

Bruckard, W.J., Kyriakidis, I. and Woodcock, J.T., 2007. The flotation of metallic arsenic as a function of pH and pulp potential -- A single mineral study. International Journal of Mineral Processing, 84(1-4): 25-32.

Castro, S.H. and Baltierra, L., 2005. Study of the surface properties of enargite as a function of pH. International Journal of Mineral Processing, 77(2): 104-115.

Castro, S.H., Baltierra, L. and Munoz, P., 2003. Depression of enargite by magnesium-ammonium mixtures. Proceedings of the Copper 2003-Cobre 2003 The 5th International Conference, Volume III-Mineral Processing: 257-269.

Castro, S.H. and Honores, S., 2000. Surface properties and floatability of enargite. In: P. Massacci (Editor), Proceedings of the XXI International Mineral Processing Conference. Elsevier Science B. V., Rome, Italy, pp. B8b-47 - B8b-53.

Chander, S., 2003. A brief review of pulp potentials in sulfide flotation. International Journal of Mineral Processing, 72(1-4): 141-150.

Cordova, R., Gomez, H., Real, S.G., Schrebler, R. and Vilche, J.R., 1997. Characterization of natural enargite/aqueous solution systems by electrochemical techniques. J. Electrochem. Soc., 144(8): 2628-2636.

Cordova, R., Gomez, H., Schrebler, R., Real, S.G. and Vilche, J.R., 1996. An electrochemical study of enargite in aqueous solutions by transient techniques. Proc. - Electrochem. Soc., 96-6(Electrochemistry in Mineral and Metal Processing): 356-367.

Dai, Z., Garritsen, J., Wells, P.F. and Xu, M., 2005. Arsenic rejection in the flotation of Garson Ni-Cu ore. Publ. Australas. Inst. Min. Metall., 5/2005(Centenary of Flotation Symposium, 2005): 939-946.

Filippou, D., St-Germain, P. and Grammatikopoulos, T., 2007. Recovery of metal values from copper-arsenic minerals and other related resources. Miner. Process. Extr. Metall. Rev., 28(4): 247-298.

Fornasiero, D., Fullston, D., Li, C. and Ralston, J., 2001. Separation of enargite and tennantite from non-arsenic copper sulfide minerals by selective oxidation or dissolution. International Journal of Mineral Processing, 61(2): 109-119.

Fullston, D., Fornasiero, D. and Ralston, J., 1999a. Oxidation of synthetic and natural samples of enargite and tennantite: 1. Dissolution and zeta potential study. Langmuir, 15(13): 4524-4529.

Fullston, D., Fornasiero, D. and Ralston, J., 1999b. Oxidation of synthetic and natural samples of enargite and tennantite: 2. X-ray photoelectron spectroscopic study. Langmuir, 15(13): 4530-4536.

Fullston, D., Fornasiero, D. and Ralston, J., 1999c. Zeta potential study of the oxidation of copper sulfide minerals. Colloids and Surfaces A: Physicochemical and Engineering Aspects, 146(1-3): 113-121.

Guo, B.H. and Yen, W.-T., 2001. Electrochemical investigation on wettability of enargite. Interact. Miner. Process., Proc. UBC-McGill Int. Symp. Fundam. Miner. Process., 4th: 325-336.

Guo, H. and Yen, W.T., 2002. Surface potential and wettability of enargite in potassium amyl xanthate solution. Minerals Engineering, 15(6): 405-414.

Guo, H. and Yen, W.T., 2005. Selective flotation of enargite from chalcopyrite by electrochemical control. Minerals Engineering, 18(6): 605-612.

Guo, H. and Yen, W.T., 2006. Electrochemical floatability of enargite and effects of depressants. In: G. Önal et al. (Editors), Proceedings of the XXIII International Mineral Processing Conference. Promed, Istanbul, Turkey, pp. 504-509.

Guo, H. and Yen, W.T., 2008. Electrochemical study of synthetic and natural enargites. Proc. Int. Miner. Process. Congr., 24th, 1: 1138-1145.

Heyes, G.W. and Trahar, W.J., 1979. Oxidation-reduction effects in the flotation of chalcocite and cuprite. Int. J. Miner. Process., 6(3): 229-52.

Huch, R.O., (Tucson, AZ), 1994. Method for achieving enhanced copper-containing mineral concentrate grade by oxidation and flotation. Cyprus Mineral Company (Englewood, CO), United States.

Kantar, C., 2002. Solution and flotation chemistry of enargite. Colloids and Surfaces A: Physicochemical and Engineering Aspects, 210(1): 23-31.

Kydros, K.A., Angelidis, T.N. and Matis, K.A., 1993. Selective flotation of an auriferous bulk pyrite - arsenopyrite concentrate in presence of sodium sulfoxy - salts. Miner. Eng., 6(12): 1257-64.

Pauporté, T. and Schuhmann, D., 1996. An electrochemical study of natural enargite under conditions relating to those used in flotation of sulphide minerals. Colloids and Surfaces A: Physicochemical and Engineering Aspects, 111(1-2): 1-19.

Sasaki, K., Takatsugi, K., Ishikura, K. and Hirajima, T., 2010. Spectroscopic study on oxidative dissolution of chalcopyrite, enargite and tennantite at different pH values. Hydrometallurgy, 100(3-4): 144-151.

Schwedt, G. and Rieckhoff, M., 1996. Separation of thio- and oxothioarsenates by capillary zone electrophoresis and ion chromatography. Journal of Chromatography A, 736(1-2): 341-350.

Senior, G.D., Guy, P.J. and Bruckard, W.J., 2006. The selective flotation of enargite from other copper minerals -- a single mineral study in relation to beneficiation of the Tampakan deposit in the Philippines. International Journal of Mineral Processing, 81(1): 15-26.

Smith, L.K. and Bruckard, W.J., 2007. The separation of arsenic from copper in a Northparkes copper-gold ore using controlled-potential flotation. International Journal of Mineral Processing, 84(1-4): 15-24.

Tajadod, J. and Yen, W.T., 1997a. A comparison of surface properties and flotation characteristics of enargite and chalcopyrite. Proc. of the XX IMPC, Aachen, Germany, 3: 409-418.

Tajadod, J. and Yen, W.T., 1997b. Arsenic content reduction in copper concentrates. Process. Complex Ores Miner. Process. Environ., Proc. UBC-McGill Bi-Annu. Int. Symp. Fundam. Miner. Process., 2nd: 153-164.

Tapley, B. and Yan, D., 2003. The selective flotation of arsenopyrite from pyrite. Miner. Eng., 16(11): 1217-1220.

Velásquez, P. et al., 2000b. SEM, EDX and EIS study of an electrochemically modified electrode surface of natural enargite (Cu3AsS4). Journal of Electroanalytical Chemistry, 494(2): 87-95.

Velasquez, P., Ramos-Barrado, J.R., Cordova, R. and Leinen, D., 2000a. XPS analysis of an electrochemically modified electrode surface of natural enargite. Surf. Interface Anal., 30(1): 149-153.

Welham, N.J., 2001. Mechanochemical processing of enargite (Cu3AsS4). Hydrometallurgy, 62(3): 165-173.

Woods, R., 2003. Electrochemical potential controlling flotation. International Journal of Mineral Processing, 72(1-4): 151-162.

Yen, W.T. and Tajadod, J., 2000. Selective flotation of enargite and chalcopyrite. Proceedings of the XXI International Mineral Processing Conference, B: B8a-49 - B8a-55.

Chapter III

The effects of X-ray irradiation and temperature on the formation and stability of chemical species on enargite surfaces during XPS

Chris Plackowski, Marc A. Hampton, Anh V. Nguyen, and Warren J. Bruckard

Published in Minerals Engineering, 2013, 45(0), 59-66.

1. Abstract

An investigation of the species present on the surface of natural enargite and the effects of X-ray radiation on the surface after electrochemical oxidation at pH 10 has been carried out using X-ray photoelectron spectroscopy. Surface species present on fractured and polished unoxidized enargite have been compared with those present on the polished surface after oxidation at pH 10. The effect of X-ray irradiation time as a function of temperature on the forms and intensities of the photoelectron signals from the enargite surface was studied. High BE components and shake-ups of the Cu 2p signals, characteristic of a copper (II) hydroxide surface layer, reduced in intensity with increasing X-ray exposure time. Associated changes in the relative concentrations of surface oxygen species were also observed. Comparing a surface exposed to X-rays at 35 °C with that maintained at -135 °C, temperature was shown to significantly influence the rate of change. The observed changes were evaluated in terms of a proposed two-stage mechanism involving the dehydration of $Cu(OH)_2$ to CuO, followed by photoreduction of CuO to Cu_2O. The photoreduction effects of X-ray irradiation should be significantly reduced by sample cooling for consistent analysis of the enargite surface using XPS.

Keywords: oxidation, surface, copper, sulfur, arsenic, sulfide, enargite

2. Introduction

In the flotation separation of enargite from other copper sulfides using conventional froth flotation processes, a better understanding of the surface electrochemistry of enargite is important if effective flotation separation techniques are to be developed. Previous research has shown that crude separation may be achieved using selective oxidation techniques, or through the use of pulp potential control (Huch, 1994; Fornasiero et al., 2001; Kantar, 2002; Guo and Yen, 2005; Smith and Bruckard, 2007). However, the fundamental mechanisms involved and the species present are not well understood. Of particular interest are the chemical species formed by oxidation of the mineral surface.

An understanding of surface oxidation, the species formed, and the nature of the surface layer also has implications for other approaches to arsenic reduction in the case of ores containing enargite. Hydrometallurgical approaches to removing arsenic have been shown to be effective (Balaz et al., 2000; Curreli et al., 2005). In addition, the surface species and formation of a surface layer are important considerations in the leaching of enargite in acid environments (Fantauzzi et al., 2007) where the release of arsenic can have serious environmental consequences.

A recent review of studies relating to the surface properties of enargite showed that formation of different species, including copper sulfate or hydroxide and elemental sulfur, on the mineral

surface has been variously identified. However, disagreement exists about the nature of the oxidation products formed and it is uncertain whether species such as copper hydroxide or oxide, or Cu(II) species associated with sulfate and chloride, are in fact the main oxidation products (Plackowski et al., 2012).

To better understand the formation of oxidation products on the surface of enargite at pH 10, oxidized and unoxidized enargite has been studied using X-ray photoelectron spectroscopy (XPS). An important issue in surface analysis by XPS is the potential for damage, or changes to the surface chemistry due to the conditions the sample is exposed to during XPS, to affect the measurement results.

The purpose of this study was to investigate the chemical species present on the surface of enargite after electrochemical oxidation in pH 10 solutions, and to study the chemical changes that take place during exposure to an ultrahigh vacuum (UHV) environment and X-ray irradiation during the XPS process. The two variables of particular significance are the period of time for which the specimen is exposed to the XPS analysis environment (UHV and X-ray irradiation), and the temperature during measurement. The expected effects are, a greater extent of reduction of unstable surface species with increasing exposure time, and stabilization of these species against photoreduction when the temperature is reduced with liquid nitrogen cooling.

In the study of mineral surface chemistry related to froth flotation separation, XPS is a widely used technique for the identification of surface chemical species. However it is known that exposure of a surface to the conditions that exist during measurement can alter its chemical composition (Larson, 1974; Skinner et al., 1996). At present no published work is available that specifically considers the effects of photoreduction during XPS measurements of the oxidized enargite surface. The present study seeks to investigate those effects and propose a means of minimizing their impact on measurement results.

3. Experimental

3.1. Materials

A high purity enargite (Cu_3AsS_4) sample was obtained from Wright's Rock Shop (USA) and analyzed by x-ray photoelectron spectroscopy (XPS) to confirm its chemical surface composition. X-ray diffraction (XRD) was used to determine its crystal structure and identify the mineral phases present. The predominant phase determined was enargite, Cu_3AsS_4 (Appendix 1), with no other phases detected. A resin mounted thin polished section was prepared with the mineral exposed on both sides, and mounted on a fabricated PVC sample holder. An insulated copper lead was attached to the lower surface using silver epoxy (ITW Chemtronics, USA) to ensure good electrical contact.

Prior to each measurement any pre-existing surface oxidation was removed by machine polishing sequentially with 9, 3 and 1 micron diamond suspensions (Dia-duo, Struers Australia) to ensure a fresh surface was exposed. The surface was then washed with ethanol (AR grade) and dried with high purity compressed nitrogen, then immediately placed in the electrochemical cell and an oxidizing potential applied. AR grade di-sodium tetraborate decahydrate (Scharlau Chemie S.A., Spain) and technical grade sodium hydroxide (Sigma-Aldrich, Australia) were used to prepare a pH 10.0 buffer solution (0.05 M). Water used in the experiments was freshly purified using a reverse osmosis RIO's unit and an Ultrapure Academic Milli-Q system (Millipore, USA). The Milli-Q water had a specific resistance of 18.2 $M\Omega cm^{-1}$.

3.2. Sample Preparation

The freshly polished mineral surface was prepared for XPS by electrochemical oxidation in a pH 10.0 buffer solution using an Asylum AFM electrochemical cell (Santa Barbara, USA) and a Gamry Reference 600 potentiostat (Warminster, U.S.A). The enargite working electrode was connected to the potentiostat working electrode cable by an insulated copper wire bonded to the sample by conductive silver epoxy (ITW Chemtronics, USA), while a platinum wire formed the counter electrode. An Ag/AgCl 3M KCl microelectrode (Microelectrodes Inc., USA) was used as the reference electrode.

In preparation for XPS, the sample was polished, washed with ethanol, dried with high purity nitrogen and immediately transferred to the electrochemical cell. The reference and counter electrodes were then attached to the cell, the enargite surface covered with buffer solution and the oxidizing potential initiated. All voltages are quoted with respect to the standard hydrogen electrode (SHE) unless otherwise stated. Surface oxidation was performed as a single step experiment using a constant potential of +869 mV applied for 30 min at 25 ^{o}C. This potential was selected as it has previously been shown to produce significant oxidation at the enargite surface (Guo and Yen 2008).

3.3. X-ray photoelectron spectroscopy

XPS measurements of the enargite surface oxidized using the experimental procedure described above were carried out to identify the chemical species formed, and the response to UHV and X-ray exposure. Data was acquired using a Kratos Axis ULTRA X-ray Photoelectron Spectrometer incorporating a 165 mm hemispherical electron energy analyzer.

The incident radiation was Monochromatic Al Kα X-rays (1486.6 eV) at 150 W (15 kV, 15 mA). Survey (wide) scans were taken at an analyzer pass energy of 160 eV and multiplex (narrow) high resolution scans at 20 eV. Survey scans were carried out over 1200-0 eV binding energy (BE) range with 1.0 eV steps and a dwell time of 100 ms. Narrow high-resolution scans were run with

0.05 eV steps and 250 ms dwell time. Base pressure in the sample analysis chamber (SAC) was $1.0x10^{-9}$ torr and during sample analysis $1.0x10^{-8}$ torr. The analysis depth of the sample surface is 5-7 nanometers, and detection limits range from 0.1 to 0.5 atomic percent depending on the element. The instrument work function was calibrated to give a BE of 83.96 eV for the Au $4f_{7/2}$ line for metallic gold and the spectrometer dispersion was adjusted to give a BE of 932.67 eV for the Cu $2p_{3/2}$ line of metallic copper. The Kratos charge neutralizer system was used on all specimens. Survey scan and high resolution analyses were carried out with an analysis area of 300 x 700 microns. Spectra have been charge corrected using the main line of the carbon 1s spectrum produced by surface deposition of adventitious hydrocarbon with an assigned BE of 284.8 eV as an internal reference. Spectra analysis and peak fitting was carried out using CasaXPS software (Version 2.3.14).

Conductive tape was used to secure the sample to a metal stub, which was then attached to the sample holder and inserted into the loading chamber. Where sample cooling was required, a cold probe was utilized to pre-cool the sample holder to liquid nitrogen temperatures before evacuation in the loading chamber of the XPS instrument. This procedure attempted to preserve volatile species on the surface of the samples. During initial cooling the chamber was continuously flushed with high purity dry nitrogen to remove moisture and oxygen. Once a temperature of -100 °C was reached the chamber was sealed and evacuation commenced. Once the required vacuum was reached it was then transferred to the SAC and attached to the pre-cooled sample stage, where it was maintained at -135 °C throughout the measurement. The surface was first analyzed by a single survey (wide) scan to identify the elements present, then multiplex (narrow) high resolution scans of each elemental region were carried out to identify the relative elemental concentrations as well as oxidation state and chemical bonding associations. High resolution scans were then repeated over time to quantify the chemical changes resulting from extended exposure to X-ray irradiation. Relative elemental atomic concentrations were determined by peak fitting using the CasaXPS software package and the Kratos library of sensitivity factors. XPS data for the Cu 2p, O 1s, C 1s, S 2p and As 3d regions were fitted using Shirley background subtraction and Gaussian-Lorenztian peak profiles. Two experimental conditions were compared, where measurements were carried out at 35 °C, and with sample cooling using a liquid nitrogen cooled cold stage (-135 °C) to preserve unstable surface species.

The XPS analysis of oxidized enargite has been shown to be dependent on the temperature at which it is carried out (Fantauzzi et al. 2006), as is the case for other sulfides (Hampton et al. 2011, Wittstock et al. 1996). At ambient temperature, the ultrahigh vacuum required during analysis ($1.0x10^{-8}$ torr) creates an environment where elemental sulfur formed on the surface is unstable and

quickly evaporates. In addition, it has been reported that Cu (II) species, in particular $Cu(OH)_2$, undergo a combination of vacuum and thermal dehydration and decomposition to CuO at ambient temperature (Skinner et al. 1996), typically found to be about 35 °C in the XPS sample analysis chamber. This effect can be controlled by pre-cooling the sample (below -130 °C) before evacuation thereby limiting evaporation of sulfur and decomposition of $Cu(OH)_2$ and other unstable compounds on the surface. Without cooling, elemental sulfur, if present on the surface, is quickly lost and not detected. Therefore, the sample was cooled in the loading chamber to below -130 °C prior to evacuation using a liquid nitrogen system, and maintained at that temperature in the SAC.

4. Results and Discussion

4.1. XPS of natural enargite surfaces: freshly polished surfaces and freshly crushed particles

Characterization of the natural enargite used for the study by XPS was completed to confirm its composition. Characteristic photoelectron spectra and peaks were detected for copper, arsenic and sulfur, as well as oxygen and carbon. The results of deconvoluting the obtained XPS spectra by peak fitting using the CasaXPS software package and Kratos element library are shown in Table 1 and the spectra in Appendix 2. The relative elemental atomic concentrations were found to be: Cu 2p 16.9 %, As 3d 5.0 % and S 2p 25.4 %. Compared to the stoichiometric ratio (Cu_3AsS_4), reasonable agreement was found. Specifically, normalizing with respect to copper gives a Cu:As:S ratio of 3:0.9:4.5, indicating a small arsenic deficiency, while the sulfur content is higher than the stoichiometrically expected value. Other elements detected were C 1s (40.2 %) and O 1s (12.5 %), of which the former has been used as an internal reference for charge correction as noted in Section 3.3. The high levels of C and O are indicative of surface contamination, due in part to adventitious hydrocarbons and possibly polishing compound residue and traces of epoxy resin transferred to the mineral surface during the polishing process. The photoelectron spectra for Cu $2p_{3/2}$ are shown in Figure 1, where the Cu $2p_{3/2}$ spectrum peak is situated at a BE of 932.0 eV.

Previous findings (Velasquez et al. 2000) have shown differences in BE between enargite surfaces prepared by fracturing or polishing, attributed to localized structural changes at the surface due to the polishing process. It was therefore important to establish that the polished surface was a suitable baseline from which the oxidized surfaces were prepared by applying +869 mV for 30 min at 25 °C and pH 10.

A freshly crushed enargite sample was prepared to expose unaltered mineral from the bulk, effectively creating a newly fractured surface. After crushing the enargite crystals in air using a mortar and pestle, the sample was immediately transferred to the XPS loading chamber to minimize

oxidation, and the measurement carried out. The photoelectron peaks for Cu $2p_{3/2}$ for both freshly crushed and polished surfaces compare well (Figure 1). The respective peak binding energies, full width half maxima, and atomic concentrations obtained with the freshly crushed sample are given in Table 2. Again, the results for the fractured sample show reasonable agreement with the stoichiometric formula of enargite, i.e. Cu_3AsS_4, with Cu 2p 28.1 %, As 3d 11.95 % and S 2p 35.43 %. A Cu:As:S ratio of 3:1.3:3.8 was found after normalizing with respect to copper, showing that the arsenic content of the mineral sample is slightly higher than the stoichiometric amount, while the content of sulfur is lower than expected. A single O 1s spectrum is located at 529.5 eV.

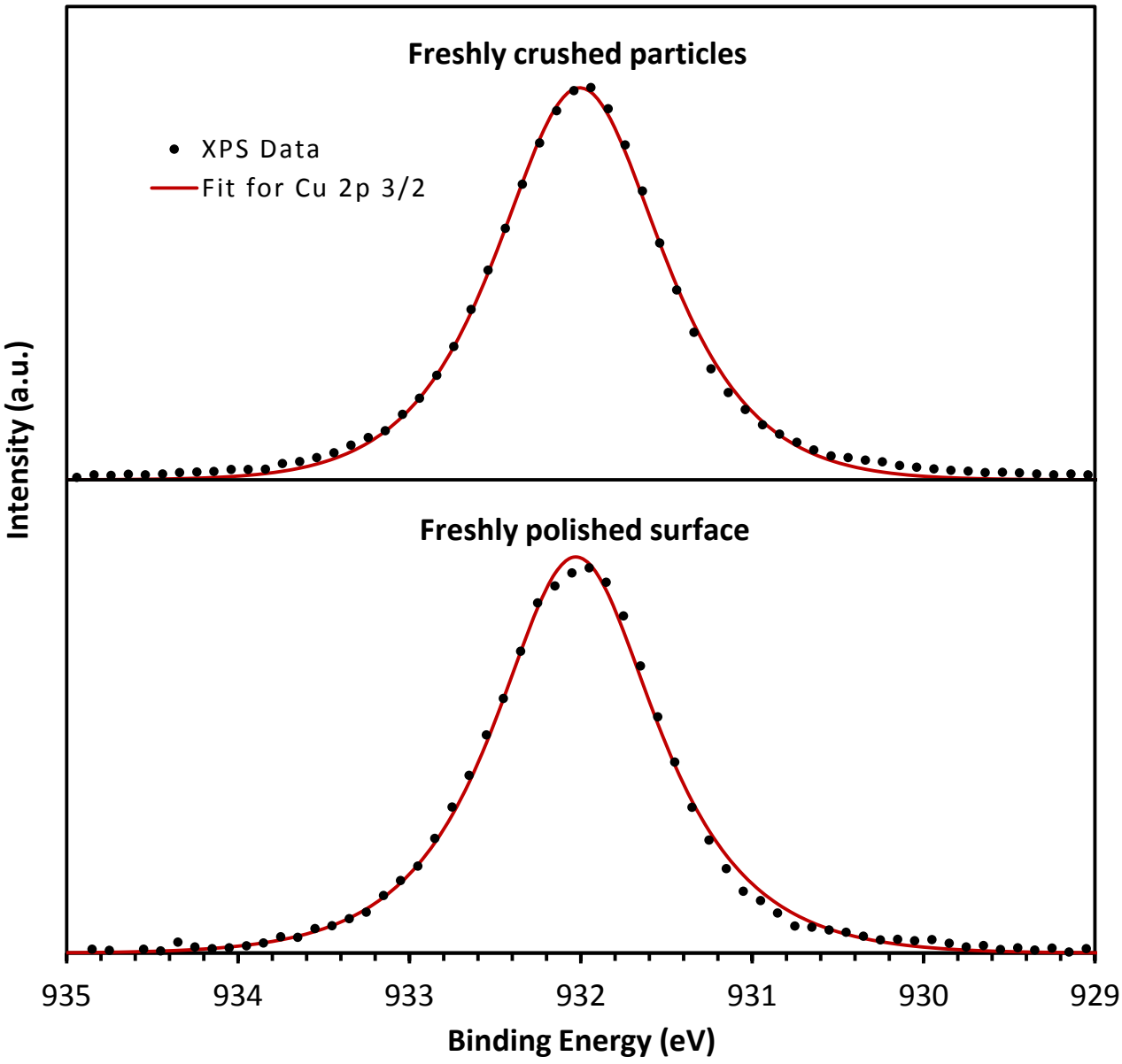

Figure 1. Comparison of Cu $2p_{3/2}$ photoelectron spectra recorded from the freshly polished enargite surface and freshly crushed enargite particles.

The S 2p spectrum for the fractured surface (Appendix 2) is resolved into a spin-orbit doublet, the components situated at binding energies of 161.8 and 162.99 eV for the S $2p_{3/2}$ and S $2p_{1/2}$ peaks respectively. In the case of polished enargite two sulfur species are evident, the S $2p_{3/2}$ components of which are situated at 161.7 and 162.9 eV. The As 3d spectrum for the bulk (fractured) enargite matrix is resolved with a spin-orbit doublet, the 5/2 component of which is located at 43.2 eV, and the low BE shoulder is resolved with another doublet, the 5/2 component at 42.3 eV. The result for polished enargite returns lower binding energies of 43.1 and 42.2 eV, respectively. Comparing the polished and fractured surfaces relatively little difference is seen, with a small (0.1 eV) shift of the As 3d and S 2p peaks to lower binding energies and peak broadening observed, however this small change can be within experimental error. Velasquez et al. (2000) reported such changes however, attributing the difference to changes of As and S co-ordination at the surface due to the polishing process.

Compared with the findings of Pratt (2004) in an XPS study of natural enargite, good agreement has been found for both fractured and polished natural enargite. Peak locations of the elements detected at the fractured surface differ by less than 0.2 eV from published data, and comparable results were obtained for the polished specimen. Analysis of a fractured sample of natural enargite by Velasquez et al. (2000) also demonstrates good agreement with the present work, where binding energies for Cu $2p_{3/2}$, As 3d, S 2p and C 1s of 932.4, 43.4, 162.1 and 284.8 eV respectively were found.

Table 1. Peak binding energies, full width half maximum (FWHM), and abundance (atomic %) of the chemical elements identified on the polished, untreated natural enargite surface.

Element	Position (eV)	FWHM (eV)	Atomic %
Cu 2p	932.0	1.1	16.9
S 2p 3/2	161.7	0.8	14.5
S 2p 1/2	162.9	0.9	7.3
S 2p 3/2	162.9	0.9	2.4
S 2p 1/2	164.1	0.9	1.2
As 3d 5/2	42.2	0.6	1.1
As 3d 3/2	42.9	0.6	0.7
As 3d 5/2	43.1	0.6	1.9
As 3d 3/2	43.8	0.6	1.3
O 1s	529.3	1.1	1.6
O 1s	531.0	1.3	1.1
O 1s	532.5	1.3	9.8
C 1s C-O	286.2	1.3	20.3
C 1s C-C ref	284.8	1.2	19.9

In the case of the polished sample a shift in the As 3d and S 2p peaks to 42.7 and 161.7 eV was found compared to the fractured sample. However the C 1s peak was recorded at 284.1 eV. No attempt was made to resolve the high resolution spectra of S 2p and As 3d into spin-orbit doublets.

The existence of two distinct contributions to the As 3d spectrum (Tables 1 and 2) is explained by Pratt (2004) as attributable to As in the bulk matrix (As $3d_{5/2}$ at 43.2 eV) and As atoms at the surface (As $3d_{5/2}$ at 42.2 eV). Rossi et al. (2001) reported binding energies of Cu $2p_{3/2}$, As $3d_{5/2}$ and S 2p as 932.5 ± 0.2, 43.9 ± 0.2 and 162.2 ± 0.2 respectively, for natural (as received), as well as natural and synthetic powdered enargite samples. In natural enargite the elemental oxidation states are copper as Cu (I), arsenic as As (V) and sulfur as S (II^-) (Cordova et al. 1997, Fullston et al. 1999, Pauporté and Schuhmann 1996, Pratt 2004, Velasquez et al. 2000).

Table 2. Peak binding energies, FWHM and abundance (atomic %) of the chemical elements identified from the freshly crushed (fractured) surface of enargite crystals.

Element	Position (eV)	FWHM (eV)	Atomic %
Cu 2p	932.0	1.1	28.1
S 2p 3/2	161.8	0.7	23.1
S 2p 1/2	163.0	0.8	12.3
As 3d 5/2	43.2	0.7	4.7
As 3d 3/2	43.9	0.6	3.1
As 3d 5/2	42.3	0.7	2.5
As 3d 3/2	43.0	0.6	1.7
O 1s	529.5	0.9	3.2
C 1s C-C ref	284.8	1.5	21.4

4.2. Electrochemically oxidized enargite surface at pH 10: XPS at 35 °C

After application of an anodic potential of +869 mV SHE at pH10 for 30 min the enargite surface was heavily oxidized, as shown in the first XPS sweep of Cu $2p_{3/2}$ (Spectra 1, Figure 2), by the formation of a Cu 2p spectra characteristic of Cu (II) species where the shake-up structure is clearly visible. These "shake-up" peaks occur as a part of the photoionisation process, which results in the emission of a photoelectron from an ion. It is possible that excitation by the outgoing photoelectron can leave the ion in an energy state a few eV above the ground state. As energy is transferred to the ion, the kinetic energy of the emitted photoelectron is reduced, and these low-energy electrons will be seen as a "shake-up" peak at a higher BE than the main peak.

In addition, a broadening of the As $3d_{5/2}$ peak and shift to 43.7 eV suggest As_2O_3 formation (Velasquez et al. 2000). A broadening of the S $2p_{3/2}$ peak such that three separate sulfur species can be identified, is also seen (Table 3). A new peak at 168.5 eV is also present, which is attributable

to the formation of $CuSO_4$ at the surface (Velasquez et al. 2000). The BE data for enargite at 35 °C is also contained in Table 3.

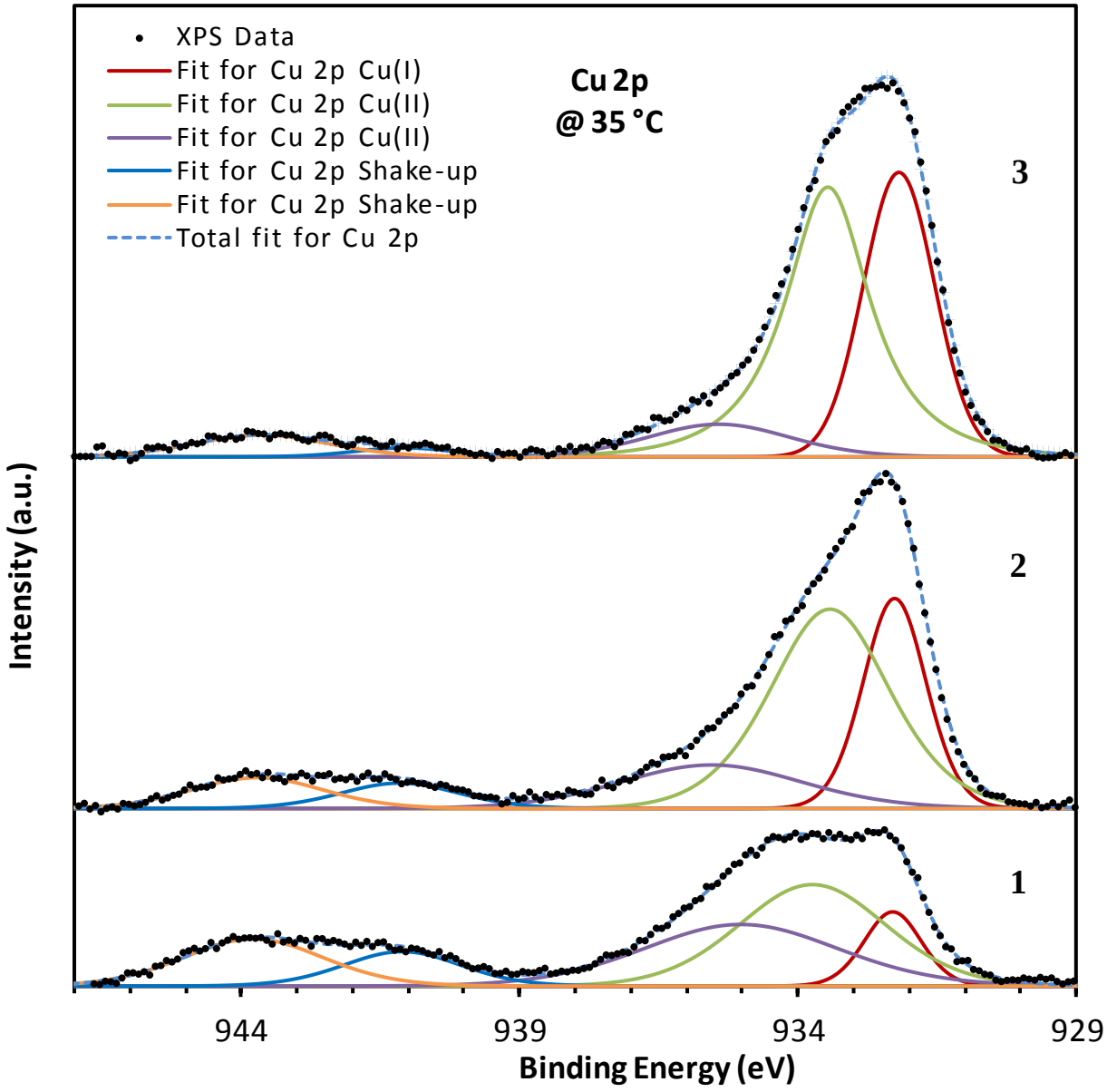

Figure 2. Effect of X-ray exposure time on Cu $2p_{3/2}$ photoelectron spectra recorded from the enargite surfaces oxidized by applying an anodic potential of +869 mV SHE for 30 min at pH10 and 25 °C. The XPS analysis was performed at 35 °C. Spectra 1 to 3 represent X-ray exposure times of approximately 20, 65 and 105 min, respectively.

Table 3. Binding energies for the elements Cu, As, S, C and O identified by XPS on unoxidized (reference) samples and on oxidized enargite at 35 °C.

	Unoxidized		Oxidized at +869 mV SHE		
Element	Fractured	Polished	Spectra 1	Spectra 2	Spectra 3
Cu 2p 3/2 (I)	932.0	932.0	932.3	932.3	932.2
Cu 2p 3/2 (II)			933.7	933.4	933.5
Cu 2p 3/2 (II)			935.0	935.6	935.4
Cu 2p (Shake-up)			941.1	941.2	941.1
Cu 2p (Shake-up)			943.8	943.7	943.7
S 2p 3/2 (1)	161.8	161.7	162.3	162.1	162.3
S 2p 1/2 (1)	163.0	162.9	163.4	163.3	163.5
S 2p 3/2 (2)		162.9	163.3	163.4	163.3
S 2p 1/2 (2)		164.1	164.5	164.6	164.5
S 2p 3/2 (3)			164.2	164.9	164.5
S 2p 1/2 (3)			165.4	166.1	165.6
S 2p SO_4			168.5	168.7	168.8
As 3d 5/2	43.2	42.2	43.7	44.2	44.7
As 3d 3/2	43.9	42.9	44.4	44.9	45.4
As 3d 5/2	42.3	43.1	45.1	46.0	46.6
As 3d 3/2	43	43.8	45.7	46.6	47.2
O 1s	529.5	529.3	531.1	531.0	531.0
O 1s		531.0	532.3	532.3	532.3
O 1s		532.5	534.4	534.0	533.8
C 1s C-O		289.2	286.3	286.2	286.0
C 1s C=O			288.0	287.9	287.6
C 1s C-C ref	284.8	284.8	284.8	284.8	284.8

Of the three species that appear to be present in the S 2p spectrum, the doublet fit to the low BE shoulder at 162.3 eV is indicative of the presence the copper monosulfide, CuS, or covellite, and the presence of this peak in combination with the Cu $2p_{3/2}$ peak at 932.3 eV provides good evidence for the formation of CuS, according to BE data published by Skinner et al. (1996).The other S $2p_{3/2}$ peaks are located at 163.3 and 164.2 eV. Based on their BE's it would appear reasonable for the peak at 163.3 eV to be assigned to metal-deficient sulfide or polysulfides (S_n^{2-}) which for the latter fall in the range 162.0-163.6 eV (Smart et al. 1999).

Fullston et al. (1999) used XPS to investigate the natural enargite surface after chemical oxidization at pH 11, and attributed a S 2p component identified at about 162 eV as indicative of metal deficient sulfide or disulfide. Although the oxidation mechanism is different and care is needed in applying this result to the present study, given that copper loss from the mineral is likely with electrochemical oxidation (Guo and Yen 2008) the presence of metal deficient species or disulfide should be considered. Although 162.1-162.3 eV found in the present work may seem too high to correlate with this result, Fullston et al. (1999) used C 1s at 284.6 eV as an internal

reference, which is 0.2 eV lower than the 284.8 eV used in the present work. Taking this into account reduces the difference, but further investigation is needed to confirm or otherwise the result before any conclusion can be made.

The nature of the S $2p_{3/2}$ species identified in the range 164.2-164.9 eV is not so clear. The BE is known to be characteristic of elemental sulfur, however this species is also known to be unstable under conditions of ultrahigh vacuum (UHV) as exist in the XPS sample analysis chamber, resulting in sublimation of this or other volatile compounds formed on the surface (Fantauzzi et al. 2006, Hampton et al. 2011, Wittstock et al. 1996). Given that it persists over an extended period of exposure to X-ray irradiation and UHV conditions, the possibility that it represents elemental sulfur can be discounted. However, it has been suggested that a S 2p peak at about 164 eV also corresponds to the formation of polysulfides (Buckley et al. 1994, Kartio et al. 1998, Wittstock et al. 1996), a more likely explanation.

4.3. Electrochemically oxidized enargite surface at pH 10: XPS under cryogenic conditions

When enargite oxidized under the same conditions is subject to repeated XPS measurements while maintained at -135 °C, the results are significantly different to that carried out at the ambient temperature of the SAC (35 °C). This will be discussed in more detail in Section 4.4. The fitted Cu $2p_{3/2}$ photoelectron peaks from five successive measurements are shown in Figure 3, while the resulting binding energies are presented in Table 4.

Electrochemical oxidation of enargite at pH10 was found to produce a surface that was heavily oxidized, shown by a Cu $2p_{3/2}$ spectra characteristic of the presence of Cu (II) species as demonstrated in Figures 2 and 3, and Tables 3 and 4, changes to the As 3d component indicative of As_2O_3 formation (Velasquez et al.2000a), a shift of the S $2p_{3/2}$ peak to 163.7 eV (Table 4), and the presence of a new peak at 168.8 eV, indicative of $CuSO_4$ formation. Taken together this data supports the formation of CuO, and $Cu(SO)_4$, and is in good agreement with the work of Velasquez et al. (2000). However in their work a relatively lower oxidizing potential of +745 mV was used, thus in this study, where a higher oxidizing potential of 869 mV was used, a relatively higher degree of oxidation is possible.

Fullston et al. (1999) also attributed a S 2p component identified in the range 163.5-164.2 eV as indicative of polysulfide. Again the oxidation mechanism is different to that used in this study but, as discussed previously, electrochemical oxidation resulting in copper dissolution from the mineral surface is likely (Guo and Yen 2008), resulting in a metal deficient surface.

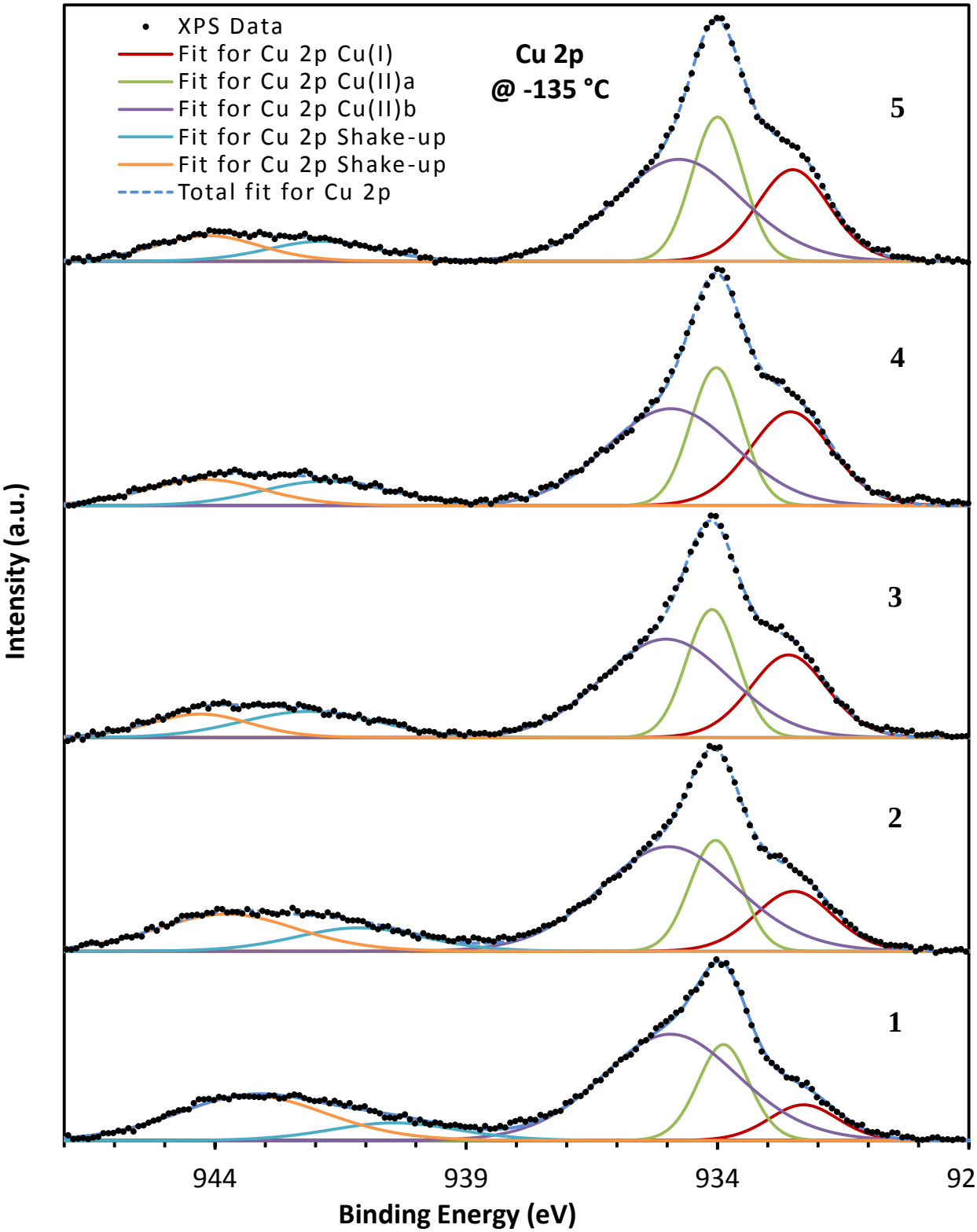

Figure 3. Effects of increasing X-ray exposure time on Cu $2p_{3/2}$ photoelectron spectra recorded from enargite surfaces oxidized by applying an anodic potential of +869 mV SHE for 30 min at pH10 and 25 °C. The XPS analysis was performed at -135 °C. Spectra 1 to 5 represent X-ray exposure times of approximately 24, 63, 105, 144 and 184 min, respectively.

Thus metal deficient sulfide and polysulfide species can occur and the latter can be ascribed to the BE range 163.7-163.8 eV found in the present work. The high BE of S $2p_{3/2}$ species identified in

the range 164.7-165.2 eV is more difficult to identify and although it could be ascribed to the presence of a form of polysulfide, the measured BE lies at the upper end of what would be expected.

Table 4. Peak binding energies for the elements Cu, As, S, C and O identified by XPS on unoxidized (reference) samples and on oxidized enargite with liquid nitrogen cooling (-135 °C).

	Unoxidized		Oxidized at +869 mV				
Element	Fractured	Polished	Spectra 1	Spectra 2	Spectra 3	Spectra 4	Spectra 5
Cu 2p 3/2 (I)	932.0	932.0	932.3	932.5	932.6	932.5	932.5
Cu 2p 3/2 (II)a			933.9	934.0	934.1	934.0	934.0
Cu 2p 3/2 (II)b			934.9	935.0	935.0	934.9	934.8
Cu 2p (Shake-up)			940.4	941.1	942.1	941.8	941.9
Cu 2p (Shake-up)			943.3	943.8	944.3	944.2	944.1
S 2p 3/2 (1)	161.8	161.7	163.7	163.8	163.8	163.7	163.8
S 2p 1/2 (1)	163.0	162.9	164.9	164.9	165	164.8	164.9
S 2p 3/2 (2)		162.9	164.7	165.1	165.2	165.1	165.2
S 2p 1/2 (2)		164.1	165.9	166.3	166.4	166.3	166.4
S 2p SO_4			168.8	168.8	168.9	169.0	169.2
As 3d (1)			45.5	45.6	45.6	45.4	46.8
As 3d (2)					47.1	46.9	45.5
As 3d 5/2	43.2	42.2					
As 3d 3/2	43.9	42.9					
As 3d 5/2	42.3	43.1					
As 3d 3/2	43	43.8					
O 1s	529.5	529.3	530.9	531.1	531.1	531	531.1
O 1s		531	532	532.1	532.1	532.1	532.2
O 1s		532.5	533	533.3	533.2	533.2	533.3
C 1s C-O		289.2	285.9	286	286.1	286.1	286.1
C 1s C=O			287.1	287.4	287.6	286.9	286.7
C 1s C-C ref	284.8	284.8	284.8	284.8	284.8	284.8	284.8

4.4. Photoreduction effects

In considering the effects of X-ray induced photoreduction of oxidation products on the enargite surface, copper-containing compounds are of principal interest. Comparison of the XPS results obtained at ambient temperature with those from the specimen analyzed using liquid nitrogen cooling shows that temperature has a clear effect on the resulting spectra recorded as a function of increasing X-ray exposure time. Figures 2 and 3 compare the Cu $2p_{3/2}$ photoelectron spectra for the two analysis temperature conditions as a function of X-ray exposure time. Clearly

the proportionate increase of Cu (I) species is more pronounced at 35 °C, and the rate of change is significantly greater (Table 3). The total X-ray exposure time represented by the Cu $2p_{3/2}$ photoelectron spectra in Figure 2 is 105 min, and over this time the atomic concentration of the Cu (I) species increased from 1.3 to 5.9 atomic %. In contrast, Figure 3 depicts the Cu $2p_{3/2}$ photoelectron spectra over a total exposure time of 184 min, where the proportion of Cu (I) was found to increase from 1.1 to 3.1 atomic %, while the total Cu (II) species varied between 8.6 and 9.4 atomic %. Table 5 depicts the atomic concentrations for all the elements detected. Copper is resolved into Cu (I), Cu (II) (low and high BE species) and total copper.

Table 5. Elemental atomic concentrations for the reference and oxidized enargite under different analysis temperature conditions. Concentrations of Cu (I) and Cu (II) (low and high BE) species are also shown.

	Atomic concentration (%)							
Element	Cu (I)	Cu (II)	Cu (II)	Total Cu	O 1s	C 1s	S 2p	As 3d
Fractured	28.1	-	-	28.1	3.2	21.4	35.4	11.9
Polished	17.0	-	-	17.0	12.4	40.2	25.3	5.2
35 °C Spectra 1	1.3	4.5	3.6	11.9	37.9	36.2	11.6	2.8
35 °C Spectra 2	4.1	7.9	1.2	14.9	35.9	33.2	12.6	3.4
35 °C Spectra 2	5.9	7.8	1.3	15.9	35.9	31.4	12.9	4.0
-135 °C Spectra 1	1.1	2.2	6.4	13.7	34.9	26.2	21.5	3.7
-135 °C Spectra 2	2.1	2.5	6.3	14.3	35.2	27.1	19.5	3.8
-135 °C Spectra 3	2.9	2.9	5.6	14.1	35.8	25.9	20.2	4.0
-135 °C Spectra 4	3.4	3.1	5.4	14.5	34.2	28.4	18.8	4.0
-135 °C Spectra 5	3.1	3.3	6.0	14.7	35.3	27.2	18.8	4.1

According to Skinner et al. (1996), sample degradation during XPS is a result of two factors that cause reduction of $Cu(OH)_2$ during prolonged X-ray exposure. The first is the dehydration and decomposition of $Cu(OH)_2$ to CuO due to exposure to UHV conditions and elevated temperature in the loading chamber and SAC. The first step of $Cu(OH)_2$ reduction can be represented by:

$$Cu(OH)_2 = CuO + H_2O \qquad [1]$$

The second step is the photoreduction of CuO to Cu_2O by X-ray exposure according to the following redox reaction:

$$4CuO = 2Cu_2O + O_2 \qquad [2]$$

According to this mechanism the presence of $Cu(OH)_2$ on the surface is expected. Identification of the Cu $2p_{3/2}$ peaks shown in Figure 2 according to binding energy (spectra 1) shows a minor peak at 932.3 eV, which can be ascribed to either Cu or Cu_2O (Table 6). The majority of the copper is represented by the peaks at 933.7 eV, which corresponds to CuO, and

935.0, likely to be $Cu(OH)_2$ although the BE is higher than those values in Table 6. Further support for $Cu(OH)_2$ is given by the presence of an O 1s peak (not shown) at 531.1 eV, which can also be ascribed to $Cu(OH)_2$ (Chawla et al. 1992, McIntyre and Cook 1975, Skinner et al. 1996). McIntyre et al. (1981) reported a Cu $2p_{3/2}$ photoelectron peak BE for $Cu(OH)_2$ as high as 935.1 eV. Thus the Cu (II) species identified in Table 4 ranging in BE from 934.8 to 935 eV can be ascribed to $Cu(OH)_2$. Published binding energies from several authors for a number of elements in different compounds, as summarized by Skinner et al. (1996) are presented in Table 6.

Table 6. Reported binding energies for the Cu $2p_{3/2}$, S 2p and O 1s XPS peaks for selected Cu (I) and Cu (II) oxides and sulfides (Skinner et al., 1996). The figures in brackets denote the respective FWHM for that photoelectron peak.

	Cu 2p3/2	S 2p	O 1s	Reference
Cu	932.5 (1.3)			Chawla et al. (1992)
	932.7			Deroubaix and Marcus (1992)
	932.5 (1.1)			McIntyre and Cook (1975)
Cu_2O	932.4 (1.5)		530.0 (1.8)	Chawla et al. (1992)
	932.5		530.4	Deroubaix and Marcus (1992)
	932.5 (1.5)		530.5 (1.2)	McIntyre and Cook (1975)
CuO	933.7 (3.2)		529.5 (1.6)	Chawla et al. (1992)
	933.6		529.6	Deroubaix and Marcus (1992)
	933.8 (2.9)		529.6 (1.3)	McIntyre and Cook (1975)
$Cu(OH)_2$	934.6 (3.9)		531.2 (2.2)	Chawla et al. (1992)
	934.4 (2.6)		530.9	McIntyre and Cook (1975)
	934.6 (3.0)		530.8 (2.2)	Skinner et al. (1996)
H_2O ads.			532.2	McIntyre et al. (1981)
			532.4	Pratt et al. (1994)
			532.5 (2.1)	Skinner et al. (1996)
Cu_2S	932.6 (2.0)	162.0		Nakai et al. (1978)
	932.6 (1.9)	161.7 (2.6)		Chawla et al. (1992)
	932.9	161.9		Deroubaix and Marcus (1992)
CuS	932.1 (2.6)	162.8		Chawla et al. (1992)
	932.5 (1.8)	162.4 (2.9)		Deroubaix and Marcus (1992)

From Tables 3 and 4, it can be seen that a number of copper species are present after oxidation, and their relative concentrations (atomic %), and therefore the predominant copper species, varies with increasing X-ray exposure time. Although the Cu (I) species remains consistent with an observed BE range of 932.2 to 932.7 eV, the Cu (II) species shows greater variability. The species with a BE of 933.6 ± 1 eV (Sweep 2, Table 3) has been reported as characteristic of CuO (Deroubaix and Marcus 1992, Larson 1974), as shown in Table 6, although there does not appear to be a corresponding O 1s peak which, according to values referenced by Skinner et al. (1996),

should be found around 529.6 eV.

The effects of liquid nitrogen cooling on the dehydration and photoreduction processes proposed by Skinner et al. (1996) are demonstrated by the photoelectron peaks for Cu $2p_{3/2}$ as a function of increasing X-ray exposure time, as shown in Figure 3. Clearly, there are both Cu (I) and Cu (II) species present; however, the changes seen in Figure 2 are greatly reduced when the sample is cooled. This can be seen in Figure 3 where, after nearly double the exposure time, very little change is evident. Comparing the data in Tables 3 and 4, the binding energies of the photoelectron peaks and the relative proportions of each species (Table 5) are reasonably constant at -135 °C, showing less variation compared to the data obtained from the analysis at 35 °C.

5. Conclusions

The effects of X-ray exposure over time as a function of temperature during the XPS analysis of natural enargite electrochemically oxidized at pH 10 have been investigated. The presence of $Cu(OH)_2$ on the surface after oxidation has been confirmed, and photoelectron peaks that can be ascribed to Cu_2O and CuO have been identified. The reduction of Cu (II) to Cu (I) species at 35 °C has also been confirmed by the change in Cu (I) to Cu (II) ratio from an initial value of 1:6.4 to a value after 105 min of X-ray exposure of 1:1.6. Additionally the Cu (II) photoelectron spectrum with its characteristic shake-up peaks is greatly reduced in intensity, indicative of the loss of Cu (II) species at the surface. In comparison, at -135 °C this ratio varies from 1:7.8 to 1:3.0 after 184 min.

These findings correlate with the mechanism proposed by Skinner et al. (1996) involving a two-stage process of decomposition or dehydration of $Cu(OH)_2$ to CuO due to heating effects of X-ray exposure and/or exposure to ultra-high vacuum effects, followed by photoreduction of CuO to Cu_2O. Reducing the surface temperature with liquid nitrogen cooling prior to evacuation and X-ray exposure reduces the reduction of Cu (II) significantly, further supporting the mechanism proposed by Skinner et al. (1996), where the reduction process can be limited by reducing the decomposition of $Cu(OH)_2$.

These results have significant implications where the quantitative surface analysis of copper sulfide minerals, and particularly measurement of surface oxidation species, is important. The XPS measurement process can alter the proportions of surface oxidation products significantly. This may result in an underestimation of the degree of oxidation and potentially failure to identify species that are important in the interaction of the mineral surface with other chemicals such as flotation reagents. The use of liquid nitrogen cooling to minimize degradation of surface oxidation products has been demonstrated as an effective means to enable accurate quantification of these chemical species, and permit extended multiple-element analyses to be completed.

Acknowledgments

The authors gratefully acknowledge the University of Queensland for an APA Scholarship and the CSIRO for scholarship (C.P.) and research expenses support. The authors acknowledge the facilities, and the scientific and technical assistance of the Australian Microscopy & Microanalysis Research Facility at the Centre for Microscopy and Microanalysis, The University of Queensland.

References

Buckley, A.N., Kravets, I.M., Shchukarev, A.V. and Woods, R. (1994) Interaction Of Galena With Hydrosulfide Ions Under Controlled Potentials. J. Appl. Electrochem. 24(6), 513-520.

Chawla, S.K., Sankarraman, N. and Payer, J.H. (1992) Diagnostic Spectra for XPS Analysis of Cu-O-S-H Compounds. Journal of Electron Spectroscopy and Related Phenomena 61(1), 1-18.

Cordova, R., Gomez, H., Real, S.G., Schrebler, R. and Vilche, J.R. (1997) Characterization of natural enargite/aqueous solution systems by electrochemical techniques. J. Electrochem. Soc. 144(8), 2628-2636.

Deroubaix, G. and Marcus, P. (1992) X-Ray Photoelectron-Spectroscopy Analysis of Copper and Zinc-Oxides and Sulfides. Surf. Interface Anal. 18(1), 39-46.

Fantauzzi, M., Atzei, D., Elsener, B., Lattanzi, P. and Rossi, A. (2006) XPS and XAES analysis of copper, arsenic and sulfur chemical state in enargites. Surf. Interface Anal. 38(5), 922-930.

Fullston, D., Fornasiero, D. and Ralston, J. (1999) Oxidation of synthetic and natural samples of enargite and tennantite: 2. X-ray photoelectron spectroscopic study. Langmuir 15(13), 4530-4536.

Guo, H. and Yen, W.T. (2008) Electrochemical study of synthetic and natural enargites. Proc. 24th Int. Miner. Process. Congr. 1, 1138-1145.

Hampton, M.A., Plackowski, C. and Nguyen, A.V. (2011) Physical and Chemical Analysis of Elemental Sulfur Formation during Galena Surface Oxidation. Langmuir 27(7), 4190-4201.

Kartio, I.J., Basilio, C.I. and Yoon, R.H. (1998) An XPS study of sphalerite activation by copper. Langmuir 14(18), 5274-5278.

Larson, P.E. (1974) X-Ray Induced Photoelectron and Auger-Spectra of Cu, CuO, Cu_2O, and Cu_2S Thin-Films. Journal of Electron Spectroscopy and Related Phenomena 4(3), 213-218.

McIntyre, N.S. and Cook, M.G. (1975) X-ray photoelectron studies on some oxides and hydroxides of cobalt, nickel, and copper. Analytical Chemistry 47(13), 2208-2213.

McIntyre, N.S., Sunder, S., Shoesmith, D.W. and Stanchell, F.W. (1981) Chemical Information from XPS - Applications to the Analysis of Electrode Surfaces. Journal of Vacuum Science & Technology 18(3), 714-721.

Nakai, I., Sugitani, Y., Nagashima, K. and Niwa, Y. (1978) X-Ray Photoelectron Spectroscopic Study of Copper Minerals. Journal of Inorganic & Nuclear Chemistry 40(5), 789-791.

Pauporté, T. and Schuhmann, D. (1996) An electrochemical study of natural enargite under conditions relating to those used in flotation of sulphide minerals. Colloids and Surfaces A: Physicochemical and Engineering Aspects 111(1-2), 1-19.

Pratt, A. (2004) Photoelectron core levels for enargite, Cu3AsS4. Surf. Interface Anal. 36(7), 654-657.

Pratt, A.R., Muir, I.J. and Nesbitt, H.W. (1994) X-Ray Photoelectron and Auger-Electron Spectroscopic Studies of Pyrrhotite and Mechanism of Air Oxidation. Geochimica Et Cosmochimica Acta 58(2), 827-841.

Rossi, A., Atzei, D., Da Pelo, S., Frau, F., Lattanzi, P., England, K.E.R. and Vaughan, D.J. (2001) Quantitative X-ray photoelectron spectroscopy study of enargite (Cu3AsS4) surface. Surf. Interface Anal. 31(6), 465-470.

Skinner, W.M., Prestidge, C.A. and Smart, R.S.C. (1996) Irradiation effects during XPS studies of Cu(II) activation of zinc sulphide. Surf. Interface Anal. 24(9), 620-626.

Smart, R.S.C., Skinner, W.M. and Gerson, A.R. (1999) XPS of sulfide mineral surfaces: Metal-deficient, polysulfides, defects and elemental sulphur. Surf. Interface Anal. 28(1), 101-105.

Velasquez, P., Ramos-Barrado, J.R., Cordova, R. and Leinen, D. (2000) XPS analysis of an electrochemically modified electrode surface of natural enargite. Surf. Interface Anal. 30(1), 149-153.

Wittstock, G., Kartio, I., Hirsch, D., Kunze, S. and Szargan, R. (1996) Oxidation of Galena in Acetate Buffer Investigated by Atomic Force Microscopy and Photoelectron Spectroscopy. Langmuir 12(23), 5709-5721.

Appendix 1

X-ray diffraction result obtained for the enargite sample

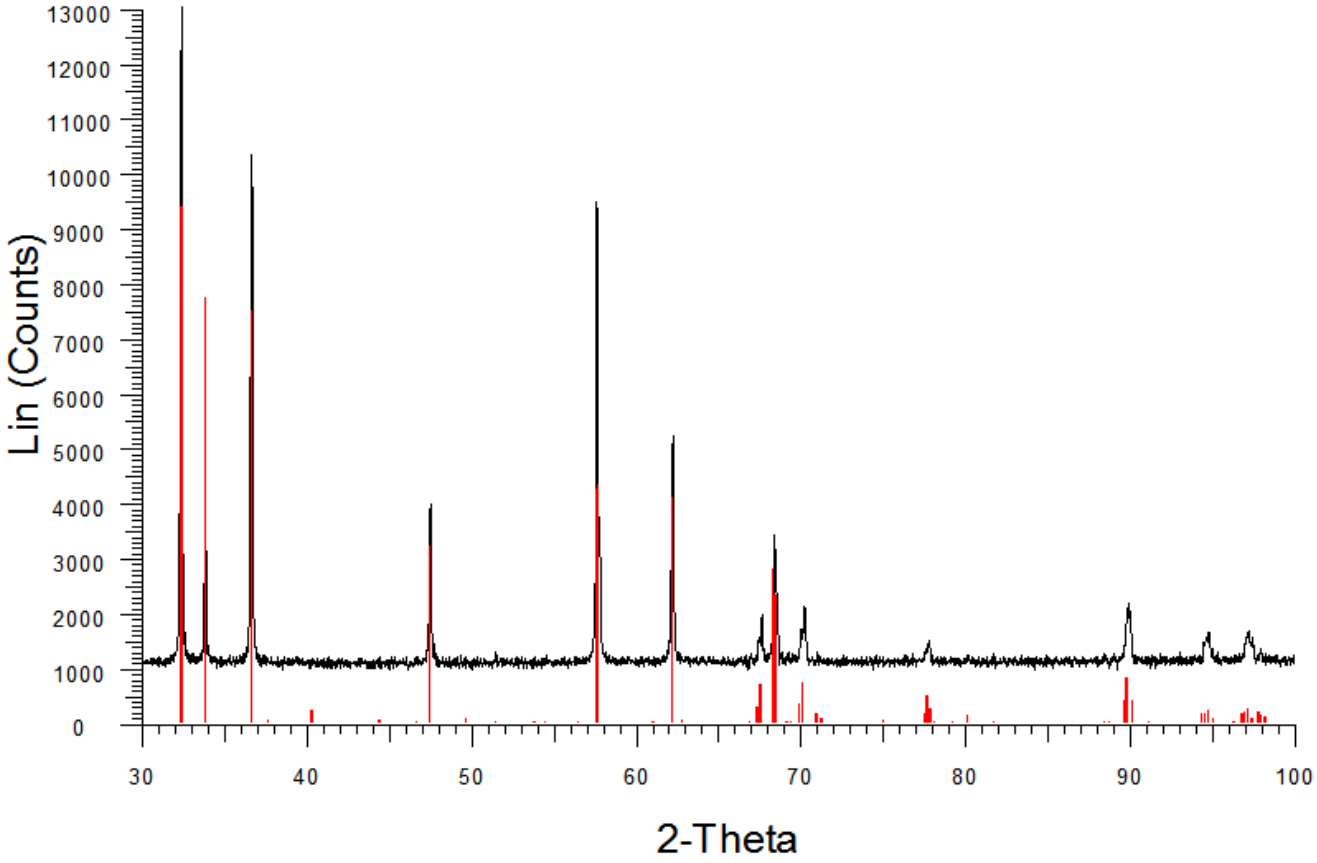

Figure 4. XRD analysis of the natural enargite used in the experimental work. The continuous trace represents the measured data while the individual peaks represent Pattern 03-065-1097 (A) - Enargite - $AsCu_3S_4$, incorporated in the Diffrac$^{(plus)}$ Evaluation Package Release 2009 and PDF-2 Release 2009 software package.

XRD analysis was performed on a natural enargite sample pulverized to a fine powder. The sample was analyzed in a Bruker Advance D8 X-Ray Diffractometer equipped with a LynxEye detector, Co tube radiation, and operated at 35 kV and 40 mA. Conditions of analysis are as follows:

- 30-100 degrees 2-theta
- 0.02 degree increment
- 1.2 s/step time per step
- 0.26 mm fixed divergence slit
- 5.0 mm fixed anti-scatter slit
- 68 min scan time

Traces were processed using the Diffrac$^{(plus)}$ Evaluation Package Release 2009 and PDF-2 Release 2009. X-ray diffraction analysis confirmed that the predominant mineral phase in the sample was enargite, Cu_3AsS_4, and no other phases were detected.

Appendix 2

XPS results for polished and fractured natural enargite

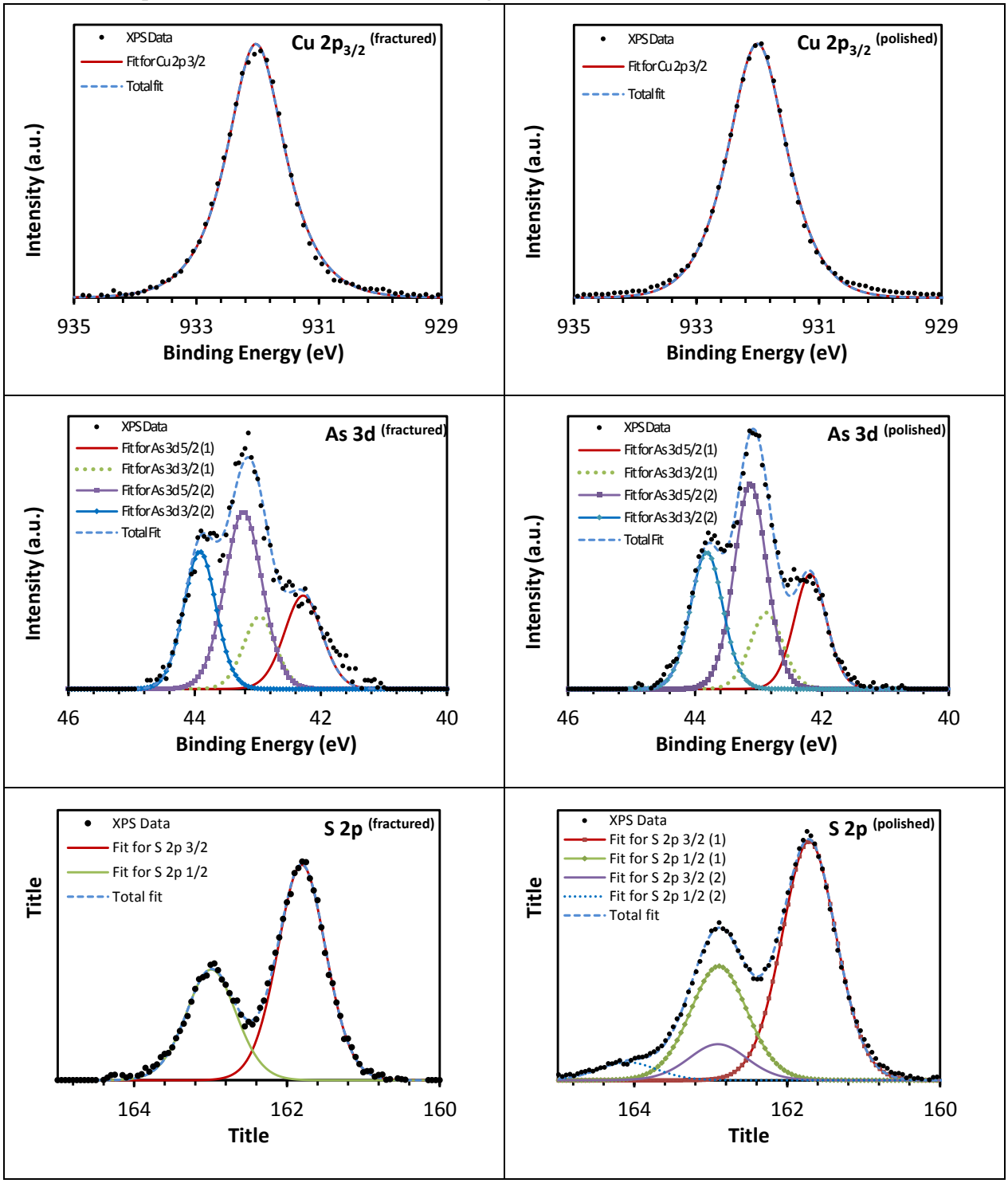

Figure 5. XPS spectra of Cu, As and S for fractured and polished natural enargite.

Chapter IV

Fundamental Studies of Electrochemically Controlled Surface Oxidation and Hydrophobicity of Natural Enargite

Chris Plackowski, Marc A. Hampton, Anh V. Nguyen, and Warren J. Bruckard

Published in Langmuir, 2013, 29(7), 2371-2386.

1. Abstract

The surface oxidation and hydrophobicity of natural enargite (Cu_3AsS_4), and formation of oxidation species at the mineral surface have been examined by a novel experimental approach that combines electrochemical techniques and atomic force microscopy (AFM). This approach allows for in-situ, synchronized electrochemical control and examination of the oxidative surface morphology of enargite. Combined with ex-situ cryo XPS surface analysis, the surface speciation of enargite surface oxidation has been obtained, comparing the newly fractured natural enargite surface with those which have been electrochemically oxidized at pH 4 and pH 10. At pH 4 surface layer formations consisting of metal deficient sulfide and elemental sulfur were identified, associated with a limited increase in RMS roughness (1.23 to 3.14 nm) and apparent heterogeneous distribution of surface products as demonstrated by AFM imaging. A mechanism of initial rapid dissolution of Cu followed by diffusion limited surface layer deposition was identified. At pH 10, a similar mechanism was identified although the differences between the initial and diffusion limited phases were less definitive. Surface species were identified as copper sulfate and hydroxide. A significant increase in surface roughness was found as RMS roughness increased from 0.79 to 9.72 nm. Dynamic (receding) contact angle measurements were obtained by a droplet evaporation method. No significant difference in the contact angle on a surface oxidized at pH 10, and the freshly polished surface was found. A significant difference was found between the polished surface and that oxidized at pH 4, with an increase in contact angle of about 13° (46° to 59°) after oxidation. Competing effects of hydrophilic (copper oxides and hydroxides) and hydrophobic (elemental sulfur) species on the mineral surface under oxidizing conditions at pH 4, and the change in surface roughness at pH 10, may contribute to the observed effects of electrochemically-controlled oxidation on enargite hydrophobicity.

Key words: Surface electrochemistry; flotation; enargite; AFM, contact angle, XPS

2. Introduction

Arsenic is a highly toxic inorganic pollutant, responsible for serious environmental and human health problems in several parts of the world. Specifically, arsenic emissions from downstream processing of arsenic-bearing minerals, such as smelting, must be captured and rendered inert for safe disposal. Such treatments are expensive and significant financial penalties are increasingly imposed to process smelter feeds containing typically more than 0.2wt% arsenic (Smith and Bruckard, 2007). Arsenic in the final copper product also decreases the value as arsenic is known to be detrimental to properties of copper metal such as electrical conductivity and

annealability, both of which are critical for electrical copper (Cordova et al., 1997, Biswas and Davenport, 1994).

Arsenic can occur naturally in elemental form, but more commonly as a compound in several mineral types which include copper arsenic sulfides such as enargite (Cu_3AsS_4) and tennantite ($Cu_{12}As_4S_{13}$), and associated arsenic-bearing minerals such as arsenopyrite (FeAsS). Enargite, which is the main form of copper arsenic mineralization in many deep epithermal copper-gold deposits, is commonly associated with copper sulfides such as chalcopyrite ($CuFeS_2$) and chalcocite (Cu_2S). All these minerals are significant in the formation of copper sulfide ore mineralization and are economically important sources of copper.

Since arsenic is a significant penalty element for base metal smelters, it is of economic interest to remove arsenic minerals during the metallurgical processes. There are significant economic advantages to achieving a separation of arsenic bearing minerals at an early stage of processing, but to date no feasible widely applicable commercial method of separation at the early (flotation) stage has been developed. In copper sulfide systems, one of the most problematic arsenic minerals is enargite which has surface properties suitable for air bubble attachment (Leja, 1982) and can be separated by froth flotation using air bubbles (Nguyen and Schulze, 2004). However, due to their similar flotation properties, enargite and most copper-bearing sulfides such as bornite, chalcocite and chalcopyrite are difficult to separate using conventional froth flotation processes. A better understanding of surface electrochemistry of enargite is important if effective separation techniques using flotation are to be developed. Previous research has shown that crude separation may be achieved using selective oxidation techniques (Guo and Yen, 2005), or through the use of pulp potential control (Senior et al., 2006). However, the fundamental mechanisms involved in these separations and the species present are not yet well understood. Oxidation and precipitation mechanisms have been proposed and argued. The present work seeks to contribute to a better understanding of the formation of oxidation products and the effects on the surface morphology of electrochemically controlled enargite at pH 10 and 4.

Although some promising studies have been completed on arsenic sulphide minerals (Senior et al., 2006, Bruckard et al., 2007, Smith and Bruckard, 2007, Bruckard et al., 2010), compared to other sulfide mineral types, relatively limited research has been carried out on the selective flotation of enargite and methods of achieving an effective separation from non-arsenic copper sulfides. An understanding of surface oxidation, the species formed and the nature of the surface layer also has implications for other approaches to arsenic reduction in the case of ores containing enargite. Hydrometallurgical approaches to removing arsenic, particularly leaching processes, have been shown to be effective (Balaz et al., 2000, Curreli et al., 2005). In addition the surface species and

formation of a surface layer are important considerations in the leaching of enargite in acid environments (Fantauzzi et al., 2007) where the release of arsenic can have serious environmental consequences.

A recent review of studies (Plackowski et al., 2012) relating to the surface properties of enargite showed that formation of different species including copper sulfate or hydroxide and elemental sulfur on the mineral surface could occur. However, disagreement exists about the nature of oxidation products formed and it is uncertain whether species such as copper hydroxide or oxide, or Cu^{2+} species associated with sulfate and chloride, are the main oxidation products (Plackowski et al., 2012).

Another review (Lattanzi et al., 2008) considered enargite oxidation both in the natural environment and laboratory setting. Oxidation was found to be a slow process, as evidenced by the low current densities seen in electrochemical oxidation. At low pH it was found copper dissolution accompanied by formation of elemental sulfur predominates. At high pH, Cu^{2+} species are evident along with oxides of arsenic, and formation of polysulfides, sulfite and sulfate as a result of sulfur oxidation, as shown by XPS studies.

The purpose of this study is to investigate the electrochemical characteristics of enargite using cyclic voltammetry (CV) and chronoamperometry (CA), to characterize the corresponding surface chemical changes by X-ray photoelectron spectroscopy (XPS), and examine morphological changes with atomic force microscopy (AFM). Contact angle measurements using a droplet evaporation technique are used to investigate surface hydrophobicity. Using this approach characterization of surface oxidation of natural enargite and correlation with surface hydrophobicity under the same conditions of applied potential has been achieved. In this way this study seeks to develop some insight into the mechanisms underlying the enargite surface oxidation and hydrophobicity, and inform the future development of various approaches to achieving selectivity in the separation by flotation of enargite and copper sulfide minerals.

3. Experimental

3.1. Materials

A high purity enargite sample was obtained from Wright's Rock Shop (USA) and analyzed by X-ray diffraction (XRD) using a Bruker Advance D8 X-Ray Diffractometer (Bruker AXS Inc., Madison, WI, USA) equipped with a LynxEye detector, Co tube and operated at 35kV and 40mA. Further conditions of analysis are available in the Supporting Information. The XRD analysis identified the predominant mineral phase to be enargite with no other phases detected. For the surface electrochemistry, AFM, and contact angle experiments, a resin mounted thin polished

section was prepared and attached to a fabricated PVC sample holder. An insulated copper lead was attached to the underside using silver epoxy (ITW Chemtronics, USA) to ensure good electrical contact. A fresh surface was created before each experiment by machine polishing with 9, 3 and 1 micron diamond suspension (Dia-duo, Struers Australia). The surface was then washed with ethanol (A.R. grade) and dried with high purity compressed nitrogen. The sample was then immediately placed in the electrochemical cell and the experiment initiated. AR grade di-sodium tetraborate decahydrate (Scharlau Chemie S.A., Spain) and technical grade sodium hydroxide (Sigma-Aldrich, Australia) were used to prepare a pH 10.0 buffer solution (0.05M). Acetic acid glacial (Rowe Scientific, Australia, purity min. 99.85% w/w) and sodium acetate (Sigma-Aldrich, Australia, ACS reagent, >99 %) were used to prepare a 0.1M pH 4 buffer solution. Water used in the experiments was freshly purified using a reverse osmosis RIO's unit and an Ultrapure Academic Milli-Q system (Millipore, USA). The Milli-Q water had a specific resistance of 18.2 $M\Omega cm^{-1}$.

3.2. Electrochemistry

The cyclic voltammetry (CV) experiments were performed with a freshly polished enargite sample in pH 10.0 and pH 4 buffer solutions using the Asylum AFM electrochemical cell (Santa Barbara, USA) and a Gamry Reference 600 potentiostat (Warminster, USA). The polished enargite section formed the working electrode, a platinum wire was used as the counter electrode and an Ag/AgCl 3M KCl microelectrode (Microelectrodes Inc., USA) was used as the reference electrode. All voltages are converted and reported relatively to standard hydrogen electrode (SHE).

In a typical experiment, the sample was polished, washed with ethanol, dried with high purity N_2 and immediately transferred to the electrochemical cell. The reference and counter electrodes were then attached to the cell, the enargite surface covered with buffer solution and the CV initiated. All experiments were conducted at a scan rate of 1 mV/s and initiated in the positive sweep direction. All CV curves were initiated from a potential of 0 mV at a sweep rate of 1 mV/s in the positive direction then switched back at 1100 mV to -690 mV, then terminated at 0 mV. Deoxygenation of the buffer solution and electrochemical cell was not considered necessary. The effects of oxygen on the cyclic polarization of synthetic enargite was investigated by Guo and Yen (2008), where almost identical results for oxygenated buffer compared to untreated and deoxygenated solutions were found. It was concluded that oxygen concentration does not have a significant effect on enargite cyclic polarization.

The chronoamperometry (CA) experiments were performed as a single step experiment at +610 mV (pH 4) and +869 mV (pH 10) where the desired potential was applied for 1800 s, using a freshly polished enargite surface immersed in a quiescent pH 10 or pH 4 buffer solution. These potentials were selected based on the CV data and represent the main anodic current peak for the

pH 4 system, and a sufficiently high potential to ensure significant surface oxidation for the pH 10 system.

3.3. Atomic force microscopy

AFM AC mode imaging was carried out using a MFP3D Asylum AFM (Asylum Research, CA, USA) using NT-MDT HANC High Accuracy Etalon cantilevers (NT-MDT, Russia) with a resonant frequency of 120 kHz and spring constant of 3.4 N/m. The sample was prepared and mounted as previously described and placed in an Asylum electrochemical cell supplied as an accessory for the AFM for imaging. Prior to imaging, the cantilevers were cleaned with ethanol and Milli-Q water then dried using high purity compressed nitrogen to ensure they were free from contamination.

The AFM was then set up, taking approximately 5 min before the first image at open circuit potential was initiated. Images were taken at a scan rate of 1.5Hz over an area of 2 μm^2. After the first image, the cantilever was disengaged, the potential was set and left for the desired interval before another image was taken. AFM images were processed using the Asylum in-built median filter (5x5 and 3 passes) to remove noise. No additional processing was necessary.

3.4. X-ray photoelectron spectroscopy (cold stage)

XPS measurements were performed to analyze an enargite surface oxidized using the same experimental procedure as the CA experiments (i.e. mimicking conditions of the AFM experiment) to identify the chemical species produced on the surface. Data was acquired using a Kratos Axis ULTRA X-ray Photoelectron Spectrometer (Kratos Analytical Ltd, Manchester, UK) incorporating a 165mm hemispherical electron energy analyzer. The incident radiation was Monochromatic Al Kα X-rays (1486.6 eV) at 150 W (15 kV, 15 mA). Survey (wide) scans were taken at an analyzer pass energy of 160 eV and multiplex (narrow) high resolution scans at 20 eV. Survey scans were carried out over 1200-0 eV binding energy range with 1.0 eV steps and a dwell time of 100 ms. Narrow high-resolution scans were run with 0.05 eV steps and 250 ms dwell time. Base pressure in the analysis chamber was $1.0x10^{-9}$ torr and during sample analysis it was $1.0x10^{-8}$ torr. Spectra analysis and peak fitting was carried out using CasaXPS software (Version 2.3.14). Atomic concentrations were determined using Shirley background subtraction and sensitivity factors provided by the Kratos library.

The analysis depth of the sample surface is 5 to 7 nm, and detection limits range from 0.1 to 0.5 atomic %, depending on the element of interest. The instrument work function was calibrated to give a BE of 83.96 eV for the Au $4f_{7/2}$ line for metallic gold and the spectrometer dispersion was adjusted to give a BE of 932.67 eV for the Cu $2p_{3/2}$ line of metallic copper. The Kratos charge

neutralizer system was used on all specimens. Survey scan and high resolution analyses were carried out with an analysis area of 300 μm x 700 μm. Spectra have been charge corrected using the main line of the carbon 1s spectrum produced by surface deposition of adventitious hydrocarbon with an assigned BE of 284.8 eV as an internal reference.

The XPS analysis of oxidized enargite is very much dependent on the temperature at which it is carried out (Fantauzzi et al., 2006), as found for other sulfides (Wittstock et al., 1996, Hampton et al., 2011). If carried out at ambient temperature, the ultrahigh vacuum required during analysis ($1.0x10^{-8}$ torr) results in sublimation of any elemental sulfur or other volatile compounds formed on the surface. However, where the sample was pre-cooled (below -130 °C) before evacuation of the chamber, these compounds remained on the surface and could be detected. Therefore, the sample was cooled in the loading chamber to below -130 °C with liquid nitrogen prior to evacuation, and maintained at that temperature in the sample analysis chamber. Conductive tape was used to attach the sample to a metal stub, which was then quickly inserted into the loading chamber onto a pre-cooled sample holder and the chamber evacuated. Once the required vacuum was reached it was then transferred to the analysis chamber and attached to the pre-cooled sample stage.

3.5. Surface hydrophobicity and contact angle

The change in the enargite surface hydrophobicity with oxidation was measured directly using the sessile droplet evaporation method (Nguyen et al., 2012) whereby a water droplet was placed directly on the mineral surface and allowed to evaporate in a controlled (unsaturated) humidity environment. The transient (receding) contact angle and/or contact base radius were determined from the droplet shape/volume transiently reduced by diffusion-limited evaporation. Experimentally, the polished enargite sample was first placed in a sealed box containing a saturated magnesium nitrate solution (to control the relative humidity inside the box to 53 ± 1 %). To initiate the experiment a 0.5 μL droplet of Milli-Q water was placed on the surface using an Eppendorf pipette (Eppendorf Research, Germany). A progressive scan CCD camera (model XCD-SX910, Sony, Japan) fitted with a 10x magnification objective lens (Nikon, Japan) was used to capture video images of the evaporating droplet at a frame rate of 1.875 fps. A fiber light with diffuser was used to illuminate the droplet from behind. The video was then extracted into single images using the Photron Fastcam Viewer 3 software package and further analysis completed using in-house Matlab code for the given droplet parameters and dimensions. Since the diameter of all water droplets used in this study was much smaller than the capillary length (2.7 mm), the sessile droplets were subject to negligible deformation by gravity. The resulting shape was that of a spherical cap and the detected droplet profiles were well fitted to a circle. The droplet contact angle and contact radius were calculated using the fitted droplet profiles.

4. Results

4.1. Surface electrochemistry

Typical cyclic voltammetry (CV) curves for pH 10 and 4 for freshly polished natural enargite are shown in Figure 1. The results are similar to those of Guo and Yen (2008, 2006) who compared natural and synthetic enargite at pH 10, and Velasquez et al. (2000) and Cordova et al. (1997) who investigated natural enargite at pH 9.2. Small differences between the current CV results and the published data are likely due to variation in sample composition including type and concentrations of impurities present, sample preparation and experimental technique.

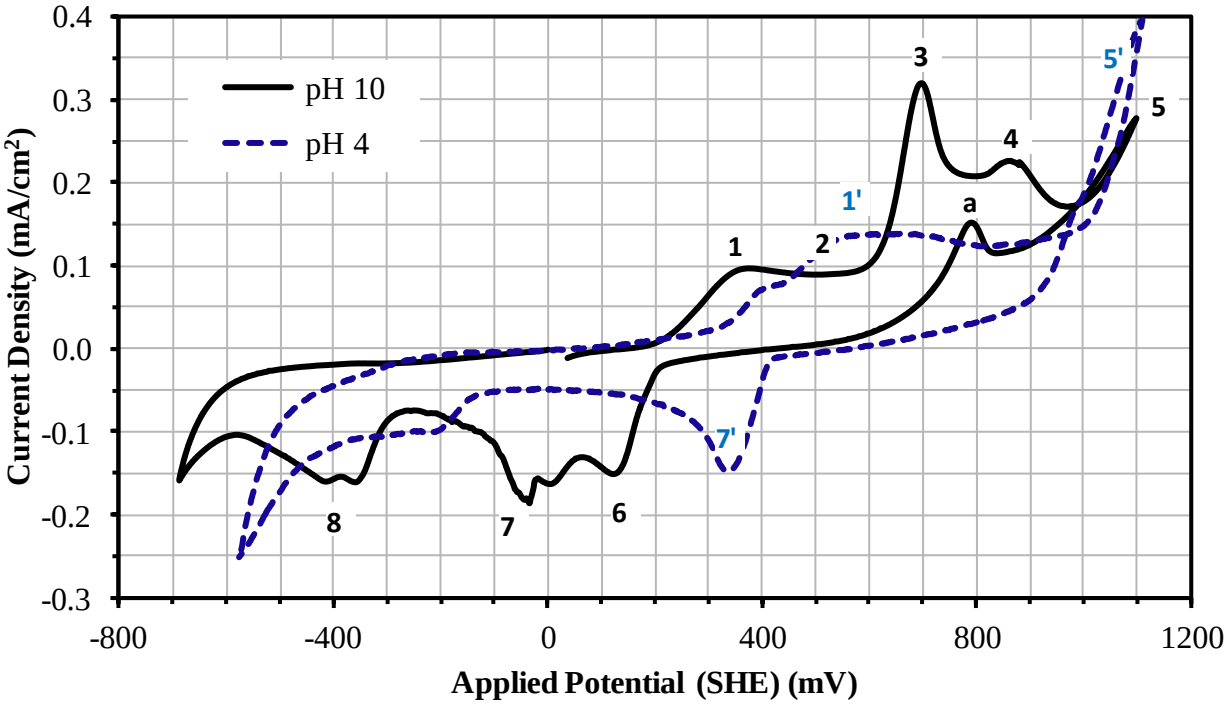

Figure 1. Typical cyclic polarization curves for natural enargite at pH 10 (black, solid line) and 4 (blue, dashed line) obtained using a scan rate of 1 mV/s. The curves were initiated at 0 mV in the anodic direction, returned to the cathodic scan at 1100 mV to -590 (pH 4) or -690 (pH 10) mV, and terminated at 0 mV.

Considering the anodic scan at pH 10 shown in Figure 1, five current peaks can be identified at potentials of 347 (peak 1), 516 (peak 2), 705 (peak 3), 869 (peak 4) and 1100 (peak 5) mV. Whether there is a peak at 516 mV is not clear from the figure however, examination of the numerical data does indicate a local current maximum at this potential. There are also a few current peaks on the cathodic scan at pH 10, namely, 100 mV (peak 6), -100 mV (peak 7) and -400 mV (peak 8). An additional peak at about 790 mV is observed on the return sweep from 1100 mV in the oxidative range that was not found by Guo and Yen (2008). It is possible that its existence is due to

the continuation of incomplete reaction processes taking place at potentials around 800 mV during the forward potential sweep. The relatively high current density observed at peak 3 in the positive sweep direction suggests greater reactivity at this potential which, even at the low sweep rate of 1 mV/sec used in the CV does not reach equilibrium.

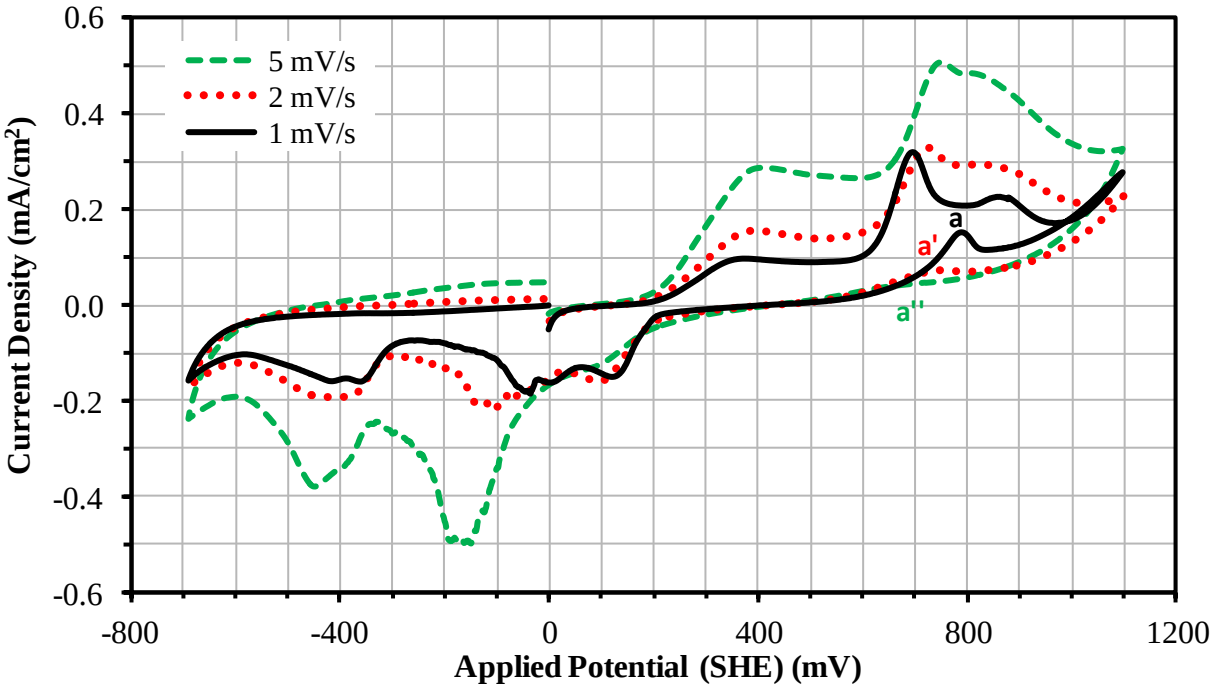

Figure 2. Effect of scan rate on natural enargite cyclic polarization at pH 10.

When the pH is reduced to 4 the peak at 347 mV is shifted upscale to 400 mV while the individual oxidative peaks seen at pH 10 (peaks 2-4) are no longer apparent and have become merged into a single broad peak, similar to the findings of Guo and Yen (2008). Analysis of the numerical data indicates a current peak at 610 mV (peak 1', highlighted in blue), which is the most significant change at pH 4. The cathodic scan at pH 4 also displays a current peak at 420 mV (peak 7') and -200 mV.

Investigation of the effects of scan rate, shown in Figure 2, demonstrates that the presence of a peak (labeled a) in the oxidative range of the return sweep is related to rate. The peak is clearly present at a scan rate of 1 mV/s, greatly diminished at 2 mV/s, and no longer discernible at 5 mV/s, as shown in Figure 2. The nature of the chemical reaction taking place at this point in the cyclic polarization at 1 mV/s was investigated further by XPS measurement of a surface prepared by applying a cyclic polarization with an initial potential of 0 mV, anodic scan limit of 1100 mV, and terminating at a final potential of 790 mV. The surface species identified are discussed in Section 4.3. These results also support the findings of Guo and Yen (2008), where increasing scan rate was

found to increase measured current density, and cause a broadening of some peaks without affecting the commencement point. However, the focus of this study is not to quantify the effects of scan rate on surface reactivity and speciation, and the limited investigation of these effects is intended only to acknowledge their existence, and enable some understanding of the potential cause of the current peak observed on the return sweep at 790 mV, the presence of which has been shown to be related to scan rate.

The CA experiments (Figure 3) focused on selected potentials based on the CV results. A potential of 610 mV (pH 4) was selected since it represents the highest current density in the oxidative range and therefore could be expected to result in a greater degree of change at the mineral surface. At pH 10 a current of 869 mV was selected to correspond to the fourth peak identified in the cyclic polarization studies. The purpose in selecting this value was to ensure the use of an applied potential sufficiently high in the anodic range to produce significant oxidation at the mineral surface. According to Guo and Yen (2008) at this potential enargite is oxidized to form a copper deficient surface with the formation of copper hydroxide, oxides of arsenic and elemental sulfur, suggesting the formation of a surface layer structure which may affect the rate of reaction at the surface. The chronoamperometry results (Figure 3) indicate that current decay characteristic of the formation of a passivating surface layer occur, where the initially high current in the CA falls rapidly then tends towards a constant or slightly decreasing value over time (Nava et al., 2002, Biegler and Swift, 1979). To confirm the changes in morphology at the surface, AFM was used to image the oxidizing surface *in-situ*.

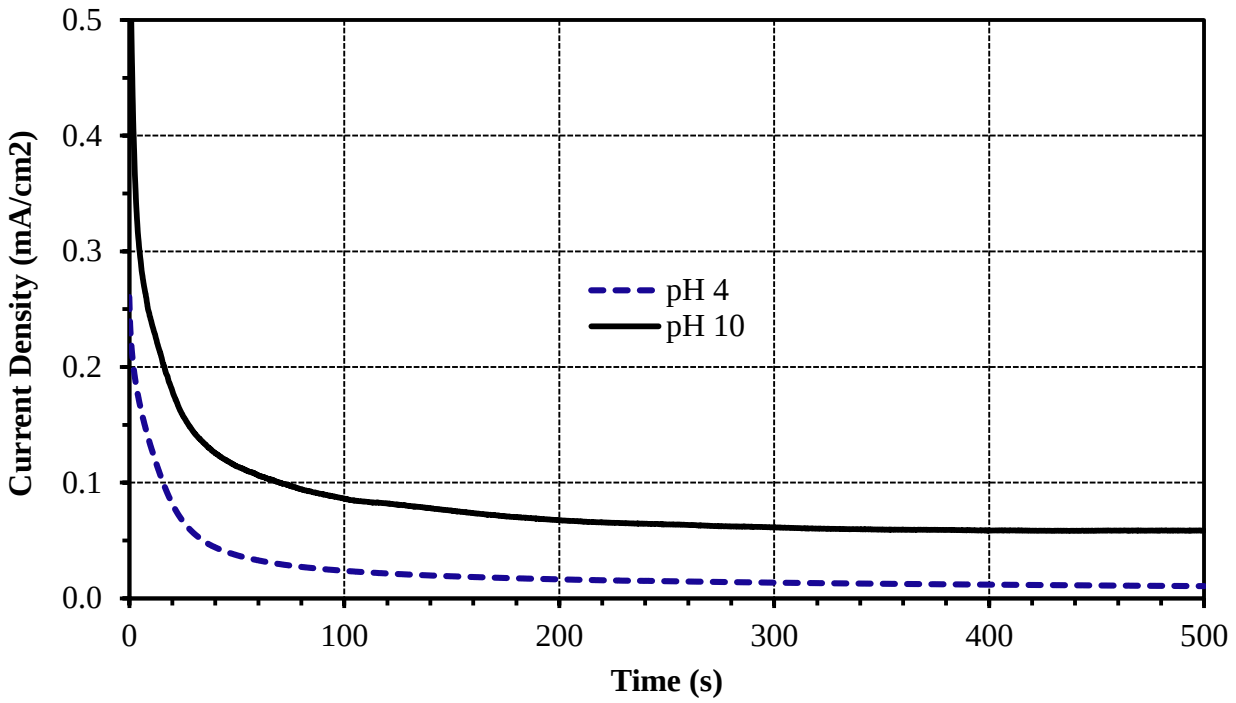

Figure 3. CA of enargite in pH 10 and pH 4 buffers performed using a freshly polished mineral surface. The time is offset to when the potential was applied.

4.2. Atomic force microscopy

AFM imaging was carried out to visualize the morphological changes taking place at the surface and develop some understanding of the mechanisms of mineral surface dissolution and precipitation of a surface layer. For this purpose a relatively high oxidizing potential of 869 mV (pH 10) was considered suitable to demonstrate these changes. At pH 4 a potential of 610 mV was selected. The changes in surface morphology over time are shown in Figure 4, where a freshly polished surface is compared before and after oxidation. Figure 4 (images **a** & **f**) shows the surface before oxidation while images **b** to **e** depict oxidation times of 2.5, 5, 10 and 30 minutes at 869 mV and pH 10, while images **g** to **j** show the surface after the same oxidation times at 610 mV and pH 4. The images in Figure 4 demonstrate the surface morphological changes observed over a 2 x 2 µm area.

Considering oxidation at pH 10 the initial changes depict a roughening and loss of surface detail where previously clearly visible surface scratches caused by polishing become less obvious (Figure 4b). This is thought to represent the initial rapid dissolution of Cu from the surface, and the beginning of surface layer deposition, represented by the initially high but rapidly declining current seen in the CA results (Figure 3).

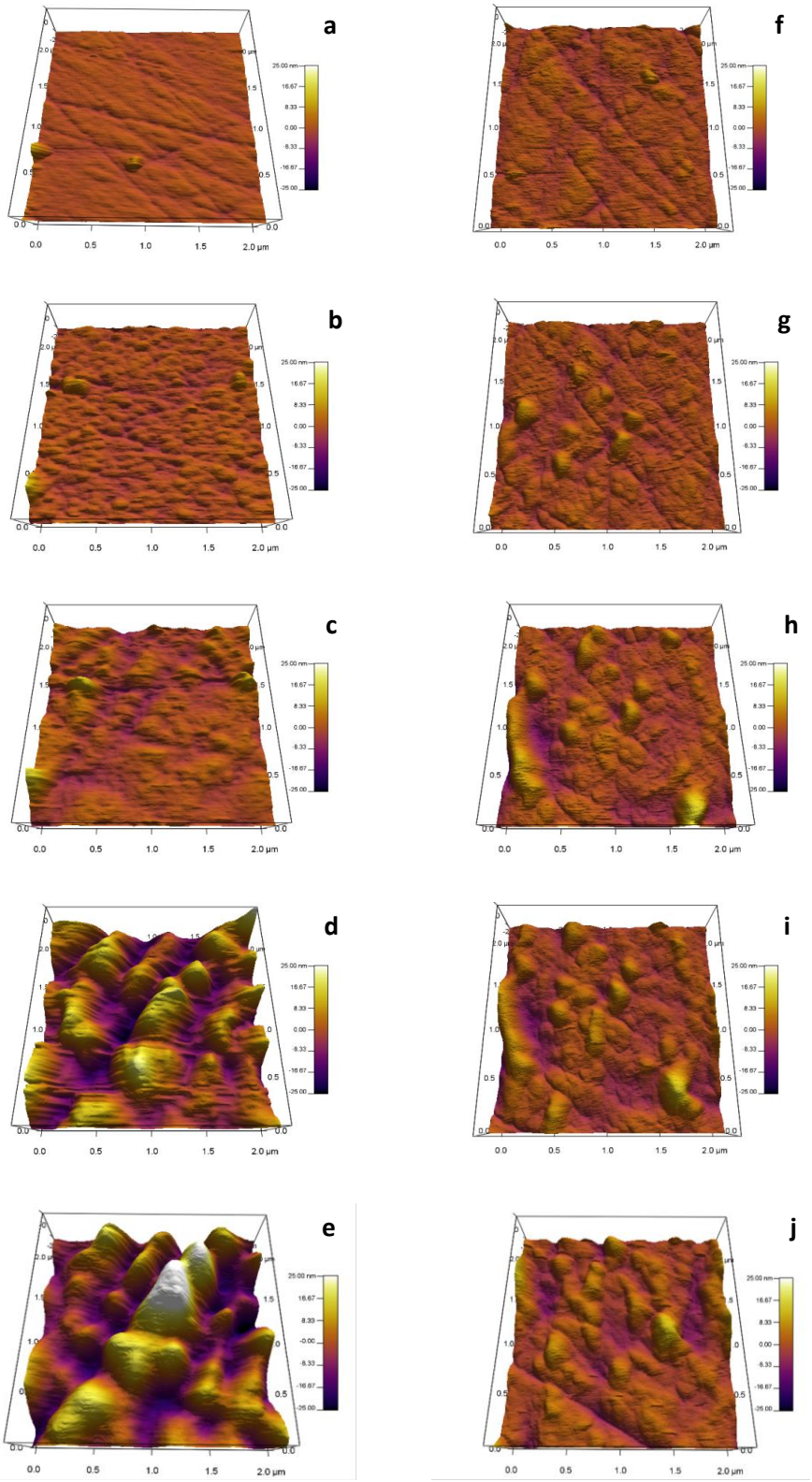

Figure 4. AFM images of a freshly polished enargite surface (**a** & **f**) and the same surface after oxidation at an applied potential of 869 mV at pH 10 (**b** to **e**) and 610 mV at pH 4 (**g** to **j**) for 30 min.

As oxidation progresses the formation and growth of surface structures becomes apparent. There does not appear to be an obvious pattern of formation of individual nucleation sites from which surface layer growth originates, but rather development of a continuous although uneven surface layer. As oxidation continues beyond 5 minutes the surface topography changes significantly, as greatly increased surface roughness becomes apparent. These images can be interpreted to show a combination of surface dissolution, and deposition and growth of surface species in a discontinuous layer. Thus the processes of dissolution and deposition occur together, and as oxidation progresses lateral growth of the deposits progressively decreases the area available where dissolution can occur. This is in agreement with the pattern of current decay in the CA experiments where the rapid decrease in initial current to a non-zero value suggests the formation of a porous or discontinuous surface layer. Further consideration of the chemical species present and the mechanisms of formation will be considered in later sections.

Oxidation at pH 4 produces a surface morphology that is significantly different to that seen at pH 10. The CA results show that an initially high current decays rapidly to a level significantly below that occurring where oxidation takes place at pH 10, and this behavior is indicative of the formation of a layer structure that inhibits diffusion. This is supported by the AFM images which demonstrate the formation and growth of a layer over the surface, which appears to form as dissolution of the surface is taking place, evident by progressive loss of the surface detail previously seen on the un-oxidized surface.

There also appear to be localized areas of surface deposition, seen as isolated domains of preferential growth on the surface which increase in size over time. These formations are similar to those described by Wittstock et al. (1996) and are thought to be deposits of elemental sulfur. The chemical evidence for sulfur formation and proposed mechanisms will be explained in later sections. The exact reason why the sulfur deposits form preferentially in certain areas is thought to be due to the presence of impurities and/or crystal defects. It is obvious from the AFM imaging that the occurrence of oxidation over the enargite surface is not homogeneous. The preferential spatial location of the domains indicates that sulfur formed during the oxidation process is released into solution from the surface and redeposited at favorable sites. However these domains remain relatively small and isolated and the formation of a surface layer by the nucleation, growth and overlap of discrete domains is not supported.

4.3. X-ray photoelectron spectroscopy

4.3.1. Crushed Natural Enargite

XPS was first used to characterize the natural enargite used for the study and confirm its composition. The sample was prepared by crushing a freshly cleaved fragment of natural enargite to a fine powder, which was then immediately transferred to the loading chamber and evacuation commenced. The sample analysis chamber was maintained at room temperature throughout the measurements.

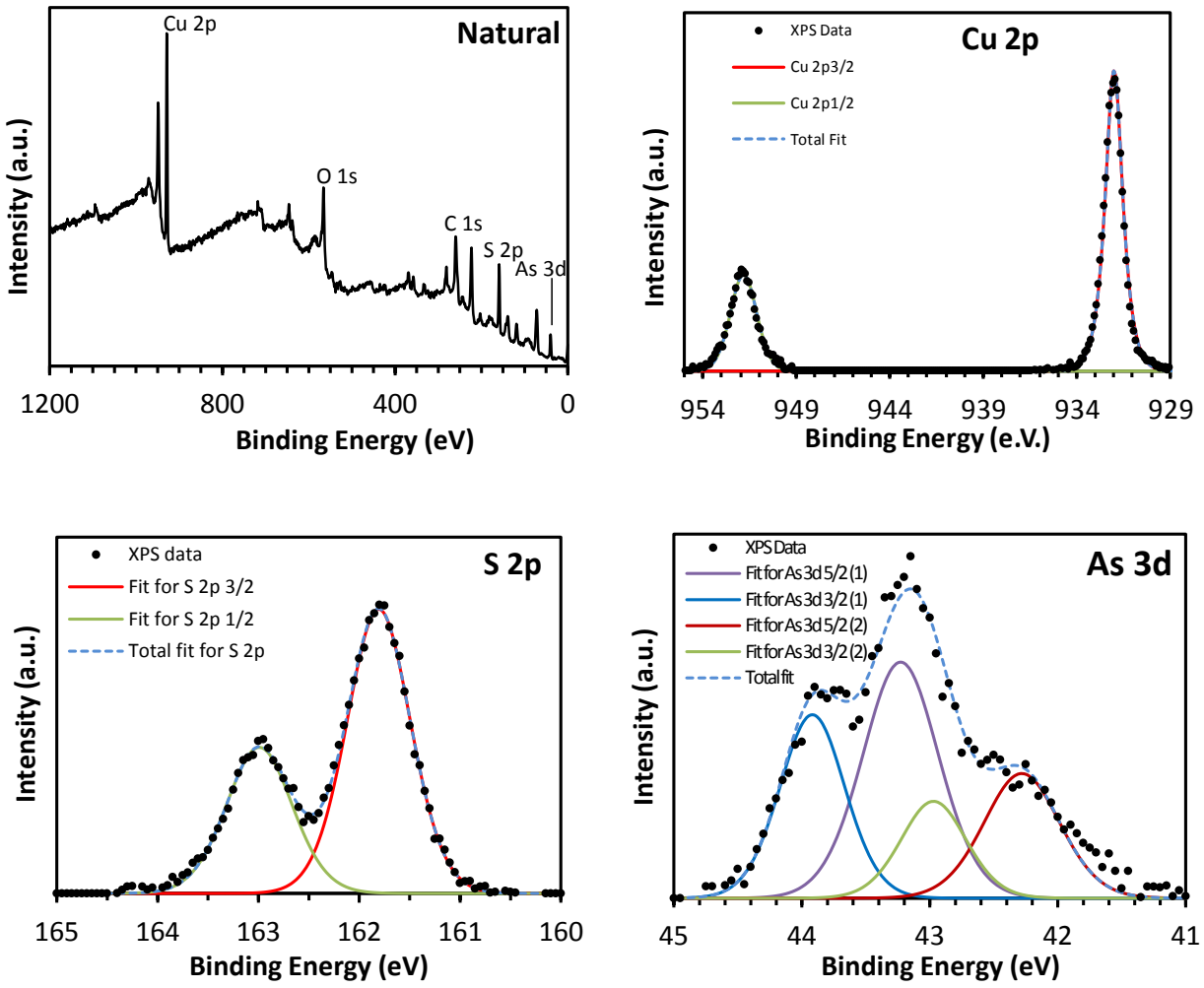

Figure 5. Survey and high resolution photoelectron spectra recorded from the fractured surface of natural enargite prepared by crushing an unoxidized crystalline sample to a fine powder.

Characteristic photoelectron peaks were detected for copper, arsenic and sulfur, as well as oxygen and carbon. The relative atomic concentrations of all elements (Table 1) show small deviations with respect to the stoichiometric formula of enargite, i.e. Cu_3AsS_4, with concentrations of Cu 2p 28.1%, As 3d 11.9% and S 2p 35.5r% detected. Normalizing with respect to copper gives a Cu:As:S ratio of 3:1.3:3.8 which indicates that the content of arsenic contained in the mineral

sample is slightly higher than the stoichiometric content, while the content of sulfur is a little bit lower than the stoichiometrically expected value. Other elements detected include (O 1s 3.19%) and C 1s (21.35%), of which the latter is used for charge correction.

Shown in Figure 5 is the photoelectron spectrum of the survey scan and high resolution photoelectron spectra for Cu 2p, S 2p and As 3d. The Cu $2p_{3/2}$ spectrum peak is situated at a binding energy of 932.0 eV. The S 2p spectrum is fit with one spin-orbit doublet situated at binding energies of 161.8 and 162.99 eV for the S $2p_{3/2}$ and S $2p_{1/2}$ peaks, respectively.

The As 3d spectrum for the bulk enargite matrix is fitted with a spin-orbit doublet, the 5/2 component located at 43.2 eV, and the low binding energy shoulder is fitted with another doublet with the 5/2 component at 42.3 eV. A single O 1s spectrum (not shown) was located at 529.5 eV while the position of each peak has been corrected to account for charging effects by reference to the C 1s spectrum which has been fixed at 284.8 eV.

Table 1. Binding energies, full width half maximum and atomic concentrations of the elements identified on the freshly fractured surface of enargite.

Element	Position (eV)	FWHM	Atomic%
Cu $2p_{3/2}$ (sulfide)	932.0	1.1	18.9
Cu $2p_{1/2}$ (sulfide)	951.9	1.6	8.2
As $3d_{5/2}$ (bulk)	43.2	0.7	4.7
As $3d_{3/2}$ (bulk)	43.9	0.6	3.1
As $3d_{5/2}$ (surface)	42.3	0.7	2.5
As $3d_{3/2}$ (surface)	43.0	0.6	1.7
S $2p_{3/2}$ (sulfide)	161.8	0.7	22.8
S $2p_{1/2}$ (sulfide)	163.0	0.8	12.7
C 1s (reference)	284.8	1.5	21.4

4.3.2. Natural Enargite Oxidized at pH 10

After application of an anodic potential of +869 mV SHE at pH10 for 1800 s the surface has been heavily oxidized, as shown by the formation of a Cu 2p spectra characteristic of Cu^{II}, a broadening and shift of the As 3d peak to 45.2 eV suggesting As_2O_3 formation (Velasquez et al., 2000), and a shift of the S $2p_{3/2}$ peak to 163.9 eV, which may be polysulfides, metal-deficient sulfides or elemental sulfur (Figure 6). In addition a new peak at 168.4 eV is present, which is attributable to the formation of $CuSO_4$ at the surface (Velasquez et al., 2000).

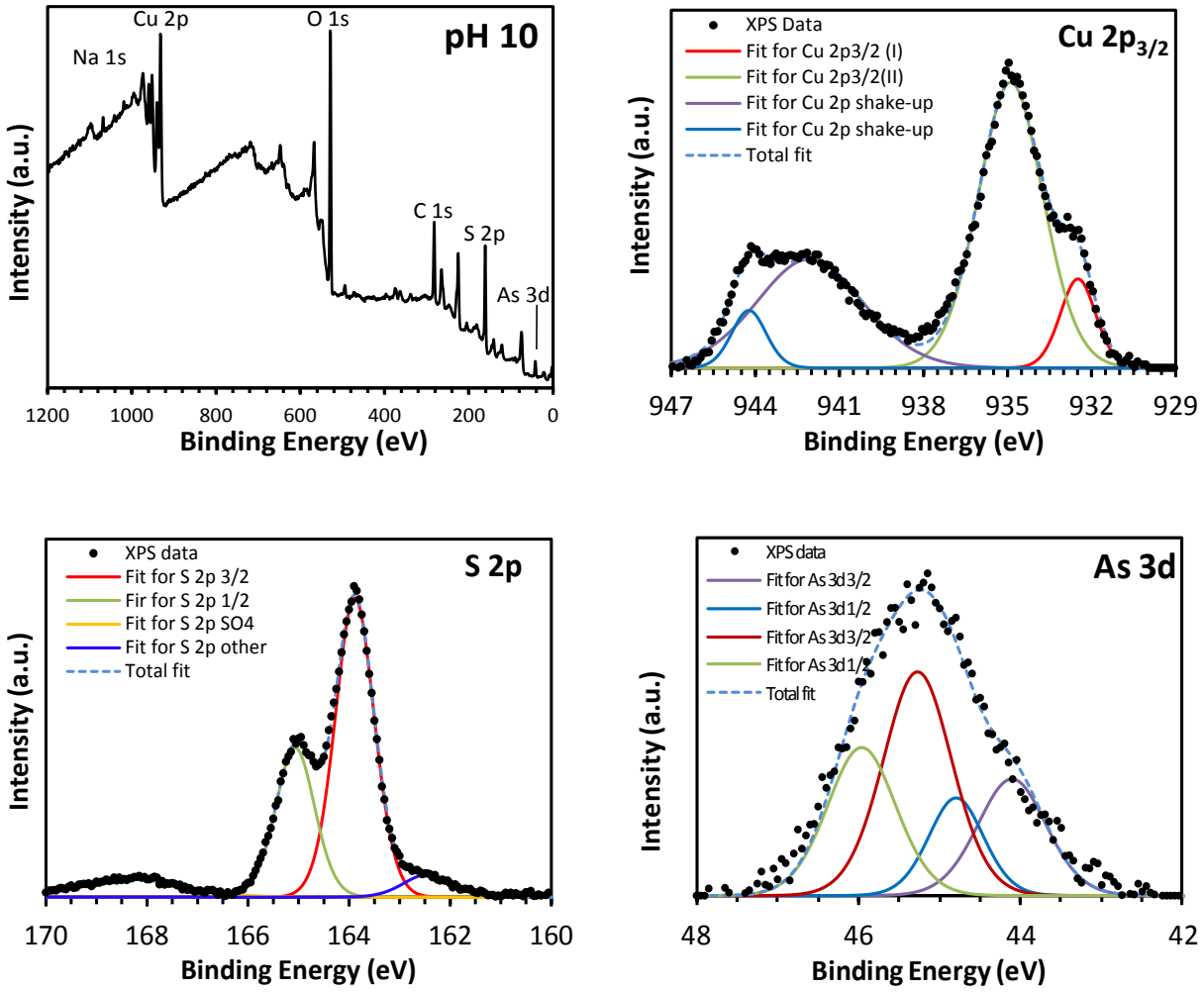

Figure 6. Survey and high resolution photoelectron spectra recorded from the enargite electrode surface at -130 °C after application of +869 mV at pH 10.

The S 2p spectrum also shows what appears to be a low binding energy shoulder at 162.5 eV which can be fitted with an additional S 2p minor peak. Attempts to fit a S 2p doublet were unsuccessful and resulted in an overall worse fit than the single peak shown. The binding energy is correct for a copper sulfide species such as CuS (Brion, 1980, Perry and Taylor, 1986) or Cu_2S (Strohmeier et al., 1985) and the corresponding Cu $2p_{3/2}$ peak at 934.9 eV supports the presence of

CuS. However it is not clear whether this represents a real contribution or some form of interference with the spectrum such as an As auger or energy loss peak, and care should be exercised in making any conclusions in this regard. Since the measured elemental concentration is 0.9%, which is close to the detection limit, Binding energy data are given in Table 2.

Table 2. Binding energies, full width half maximum and atomic concentrations of the elements identified on enargite at -130 °C after application of +869 mV at pH 10.

Element	Position (eV)	FWHM	Atomic%
Cu $2p_{3/2}$ (I) (sulfide)	932.5	1.5	1.1
Cu $2p_{3/2}$ (II) (CuS)	934.9	2.7	4.1
Cu 2p (shake-up)	942.1	4.5	2.5
Cu 2p (shake-up)	944.2	1.5	0.4
As $3d_{5/2}$ (bulk)	45.3	1.0	0.9
As $3d_{3/2}$ (bulk)	46.0	1.0	0.6
As $3d_{5/2}$ (surface)	44.1	1.0	0.5
As $3d_{3/2}$ (surface)	44.8	1.0	0.3
S $2p_{3/2}$ (sulfide)	163.9	0.9	10.1
S $2p_{1/2}$ (sulfide)	165.1	0.9	5.0
S 2p (SO_4)	168.4	2.5	1.7
S 2p (CuS)	162.5	1.1	0.9
C 1s (reference)	284.8	1.15	14.92

4.3.3. Natural Enargite Oxidized at pH 4

Oxidation at pH 4 (Figure 7) results in significant differences in the chemical species formed at the enargite surface. Compared to the polished enargite (Figure 5) both the intensity and the

relative concentration of Cu at the surface are diminished, the latter decreasing from 28 to less than 12 atomic%. This is supportive of two processes taking place, firstly the dissolution of Cu ions into solution leaving a Cu deficient surface, and the deposition of a surface layer composed primarily of species other than Cu.

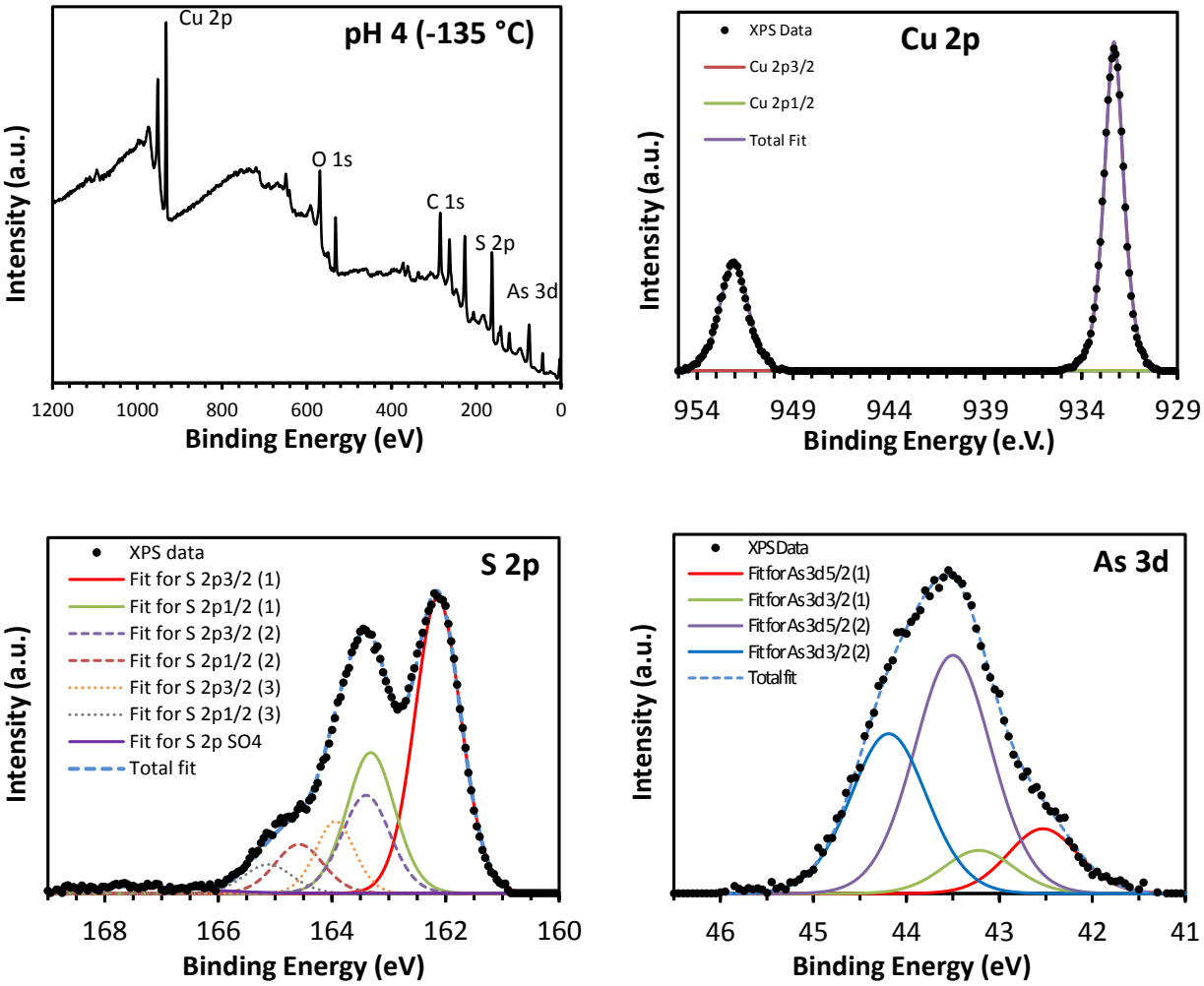

Figure 7. Survey and high resolution photoelectron spectra recorded from the enargite electrode surface at -130 °C after application of +610 mV at pH 4.

Examining the spectrum for S 2p reveals the presence of three distinct sulfur species, the S $2p_{3/2}$ peaks located at 162.1, 163.4 and 164.0 eV. An additional peak has been fitted at 167.4 eV and is ascribed to the presence of sulfate (SO_4) species. However its contribution is minimal and with a measured concentration of less than 0.8% it is not certain if it is real. The major S 2p species at 162.1 eV corresponds to the sulfide (S^{2-}), or sulfur component of enargite as previously discussed. The binding energy data are given in Table 3.

Assignment of the S $2p_{3/2}$ peaks identified at 163.4 and 164.0 eV is not so straightforward. Similar to the S $2p_{3/2}$ peak at 163.9 eV after oxidation at pH 10, a number of different assignments to the higher BE components are possible, including polysulfides, metal-deficient sulfides, elemental sulfur and defect electronic states. The BE ranges for these S $2p_{3/2}$ components overlap, so identification cannot be based on this alone.

Table 3. Binding energies, full width half maximum and atomic concentrations of the elements identified on enargite at -130 °C after application of +610 mV at pH 4.

Element	Position (Be)	FWHM	Atomic%
Cu $2p_{3/2}$ (sulfide)	932.3	1.2	7.8
Cu $2p_{1/2}$ (sulfide)	952.1	1.8	3.5
As $3d_{5/2}$ (surface)	42.5	0.9	0.7
As $3d_{3/2}$ (surface)	43.2	0.9	0.5
As $3d_{5/2}$ (bulk)	43.5	1.0	2.8
As $3d_{3/2}$ (bulk)	44.2	1.0	1.9
S $2p_{3/2}$ (sulfide)	162.1	1.0	12.9
S $2p_{1/2}$ (sulfide)	163.3	1.0	6.4
S $2p_{3/2}$ (S_n^{2-})	163.4	1.0	4.5
S $2p_{1/2}$ (S_n^{2-})	164.6	1.0	2.2
S $2p_{3/2}$ (S°)	164.0	0.8	2.6
S $2p_{1/2}$ (S°)	165.1	1.0	1.3
S 2p (SO_4)	167.4	2.5	0.8
C 1s (reference)	284.8	1.3	19.6

However analysis based on BE suggests it would appear reasonable for the peak at 163.4 eV to be assigned to metal-deficient sulfide or polysulfides (S_n^{2-}) which for the latter fall in the range 162.0-163.6 eV, and the peak at 164.0 eV is likely due to elemental sulfur (S^0) (Smart et al., 1999).

The latter is confirmed by allowing the sample to warm to room temperature (30°C) in situ and repeat the XPS analysis, in which case the high binding energy S 2p doublet is seen to disappear, as shown in Figure 8. The associated binding energy data are shown in Table 4.

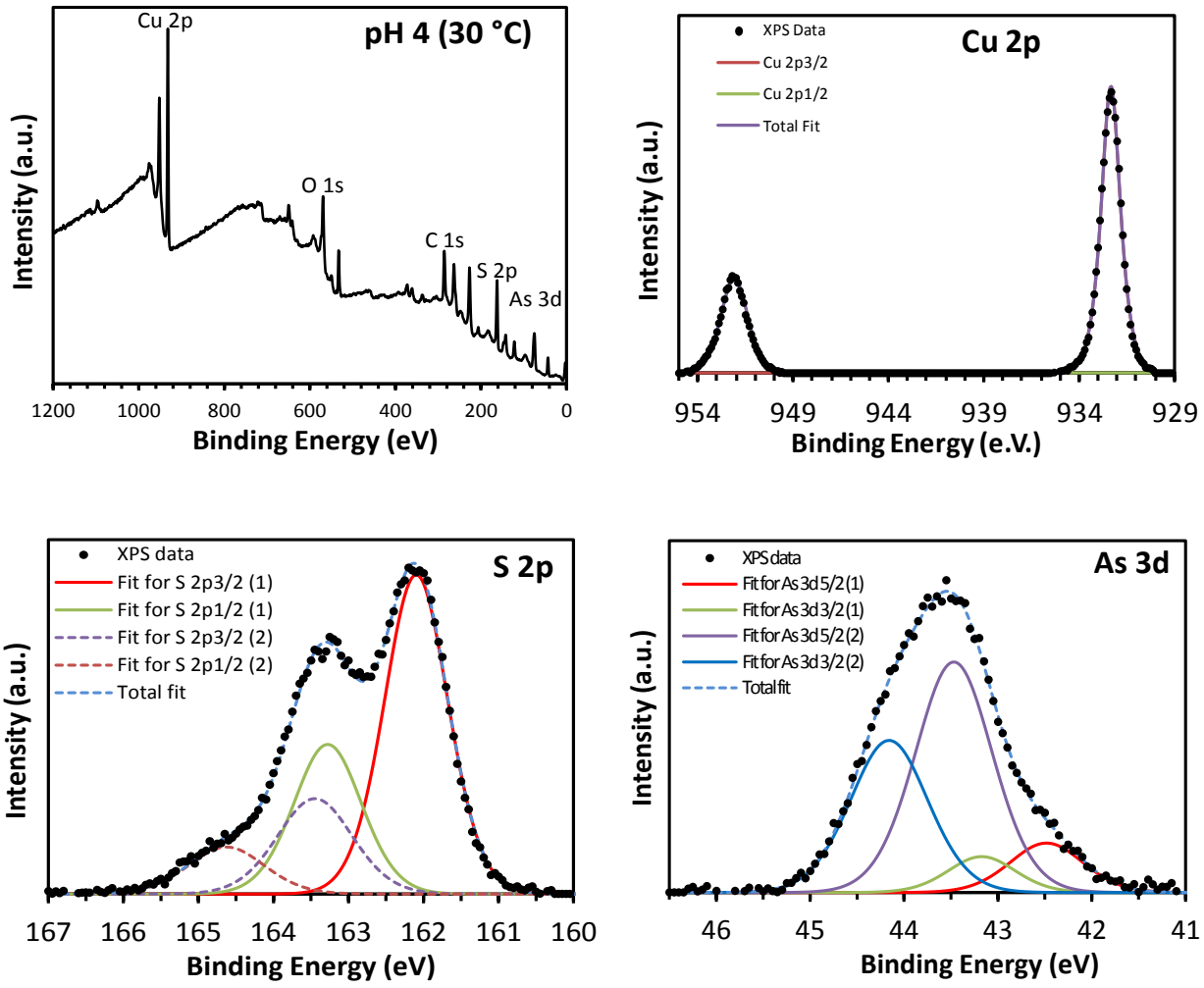

Figure 8. Survey and high resolution photoelectron spectra recorded from the enargite electrode surface at 30 °C after application of +610 mV at pH 4.

Table 4. Binding energies, full width half maximum and atomic concentrations of the elements identified on enargite at 30 °C after application of +610 mV at pH 4.

Element	Position (eV)	FWHM	Atomic%
Cu $2p_{3/2}$	932.3	1.2	11.0
Cu $2p_{1/2}$	952.1	1.7	4.7
As $3d_{5/2}$ (surface)	42.5	0.9	0.6
As $3d_{3/2}$ (surface)	43.2	0.9	0.4
As $3d_{5/2}$ (bulk)	43.5	1.0	3.2
As $3d_{3/2}$ (bulk)	44.2	1.0	2.1
S $2p_{3/2}$ (sulfide)	162.1	1.0	13.7
S $2p_{1/2}$ (sulfide)	163.3	1.1	6.8
S $2p_{3/2}$ (poly-S)	163.5	1.2	4.8
S $2p_{1/2}$ (poly-S)	164.6	1.2	2.4
C 1s (reference)	284.8	1.3	14.7

There is a clear difference in the S 2p spectrum, showing the complete absence of the S $2p_{3/2}$ component at 164.0 eV due to evaporative loss, providing the necessary confirmation of elemental sulfur. The peaks at 162.1 and 163.5 eV remain with no significant change in BE. However there are clear differences in atomic concentration, as shown in Table 5. The most significant change is seen for copper.

Table 5. Atomic concentration of all elements identified in crushed natural enargite and enargite electrochemically oxidized at pH 4, analyzed at -130 and 30 °C.

Conditions	Cu	As	S^{2-}	S_n^{2-}	S_n^0	O	C
Crushed	28.1%	11.9%	35.5%	0.0	0.0	3.2%	21.4%
-130 °C	11.7%	5.8%	19.3%	6.7%	4.0%	12.0%	39.6%
30 °C	16.3%	6.3%	20.3%	7.2%	0.0%	14.6%	35.4%

4.3.4. Investigation of CV Peak at 790 mV in the Cathodic Sweep Direction

To identify the surface chemical species that exist at the peak identified at 790 mV in the 1 mV/s CV during the return sweep, a sample was prepared as described in Section 4.1, and then subject to XPS analysis using the cold stage procedure described previously. The results are shown in Figure 9, while the binding energy and elemental concentration data are presented in Table 6.

Two Cu $2p_{3/2}$ species were identified at binding energies of 933.1 and 935.1 eV, showing that only Cu^{II} species exist on the surface. The peak at 935.1 can be identified as Cu in $Cu(OH)_2$, and is confirmed by the corresponding O 1s peak (not shown) at 531.3 (McIntyre et al., 1981). However $CuSO_4$ is also a possibility, with reported BE's for Cu $2p_{3/2}$ of 934.9 eV using C 1s reference BE of 284.6 eV , S $2p_{3/2}$ of 168.3 eV (Klein et al., 1984), and O 1s of 532.2 eV (Strohmeier et al., 1985), which is in good agreement with the measured values of 935.1, 168.4 and 532.6 eV respectively.

The identity of the Cu $2p_{3/2}$ species at 933.1 eV possibly represents CuO, with reported binding energy of 933.2 eV (Gauzzi et al., 1990), however there is no corresponding O 1s detected, which would be expected at about 529.6 eV (Skinner et al., 1996). Copper in Cu_2S is another possibility with reported binding energies for Cu $2p_{3/2}$ of 932.6 to 932.9 eV (Skinner et al., 1996), which is supported by a corresponding S 2p species identified as a single minor peak at 162.6 eV, in agreement with published data (Strohmeier et al., 1985).

Given the relatively complex chemistry of the surface resulting from the presence of multiple compounds composed of Cu, S, As and O resolving the individual species is not straightforward,

particularly given the degree of variability of binding energies for these elements in different compounds reported in the literature.

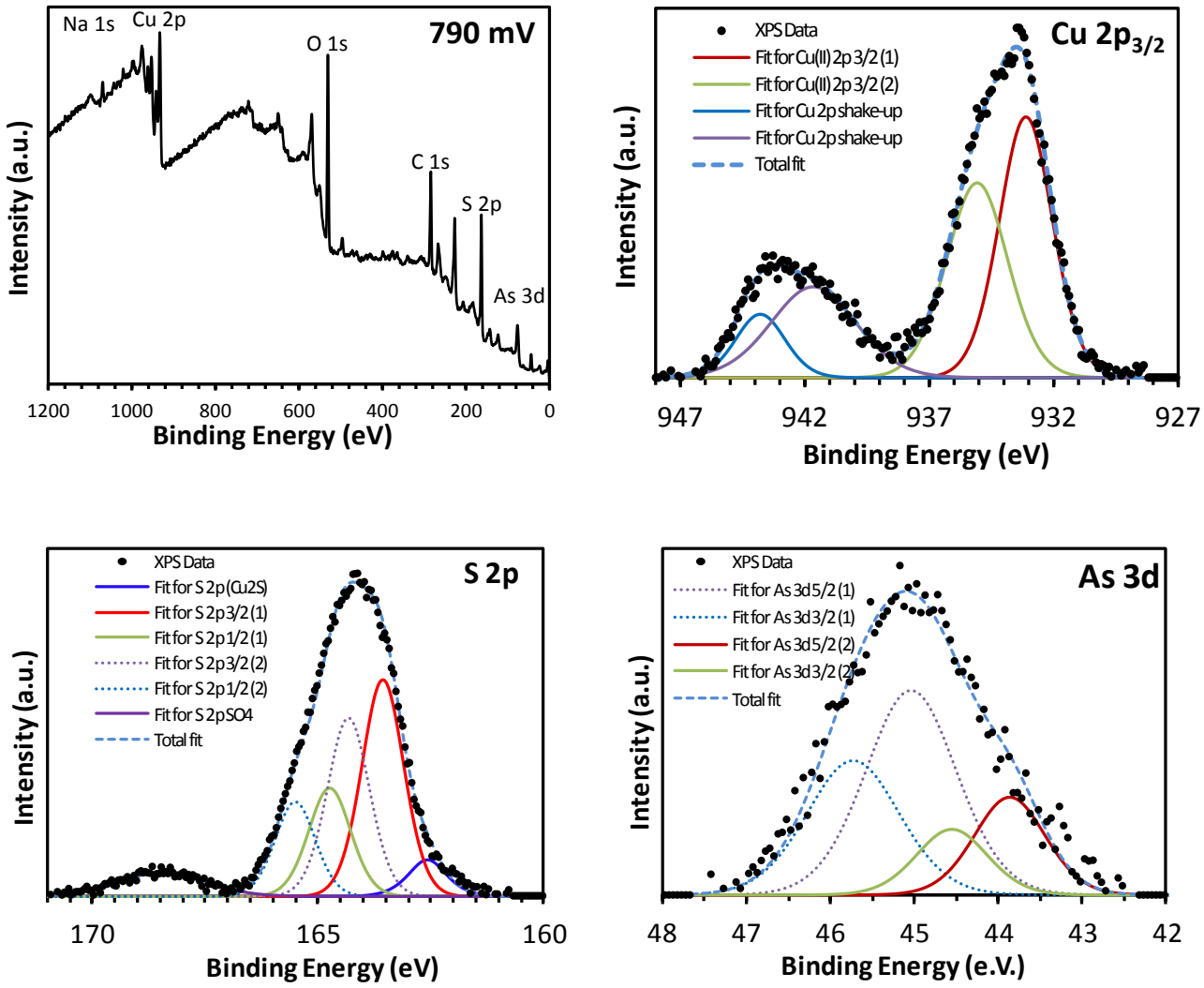

Figure 9. Survey and high resolution photoelectron spectra recorded from the enargite electrode surface at -135 °C after application of cyclic polarization in a pH 10 buffer solution initiated at 0 mV in the positive direction, switching at +1100 mV, and terminating at +790 mV.

Thus the major difference between this current peak and those examined in the positive sweep direction of the anodic range of the cyclic voltammogram is the absence of any cuprous Cu^{I} species detected on the surface. Combined with the fact that the XPS peak for copper is shifted higher in the binding energy range suggests a higher degree of surface oxidation and a thicker or continuous surface oxide layer is formed.

Table 6. Binding energies, full width half maximum and atomic concentrations of the elements identified on enargite at -130 °C after application of a partial CV scan terminating at +790 mV at pH 10.

Element	Position (eV)	FWHM	Atomic%
Cu $2p_{3/2}$ (^{II}) (Cu_2S)	933.1	2.5	4.2
Cu $2p_{3/2}$ (^{II}) ($Cu(OH)_2$)	935.1	2.9	3.6
Cu 2p (shake-up)	941.7	4.0	2.3
Cu 2p (shake-up)	943.8	2.3	0.9
As $3d_{5/2}$ (bulk)	45.0	1.3	1.3
As $3d_{3/2}$ (bulk)	45.7	1.3	0.9
As $3d_{5/2}$ (surface)	43.9	1.0	0.5
As $3d_{3/2}$ (surface)	44.6	1.0	0.3
S 2p (Cu_2S)	162.6	1.0	1.1
S $2p_{3/2}$ (sulfide)	163.6	1.1	6.9
S $2p_{1/2}$ (sulfide)	164.8	1.1	3.4
S 2p3/2	164.3	1.1	5.7
S 2p1/2	165.5	1.0	2.9
S 2p (SO_4)	168.5	2.2	1.5
O 1s ($Cu(OH)_2$)	531.3	1.6	20.7
O 1s ($CuSO_4$)	532.6	1.6	12.0
C 1s (reference)	284.8	1.4	17.6

In addition, the first switching potential is high at 1100 mV, which places the system close to the upper limit of the water stability region prior to commencing the return sweep. Thus the

potential exists for the complete breakdown of the enargite surface and deposition of a chemically complex surface layer composed largely of oxides of copper and arsenic, as well as sulfur containing species such as Cu_2S and $CuSO_4$.

4.4. Contact angle

To investigate further any changes in surface hydrophobicity associated with surface oxidation, contact angle measurements were carried out on a freshly polished enargite surface subject to three separate preparation conditions. These are the polished surface with no further treatment, the polished surface after oxidation for 60 min at + 869 mV (pH 10) and the polished surface after oxidation for 60 min at +610 mV (pH 4). Contact angle as a function of normalized base radius for these three conditions is shown in Figure 10. The normalized base radius was obtained by dividing the actual (measured) base radius of the water droplet by the initial base radius when it was first placed on the surface.

The initial contact angle of a droplet placed on the surface was found to be 46 ± 4° for a freshly polished surface, 44 ± 9° for a surface oxidized at pH 10, and 59 ± 7° for a surface oxidized at pH 4, at a 95% confidence level. This would indicate there is a significant difference between the polished surface and oxidized surface prepared at pH 4. Where the surface was oxidized at pH 10, the results are not so clear. The variation in initial contact angle is large, ranging from a minimum of 35° to a maximum measured value of 55°, and this is reflected in the wide confidence interval (± 9°). Different values were obtained depending on the particular location on the specimens' surface that was selected for drop placement. This would suggest that the oxidation layer is not uniform over the surface. From these results no significant difference in initial contact angle was found between the surface oxidized at pH 10 and the polished sample.

As shown in Figure 10, the polished only, and oxidized (pH 10) treatment conditions display very similar behavior with respect to change in contact angle with normalized base radius. Essentially the droplet is observed to remain pinned once it is placed on the surface with very limited reduction in base radius.

The observed departure from a constant radius below approximately 30°, seen as a curved line in Figure 10, was determined to be an artifact of the image processing method used to extract the data, which was based on the assumption of a circular droplet contact area, and the properties of the images themselves. Manual examination of the images was used to correct the artifact and revealed that as droplet height decreased the contact line became non-circular, resulting in measurement errors that produce the apparent decrease in base radius with contact angle.

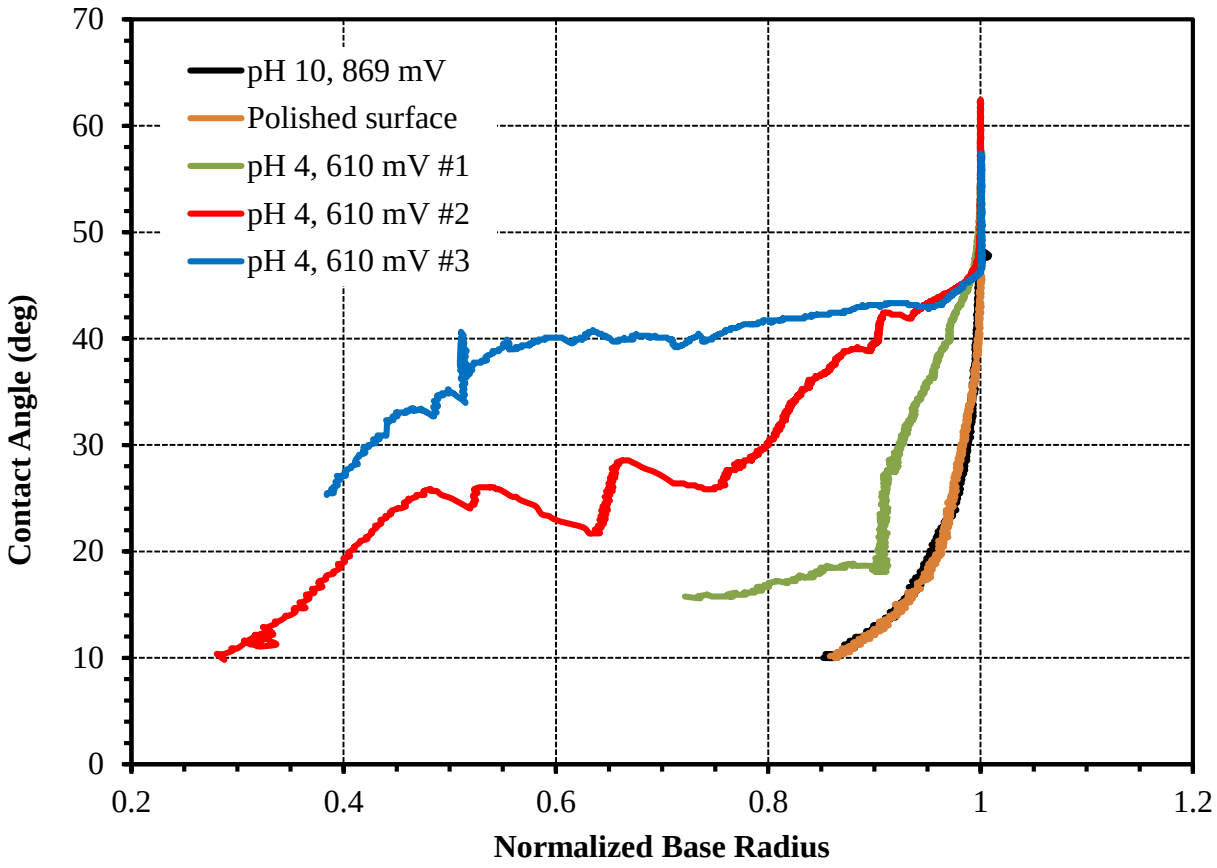

Figure 10. Dynamic (receding) contact angle versus normalized base radius of 0.5 µL water droplets evaporating on natural enargite surfaces prepared under different conditions. The curves for pH 4 were obtained at different locations on the surface.

Manually determining contact angle by measuring base radius and height of individual images to calculate contact angle, demonstrated that droplet contact radius does remain essentially pinned as contact angle decreases to a threshold of about 10°. Below 10° the data is generally considered unreliable and therefore does not contribute any meaningful information.

5. Discussion

5.1. Surface electrochemistry

The anodic peaks generated by the cyclic polarization of enargite at pH 10 represent a process of progressive dissolution of Cu from the enargite surface, Cu_3AsS_4, to Cu^{2+} in solution, which precipitates on the surface as a $Cu(OH)_2$ layer (Guo and Yen, 2008). The intermediate products produced by increasing anodic potential would include various mineral phases of the form $Cu_{3-x}AsS_4$, where $0 < x \leq 3$. As the potential increases, As can leave the enargite structure and form ions (AsO_4^{3-}) in solution, surface species such as As_2O_5 and As_2O_3, and surface S^0 and sulfate species (SO_4^{2-}) such as $CuSO_4$ may also form (Velasquez et al., 2000). Guo and Yen (2008)

postulate a series of reaction mechanisms at pH 10 corresponding to each of the CV peaks identified in their work. The reactions at peak 1, 2, 3, 4 and 5 on the anodic scan shown in Figure 2 can be presented as follows:

$$Cu_3AsS_4 + 2xOH^- = Cu_{3-x}AsS_4 + xCu(OH)_2 + 2xe^- \quad [1]$$

$$Cu_{3-x}AsS_4 + (14-2x)OH^- = (3-x)Cu(OH)_2 + AsO_4^{3-} + 4S^o + 4H_2O + (11-x)e^- \quad [2]$$

$$Cu_2AsS_4 + 12OH^- = 2Cu(OH)_2 + AsO_4^{3-} + 4S^o + 4H_2O + 9e^- \quad [3]$$

$$CuAsS_4 + 10OH^- = Cu(OH)_2 + AsO_4^{3-} + 4S^o + 4H_2O + 7e^- \quad [4]$$

$$Cu_3AsS_4 + 46OH^- = 3Cu(OH)_2 + AsO_4^{3-} + 4SO_4^{2-} + 20H_2O + 35e^- \quad [5]$$

Reaction [1] represents weak surface oxidation at low applied anodic potential, while reaction [5] describes strong surface oxidation at high applied potential, i.e., the complete decomposition of enargite by oxidation. The intermediate reactions given by Eqs. [3] and [4] can contain products of sulfur of oxidation state higher than zero-valence (elemental) sulfur as described. The main difference at lower and high potentials is the number of OH^- ions involved in the reactions. At high potential (1074 mV) SO_4^{2-} ions are present, possibly as $CuSO_4$ (Guo and Yen, 2008).

On the cathodic scan returning from high applied potential, the current peaks can present various reduction reactions such as the reduction of copper hydroxide (peak 7 in Figure 1) and the reductions of elemental sulfur and polysulfide ions (peak 8). The reduction reactions can be presented as follows (Guo and Yen, 2008):

$$2Cu(OH)_2 + 2e^- = Cu_2O + 2OH^- + 2H_2O; \quad E(SHE) = -95mV \quad [6]$$

$$2S^0 + 2e^- = S_2^{2-}; \quad E(SHE) = -670mV \quad [7]$$

$$S_2^{2-} + 2e^- = 2S^{2-}; \quad E(SHE) = -720mV \quad [8]$$

The reduction decomposition of enargite can produce arsenic sulfide and copper sulfide as shown below:

$$2Cu_3AsS_4 + 6H_2O + 6e^- = As_2S_2 + 3Cu_2S + 3H_2S + 6OH^- \quad [9]$$

Remarkably little information exists in the literature regarding electrochemical oxidation of enargite at pH 4. Guo and Yen (2008) compare the effects of pH on stationary and cyclic polarization but did not consider possible reaction mechanisms in any detail other than for pH 10. In order to gain a better theoretical understanding of possible reaction mechanisms a thermodynamic

approach is useful. Using the HSC Chemistry 7.1 software package (Outotec, Finland) Eh-pH diagrams have been generated for the enargite systems. Thermodynamic predictions of the behavior of the Cu-As-S-H_2O, As-Cu-S-H2O and S-As-Cu-H_2O systems are shown in Figure 11. Caution is required in interpreting these results, however, as the concentrations of Cu (0.003 M), As (0.001 M) and S (0.004 M) in solution and the species selected as present in solution are assumptions based on the stiochiometry of enargite.

Predicted equations for pH 10 and pH 4 for this system at the selected potentials of 869 mV and 610 mV, respectively, have been derived and are represented by the following equations:

$$Cu_3AsS_4 + 45OH^- = 3Cu(OH)_2 + HAsO_4^{2-} + 4SO_4^{2-} + 19H_2O + 35e^- \quad [10]$$

$$2Cu_3AsS_4 + 40H_2O = 3Cu^{2+} + Cu_3(AsO_4)_2 + 8SO_4^{2-} + 80H^+ + 70e^- \quad [11]$$

These predictions are included because they are useful to provide a reference over a wide range of conditions. However, they do not predict the kinetic behaviour of copper sulfide electrodes accurately. Evidence for this is seen in the potential-pH diagram for the thermodynamic systems shown in Figure 11, where oxidation of enargite is strong (corresponding to a high positive applied potential), involving the dissolution of enargite and the formation of cuprous species, sulfate species and arsenate species. It shows a very similar result to that of Asbjornsson et al. (2004) in a thermodynamic analysis of the Cu-As-S-Cl-H_2O system at 298 K.

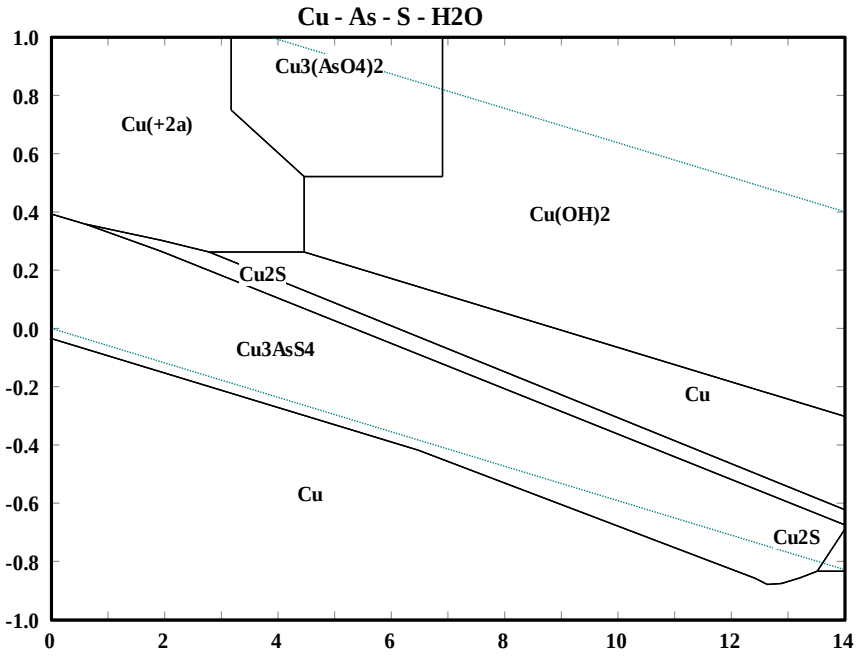

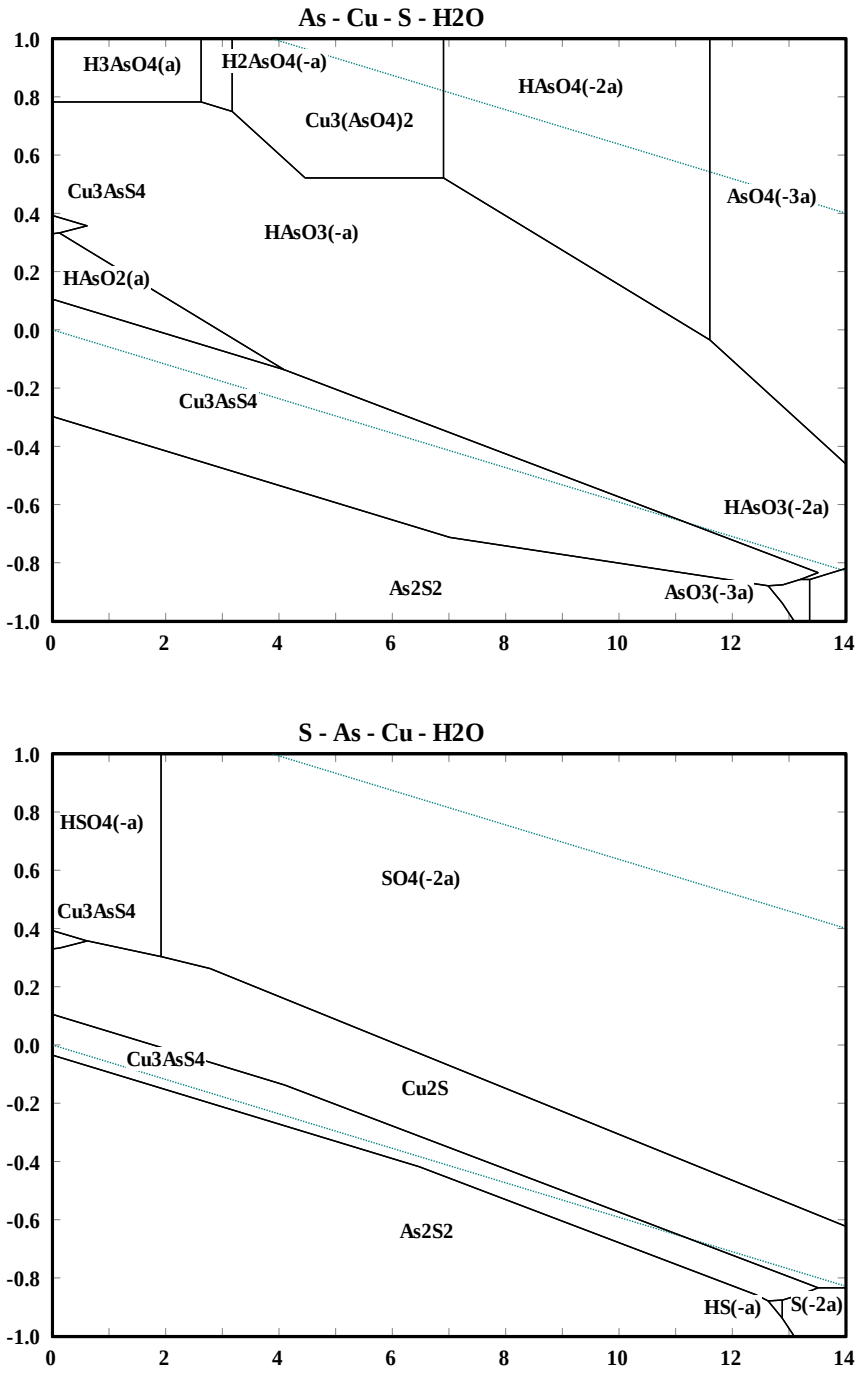

Figure 11. Eh-pH diagrams for the Cu-As-S-H_2O, As-Cu-S-H_2O and S-As-Cu-H_2O systems at 278K. Dissolved copper, arsenic and sulfur activities are assumed to be 3, 1 and $4x10^{-3}$ M, respectively. The dashed lines indicate the upper and lower limits of water stability.

The CA behavior (shown in Figure 3) is similar to that seen in the study of chalcopyrite oxidation in acidic solution by Biegler and Swift (1979), where they propose the formation of a relatively uniform compact layer of amorphous plastic sulfur at the surface. Gardner and Woods (1979) studied the floatability of chalcopyrite at pH 11 under potentiostatic control and proposed a

mechanism of formation of surface species of CuS, $Fe(OH)_3$ and S. They considered the presence of sulfur on the mineral surface as responsible for the change from a hydrophilic to a hydrophobic condition rendering chalcopyrite floatable.

In the case of enargite, as oxidation proceeds at pH 10 via mechanisms of the form of the reaction described by Eq. [10], copper is dissolved into solution and a surface layer of copper hydroxide is believed to form, which thickens over time. With increasing thickness ion transport through the surface layer into the bulk solution is increasingly hindered and the reaction becomes diffusion limited.

The behavior of diffusion controlled surface layer formation is predicted by parabolic kinetics, which is seen when the flow of current through a passivating surface layer is inversely proportional to the square root of time. In general, the existence of this relationship indicates that the rate determining step is diffusion through the surface layer. Where parabolic kinetics exist, the current resulting from an applied potential decays according to the relationship

$$I = \frac{k}{\sqrt{t}} \qquad [12]$$

where I is the current, k is the rate constant and t is time. Under these conditions a plot of I vs. $t^{-1/2}$ will be linear and pass through the origin. Given that for a diffusion limited system it is known that $I \propto t^{-0.5}$ as shown by Eq. [12], and therefore $\log I \propto -0.5 \log t$, when the t vs. I data is plotted on a log/log scale as shown in Figure 12, the resultant graph will display a slope of -0.5 where surface layer formation is diffusion controlled. Thus it would appear that the reactions taking place at the enargite surface at pH 4 are largely diffusion controlled after about the initial ten seconds of oxidation. At pH 10 the situation is more complex, and the behavior appears to be a result of a combination of mechanisms. It is probable that surface reactions are partly limited by diffusion through a partial or permeable surface layer, combined with processes of surface dissolution, which provides the species in solution necessary for precipitation and formation of the surface layer.

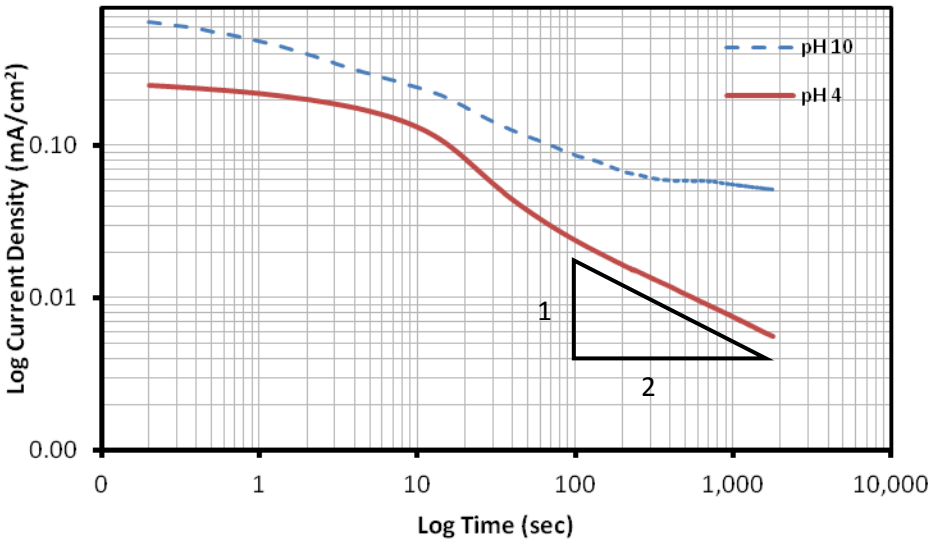

Figure 12. Log current vs. log time for CA of enargite in pH 10 and 4 buffer at an applied potential of 869 and 610 mV respectively (data from Figure 3). Linear behavior with slope -0.5 indicates that the reaction is diffusion controlled.

However it is clear from the lack of linearity over the whole of the oxidation process that diffusion is not the only mechanism affecting enargite surface layer formation under oxidizing conditions, although it appears to play a significant role. It must be noted that Eq. [12] is for a planar electrode. Therefore, the non-linear behavior may be due to the non-planar nature of the electrode, which is shown by the roughening of the surface seen in the AFM images, particularly at pH 10 (Figure 5). In this case the root mean square (RMS) roughness of the surface increased from 0.795 nm for the freshly polished surface to 9.723 nm after oxidation at 869 mV. In comparison when oxidation was carried out at pH 4 using an applied potential of 610 mV, the increase in the RMS roughness value was much less, from 1.228 nm to 3.143 nm.

As shown in Figure 12, there appear to be two distinctly different behavioral regions, which are more evident where enargite is oxidized at pH 4. These regions are indicated by the flat portion of the curve, representing initial surface polarization and charging of the electrical double layer, where fast dissolution of Cu into solution to form a metal-deficient surface enriched in S and As can occur. Evidence for Cu depletion at the surface will be discussed in the XPS section. The second region is that where the slope of the plot approximates -0.5, The CA data collected over an extended time period (Figure 3) show that the current tends towards a plateau, suggesting the surface is not completely passivated. These results suggest that the initial portion of the curve where log current is constant relative to log time (or current is proportional to $t^{-1/2}$) is due to the formation of a heterogeneous layer, while the constant current region, shown in Figure 12 where a slope of -0.5 exists, is due to flow through a completed layer (Fleischmann and Thirsk, 1955). The composition

of this surface layer will be further discussed in the XPS section, but the results indicate that at pH 10 significant amounts of $CuSO_4$ and possibly $Cu(OH)_2$ exist. This layer is, shown by AFM imaging to be discontinuous. At pH 4 the surface layer appears to be continuous, interspersed with localized deposits of what is assumed to be elemental sulfur and metal-deficient sulfide, the presence of which is confirmed by XPS.

Considering the morphological changes seen by AFM and the CA behavior described above, a mechanism of surface layer formation involving the nucleation and growth of discrete domains is not supported. If this was so, the *I(t)* curve (Figure 3) would show the presence of a second minimum. Instead, the *I(t)* curve shows an initially rapid decay in current tending towards a plateau at long oxidation times. This is indicative of the formation of a layer structure that inhibits diffusion. This existence of this mechanism is supported by the AFM images which demonstrate the formation and growth of a layer over the surface, particularly at pH 4, which appears to form as dissolution of the surface is taking place, evident by progressive loss of the surface detail previously seen on the unoxidized surface.

5.2. X-ray photoelectron spectroscopy

5.2.1. Crushed Natural Enargite

The XPS data obtained for crushed natural enargite (Figure 5) is in good agreement with the findings of Pratt (2004) for natural enargite, with peak locations differing by less than 0.2 eV for the elements detected. Good agreement is also found with the results of Velasquez et al. (2000) where, using a fractured sample of natural enargite, binding energies for Cu $2p_{3/2}$, As 3d, S 2p and C 1s of 932.4, 43.4, 162.1 and 284.8 eV, respectively, were found. For polished enargite a shift of the As 3d and S 2p peaks to 42.7 and 161.7 eV was recorded. However the C 1s peak was recorded at 284.1 eV. No attempt was made to resolve high resolution spectra of S 2p and As 3d into spin-orbit doublets.

The existence of two distinct contributions to the As 3d spectrum is explained by Pratt (2004) as attributable to As in the bulk matrix (As $3d_{5/2}$ at 43.2 eV) and As atoms at the surface (As $3d_{5/2}$ at 42.2 eV). Rossi et al. (2001) reported binding energies of Cu $2p_{3/2}$, As $3d_{5/2}$ and S 2p as 932.5 ± 0.2, 43.9 ± 0.2 and 162.2 ± 0.2 respectively, for natural 'as received', as well as natural and synthetic powdered enargite samples. In natural enargite the elemental oxidation states are copper as Cu(I), arsenic as As(V), and sulfur as S^{2-} (Velasquez et al., 2000, Cordova et al., 1997, Pauporté and Schuhmann, 1996, Pratt, 2004).

With respect to the relative atomic concentrations of copper, sulfur and arsenic there appears to be an excess of As for this sample. If the stoichiometric ratio of Cu:As were to exist (3:1), the

atomic concentration of As would be about 9.36%. Velasquez et al. (2002) found a Cu:As:S ratio of 22.4:7.8:33.1 (3:1:4.2) for a fractured natural enargite sample, indicating the atomic concentrations match the stoichiometry of enargite very closely. This was done using sensitivity factors provided by the manufacturer (Physical Electronics) of the equipment used in their study, which may differ from those provided by Kratos, as they are instrument dependent. This may account for some of the observed variation from the stoichiometric ratio. Also important is the presence of a surface layer, in this case adventitious carbon. Such a layer will act to reduce the emission rate of photoelectrons, having an increasing effect with decreasing kinetic energy of emission. Thus copper is most affected, followed by oxygen and sulfur, and arsenic is least affected. Thus copper and sulfur are likely to be underestimated with respect to arsenic. A measured atomic concentration of carbon of 21% is significant, and may partly account for the deviation of the observed Cu:As:S ratio from the expected stoichiometric ratio.

5.2.2. Natural Enargite Oxidized at pH 10

Electrochemical oxidation of enargite at pH10 was found to produce a surface that has been heavily oxidized, demonstrated by a Cu 2p spectra characteristic of Cu(II) with two Cu species, changes to the As 3d component indicative of As_2O_3 formation as a surface oxide (Velasquez et al., 2000), and a shift of the S $2p_{3/2}$ peak to 163.9 eV (Figure 6) which, when combined with the Cu $2p_{3/2}$ peak at 934.9 eV suggests CuS formation. (Perry et al., 1986) The presence of a new peak at 168.4 eV is indicative of $CuSO_4$ formation. Taken together this data supports the formation of CuO, and $Cu(SO)_4$, and possibly $Cu(OH)_2$, and is in good agreement with the work of Velasquez et al. (2000). However it should be noted that in their work a relatively lower potential of +745 mV was used. Thus, in this study, a relatively higher degree of oxidation is possible.

In an XPS investigation of natural enargite chemically oxidized at pH 11, Fullston et al. (1999) attribute a S 2p component identified at around 162 eV as indicative of metal deficient sulfide or disulfide. Some care is needed in applying this result to the present study since the oxidation mechanism is different. In addition 162.5 eV may seem too high to correlate with this result but these authors use a C1s reference of 284.6 eV, which is 0.2 eV lower than the 284.8 eV used in this study. Taking this into account reduces the difference to 0.25 eV, but further investigation is needed to confirm the result before any conclusion can be made.

5.2.3. Natural Enargite Oxidized at pH 4

Based on the evidence derived from the experimental results (Figure 7), it is not clear whether polysulfides or metal-deficient sulfides are significantly represented at the enargite surface. Further investigation with techniques such as diffraction (e.g. XRD) or X-ray absorption fine structure

(XAFS) would be required to confirm metal-deficient sulfides, or confirmation of S-S bonding by IR, Raman or XAFS in the case of polysulfides (Smart et al., 1999). However some inferences can be made. According to Kartio et al. (1998) polysulfides are composed of sulfur atoms arranged in a chain structure, resulting in different atomic charge for atoms at different locations in the chain. Those at each end exhibit a formal charge of -1, while that of the intermediate atoms is 0. These authors argue that where polysulfides are present two doublets would be expected, where the S $2p_{3/2}$ component located around 162.1 eV could represent the S^{2-} species and that at 163.1 eV the S^0 component.

In the case of the XPS data for enargite electrochemically oxidized at pH 4, the doublet with the S $2p_{3/2}$ component at 163.9 eV disappears after warming. So, this set of peaks cannot be due to S^0 in a polysulfide as it should remain after warming. This is supported by Kartio et al. (1998) where the XPS analysis was carried out at ambient temperature, and at least part of the S 2p spectrum was attributed to the presence of polysulfide. Therefore, it is likely that polysulfide is not present, just elemental sulfur. The remaining contribution to the S 2p spectrum can then be ascribed to metal deficient sulfide. The presence of metal deficient sulfide would concur with the change in the Cu% to S% ratio with treatment. Initially the ratio is 0.79, after oxidation at pH 4 (-130 °C) the ratio is reduced to 0.38, and after warming to ambient temperature, increases again to 0.59. It therefore appears that the proportion of Cu at the surface has been reduced to form a metal deficient sulfide. Further analysis of the composition of the resulting solution after completion of oxidation using a method such as ICP would help confirm this.

5.3. Contact angle

Based on the measured results (Figure 10), it was observed that differences in initial contact angle exist depending on the location on the surface where the droplet was placed, suggesting a non-uniform surface layer distribution. Visual observation would suggest this to be a reasonable assumption as areas of different color are evident, separated by clearly defined boundaries, which suggests differences in surface properties may exist. However this was not clearly supported by the XPS, which gave repeatable results for a number of sites on the same sample. The mineral specimen used for the tests does not consist of a single uniform crystal but rather is composed of multiple crystals randomly oriented with relation to each other. Thus it is likely that different orientations of the lattice structure are presented at the surface, which may contribute to the differences observed.

The behavior of the sample oxidized at pH 4 is quite different to the other treatment conditions, as shown in Figure 10. After placement the behavior of the droplet is similar to that observed for the polished and oxidized (pH 10) surfaces, but the initial contact angle is significantly

higher than that for the polished surface. Although initially the droplet remains pinned to the surface and contact angle decreases from about 57° to 47°, with further evaporation de-pinning of the triple-line is observed at about 45° where the behavior departs from that seen for the other conditions. The droplet is no longer pinned, and the radius decreases in an irregular fashion. In this stage stick-slip motion of the triple-line is observed as the contact radius decreases, with associated fluctuation in contact angle. It is also clear that there is significant variation in the behavior after de-pinning between individual measurements as shown in Figure 10, again suggesting significant variation in physical and chemical properties of the surface over the sample area.

This behavior is similar to that described by Bormashenko et al. (2011) in their investigation of contact angle observed on low-energy polymeric substrates, where an initial step with pinning of the triple-line is observed, followed by steady or irregular stick-slip behavior with decreasing contact radius and fluctuation of the contact angle above and below a certain value for at least part of the range of contact radius variation.

As previously described, the electrochemistry and XPS results support the formation of hydrophilic ($Cu(OH)_2$, $CuSO_4$) species on the mineral surface under oxidizing conditions at pH 10. Thermodynamic data published by Guo and Yen (2008) support the formation of elemental sulfur (S^0), which is hydrophobic. These competing influences may tend to alter the surface hydrophobicity in a way that is difficult to predict, such that no clear difference can be demonstrated. However the XPS results of this study do not support the formation of elemental sulfur after oxidation at pH 10, although polysulfide/metal deficient sulfide is considered likely. In addition the change in surface roughness may be a contributing factor. It is well known that the chemical and physical characteristics of a surface directly influence the hydrophobicity (Bhushan et al., 2009, Chau et al., 2009), but it is difficult to predict the net effect of these changing properties. Specifically surface roughness, where the apparent contact angle increases for hydrophobic materials and decreases for hydrophilic materials as roughness increases (Chau et al., 2009) and heterogeneity, or the degree of variation in surface chemistry, are known to affect contact angle, but many variables can influence the measurements, making it very difficult to obtain meaningful results (Chau et al., 2009).

Clearly the surface produced by electrochemical oxidation at pH 10 and pH 4 is heterogeneous and non-ideal. The variability can be explained by considering both the chemical and physical causes of contact angle variability. The former includes the chemical heterogeneity of the oxidized surface while physical characteristics such as the presence of pores and cracks, surface roughness and molecular lattice orientation at the surface need to be considered (Shanahan, 1995).

5.4. Interrelationship among surface oxidation, roughness, species and hydrophobicity

In the preceding sections consideration has been given to the results of the four main areas of investigation, these being electrochemical surface oxidation (CV & CA), morphology or roughness (AFM), chemical species present on the surface (XPS) and surface hydrophobicity (Contact Angle). In this context the discussion so far has focused on the results of individual experimental techniques. However, to better understand the effects of electrochemically induced oxidation of the enargite surface it is important to consider how these factors interrelate.

It was shown in the AFM results that significant changes in surface morphology occur with oxidation, with a significant increase in roughness demonstrated at pH 10. The CA results show initial polarization and fast dissolution of Cu into solution resulted in Cu depletion of the surface and deposition of $CuSO_4$ and $Cu(OH)_2$ species, identified by XPS. Surface layer formation became diffusion limited after this initial phase. With the presence of these species a decrease in hydrophobicity would be expected, however this was not supported by the contact angle measurements. The competing effects of hydrophilic ($Cu(OH)_2$ and $CuSO_4$) species on the mineral surface under oxidizing conditions and increased surface roughness were found to produce a surface that did not differ significantly from unoxidized enargite in terms of hydrophobicity.

Oxidation at pH 4 was found to produce a surface layer consisting of metal-deficient sulfide species and elemental sulfur, combined with a small increase in surface roughness compared to pH 10. The electrochemistry results show a pattern of initial rapid dissolution followed by diffusion limited surface layer formation more definite than that seen at pH 10. The combination of hydrophobic sulfur species and limited increase in surface roughness was found to result in an increase in initial contact angle. It can be assumed that if the increase in surface roughness was similar to that seen at pH 10 the increase in initial contact angle would have been greater.

The resulting contact angle is therefore a function of the combination of effects resulting from the presence of hydrophilic or hydrophobic species, the extent of increase in surface roughness and the degree of heterogeneity, or variation in surface chemistry, across the enargite surface. The interaction of these factors is difficult to predict but the general trend of no significant change in hydrophobicity at pH 10, and increased hydrophobicity at pH 4, is supported by the evidence.

6. Conclusions

Using a combination of experimental techniques, the effects of an applied oxidizing potential on the surface of natural enargite in pH 10 and pH 4 solutions were investigated and compared to a freshly polished natural enargite surface. Surface oxidation and the formation of surface species were confirmed by electrochemical techniques and XPS. Surface layer formation and changes in

physical characteristics such as roughness, and apparent heterogeneous distribution of surface products, were demonstrated by AFM imaging. At pH 10, the CA results suggest that after initial polarization and fast dissolution of Cu into solution, surface layer formation becomes diffusion limited. The surface layer was found to be composed of copper sulfate and hydroxide species. AFM demonstrated a significant increase in surface roughness and formation of a discontinuous surface layer. The observed structure suggests partial surface passivation by formation of the surface layer in discrete domains, which allow diffusion to occur via the inter-domain spaces but over a greatly reduced surface area exposed to the solution. In contrast to pH 10, at pH 4 two distinct regions were indicated by the CA results showing a clear difference between the initial phase of fast dissolution and that of diffusion limited surface layer formation. This is supported by the AFM imaging which shows the formation of a continuous surface layer interspersed with isolated domains of what is believed to be elemental sulfur. The presence of elemental sulfur is confirmed by XPS analysis, as is metal deficient sulfide. Contact angle measurements demonstrated no significant difference between the freshly polished surface and a surface oxidized at pH 10. A significant difference was found between the polished surface and that oxidized at pH 4, with an increase in contact angle of about 13° (46° to 59°) after oxidation. It is theorized that the competing effects of hydrophilic (copper oxides and hydroxides) and hydrophobic (elemental sulfur) species on the mineral surface under oxidizing conditions, and the change in surface roughness, contribute to the lack of significant difference in contact angle observed for a surface oxidized at pH 10. Further studies, including investigation of the effects of the presence of flotation collector on the surface chemistry and flotation response, are required to better understand the enargite flotation system.

Acknowledgements

The authors gratefully acknowledge the University of Queensland for an APA Scholarship and the CSIRO for scholarship top-up (C.P.) and research expenses support. Assistance with the contact angle measurements and processing of the captured images by T. A. H. Nguyen is gratefully acknowledged. This research is also supported under The University of Queensland's CIEF funding scheme. The authors acknowledge the facilities, and the scientific and technical assistance, of the Australian Microscopy & Microanalysis Research Facility at the Centre for Microscopy and Microanalysis, The University of Queensland.

References

Asbjornsson, J., Kelsall, G. H., Pattrick, R. A. D., Vaughan, D. J., Wincott, P. L. & Hope, G. A. 2004. Electrochemical and surface analytical studies of enargite in acid solution. *J. Electrochem. Soc.,* 151**,** E250-E256.

Balaz, P., Achimovicova, M., Bastl, Z., Ohtani, T. & Sanchez, M. 2000. Influence of mechanical activation on the alkaline leaching of enargite concentrate. *Hydrometallurgy,* 54**,** 205-216.

Bhushan, B., Jung, Y. C. & Koch, K. 2009. Micro-, nano- And hierarchical structures for superhydrophobicity, self-cleaning and low adhesion. *Philosophical Transactions of the Royal Society A: Mathematical, Physical and Engineering Sciences,* 367**,** 1631-1672.

Biegler, T. & Swift, D. A. 1979. Anodic electrochemistry of chalcopyrite. *J. Appl. Electrochem.,* 9**,** 545-554.

Biswas, A. K. & Davenport, W. G. 1994. *Extractive metallurgy of copper,* Oxford, Pergamon.

Bormashenko, E., Musin, A. & Zinigrad, M. 2011. Evaporation of droplets on strongly and weakly pinning surfaces and dynamics of the triple line. *Colloids and Surfaces A: Physicochemical and Engineering Aspects,* 385**,** 235-240.

Brion, D. 1980. Study by Photoelectron-Spectroscopy of Surface Degradation of FeS2, CuFeS2 ZnS and PbS exposed to air and water. *Appl. Surf. Sci.,* 5**,** 133-152.

Bruckard, W. J., Davey, K. J., Jorgensen, F. R. A., Wright, S., Brew, D. R. M., Haque, N. & Vance, E. R. 2010. Development and evaluation of an early removal process for the beneficiation of arsenic-bearing copper ores. *Minerals Engineering,* 23**,** 1167-1173.

Bruckard, W. J., Kyriakidis, I. & Woodcock, J. T. 2007. The flotation of metallic arsenic as a function of pH and pulp potential - A single mineral study. *International Journal of Mineral Processing,* 84**,** 25-32.

Chau, T. T., Bruckard, W. J., Koh, P. T. L. & Nguyen, A. V. 2009. A review of factors that affect contact angle and implications for flotation practice. *Advances in Colloid and Interface Science,* 150**,** 106-115.

Cordova, R., Gomez, H., Real, S. G., Schrebler, R. & Vilche, J. R. 1997. Characterization of natural enargite/aqueous solution systems by electrochemical techniques. *J. Electrochem. Soc.,* 144**,** 2628-2636.

Curreli, L., Ghiani, M., Surracco, M. & Orru, G. 2005. Beneficiation of a gold bearing enargite ore by flotation and As leaching with Na hypochlorite. *Miner. Eng.,* 18**,** 849-854.

Fantauzzi, M., Atzei, D., Elsener, B., Lattanzi, P. & Rossi, A. 2006. XPS and XAES analysis of copper, arsenic and sulfur chemical state in enargites. *Surf. Interface Anal.,* 38**,** 922-930.

Fantauzzi, M., Elsener, B., Atzei, D., Laftanzi, P. & Rossi, A. 2007. The surface of enargite after exposure to acidic ferric solutions: an XPS/XAES study. *Surf. Interface Anal.,* 39**,** 908-915.

Fleischmann, M. & Thirsk, H. R. 1955. An investigation of electrochemical kinetics at constant overvoltage. The behaviour of the lead dioxide electrode. Part 5. - The formation of lead sulphate and the phase change to lead dioxide. *Transactions of the Faraday Society,* 51**,** 71-95.

Fullston, D., Fornasiero, D. & Ralston, J. 1999. Oxidation of synthetic and natural samples of enargite and tennantite: 2. X-ray photoelectron spectroscopic study. *Langmuir,* 15**,** 4530-4536.

Gardner, J. R. & Woods, R. 1979. An electrochemical investigation of the natural flotability of chalcopyrite. *Int. J. Miner. Process.,* 6**,** 1-16.

Gauzzi, A., Mathieu, H. J., James, J. H. & Kellett, B. 1990. AES, XPS and SIMS characterization of YBa2Cu3O7 superconducting high-Tc thin-films. *Vacuum,* 41**,** 870-874.

Guo, H. & Yen, W. T. 2005. Selective flotation of enargite from chalcopyrite by electrochemical control. *Minerals Engineering,* 18**,** 605-612.

Guo, H. & Yen, W. T. 2006. Electrochemical floatability of enargite and effects of depressants. *In:* Önal, G., Acarkan, N., Çelik, M. S., Arslan, F., Ateşok, G., Güney, A., Sirkeci, A. A., Yüce, A. E. & Perek, K. T. (eds.) *Proceedings of the XXIII International Mineral Processing Conference.* Istanbul, Turkey: Promed.

Guo, H. & Yen, W. T. 2008. Electrochemical study of synthetic and natural enargites. *Proc. 24th Int. Miner. Process. Congr.,* 1**,** 1138-1145.

Hampton, M. A., Plackowski, C. & Nguyen, A. V. 2011. Physical and Chemical Analysis of Elemental Sulfur Formation during Galena Surface Oxidation. *Langmuir,* 27**,** 4190-4201.

Kartio, I. J., Basilio, C. I. & Yoon, R. H. 1998. An XPS study of sphalerite activation by copper. *Langmuir,* 14**,** 5274-5278.

Klein, J. C., Li, C. P., Hercules, D. M. & Black, J. F. 1984. Decomposition of Copper Compounds in X-Ray Photoelectron Spectrometers. *Appl. Spectrosc.,* 38**,** 729-734.

Lattanzi, P., Da Pelo, S., Musu, E., Atzei, D., Elsener, B., Fantauzzi, M. & Rossi, A. 2008. Enargite oxidation: A review. *Earth-Science Reviews,* 86**,** 62-88.

Leja, J. 1982. *Surface Chemistry of Froth Flotation,* New York, NY, Plenum Press.

Mcintyre, N. S., Sunder, S., Shoesmith, D. W. & Stanchell, F. W. 1981. Chemical Information from XPS - Applications to the Analysis of Electrode Surfaces. *Journal of Vacuum Science & Technology,* 18**,** 714-721.

Nava, J. L., Oropeza, M. T. & González, I. 2002. Electrochemical characterisation of sulfur species formed during anodic dissolution of galena concentrate in perchlorate medium at pH 0. *Electrochimica Acta,* 47**,** 1513-1525.

Nguyen, A. V. & Schulze, H. J. 2004. *Colloidal science of flotation,* New York, Marcel Dekker.

Nguyen, T. A. H., Nguyen, A. V., Hampton, M. A., Xu, Z. P., Huang, L. & Rudolph, V. 2012. Theoretical and experimental analysis of droplet evaporation on solid surfaces. *Chemical Engineering Science,* 69**,** 522-529.

Pauporté, T. & Schuhmann, D. 1996. An electrochemical study of natural enargite under conditions relating to those used in flotation of sulphide minerals. *Colloids and Surfaces A: Physicochemical and Engineering Aspects,* 111**,** 1-19.

Perry, D. L. & Taylor, J. A. 1986. X-ray photoelectron and Auger spectroscopic studies of Cu2S and CuS. *Journal of Materials Science Letters,* 5**,** 384-386.

Plackowski, C., Nguyen, A. V. & Bruckard, W. J. 2012. A critical review of surface properties and selective flotation of enargite in sulphide systems. *Minerals Engineering,* 30**,** 1-11.

Pratt, A. 2004. Photoelectron core levels for enargite, Cu3AsS4. *Surf. Interface Anal.,* 36**,** 654-657.

Rossi, A., Atzei, D., Da Pelo, S., Frau, F., Lattanzi, P., England, K. E. R. & Vaughan, D. J. 2001. Quantitative X-ray photoelectron spectroscopy study of enargite (Cu3AsS4) surface. *Surf. Interface Anal.,* 31**,** 465-470.

Senior, G. D., Guy, P. J. & Bruckard, W. J. 2006. The selective flotation of enargite from other copper minerals - a single mineral study in relation to beneficiation of the Tampakan deposit in the Philippines. *International Journal of Mineral Processing,* 81**,** 15-26.

Shanahan, M. E. R. 1995. Simple Theory of "Stick-Slip" Wetting Hysteresis. *Langmuir,* 11**,** 1041-1043.

Skinner, W. M., Prestidge, C. A. & Smart, R. S. C. 1996. Irradiation effects during XPS studies of Cu(II) activation of zinc sulphide. *Surf. Interface Anal.,* 24**,** 620-626.

Smart, R. S. C., Skinner, W. M. & Gerson, A. R. 1999. XPS of sulphide mineral surfaces: metal-deficient, polysulphides, defects and elemental sulphur. *Surf. Interface Anal.,* 28**,** 101-105.

Smith, L. K. & Bruckard, W. J. 2007. The separation of arsenic from copper in a Northparkes copper-gold ore using controlled-potential flotation. *International Journal of Mineral Processing*, 84**,** 15-24.

Strohmeier, B. R., Levden, D. E., Field, R. S. & Hercules, D. M. 1985. Surface spectroscopic characterization of CuAl2O3 catalysts. *Journal of Catalysis*, 94**,** 514-530.

Velasquez, P., Ramos-Barrado, J. R., Cordova, R. & Leinen, D. 2000. XPS analysis of an electrochemically modified electrode surface of natural enargite. *Surf. Interface Anal.*, 30**,** 149-153.

Velasquez, P., Ramos-Barrado, J. R. & Leinen, D. 2002. The fractured, polished and Ar+-sputtered surfaces of natural enargite: an XPS study. *Surf. Interface Anal.*, 34**,** 280-283.

Wittstock, G., Kartio, I., Hirsch, D., Kunze, S. & Szargan, R. 1996. Oxidation of Galena in Acetate Buffer Investigated by Atomic Force Microscopy and Photoelectron Spectroscopy. *Langmuir*, 12**,** 5709-5721.

Chapter V

An XPS Investigation of the Surface Species Formed by Electrochemically Induced Surface Oxidation of Enargite in the Oxidative Potential Range

Chris Plackowski, Marc A. Hampton, Anh V. Nguyen, and Warren J. Bruckard

Published in Minerals Engineering, 2014, 55(0), 60-74.

1. Abstract

Oxidation of the surface of natural enargite (Cu_3AsS_4) under potentiostatic control and the formation of oxidation species at the mineral surface has been investigated at selected applied potentials in the oxidative range. Potentials at which oxidation reactions were found to occur were identified by cyclic voltammetry as +347, +516, +705, +869 and +1100 mV SHE (versus Standard Hydrogen Electrode). The mineral surface was oxidized by application of these potentials in pH 10 buffer solution, and then analyzed by X-ray photoelectron spectroscopy (XPS). Liquid nitrogen cooling was used during XPS analysis to minimize the effects of exposure to X-rays, thermal degradation, and ultra-high vacuum conditions. The surface speciation of electrochemically oxidized natural enargite obtained for these anodic potentials at pH 10 demonstrated a progressively increasing level of oxidation as applied potential increases. Surface layer deposition was linked to potential, with limited evidence of oxidation products at the surface found after treatment at applied potentials of +347 and +516 mV. At these potentials no evidence of Cu(II) compounds was found, while a decrease in the proportion of copper at the surface suggests dissolution as the primary reaction mechanism. At a treatment potential of +705 mV, Cu(II) species identified as $CuSO_4$ and $Cu(OH)_2$ were found, although the presence of arsenic oxides or sulfides was not found. After treatment at +869 and +1100 mV significant evidence of oxidation was found, with Cu(II) species of $CuSO_4$ and $Cu(OH)_2$ found. Additional sulfur and arsenic species of CuS and As_2O_3 were identified that were not present after treatment at lower potentials. Comparison of the XPS findings with previously published proposed reaction mechanisms for similar treatment potentials showed that they did not account for all species identified in the XPS data. Analysis of buffer solutions post-treatment by ICP (Inductively Coupled Plasma spectroscopy) showed a pattern of change in concentrations of Cu, As and S characterized by a step-change increase in dissolution between the +516 and +705 mV treatment conditions, which correlates with the formation of Cu(II) identified on the mineral surface.

2. Introduction

Enargite is a mineral of significance in the copper industry both due to its value as a commercial source of copper, and the detrimental impact of its arsenic content, in terms of the health, environmental, economic and final product quality issues associated with its processing (Chatterjee et al., 1995, Biswas and Davenport, 1994, Cordova et al., 1997).

A number of previous studies have investigated methods of separating arsenic during the froth flotation stage of mineral processing activities (Senior et al., 2006, Smith and Bruckard, 2007, Bruckard et al., 2007, Bruckard et al., 2010) in response to the increasing importance of finding an

economic and effective means of reducing the arsenic levels in froth flotation concentrates to acceptable levels. However to date no effective approach suitable for industrial application has been developed (Plackowski et al., 2012).

In a recent review of the literature it was found that although some progress has been made, knowledge of the fundamental surface chemistry relating to enargite must be further developed before the mechanisms that enable a successful separation by froth flotation can be understood (Plackowski et al., 2012).

In a previous study (Plackowski et al., 2013b), a detailed investigation of the enargite surface subjected to oxidation at applied potentials of +869 mV (SHE) at pH 10, and + 610 mV at pH 4, was carried out. Changes is surface morphology (roughness and distribution of surface products), hydrophobicity and surface speciation were investigated. Surface layer formation consisting of metal deficient sulfide and elemental sulfur was identified, and a mechanism of Cu dissolution and diffusion-limited surface layer deposition was proposed.

However this study considered only the one applied potential of +869 mV (SHE) at pH 10. In order to quantify surface chemical changes over a broader range, five anodic potentials, as identified by cyclic voltammetry studies, were selected to determine the progression of chemical changes induced at the enargite surface. The selected potentials were +347, +516, +705, +869 and +1100 mV SHE.

The use of electrochemical techniques to characterize the enargite surface, in particular cyclic voltammetry, provides useful information about reactivity of the mineral and enables identification of those potentials at which electrochemical reactions occur. Combined with thermodynamic data it can be used to predict the reaction mechanisms that may be responsible for the chemical changes at the surface (Guo and Yen, 2008). However to date these mechanisms, and the chemical species at the enargite surface, have not been confirmed by empirical data. Hence the purpose of this study is to examine the enargite surface after treatment by oxidation at applied potentials corresponding to high current densities as identified by cyclic voltammetry studies. This was done using XPS, combined with thermodynamic data, to confirm the surface species present, and to compare such with published reaction mechanisms.

3. Experimental

3.1. Materials

A high purity natural enargite (Cu_3AsS_4) sample was obtained from Wright's Rock Shop (USA) and analyzed by XPS to confirm its chemical composition. X-ray diffraction (XRD) was used to determine its crystal structure and to identify the mineral phases present. The predominant

phase determined was enargite, Cu_3AsS_4 (Appendix 1), with no other phases detected. A resin mounted thin polished section was prepared with the mineral exposed on both sides, and mounted on a fabricated PVC sample holder to facilitate preparation, handling and application of the experimental techniques.

AR grade di-sodium tetraborate decahydrate (Scharlau Chemie S.A., Spain) and technical grade sodium hydroxide (Sigma-Aldrich, Australia) were used to prepare a pH 10.0 buffer solution (0.05 M). Water used in the experiments was freshly purified using a reverse osmosis RIO's unit and an Ultrapure Academic Milli-Q system (Millipore, USA). The Milli-Q water had a specific resistance of 18.2 $M\Omega cm^{-1}$.

3.2. Sample Preparation

The freshly polished mineral surface was prepared for XPS by electrochemical oxidation in a pH 10.0 buffer solution using an Asylum AFM electrochemical cell (Santa Barbara, USA) and a Gamry Reference 600 potentiostat (Warminster, USA). The enargite working electrode was connected to the potentiostat working electrode cable by an insulated copper wire attached to the lower surface using silver epoxy (ITW Chemtronics, USA) to ensure good electrical contact, while a platinum wire was used as the counter electrode. An Ag/AgCl 3M KCl microelectrode (Microelectrodes Inc., USA) was used as the reference electrode.

Prior to each measurement any pre-existing surface oxidation was removed by machine polishing with 9, 3 and 1 micron diamond suspensions (Dia-duo, Struers Australia) in sequence to ensure a fresh surface was exposed. The surface was then washed with ethanol (AR grade) and dried with high purity compressed nitrogen, and immediately transferred to the electrochemical cell. The reference and counter electrodes were then attached to the cell, the enargite surface covered with buffer solution and the oxidizing potential initiated.

Surface oxidation was performed as a single step experiment using the desired potential applied for 30 min at room temperature (25 °C). The selected potentials were chosen based on the cyclic voltammetry results and correspond to the current peaks identified in the anodic range of the positive sweep direction. The results of the present work were found to be comparable to previously published data (Guo and Yen, 2008). All voltages are quoted with respect to SHE.

3.3. Electrochemistry

The cyclic voltammetry (CV) experiments were performed with a freshly polished enargite sample in a pH 10.0 buffer solution using the Asylum AFM electrochemical cell and the Gamry Reference 600 potentiostat. The enargite working electrode was connected to the potentiostat working electrode cable by an insulated copper wire attached to the sample using the silver epoxy

from ITW Chemtronics (USA). A platinum wire was used as the counter electrode and an Ag/AgCl 3M KCl microelectrode (Microelectrodes Inc., USA) was used as a reference electrode. The voltages are converted and reported relative to SHE.

In a typical experiment, the sample was polished, washed with ethanol, dried with high purity N_2 and immediately transferred to the electrochemical cell. The reference and counter electrodes were then attached to the cell, the enargite surface covered with buffer solution and the CV initiated. All experiments were conducted at a scan rate of 1 mV/s and initiated in the positive potential direction. All voltages are quoted with respect to SHE. All CV curves were initiated from a potential of 0 mV at a sweep rate of 1 mV/s in the positive sweep direction, then switched to the cathodic scan direction at 1100 mV, switched back to the anodic direction at -690 mV and terminated at 0 mV. Deoxygenation of the buffer solution and electrochemical cell was not considered necessary. The effects of oxygen on the cyclic polarization of synthetic enargite was investigated by Guo and Yen (2008), where almost identical results for oxygenated buffer compared to untreated and deoxygenated solutions were found. It was concluded that oxygen concentration does not have a significant effect on enargite cyclic polarization.

Surface preparation for X-ray photoelectron spectroscopy was carried out using the electrochemical technique of chronoamperometry (CA) performed as a single step experiment at each of the potentials corresponding to the oxidative peaks identified by CV. This method involves the application of the selected potential to the enargite working electrode while the resulting current is measured over a specified period of time, which in this work, was applied for 1800 s to a freshly polished enargite surface immersed in a quiescent pH 10 buffer solution. These potentials were selected based on the CV data and represent the anodic current peaks for the pH 10 system.

3.4. X-ray Photoelectron Spectroscopy

XPS measurements of an enargite surface oxidized using the experimental procedure described above were carried out to identify the chemical species formed at oxidizing potentials corresponding to the current peaks identified in the CV measurements. Data was acquired using a Kratos Axis ULTRA X-ray Photoelectron Spectrometer incorporating a 165 mm hemispherical electron energy analyzer. The incident radiation was monochromatic Al Kα X-rays (1486.6 eV) at 150 W (15 kV, 15 mA). The instrument work function was calibrated to give a binding energy (BE) of 83.96 eV for the Au $4f_{7/2}$ line for metallic gold and the spectrometer dispersion was adjusted to give a BE of 932.62 eV for the Cu $2p_{3/2}$ line of metallic copper. Detection limits range from 0.1 to 0.5 atomic percent depending on the element. The Kratos charge neutralizer system was used on all specimens. Survey (wide) scans were taken with an analysis area of 300 x 700 microns at an analyzer pass energy of 160 eV. Multiplex (narrow) high resolution scans were carried out with an

analysis area of 300 x 700 microns and an analyzer pass energy of 20 eV. Survey scans were carried out over a 1200-0 eV binding energy range with 1.0 eV steps and a dwell time of 100 ms. Narrow high-resolution scans were run with 0.05 eV steps and 250 ms dwell time. Base pressure in the sample analysis chamber (SAC) was $1.0x10^{-9}$ torr and during sample analysis $1.0x10^{-8}$ torr. Spectra have been charge corrected using the main line of the carbon 1s spectrum photoelectron peak (adventitious carbon) as an internal reference to account for sample charging, with an assigned BE of 284.8 eV, and were analyzed using the CasaXPS software (version 2.3.14).

In preparation for the measurement conductive tape was used to secure the oxidized enargite specimen to a metal stub, which was then attached to the sample holder and inserted into the loading chamber. Sample cooling was used for all measurements. A cold probe was utilized to pre-cool the sample holder to liquid nitrogen temperatures before evacuation of the XPS instrument loading chamber. This procedure is designed to preserve volatile species on the specimen surface. During initial cooling the chamber was continuously flushed with high purity dry nitrogen to remove moisture and oxygen. Once a temperature of -100 °C was reached the chamber was sealed and evacuation commenced. Once the required vacuum was reached the specimen was then transferred to the SAC and attached to the pre-cooled sample stage, where it was maintained at -135 °C throughout the measurement.

The surface was first analyzed by a single survey scan to identify the elements present, then multiplex high resolution scans of each elemental region were carried out to identify the relative elemental concentrations as well as oxidation state and chemical bonding associations. Relative elemental atomic concentrations were determined by peak fitting using the CASA XPS software package and the Kratos library of sensitivity factors. XPS data for the Cu 2p, O 1s, C 1s, S 2p and As 3d regions was fitted using Shirley background subtraction and Gaussian-Lorenztian peak profiles.

The XPS analysis of oxidized enargite has been shown to be dependent on the temperature at which it is carried out (Fantauzzi et al., 2006), as is the case for other sulfides (Wittstock et al., 1996, Hampton et al., 2011). At ambient temperature, the ultrahigh vacuum required during analysis ($1.0x10^{-8}$ torr) creates an environment where elemental sulfur formed on the surface is unstable and evaporates. In addition, it has been reported that Cu(II) species, in particular $Cu(OH)_2$, undergo a combination of vacuum and thermal dehydration and decomposition to CuO at ambient temperature (Skinner et al., 1996), typically found to be about 30 °C in the XPS sample analysis chamber. This effect can be controlled by pre-cooling (below -130 °C) the sample before evacuation thereby limiting evaporation of sulfur and decomposition of $Cu(OH)_2$ and other unstable compounds on the surface. Without cooling, elemental sulfur, if present on the surface, is quickly lost and is not

detected. In a previous publication (Plackowski et al., 2013a) the effects of XPS analysis on the surface species present on oxidized enargite was investigated, and similar effects as observed for other sulfides were demonstrated. Therefore, in this work the sample was cooled in the loading chamber to below -130 °C prior to evacuation using a liquid nitrogen system, and maintained at that temperature in the SAC.

3.5. Inductively Coupled Plasma Spectroscopy

To obtain an indication of the extent of dissolution of the enargite surface at oxidizing potentials corresponding to the current peaks identified in the CV measurements, samples of the buffer solution were collected after the application of each potential for 30 minutes and subject to ICP atomic emission spectroscopy analysis. A Perkin Elmer Optima 7300 DV inductively coupled plasma-optical emission spectroscopy equipped with WinLab32 for ICP software was used to measure Cu, As and S concentrations. The samples were quantitated against calibration solutions of the following concentration ranges (ppm): Cu (324.752 nm) – 0.2-5; As (193.696 nm) – 0.2-5; S (181.975 nm) – 0.2-400. An internal standard solution of Yttrium & Lutetium was used and a check standard was measured at regular intervals throughout the analysis. The method parameters used to perform the analysis are described in Appendix 2.

4. Results and Discussion

4.1. Cyclic Voltammetry

A typical CV curve for enargite at pH 10, using a freshly polished natural enargite surface, is shown in Figure 1. The results are similar to those of Guo and Yen (2008, 2006) who compared natural and synthetic enargite at pH 10, and Velasquez et al. (2000) and Cordova et al. (1997), who investigated natural enargite at pH 9.2. Small differences between the CV results in this work and the published data are likely due to variation in sample composition, including type and concentrations of impurities present, sample preparation, and experimental technique.

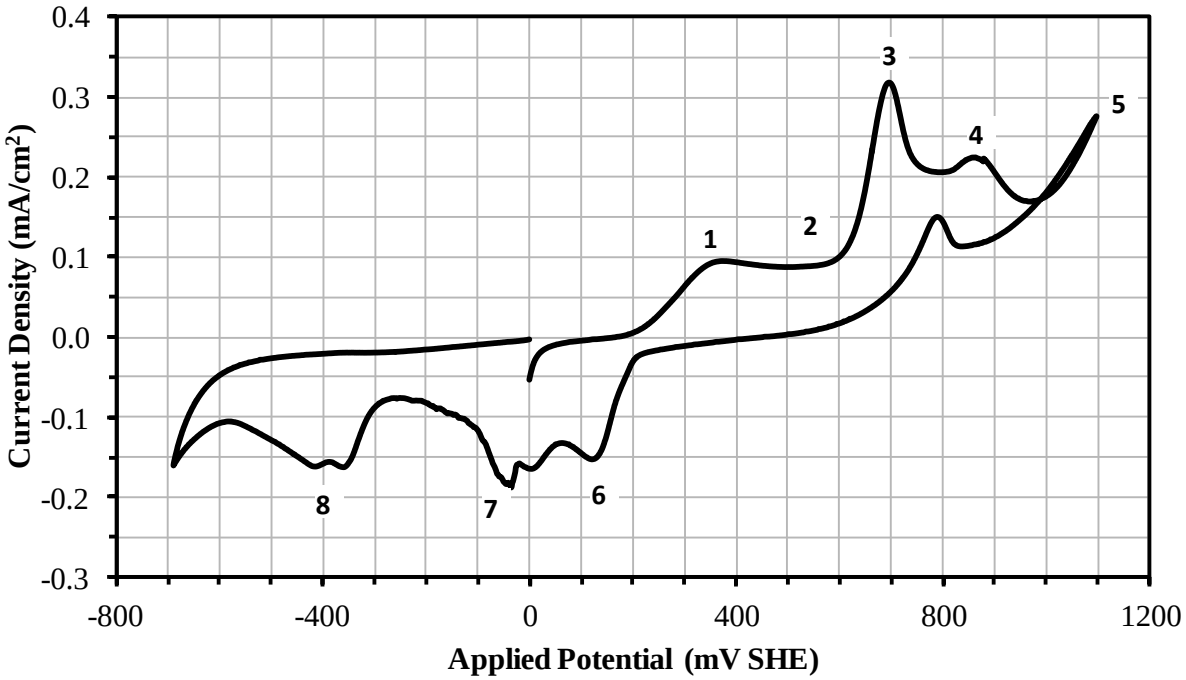

Figure 1. Typical cyclic polarization curve for natural enargite at pH 10 obtained using a scan rate of 1 mV/s. The polarization was initiated at 0 mV, returned to the cathodic scan at 1100 mV, switched to the anodic direction at -690 mV, and terminated at 0 mV (Plackowski et al. 2013).

Considering the anodic scan at pH 10 shown in Figure 1, five current peaks can be identified at potentials of 347, 516, 705, 869 and 1100 mV, designated as peaks 1-5 respectively. Whether there is a peak at 516 mV is not clear from the figure, however examination of the numerical data does indicate a local current maximum at this potential.

There are also a few current peaks on the cathodic scan at pH 10, namely, 100 mV, -100 mV and -400 mV (peaks 6-8 respectively). An additional peak at about 790 mV is observed on the return sweep from 1100 mV in the oxidative range that was not found by Guo and Yen (2008). It is possible that its existence is due to the continuation of incomplete reaction processes taking place at potentials around 800 mV during the forward potential sweep. The relatively high current density observed at peak 3 in the positive sweep direction suggests greater reactivity at this potential which, even at the low sweep rate of 1 mV/sec used in the CV, does not reach equilibrium.

4.2. Surface Composition of Unoxidized (Natural) Enargite

XPS was first used to characterize the composition of the natural enargite used for the study and confirm its composition. The sample was prepared by crushing a freshly cleaved fragment of natural enargite to a fine powder, which was then immediately transferred to the loading chamber and evacuation commenced. The sample analysis chamber was maintained at room temperature throughout the measurements. Characteristic photoelectron peaks were detected for copper, arsenic

and sulfur, as well as oxygen and carbon. The relative atomic concentrations of all elements show small deviations with respect to the stoichiometric formula of enargite, i.e. Cu_3AsS_4, with concentrations of Cu 2p 27.1%, As 3d 12.3% and S 2p 35.9% detected. Normalizing with respect to copper gives a Cu:As:S ratio of 3:1.4:4 which indicates that the content of arsenic contained in the mineral sample is slightly higher than the stoichiometric content. Other elements detected include O 1s (3.2%) and C 1s (21.6%), where C 1s is used as the internal reference for charge correction.

Shown in Figure 2 are the high resolution photoelectron spectra for Cu 2p, S 2p and As 3d. The Cu $2p_{3/2}$ spectrum peak is situated at a binding energy of 932.0 eV. The S 2p spectrum is fitted with one spin-orbit doublet situated at binding energies of 161.8 and 163.0 eV for the S $2p_{3/2}$ and S $2p_{1/2}$ peaks, respectively.

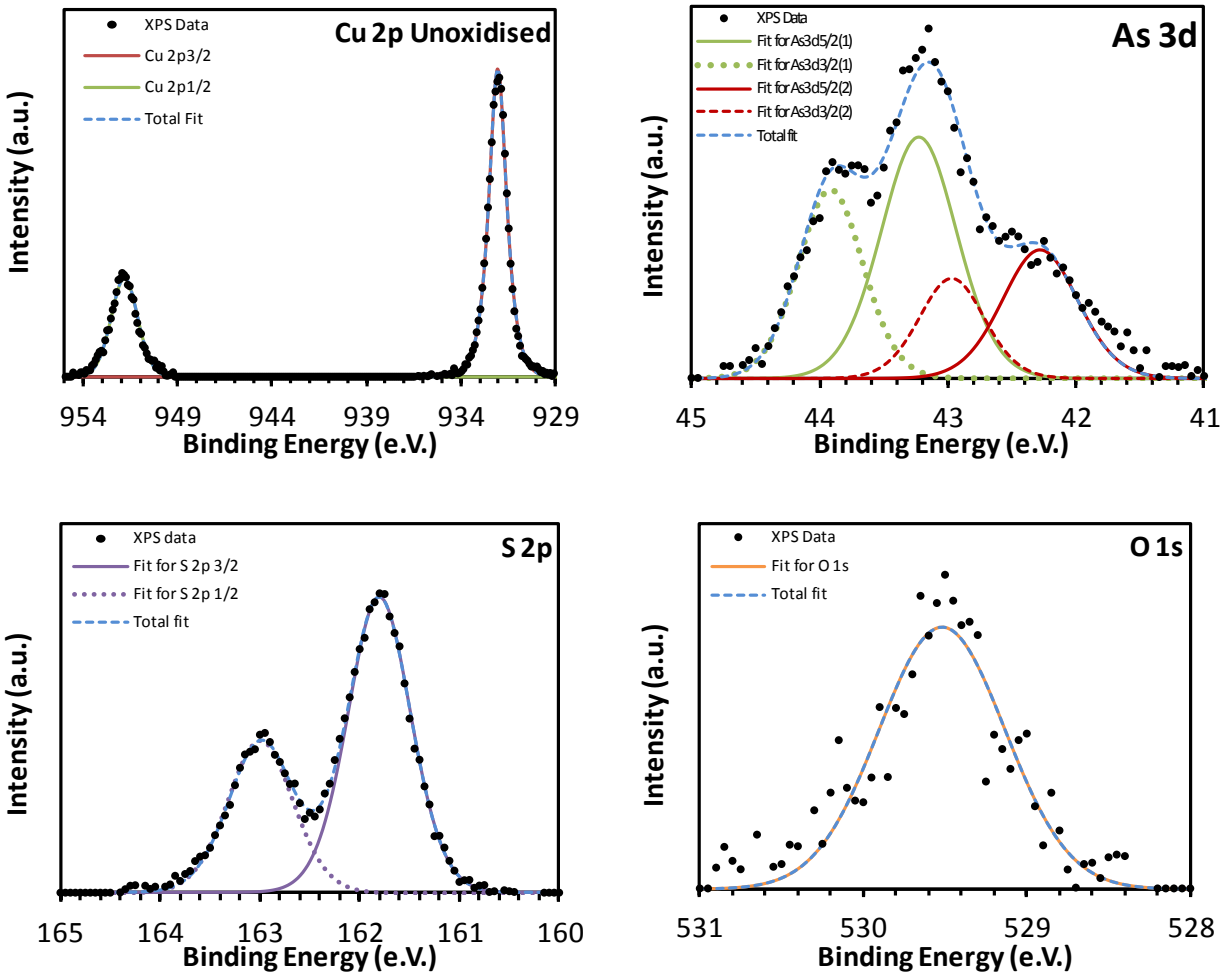

Figure 2. Cu 2p, As 3d, S 2p and O 1s high resolution photoelectron spectra recorded from the fractured surface of natural enargite prepared by crushing an unoxidized crystalline sample and immediately transferring it to the XPS instrument.

The As 3d spectrum for the bulk enargite matrix is fitted with a spin-orbit doublet, the 5/2 component located at 43.2 eV, and the low binding energy shoulder is fit with another doublet with the 5/2 component at 42.2 eV. A single O 1s spectrum was located at 529.5 eV while the position of each peak has been corrected to account for charging effects by reference to the C 1s spectrum which has been fixed at 284.8 eV. The complete XPS data is contained in Table 1.

Table 1. Binding Energies (B.E.), Full Width Half-Maxima (FWHM) and Atomic Concentrations (Atom %) of the elements identified on the freshly fractured enargite surface

	B.E.	**FWHM**	**Atom %**
Cu $2p_{3/2}$	932.0	1.1	18.9
Cu $2p_{1/2}$	951.9	1.7	8.2
O 1s	529.5	0.9	3.2
C 1s C-C ref	284.8	1.5	21.6
S $2p_{3/2}$	161.8	0.7	23.4
S $2p_{1/2}$	163.0	0.8	12.5
As $3d_{5/2}$ (bulk)	43.2	0.6	4.8
As $3d_{3/2}$ (bulk)	43.9	0.6	3.2
As $3d_{5/2}$ (surface)	42.2	0.8	2.6
As $3d_{3/2}$ (surface)	42.9	0.8	1.7

In a previous publication (Plackowski et al. 2013), consideration was given to the possible mechanisms that might exist at each of the applied potentials identified in the CV data, based on the work of Guo and Yen (2008), who proposed a number of reaction mechanisms for a system at pH 10 for each of the CV peaks at +228, +548, +728, +826 and +1074 mV, identified in their work. Guo and Yen (2008) proposed the reactions corresponding to the five peaks on the anodic scan shown in Figure 2 as follows:

$$Cu_3AsS_4 + 2xOH^- = Cu_{3-x}AsS_4 + xCu(OH)_2 + 2xe^- \quad [1]$$

$$Cu_{3-x}AsS_4 + (14-2x)OH^- = (3-x)Cu(OH)_2 + AsO_4^{3-} + 4S^o + 4H_2O + (11-x)e^- \quad [2]$$

$$Cu_2AsS_4 + 12OH^- = 2Cu(OH)_2 + AsO_4^{3-} + 4S^o + 4H_2O + 9e^- \quad [3]$$

$$CuAsS_4 + 10OH^- = Cu(OH)_2 + AsO_4^{3-} + 4S^o + 4H_2O + 7e^- \quad [4]$$

$$Cu_3AsS_4 + 46OH^- = 3Cu(OH)_2 + AsO_4^{3-} + 4SO_4^{2-} + 20H_2O + 35e^- \quad [5]$$

Reaction [1] represents weak surface oxidation at low applied anodic potential, while reaction [5] describes strong surface oxidation at high applied potential, i.e., the complete decomposition of

enargite by oxidation. The intermediate reactions given by Eqs. [3] and [4] can contain products of sulfur of oxidation state higher than zero-valence (elemental) sulfur as described. The main difference at lower and high potentials is the number of OH^- ions involved in the reactions. At high potential (+1074 mV) SO_4^{2-} ions are present, possibly as $CuSO_4$ (Guo and Yen 2008).

In order to identify the surface species present under oxidizing conditions at each of the applied potentials identified in the CV and represented by the proposed reaction mechanisms shown in equations [1] to [5], XPS was used to investigate the enargite surface after treatment at those potentials. The following sections describe and discuss the XPS results obtained for the enargite surface oxidized under each of five experimental conditions in pH 10 buffer solution, using anodic potentials of +347, +516, +705, +869 and +1100 mV, corresponding to the current peaks identified in the CV measurements.

4.3. Surface Species of Oxidized Enargite at Peak 1 (+347 mV)

According to the reaction mechanism proposed by Guo and Yen (2008) (reaction [1]) the principle effect of oxidation at 347 mV is the dissolution of Cu^{++} ions into solution leaving metal deficient sulfide, and the formation of $Cu(OH)_2$ deposited at the surface. Thus evidence of the presence of Cu(II) would be expected in the XPS data to confirm this. Figure 3 shows the XPS photoelectron spectra recorded from this surface, while the binding energies are included in Table 2.

Compared to the fresh surface, enargite oxidized at +347 mV shows the early stages of surface changes. The BE of Cu is unchanged, indicative of a lack of chemical alteration, however the relative atomic concentration decreased from 27.1% at the unoxidized surface, to 19.1%. The Cu 2p spectra is characteristic of Cu(I) species and shows no evidence of the presence of any Cu(II) compounds. Additional changes include the identification of a second sulfur species, as well as two additional oxygen species. This suggests partial dissolution of Cu from the surface into solution as the primary reaction mechanism.

The presence of an O 1s peak at 531.1 eV is suggestive of the presence of hydroxide species such as $Cu(OH)_2$ (Deroubaix and Marcus 1992, McIntyre et al. 1981), or copper oxide, such as Cu_2O (Ertl et al. 1980) however the absence of any correlating Cu species, combined with the low atomic concentration of oxygen at this BE makes any firm conclusion in this regard tenuous at best.

Examination of the S 2p photoelectron spectra reveals the formation of a second, minor sulfur component shifted 1.2 eV higher in binding energy, with the S $2p_{3/2}$ component at 162.9 eV. This represents a significant shift above the S $2p_{3/2}$ component of enargite at 161.7 eV. Possible compounds of copper that correspond to this S $2p_{3/2}$ BE include CuS (covellite) (Brion 1980, Perry and Taylor 1986) and Cu_2S (chalcocite). Another possibility is the formation of sulfur-arsenic

compounds such as As_2S_3 (orpiment), where the S component would be expected at 162.8 eV (Petkov et al. 1994).

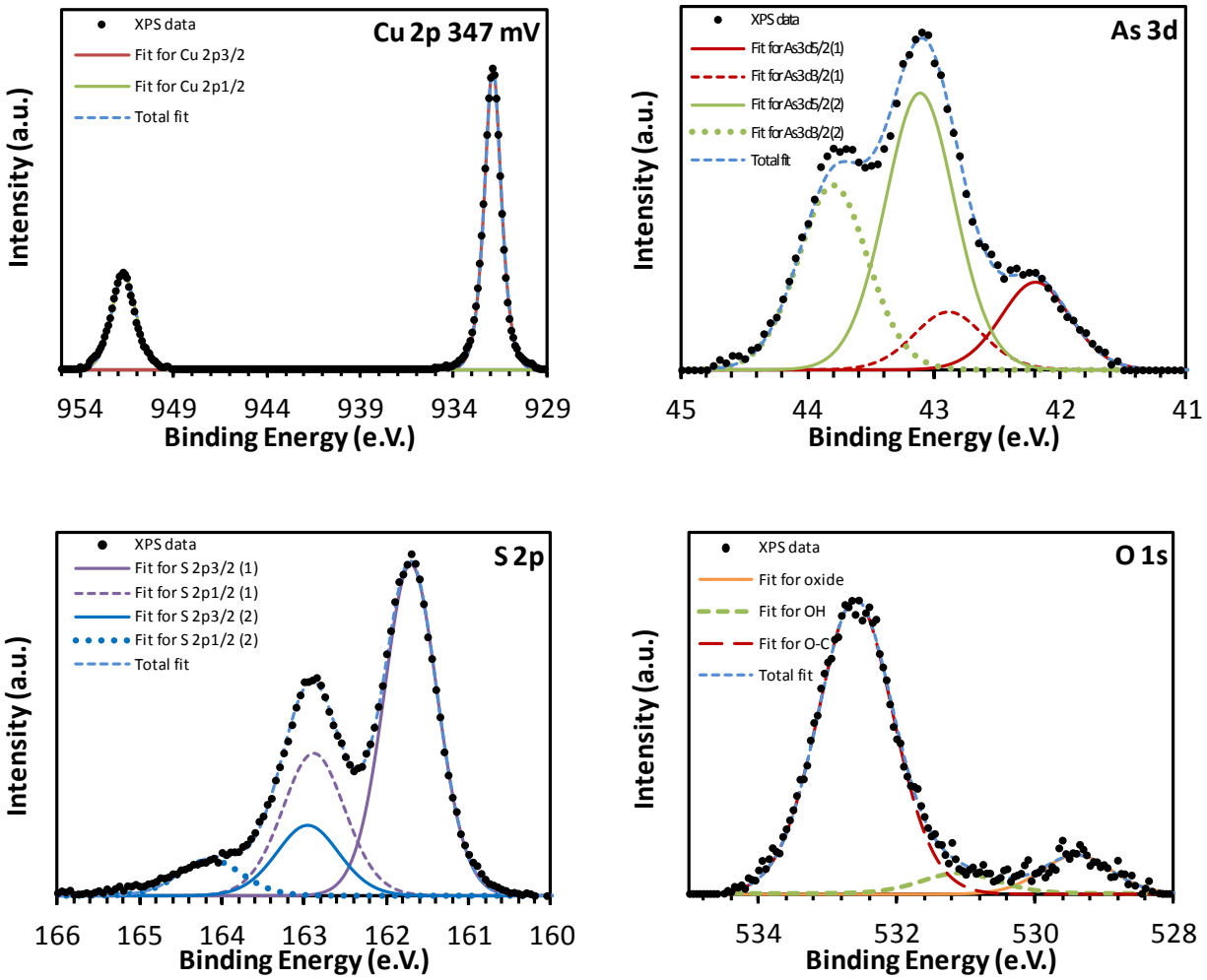

Figure 3. Cu 2p, As 3d, S 2p and O 1s high resolution photoelectron spectra recorded from the enargite electrode surface at -130 °C after application of +347 mV at pH 10.

Again, the existence of these compounds is not supported by the Cu spectrum, where a Cu $2p_{3/2}$ spectrum around 935 eV for CuS (Nefedov et al. 1980), and 935.1 eV for $Cu(OH)_2$ (McIntyre et al. 1981) would be expected. Metal-deficient sulfide or disulfide may be considered, and these species have been identified at about 162 eV (Fullston et al. 1999) but this may be too low in BE to represent the S 2p species detected here. A more likely explanation is the presence of polysulfides (S_n^{2-}), a reasonable proposition given the Cu depletion, which are known to be found in the BE range of 162.0 – 163.6 eV (Smart et al. 1999).

Table 2. Binding energies, full width half-maxima and atomic concentrations of the elements identified on the enargite surface at -130 °C after application of +347 mV at pH 10.

	B.E.	FWHM	Atom %
Cu $2p_{3/2}$	931.9	1.1	14.9
Cu $2p_{1/2}$	951.7	1.6	4.2
O 1s	529.4	1.2	1.1
O 1s ex OH	531.1	1.3	0.6
O 1s O-C	532.6	1.3	8.6
C 1s C-C ref	284.8	1.2	16.8
C 1s C-O-C	286.3	1.3	18.7
S $2p_{3/2}$ (1)	161.7	0.8	15.6
S $2p_{1/2}$ (1)	162.9	0.9	7.8
S $2p_{3/2}$ (2)	162.9	0.9	3.6
S $2p_{1/2}$ (2)	164.1	0.9	1.8
As $3d_{5/2}$ (surface)	42.2	0.7	0.9
As $3d_{3/2}$ (surface)	42.9	0.7	0.6
As $3d_{5/2}$ (bulk)	43.1	0.7	2.9
As $3d_{3/2}$ (bulk)	43.8	0.7	2.0

Considering the proposed reaction [1], the formation of copper-deficient sulfide is supported by the XPS data ($Cu_{3-x}AsS_4$), but not the presence of $Cu(OH)_2$ on the surface, where a Cu(II) peak around 935 eV (McIntyre et al. 1981) would be expected. However XPS provides no information about composition of the surrounding solution. Previously published thermodynamic data (Plackowski et al. 2013), shown in Appendix 1, predicts the presence of $Cu(OH)_2$, $HAsO_3^-$ and SO_4^{2-} species at pH 10, in which case the possible mechanism may be better represented by reaction [6], where OH^- ions as well as S and As species are included.

$$Cu_3AsS_4 + 45OH^- = 3Cu(OH)_2 + HAsO_4^{2-} + 4SO_4^{2-} + 19H_2O + 35e^- \qquad [6]$$

Such a prediction is useful to provide a point of reference over wide ranging conditions. However, it does not predict the kinetic behaviour of copper sulfide electrodes accurately. Evidence for this is seen in the potential-pH diagram for the thermodynamic systems shown in Appendix 1, where strong oxidation of enargite involving the dissolution of enargite and the formation of cuprous species, sulfate species and arsenate species is seen. It shows a very similar result to that of Asbjornsson et al (2004) in a thermodynamic analysis of the Cu-As-S-Cl-H_2O system at 298 K. However no evidence of changes in the As photoelectron spectrum are evident, with a (insignificant) 0.1 eV BE change compared to the unoxidised control, and an alternative reaction mechanism may need to be considered. This reaction may take the form of Eq. [7] shown below.

$$Cu_3AsS_4 = Cu_{3-x}AsS_4 + xCu^{2+}_{(aq)} + 2xe^- \qquad [7]$$

Considering the lack of additional Cu(II) species identified by XPS, combined with the loss of Cu at the surface, reaction [1] may be better expressed as shown in equation [7], where the Cu(II) species is represented as aqueous ions in the surrounding solution. This equation is in agreement with that of Guo and Yen (2008).

4.4. Surface Species of Oxidized Enargite at Peak 2 (+516 mV)

Increasing the oxidation potential to 516 mV produces very little change to the resulting XPS photoelectron spectra, as depicted in Figure 4. Binding energies are presented in Table 3. No evidence of Cu(II) species on the surface exists, the Cu $2p_{3/2}$ BE remains relatively unchanged at 932.1 eV, however the relative proportion of Cu has decreased further to 9.4%. The As 3d spectra is also relatively unchanged except for a 0.3 eV shift higher in the BE range.

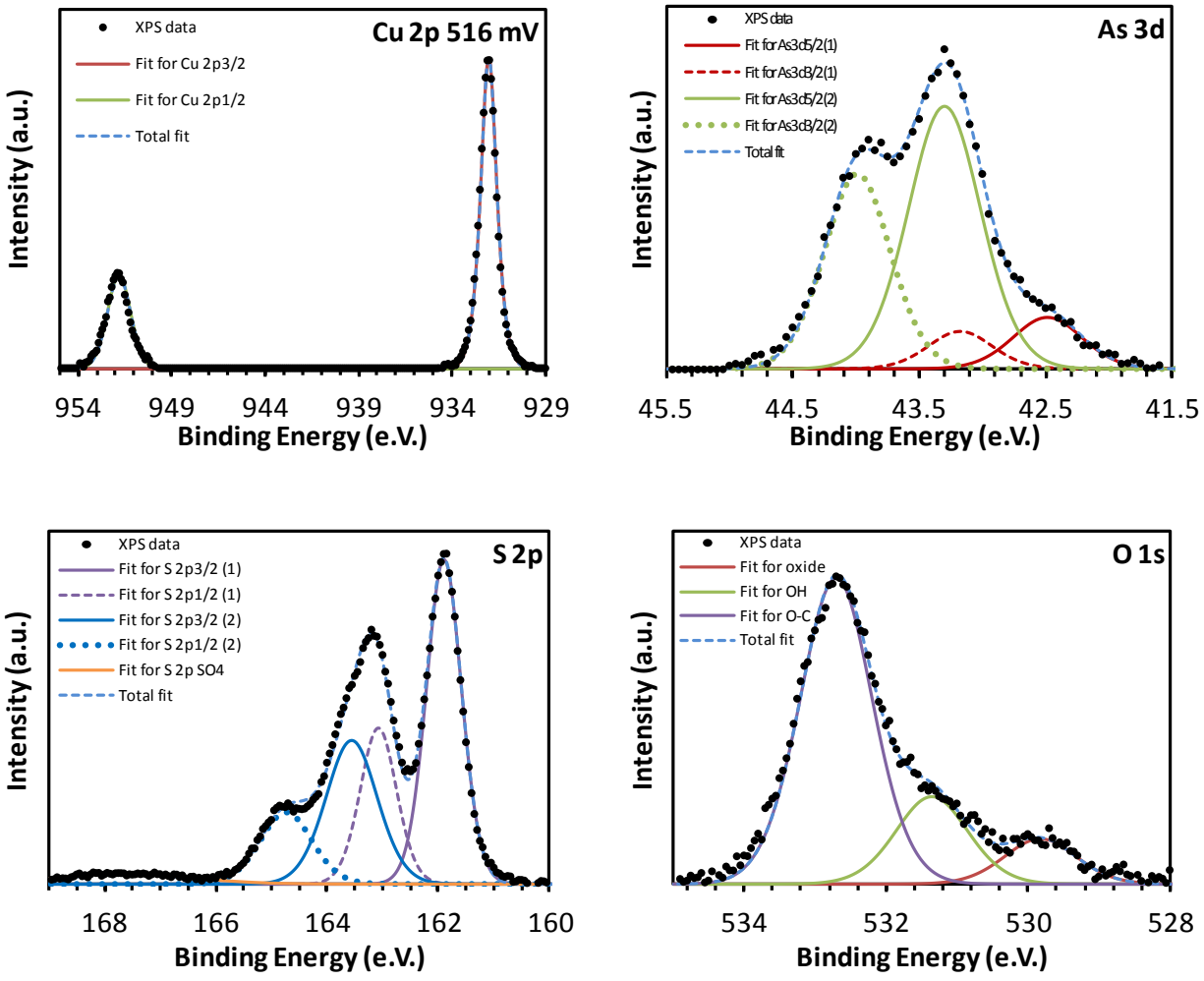

Figure 4. Cu 2p, As 3d, S 2p and O 1s high resolution photoelectron spectra recorded from the enargite electrode surface at -130 °C after application of +516 mV at pH 10.

The S 2p spectrum shows a relative increase in the proportion of the high BE component, which is now shifted about 0.7 eV higher to 163.6 eV for the S $2p_{3/2}$ component, compared to 162.9

eV where oxidation was carried out at +347 mV. However, it remains within the range where polysulfides (S_n^{2-}) may be expected, and represents a relatively higher proportion of the S 2p spectrum. When considered along with the relative decrease in Cu at the surface, these results are consistent with a greater extent of Cu dissolution and formation of polysulfide at the surface.

A significant change from the previous potential is the presence of a new broad S 2p peak at 167.7 eV representing a 1.2% contribution to the identified surface species. This BE is characteristic of the presence of sulfate (SO_4) species and, combined with the O 1s peak at 532.7 eV (Strohmeier et al. 1985), correlates with the presence of $CuSO_4$. However for definitive identification of this compound the presence of a Cu $2p_{3/2}$ peak at around 934.9 eV is required (Klein et al. 1984, Klein et al. 1983), which clearly is not present. Given the relatively low (1.2%) proportion of S 2p (SO_4) detected, it is possible any Cu(II) species are obscured by other compounds present, or constitute a very minor contribution, possibly below the detection limit of the equipment.

Table 3. Binding energies, full width half-maxima and atomic concentrations of the elements identified on the enargite surface at -130 °C after application of +516 mV at pH 10

	B.E.	**FWHM**	**Atom %**
Cu $2p_{3/2}$	932.1	1.0	7.4
Cu $2p_{1/2}$	951.9	1.5	2.0
O 1s	529.8	1.2	1.3
O 1s ex OH	531.4	1.2	2.4
O 1s (SO_4) O-C	532.7	1.2	8.5
C 1s C-C ref	284.8	1.2	24.6
C 1s C-O-C	286.4	1.3	20.4
S $2p_{3/2}$ (1)	161.9	0.7	11.0
S $2p_{1/2}$ (1)	163.1	0.8	5.5
S $2p_{3/2}$ (2)	163.6	1.1	7.1
S $2p_{1/2}$ (2)	164.7	1.1	3.5
S 2p SO_4	167.7	2.8	1.2
As $3d_{5/2}$ (1)	42.5	0.6	0.5
As $3d_{3/2}$ (1)	43.2	0.6	0.3
As $3d_{5/2}$ (2)	43.3	0.6	2.5
As $3d_{3/2}$ (2)	44.0	0.6	1.7

Considering reaction [2] in the context of the previous discussion of oxidation at +347 mV, and the XPS data for +516 mV, there is no support for the presence of Cu(II) species on the surface, nor the presence of elemental sulfur, which would require the presence of a S $2p_{3/2}$ peak in the BE range 163.5 to 163.9 eV (Buckley and Woods 1984, Hampton et al. 2011, Wittstock et al. 1996). In

addition there is no evidence to support the presence of arsenic oxides on the mineral surface. In this case a mechanism such as that shown in reaction [8], incorporating Cu and As species as aqueous ions, and polysulfide species in place of elemental sulfur, may be considered.

$$nCu_2AsS_4 + 8nOH^- = 2nCu^{2+} + nAsO_4^{3-} + 4S_n^{2-} + 4nH_2O + ne^- \quad [8]$$

However this does not account for the presence of sulfate (SO_4) species in the XPS photoelectron spectra of sulfur, and indeed it may be that one reaction mechanism is not sufficient to account for all the species detected.

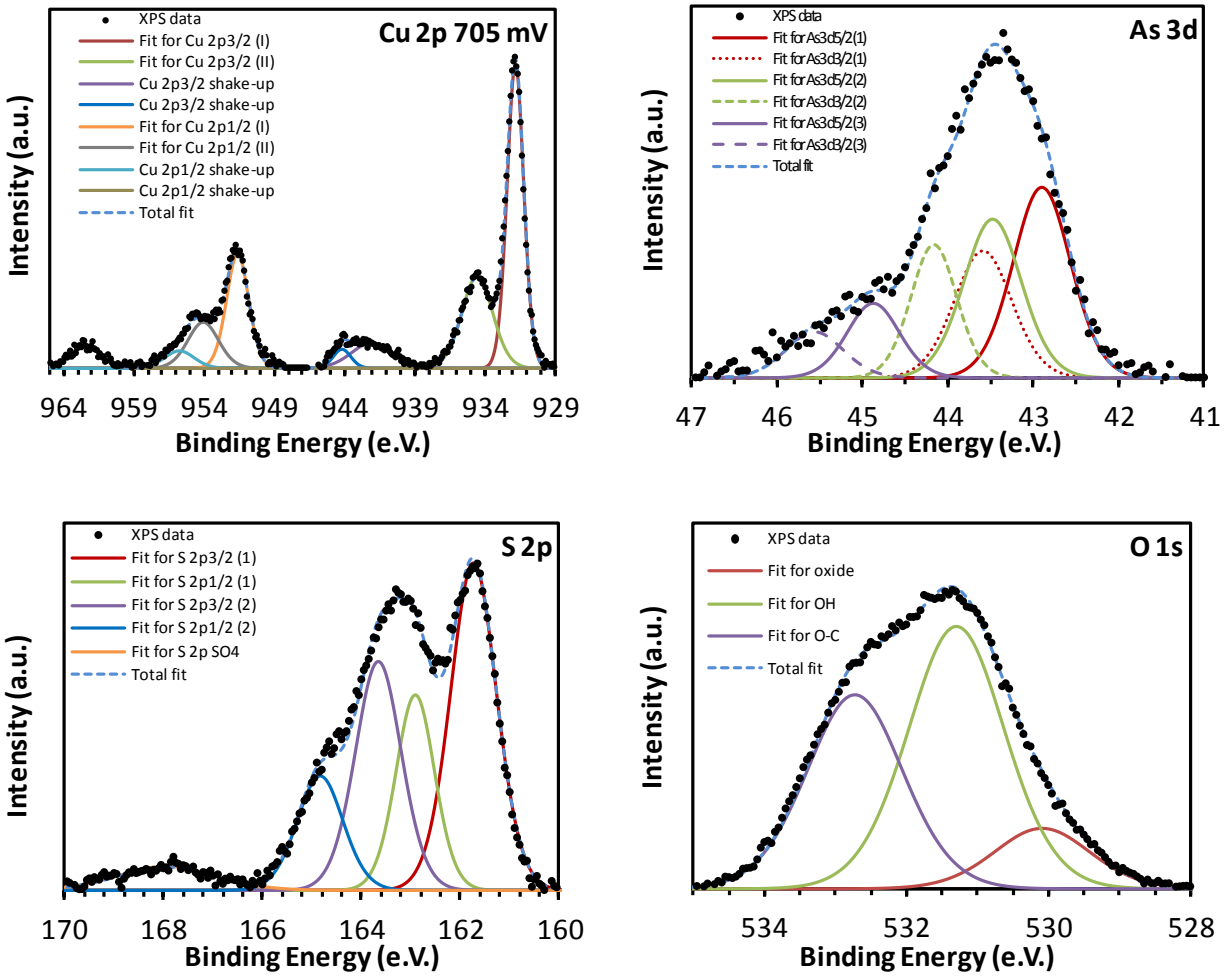

Figure 5. Cu 2p, As 3d, S 2p and O 1s high resolution photoelectron spectra recorded from the enargite electrode surface at -130 °C after application of +705 mV at pH 10.

4.5. Surface Species of Oxidized Enargite at Peak 3 (+705 mV)

At +705 mV a very different picture emerges, with clear changes in the photoelectron spectra of all the elements under consideration. The Cu 2p spectrum clearly shows the presence of both a low BE Cu(I) species (931.8 eV) and high BE Cu(II) species (934.6 eV), as well as the associated

shake-up peaks characteristic of Cu(II) compounds where the shake-up structure is clearly visible. Both the Cu $2p_{3/2}$ and Cu $2p_{1/2}$ spectra are shown (Figure 5). Binding energies are given in Table 4.

These "shake-up" peaks occur as a part of the photoionization process, which results in the emission of a photoelectron from an ion. It is possible that excitation by the outgoing photoelectron can leave the ion in an energy state a few eV above the ground state. As energy is transferred to the ion, the kinetic energy of the emitted photoelectron is reduced, and these low-energy electrons will be seen as a "shake-up" peak at a higher BE than the main peak.

Table 4. Binding energies, full width half-maxima and atomic concentrations of the elements identified on the enargite surface at -130 °C after application of +705 mV at pH 10.

	B.E.	**FWHM**	**Atom %**
Cu $2p_{3/2}$ (I)	931.8	1.4	4.0
Cu $2p_{3/2}$ (II) (SO_4)	934.6	2.6	2.3
Cu $2p_{3/2}$ (shake-up)	942.1	3.4	0.8
Cu $2p_{3/2}$ (shake-up)	944.2	1.5	0.3
Cu $2p_{1/2}$ (I)	951.6	1.9	1.3
Cu $2p_{1/2}$ (II) (SO_4)	954.1	2.6	0.7
Cu $2p_{1/2}$ (shake-up)	955.8	2.5	0.3
Cu $2p_{1/2}$ (shake-up)	962.5	2.4	0.3
O 1s M-O metal oxide	530.1	1.6	3.4
O 1s ex OH	531.3	1.6	15.0
O 1s (SO_4) (O-C)	532.7	1.6	11.1
C 1s C-C ref	284.8	1.4	19.5
C 1s C-O-C	286.4	1.4	17.1
C 1s C=O	287.9	1.4	2.7
S $2p_{3/2}$ (1)	161.7	1.1	6.7
S $2p_{1/2}$ (1)	162.9	0.9	3.4
S $2p_{3/2}$ (S_n^{2-})	163.7	1.1	4.7
S $2p_{1/2}$ (S_n^{2-})	164.8	1.1	2.4
S 2p SO_4	168.0	2.3	1.0
As $3d_{5/2}$ (surface)	42.9	0.8	0.8
As $3d_{3/2}$ (surface)	43.6	0.8	0.6
As $3d_{5/2}$ (bulk)	43.5	0.8	0.7
As $3d_{3/2}$ (bulk)	44.2	0.6	0.5
As $3d_{5/2}$ (oxide?)	44.9	0.7	0.3
As $3d_{3/2}$ (oxide?)	45.6	0.8	0.2

The Cu $2p_{3/2}$ peak at 934.6 eV is indicative of the presence of $CuSO_4$ (Klein et al. 1984, Klein et al. 1983), and combined with the presence of the S 2p peak at 168.0 eV and O 1s at 532.7 eV (Strohmeier et al. 1985), with the latter now representing a significantly increased contribution at 11.1%, the necessary confirmation of the presence of this compound is obtained.

At 931.8 eV the Cu $2p_{3/2}$ peak could be indicative of CuS (Bhide et al. 1981, Nakai et al. 1978) but its presence is not supported by a corresponding S 2p peak. If CuS was a significant surface compound, a S 2p peak at about 162.6 – 162.7 eV would be expected (Brion 1980, Perry and Taylor 1986). According to published data, the BE range for Cu in CuS is broad, ranging from 931.8 eV (Bhide et al. 1981) to as high as 935.0 eV (Nefedov et al. 1980), thus requiring the existence of a corresponding S 2p peak to confirm its presence, which is not found here.

The presence of polysulfide is again indicated by the S $2p_{3/2}$ peak identified at 163.7 eV and, combined with the reduction of Cu at the surface to 10%, similar to the proportion found for +516 mV, suggests this interpretation to be reasonable. The S 2p spectrum also indicates that the relative proportion of polysulfide in the enargite matrix compared to the contribution of sulfur has increased, from a ratio of 1.6:1($S : S_n^{2-}$) at +516 mV to 1.4:1 at +705 mV.

The arsenic spectrum now shows the presence of an additional As 3d doublet with the 5/2 component situated at 44.9 eV, corresponding to arsenic oxide, or As_2O_3 (King et al. 1990) or As_2S_5 (Stec et al. 1972), however no corresponding oxygen or sulfur peak is evident. Considering that the relative atomic proportion of this arsenic species was determined to be low at 0.5%, close to the detection limit of the equipment, caution in the interpretation of these results is required.

The formation of $Cu(OH)_2$ is also supported, both by Cu and O binding energies. Copper in $Cu(OH)_2$ can range from 932.7 eV (Deroubaix and Marcus 1992) to 935.1 (McIntyre et al. 1981) and, with the Cu 2p3/2 peak at 934.6 eV the presence of the hydroxide species is indicated. The O 1s peak at 531.1 eV provides the necessary confirmation that copper hydroxide exists on the surface.

Although the formation of elemental sulfur is predicted by reaction [3] this species is not expected to form in a system oxidized at pH 10. Electrochemical oxidation of enargite at low pH is typified by Cu dissolution and the formation of native sulfur, while at high pH sulfur is expected to oxidize to polysulfide (S_n^{2-}), sulfite (SO_3^{2-}) then sulfates (SO_4^{2-}) (Lattanzi et al. 2008). In a previous study of enargite oxidation at pH 10 and 4, and +869 mV (Plackowski et al. 2013) the presence of elemental sulfur at pH 4 was confirmed by comparing the S 2p photoelectron spectra obtained at below -130 °C with that resulting from the same surface after warming to 30 °C. No evidence of S^0 was found at pH 10.

Considering reaction [3] in light of the XPS evidence discussed above, alterations to this reaction mechanism must be considered. In this case the following mechanism may be proposed, where elemental sulfur is replaced by polysulfide and copper hydroxide and sulfates are included.

$$Cu_2AsS_4 + 18OH^- = Cu(OH)_2 + CuSO_4 + AsO_4^{3-} + 3S_n^{2-} + 8H_2O + 9e^- \qquad [9]$$

Although the As 3d spectra supports the presence of arsenic oxides or sulfides, it is not confirmed by either the O or S spectra, hence in reaction [9] it remains as an ionic aqueous species.

4.6. Surface Species of Oxidized Enargite at Peak 4 (869 mV)

In a previous paper (Plackowski et al. 2013) the effects of electrochemical oxidation in a pH 10 solution were investigated at an applied potential of +869 mV. In the present work similar results were found at this potential.

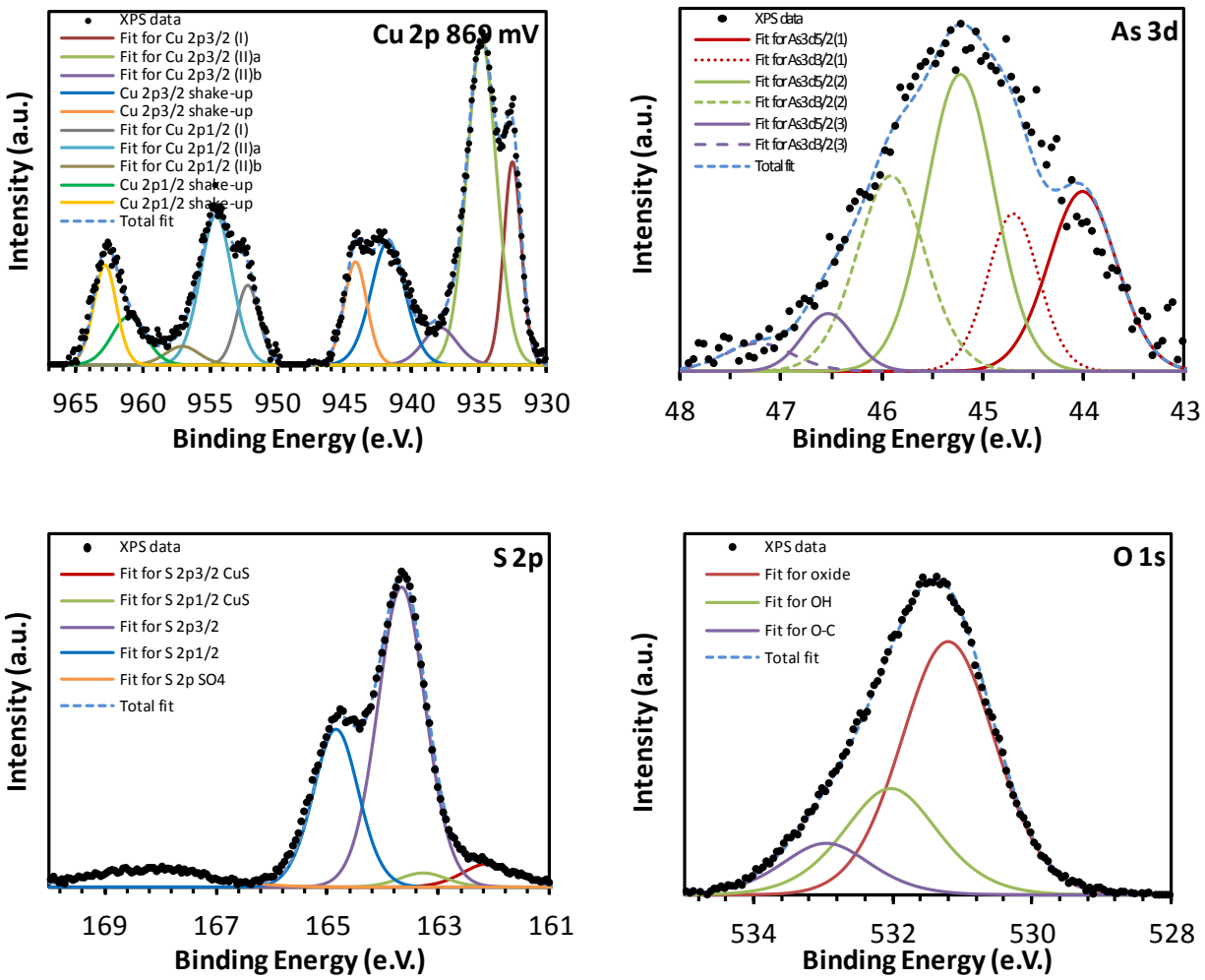

Figure 6. Cu 2p, As 3d, S 2p and O 1s high resolution photoelectron spectra recorded from the enargite electrode surface at -130 °C after application of +869 mV at pH 10.

After treatment the surface was found to be heavily oxidized, with the formation of a Cu 2p spectra characteristic of the presence of Cu(II) species, a broadening and shift of the As $3d_{5/2}$ peak to 45.2 eV, suggesting As_2O_3 formation (Velasquez et al. 2000), and a shift of the S $2p_{3/2}$ peak to 163.9 eV (Figure 6). In addition a peak at 168.2 eV is present, which is attributable to the formation of $CuSO_4$ at the surface (Velasquez et al. 2000). Binding energy data are given in Table 5.

An interesting change compared to the previous treatment condition (+705 mV) is the absence of the S 2p doublet previously identified as indicative of the presence of sulfur in the enargite matrix exposed at the surface, although a polysulfide phase (S_n^{2-}) remains with the S $2p_{3/2}$ component at 163.7 eV. The S 2p spectrum also shows what appears to be a low binding energy shoulder at 162.1 eV which can be fitted with an additional S 2p doublet which at that binding energy corresponds to CuS (Brion 1980, Perry and Taylor 1986).

Table 5. Binding energies, full width half-maxima and atomic concentrations of the elements identified on the enargite surface at -130 °C after application of +869 mV at pH 10.

	B.E.	**FWHM**	**Atom %**
Cu $2p_{3/2}$ (I)	932.5	1.6	1.4
Cu $2p_{3/2}$ (II)a CuS	934.8	2.6	3.8
Cu $2p_{3/2}$ (II)b	937.9	3.0	0.5
Cu $2p_{3/2}$ (shake-up)	941.8	3.0	1.7
Cu $2p_{3/2}$ (shake-up)	944.2	2.0	0.9
Cu $2p_{1/2}$ (I)	952.2	2.0	0.7
Cu $2p_{1/2}$ (II)a CuS	954.6	2.8	1.9
Cu $2p_{1/2}$ (II)b	957.1	3.0	0.3
Cu $2p_{1/2}$ (shake-up)	961.1	3.0	0.7
Cu $2p_{1/2}$ (shake-up)	962.9	2.0	0.9
O 1s	531.2	1.6	20.8
O 1s	532.0	1.6	8.9
O 1s	533.0	1.5	4.1
C 1s C-C ref	284.8	1.3	14.3
C 1s C-O-C	286.3	1.3	7.2
C 1s C=O	288.2	1.3	3.7
S $2p_{3/2}$ (1) CuS	162.1	1.1	1.2
S $2p_{1/2}$ (1) CuS	163.3	1.0	0.6
S $2p_{3/2}$ (2) (S_n^{2-})	163.7	1.0	14.5
S $2p_{1/2}$ (2) (S_n^{2-})	164.9	1.0	7.3
S 2p SO_4	168.2	2.4	2.1
As $3d_{5/2}$ (1) (Surface)	44.0	0.8	0.5
As $3d_{3/2}$ (1) Surface)	44.7	0.6	0.4
As $3d_{5/2}$ (2) (Bulk)	45.2	0.8	0.9
As $3d_{3/2}$ (2) (Bulk)	45.9	0.8	0.6
As $3d_{5/2}$ (oxide)	46.5	0.6	0.1
As $3d_{3/2}$ (oxide)	47.2	0.8	0.1

The Cu $2p_{3/2}$ peak at a BE of 934.8 eV corresponds to published data for Cu in CuS (Nefedov et al. 1980). Combined with the S 2p peak at 162.1 eV the necessary confirmation of the presence of CuS on the enargite surface is obtained. However it must be noted that the relative concentration

of these elements is low, hence CuS can be considered to represent a relatively minor contribution to surface species.

This Cu $2p_{3/2}$ BE can also be ascribed to $CuSO_4$ (Klein et al. 1984) and the presence of this compound is also confirmed by the S 2p peak at 168.2 eV, characteristic of sulfate species (Klein et al. 1984, Klein et al. 1983).

A second Cu(II) peak identified as Cu $2p_{3/2}$ with a BE of 937.9 eV has also been found, and could not be identified by reference to published data. This value is high even for Cu(II) species and does not seem to correlate with any compound that might reasonably be expected to exist in this system. It is possible that it represents a fitting error and should in reality be closer to 936.9 eV, which would identify it as Cu(II) in $CuSO_4$ (Strohmeier et al. 1985). Unlike the surface treated at +705 mV, the presence of $Cu(OH)_2$ is not supported by the data for Cu, although the O 1s peak at 531.2 eV is correct for this species. It may be that at this higher potential, the formation of $CuSO_4$ dominates the surface layer composition in terms of Cu species.

Further investigation of the arsenic spectrum reveals the presence of three doublets with As $3d_{5/2}$ components located at 44.0, 45.2 and 46.5 eV. The peak at 44.0 eV is indicative of As_2O_3 (Epp and Dillard 1989, Leonhardt et al. 1973), at 45.2 eV both As_2O_3 (King et al. 1990, Hollinger et al. 1994) and As_2O_5 (Cossu et al. 1992), and at 46.5 eV both As_2O_3 (Stec et al. 1972) and As_2O_5 (Hollinger et al. 1994), depending on which of the several published references is considered most applicable. What these references do show however, is the inherent variability in BE that may be seen for these arsenic oxides, and the significant overlap in the BE ranges in which their respective peaks may appear.

Further evidence can be sought from the O 1s spectra, and the peak at 532.0 eV can be ascribed to the presence of both forms of arsenic oxide, according to Mizokawa et al. (1978), while Hollinger et al. (1994) places O in As_2O_3 at 531.9 eV, and in As_2O_5 at 532.4 eV, in which case the presence of As_2O_3 is supported. While the specific form of arsenic oxide on the surface of enargite that has been oxidized at +869 mV may not be clear due to the degree of overlap of BE ranges and lack of resolving power of conventional XPS techniques, it is clear that arsenic at the surface has been oxidized to a significant degree.

With these findings in mind, and considering the thermodynamic data presented in Appendix 3, a more suitable form of reaction [4] may be expressed by the following mechanism:

$$Cu_3AsS_4 + 45OH^- = 3Cu(OH)_2 + HAsO_4^{2-} + 4SO_4^{2-} + 19H_2O + 35e^- \qquad [10]$$

Here both As and S species are shown as aqueous ions since this is supported by the thermodynamic data, although it would also be reasonable to show the presence of $CuSO_4$ and arsenic oxides such as As_2O_3 as compounds present on the surface.

4.7. Surface Species of Oxidized Enargite at Peak 5 (+1100 mV)

Compared to oxidation at +869 mV, when the XPS photoelectron spectra for the enargite surface oxidized at +1100 mV are examined (Figure 7), relatively little evidence of further change exists and the species identified are largely the same.

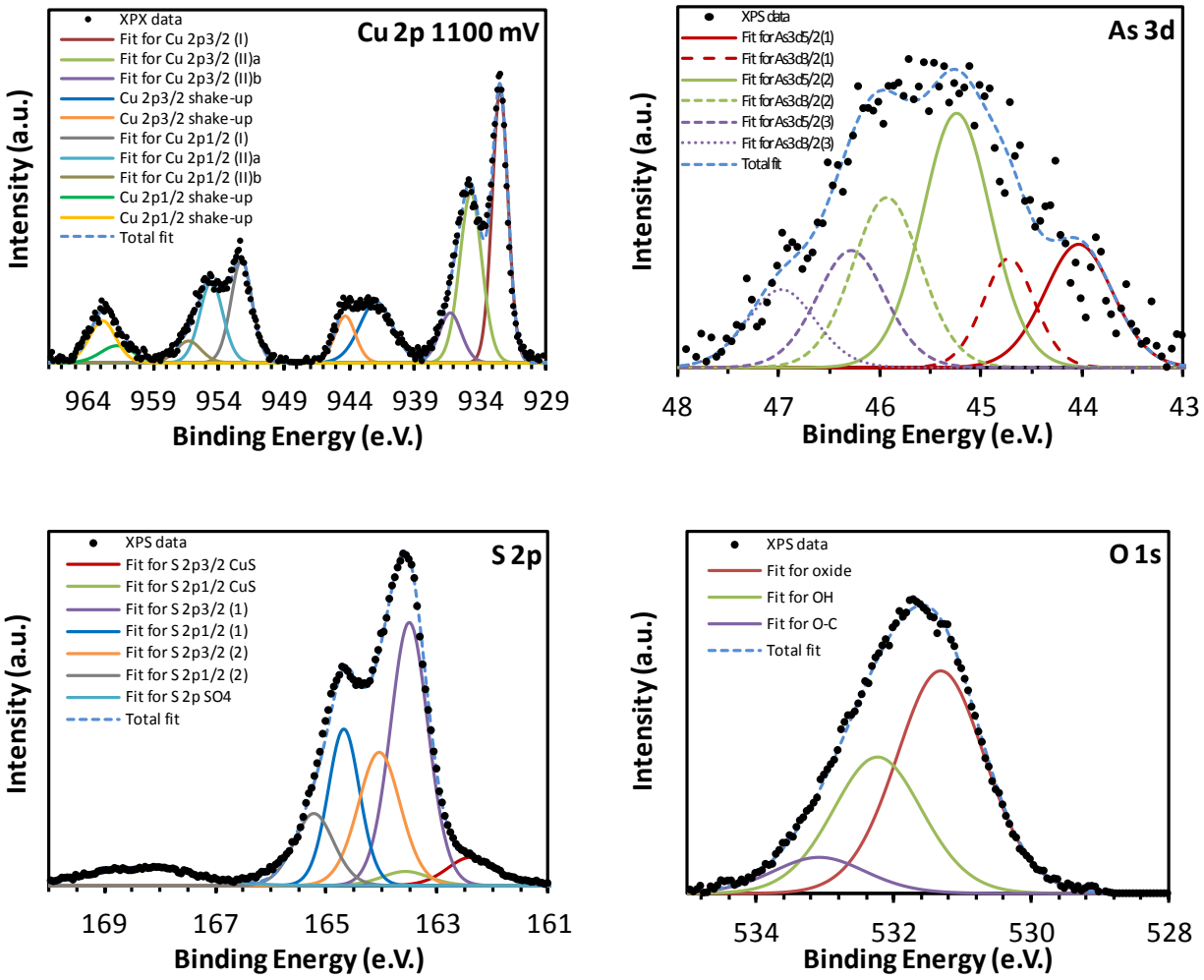

Figure 7. Cu 2p, As 3d, S 2p and O 1s high resolution photoelectron spectra recorded from the enargite electrode surface at -130 °C after application of +1100 mV at pH 10.

However notable differences are to be seen in the Cu spectra, where the second Cu(II) peak has now been identified at a BE of 936.4 eV for the Cu $2p_{3/2}$ component, with fits well with published data for Cu in $CuSO_4$. Binding energies are given in Table 6.

In addition, examination of the S 2p spectrum reveals the presence of two main S $2p_{3/2}$ components at 163.5 and 164.1 eV, corresponding to polysulfide (S_n^{2-}) and S_n^{2-}/S^0 respectively,

while the high BE peak at 168.3 eV ($CuSO_4$) and low BE shoulder at 162.4 (CuS) remain unchanged. The As and O photoelectron spectra are unchanged in terms of the number of peaks and their relative intensities, where the shift in BE's is of the order of 0.1-0.3 eV, which is not considered significant.

Table 6. Binding energies, full width half-maxima and atomic concentrations of the elements identified on the enargite surface at -130 °C after application of +1100 mV at pH 10.

	B.E.	**FWHM**	**Atom %**
Cu $2p_{3/2}$ (I)	932.5	1.4	2.3
Cu $2p_{3/2}$ (II)a	934.8	2.0	2.0
Cu $2p_{3/2}$ (II)b	936.4	2.0	0.6
Cu $2p_{3/2}$ (shake-up)	942.0	3.0	1.1
Cu $2p_{3/2}$ (shake-up)	944.4	1.9	0.5
Cu $2p_{1/2}$ (I)	952.4	1.9	1.1
Cu $2p_{1/2}$ (II)a	954.7	2.1	1.0
Cu $2p_{1/2}$ (II)b	956.4	2.3	0.3
Cu $2p_{1/2}$ (shake-up)	961.9	3.0	0.3
Cu $2p_{1/2}$ (shake-up)	963.0	2.4	0.6
O 1s	531.3	1.5	15.0
O 1s	532.3	1.5	9.2
O 1s	533.1	1.6	2.5
C 1s C-C ref	284.8	1.3	12.3
C 1s C-O-C	286.3	1.3	8.4
C 1s C=O	288.0	1.3	1.6
S $2p_{3/2}$ (1) CuS	162.4	1.0	1.9
S $2p_{1/2}$ (1) CuS	163.6	1.0	1.0
S $2p_{3/2}$ (2) (S_n^{2-})	163.5	0.8	14.3
S $2p_{1/2}$ (2) (S_n^{2-})	164.7	0.7	7.2
S $2p_{3/2}$	164.1	0.9	8.2
S $2p_{1/2}$	165.2	0.8	4.1
S 2p SO_4	168.3	2.1	2.7
As $3d_{5/2}$ (1) (Surface)	44.1	0.8	0.3
As $3d_{3/2}$ (1) Surface)	44.7	0.6	0.2
As $3d_{5/2}$ (2) (Bulk)	45.3	0.8	0.7
As $3d_{3/2}$ (2) (Bulk)	45.9	0.8	0.4
As $3d_{5/2}$ (oxide)	46.3	0.8	0.3
As $3d_{3/2}$ (oxide)	47.0	0.8	0.2

A notable difference is the presence of the high BE S 2p doublet, the S $2p_{3/2}$ component of which is found at 164.1 eV, which was not present after oxidation at +859 mV. While this falls into the BE range where polysulfide would be expected, it is also in the range where elemental sulfur would appear if it were present. However this is not considered likely for a system at pH 10, as discussed previously, and a possible explanation is the formation of a sulfur species of a higher

oxidation state, as discussed by Lattanzi et al. (2008), where it may represent the presence of sulfite (SO_3^{2-}), although these authors did not specify a BE.

Given the relatively high applied potential it is reasonable to expect a greater degree of surface oxidation than was evident at the lower potentials discussed previously, since the system is now well outside the water stability region (as indicated by the thermodynamic data in Appendix 1). As a result the dissolution of Cu and As may be increased, in which case the proportion of S species at the surface may increase to such an extent that this species will tend to predominate as the breakdown of the enargite structure become more pronounced.

The following mechanism (reaction [11]) has been formulated based on the XPS findings, which provide the necessary confirmation of the presence of $CuSO_4$ and a form of arsenic oxide, most likely As_2O_3, as part of a layer deposited on the oxidized enargite surface.

$$2Cu_3AsS_4 + 3Cu^{2+}_{(aq)} + 74OH^- = Cu(OH)_2 + 8CuSO_4 + As_2O_3 + 37H_2O + 68e^- \qquad [11]$$

In this case the aqueous species identified in the thermodynamic data have been neglected in favor of these copper and arsenic compounds, as at this potential complete decomposition of enargite by oxidation is likely (Guo and Yen 2008). This contention is supported by ICP analysis of the change in solution concentration of Cu, As and S, described in the following section, as applied potential increases.

An overall comparison, by element, of the changes in binding energy and relative intensity of the photoelectron spectra as a function of applied potential, is given in Figures 11-14 of Appendix 4 for Cu, As, S and O. Clearly evident is the transition that occurs at some potential between + 516 and +705 mV. That this transition occurs at a relatively high potential suggests enargite is resistant to electrochemically induced oxidation. Furthermore the decrease in intensity of both the Cu and As photoelectron spectra, and to a lesser extent the O, without a significant change in S, may be interpreted as an increase in the relative proportion of S species at the surface compared to Cu and As. This provides support for the notion of a progressive oxidation process that involves dissolution of Cu and As, leaving a surface composed of metal-deficient sulfide or polysulfide, accompanied by the progressive deposition of a surface layer consisting of hydroxide and sulfates compounds and, at higher potentials (+869 and +1100 mV), the formation of CuS and As_2O_3.

4.8. ICP of CA Solutions

Although the proposed reaction mechanisms and the results of the XPS investigations of species present at the surface provide a good indication of surface changes, further confirmation can

be sought based on the measured concentrations of As, Cu, and S in the buffer solution after treatment.

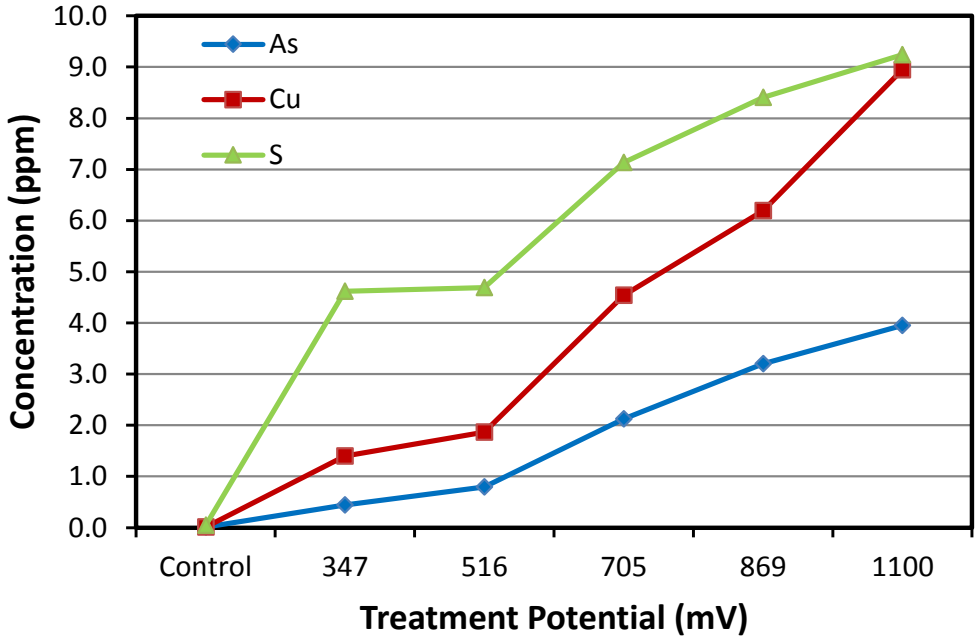

Figure 8. Solution concentration of As, Cu and S after application of selected treatment potentials for 30 minutes in pH 10 borate buffer solution. "Control" shows the (zero) concentration detected using a blank solution (water).

Figure 8 shows the variation in concentration according to the applied treatment potential. All solutions were collected after completion of surface preparation for XPS analysis using the previously described CA technique. The numerical data is shown in Appendix 6 and includes the measured concentration in parts per million (ppm) and the calculated molar concentration.

The measured concentrations are significantly lower than those assumed for the generation of the Eh/pH diagrams in Appendix 3, where the values for Cu, As and S were assigned as $3x10^{-3}$ M, $1x10^{-3}$ M and $4x10^{-3}$ M respectively. However when the lowest measured values of $2.2x10^{-5}$ M, $5.95x10^{-6}$ M and $1.4x10^{-4}$ M for Cu, As and S respectively, obtained for the surface treated at +347 mV, are specified as the molality in the HSC 7 software package and the Eh/pH diagrams recalculated (Appendix 5), no change in the species predicted to occur at pH 10 is found when compared to the data in Appendix 3.

In the preceding discussion it was shown that significant changes in the composition of surface species occurs when the oxidizing potential applied to the enargite surface is raised from +516 to +706 mV. The most obvious of these changes is the appearance of Cu(II) species, identified as copper sulfates and hydroxide, and the subsequent appearance of the copper sulfide CuS and

arsenic oxide As_2O_3 at higher applied potentials. Below +706 mV the principal reaction processes were determined to be dissolution of copper leaving a metal deficient surface, and the likely formation of polysulfide species.

Similarly these changes are reflected in the solution concentrations of Cu, As and S, with a step-change between +516 and +706 mV, accompanied by a significant increase in dissolution rate. This data is suggestive of the existence of a threshold potential, above which sufficient energy is applied to the system to enable oxidation and precipitation reactions to proceed at the mineral surface, resulting in the formation of Cu(II) compounds, copper sulfide species and oxides of arsenic.

5. Summary and Conclusions

Electrochemically controlled oxidation of natural enargite in a pH 10 buffer solution was investigated at potentials of +347, +516, +705, +869 and +1100 mV using XPS to identify the resulting surface species. At +347 and +516 mV the predominant changes were found to be dissolution of copper resulting in a Cu deficient surface, while no evidence of the formation of Cu(II) species predicted by other authors, such as hydroxides or sulfates, was found. This is in contrast to the findings of Guo and Yen (2008), who concluded that the first oxidation peak identified at +288 mV is a result of the oxidation of copper to Cu^{2+} which then precipitates as $Cu(OH)_2$ on the enargite surface. In the present work no evidence of the formation of Cu(II) compounds on the enargite surface was found after oxidation at applied potentials below +705 mV, and the principal mechanism at these lower potentials is considered to be dissolution of Cu leaving metal-deficient sulfide species at the enargite surface, and possibly the formation of polysulfide species.

The presence of sulfates (SO_4) species was first evident after oxidation at +516 mV and persisted for each applied potential above that, while additional S species (polysulfide) first appeared after oxidation at +705 mV. However no corresponding Cu species were detected to support the presence of a $CuSO_4$ surface layer. Formation of Cu(II) species was first identified on the surface after oxidation at +705 mV, and persisted as the oxidizing potential was increased to +869 and further to +1100 mV. The presence of both $CuSO_4$ and $Cu(OH)_2$ was confirmed after treatment at +705 mV, however the hydroxide species was not found on the surface after treatment at higher potentials. In its place, CuS was confirmed, and the presence of an arsenic oxide, most likely As_2O_3, was also detected.

Thermodynamic data (Appendix 3) supports the formation of both copper hydroxide and sulfate species at pH 10 above about +100 mV, while $HAsO_4^{2-}{}_{(aq)}$ is predicted above about +200

mV. The XPS data has been found to support the presence of both these copper species, while although As oxides are shown to exist, the precise form they take is not so obvious. The presence of both As_2O_3 and As_2O_5 was found to be supported by the As 3d and O 1s BE data although the former is considered more likely.

Appendix 4 show the photoelectron spectra for Cu, As, S and O for each of the applied potentials, enabling the shift in BE with increasingly anodic potential, as well as the change in relative proportion of each component, to be compared directly for each element. This shows that after +705 mV, there is a significant decrease in the intensity of both Cu and As, and to a lesser extent O, while the change in S is limited by comparison. This may be interpreted as indicative of an increase in the proportion of S species at the surface relative to Cu and As, and provides support for the proposition of an oxidation process that involves the progressive dissolution of Cu and As leaving a metal-deficient sulfide or polysulfide surface layer, accompanied by the progressive deposition of a surface layer consisting of sulfates and, at +869 and +1100 mV, the formation of CuS and As_2O_3 on the surface.

Investigation of resulting concentrations of Cu, As and S in the buffer solutions post-treatment by ICP shows a pattern of change that correlates with the XPS findings, with a step-change in concentration observed between +516 and +705 mV, as a consequence of an increase in dissolution rate. From these observations and the XPS findings it can be concluded that enargite is resistant to electrochemically induced oxidation and subsequent precipitation of other species on the mineral surface until a threshold potential, somewhere between +516 and +705 mV, is reached. Additional thermodynamic data using the measured solution concentrations of Cu, As and S, presented in Figure 15, Appendix 5, shows there is no difference in predicted species at pH 10, compared to the data in Figure 10 where assumed activities were used.

Reaction mechanisms for each of the applied potentials investigated as treatment conditions have been devised based on the thermodynamic data and the XPS results, and differences have been identified in the resulting chemical species compared to published mechanisms (Guo and Yen 2008). These alternative reaction mechanisms are presented below for each of the five applied potentials chosen as treatment conditions in preparation of the enargite species prior to XPS investigation.

Guo and Yen (2008) use primarily electrochemical techniques combined with thermodynamic data to deduce the nature of the reactions taking place on the enargite surface at different applied potentials. While this method is sound they did not directly investigate the compounds formed using surface sensitive analytical techniques. In this work we used electrochemical techniques to confirm

their results, and combined it with thermodynamic data and XPS analysis. Thus direct evidence of the species present has been obtained to give more reliable data.

Peak 1 (approximately +347 mV):

$$Cu_3AsS_4 = Cu_{3-x}AsS_4 + xCu^{2+}_{(aq)} + 2xe^- \quad [12]$$

Peak 2 (approximately +526 mV):

$$nCu_2AsS_4 + 8nOH^- = 2nCu^{2+} + nAsO_4^{3-} + 4S_n^{2-} + 4nH_2O + ne^- \quad [13]$$

Peak 3 (approximately +705 mV):

$$Cu_2AsS_4 + 18OH^- = Cu(OH)_2 + CuSO_4 + AsO_4^{3-} + 3S_n^{2-} + 8H_2O + 9e^- \quad [14]$$

Peak 4 (approximately +869 mV):

$$Cu_3AsS_4 + 45OH^- = 3Cu(OH)_2 + HAsO_4^{2-} + 4SO_4^{2-} + 19H_2O + 35e^- \quad [15]$$

Peak 5 (approximately +1100 mV):

$$2Cu_3AsS_4 + 3Cu^{2+}_{(aq)} + 74OH^- = Cu(OH)_2 + 8CuSO_4 + As_2O_3 + 37H_2O + 68e^- \quad [16]$$

However, it should be noted that the presence of aqueous species such as $HAsO_4^{2-}$ is assumed based on the thermodynamic data and has not been confirmed, since this study has focused on quantification of the chemical species present as a surface layer on electrochemically oxidized enargite, rather than the solution chemistry. Further study of the ionic species contained in the surrounding buffer solution would be useful to enable quantification of these species, and so devise reaction mechanisms that more accurately represent the actual processes taking place.

Acknowledgments

The authors gratefully acknowledge the University of Queensland for an APA Scholarship and the CSIRO for the top-up scholarship (C.P.) and research expenses support. This research is also supported under The University of Queensland's CIEF funding scheme (A.V.N.). The authors acknowledge the facilities, and the scientific and technical assistance, of the Australian Microscopy & Microanalysis Research Facility at the Centre for Microscopy and Microanalysis, The University of Queensland.

References

Guo, H. and Yen, W.T. (2008) Electrochemical study of synthetic and natural enargites. Proc. 24th Int. Miner. Process. Congr. 1, 1138-1145.

Guo, H. and Yen, W.T. (2006) Proceedings of the XXIII International Mineral Processing Conference. Önal, G., Acarkan, N., Çelik, M.S., Arslan, F., Ateşok, G., Güney, A., Sirkeci, A.A., Yüce, A.E. and Perek, K.T. (eds), pp. 504-509, Promed, Istanbul, Turkey.

Velasquez, P., Ramos-Barrado, J.R., Cordova, R. and Leinen, D. (2000) XPS analysis of an electrochemically modified electrode surface of natural enargite. Surf. Interface Anal. 30(1), 149-153.

Small, G.L., Grano, S.R., Ralston, J. and Johnson, N.W. (1997) Methods to Increase Fine Mineral Recovery in the Mount Isa Mines Lead/Zinc Concentrator. Minerals Engineering 10(1), 1-15.

Plackowski, C., Hampton, M.A., Nguyen, A.V. and Bruckard, W.J. (2013) Fundamental Studies of Electrochemically Controlled Surface Oxidation and Hydrophobicity of Natural Enargite. Langmuir 29(7), 2371-2386.

Deroubaix, G. and Marcus, P. (1992) X-Ray Photoelectron-Spectroscopy Analysis of Copper and Zinc-Oxides and Sulfides. Surf. Interface Anal. 18(1), 39-46.

McIntyre, N.S., Sunder, S., Shoesmith, D.W. and Stanchell, F.W. (1981) Chemical Information from XPS - Applications to the Analysis of Electrode Surfaces. Journal of Vacuum Science & Technology 18(3), 714-721.

Ertl, G., Hierl, R., Knözinger, H., Thiele, N. and Urbach, H.P. (1980) XPS study of copper aluminate catalysts. Applications of Surface Science 5(1), 49-64.

Brion, D. (1980) Study by Photoelectron-Spectroscopy of Surface Degradation of FeS2, CuFeS2 ZnS and PbS exposed to air and water. Appl. Surf. Sci. 5(2), 133-152.

Perry, D.L. and Taylor, J.A. (1986) X-ray photoelectron and Auger spectroscopic studies of Cu2S and CuS. Journal of Materials Science Letters 5(4), 384-386.

Petkov, K., Krastev, V. and Marinova, T. (1994) XPS Study of Amorphous As2S3 Films Deposited Onto Chromium Layers. Surf. Interface Anal. 22(1-12), 202-205.

Nefedov, V.I., Salyn, Y.V., Solozhenkin, P.M. and Pulatov, G.Y. (1980) X-ray photoelectron study of surface compounds formed during flotation of minerals. Surf. Interface Anal. 2(5), 170-172.

Fullston, D., Fornasiero, D. and Ralston, J. (1999) Oxidation of synthetic and natural samples of enargite and tennantite: 2. X-ray photoelectron spectroscopic study. Langmuir 15(13), 4530-4536.

Smart, R.S.C., Skinner, W.M. and Gerson, A.R. (1999) XPS of sulphide mineral surfaces: metal-deficient, polysulphides, defects and elemental sulphur. Surf. Interface Anal. 28(1), 101-105.

Asbjornsson, J., Kelsall, G.H., Pattrick, R.A.D., Vaughan, D.J., Wincott, P.L. and Hope, G.A. (2004) Electrochemical and surface analytical studies of enargite in acid solution. J. Electrochem. Soc. 151(7), E250-E256.

Strohmeier, B.R., Levden, D.E., Field, R.S. and Hercules, D.M. (1985) Surface spectroscopic characterization of CuAl2O3 catalysts. Journal of Catalysis 94(2), 514-530.

Klein, J.C., Li, C.P., Hercules, D.M. and Black, J.F. (1984) Decomposition of Copper Compounds in X-Ray Photoelectron Spectrometers. Appl. Spectrosc. 38(5), 729-734.

Klein, J.C., Proctor, A., Hercules, D.M. and Black, J.F. (1983) X-ray excited Auger intensity ratios for differentiating copper compounds. Analytical Chemistry 55(13), 2055-2059.

Buckley, A.N. and Woods, R. (1984) An X-Ray Photoelectron Spectroscopic Study Of The Oxidation Of Galena. Appl. Surf. Sci. 17(4), 401-414.

Hampton, M.A., Plackowski, C. and Nguyen, A.V. (2011) Physical and Chemical Analysis of Elemental Sulfur Formation during Galena Surface Oxidation. Langmuir 27(7), 4190-4201.

Wittstock, G., Kartio, I., Hirsch, D., Kunze, S. and Szargan, R. (1996) Oxidation of Galena in Acetate Buffer Investigated by Atomic Force Microscopy and Photoelectron Spectroscopy. Langmuir 12(23), 5709-5721.

Bhide, V.G., Salkalachen, S., Rastog, A.C., Rao, C.N.R. and Hegde, M.S. (1981) Depth profile composition studies of thin film CdS:Cu 2 S solar cells using XPS and AES. Journal of Physics D: Applied Physics 14(9), 1647.

Nakai, I., Sugitani, Y., Nagashima, K. and Niwa, Y. (1978) X-Ray Photoelectron Spectroscopic Study of Copper Minerals. Journal of Inorganic & Nuclear Chemistry 40(5), 789-791.

King, D.E., Fernandez, J.E. and Swartz, W.E. (1990) An XPS Study of the Doping of Trans, Trans Para-Distyrylbenzene with AsF5 - A Model Conducting Polymer System. Appl. Surf. Sci. 45(4), 325-339.

Stec, W.J., Morgan, W.E., Albridge, R.G. and Van Wazer, J.R. (1972) Measured binding energy shifts of "3p" and "3d" electrons in arsenic compounds. Inorganic Chemistry 11(2), 219-225.

Lattanzi, P., Da Pelo, S., Musu, E., Atzei, D., Elsener, B., Fantauzzi, M. and Rossi, A. (2008) Enargite oxidation: A review. Earth-Science Reviews 86(1-4), 62-88.

Epp, J.M. and Dillard, J.G. (1989) Effect of ion bombardment on the chemical reactivity of gallium arsenide(100). Chemistry of Materials 1(3), 325-330.

Leonhardt, G., Berndtsson, A., Hedman, J., Klasson, M., Nilsson, R. and Nordling, C. (1973) ESCA studies of some AIIIBv compounds with Ga and As. physica status solidi (b) 60(1), 241-248.

Hollinger, G., Skheyta-Kabbani, R. and Gendry, M. (1994) Oxides on GaAs and InAs surfaces: An x-ray-photoelectron-spectroscopy study of reference compounds and thin oxide layers. Physical Review B 49(16), 11159-11167.

Cossu, G., Ingo, G.M., Mattogno, G., Padeletti, G. and Proietti, G.M. (1992) XPS Investigation on Vacuum Thermal-Desorption of UV Ozone Treated GaAs(100) Surfaces. Appl. Surf. Sci. 56-8, 81-88.

Mizokawa, Y., Iwasaki, H., Nishitani, R. and Nakamura, S. (1978) Esca studies of Ga, As, GaAs, Ga2O3, As2O3 and As2O5. Journal of Electron Spectroscopy and Related Phenomena 14(2), 129-141.

Appendix 1 – Enargite mineral X-ray diffraction

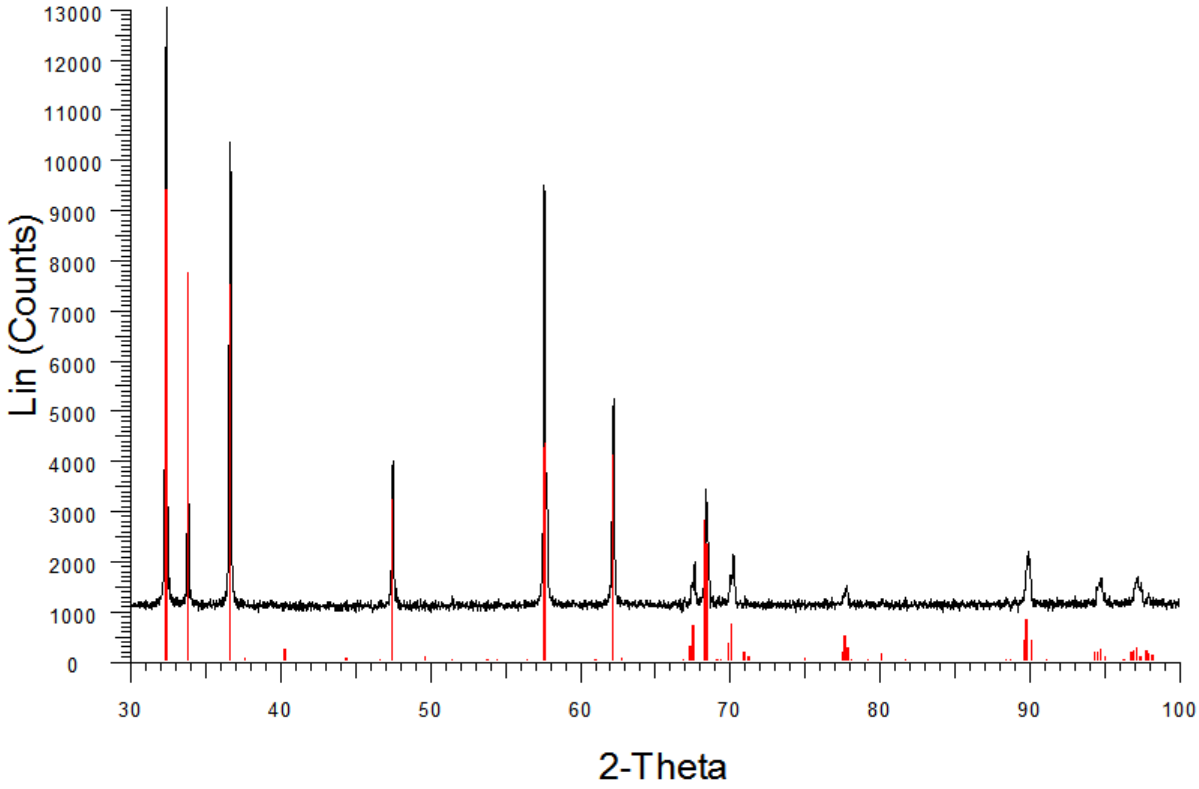

Figure 9. XRD analysis of the natural enargite used in the experimental work. The continuous trace represents the measured data while the individual peaks represent Pattern 03-065-1097 (A) - Enargite - $AsCu_3S_4$, incorporated in the Diffrac$^{(plus)}$ Evaluation Package Release 2009 and PDF-2 Release 2009 software package.

XRD analysis was performed on a natural enargite sample pulverized to a fine powder. The sample was analyzed in a Bruker Advance D8 X-Ray Diffractometer equipped with a LynxEye detector, Co tube radiation, and operated at 35 kV and 40 mA. Conditions of analysis are as follows:

- 30-100 degrees 2-theta
- 0.02 degree increment
- 1.2 s/step time per step
- 0.26 mm fixed divergence slit
- 5.0 mm fixed anti-scatter slit
- 68 min scan time

Traces were processed using the Diffrac$^{(plus)}$ Evaluation Package Release 2009 and PDF-2 Release 2009. X-ray diffraction analysis confirmed that the predominant mineral phase in the sample was enargite, Cu_3AsS_4, and no other phases were detected.

Appendix 2 – ICP-OES parameters used for chemical analysis of elements contained in buffer solutions obtained after applying various potentials

Plasma	Peristaltic Pump	Sample Introduction
RF power: 1450 W	Flow rate: 1.00 mL/min	Nebulizer: sea spray 2 mL
Plasma gas: argon (Ar)	Flush time: 40 seconds	Torch: one piece quartz
Plasma flow rate: 15 L/min		Injector: alumina 2.0 mm i.d.
Auxiliary flow rate: 0.2 L/min		
Nebulizer Ar flow rate: 0.8 L/min		
Read delay: 15 seconds		
Replicates: 3		

Appendix 3 – HSC7 thermodynamic data (assumed molality for total concentrations of dissolved copper, arsenic and sulfur activities being equal to 3, 1 and $4x10^{-3}$ M, respectively).

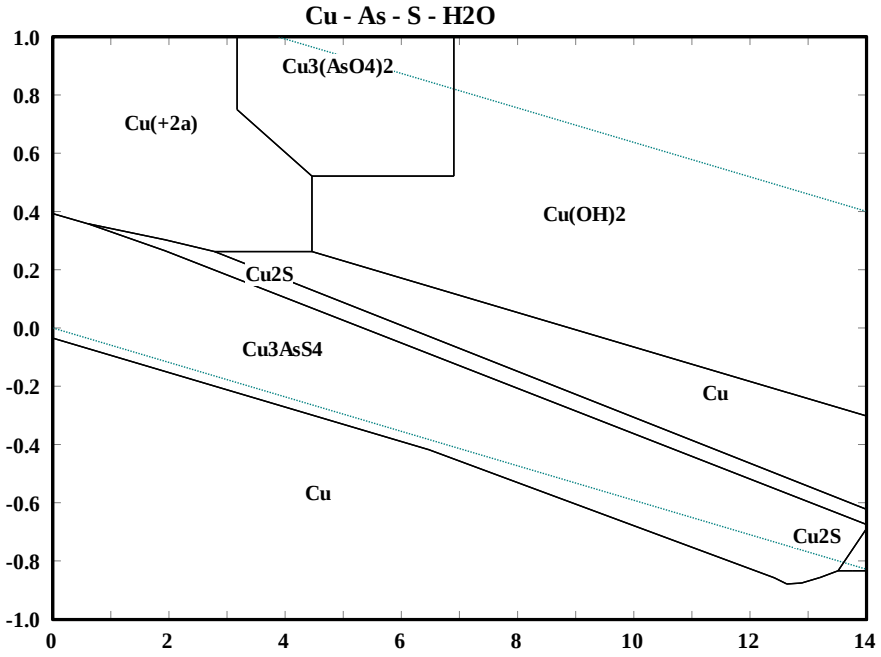

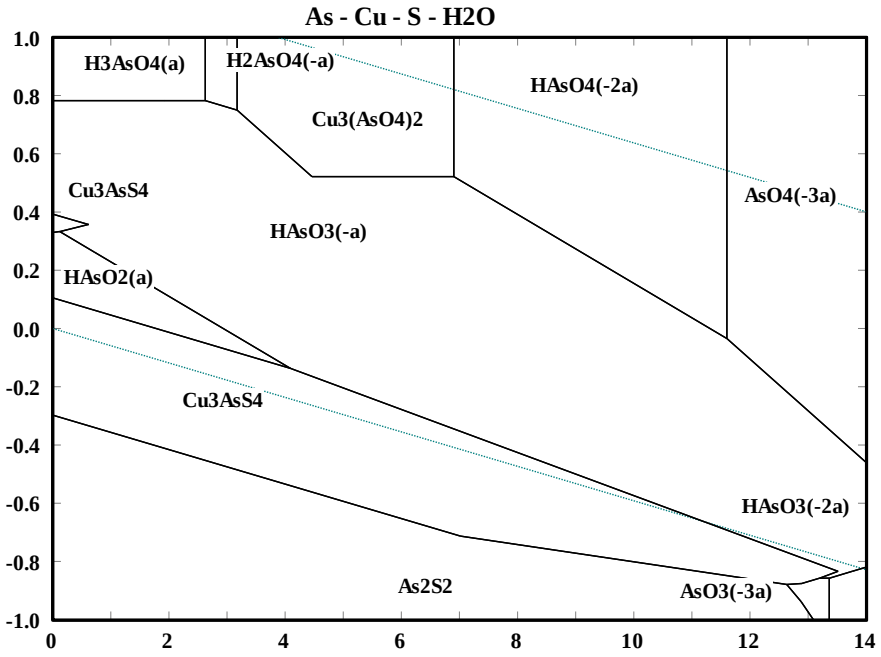

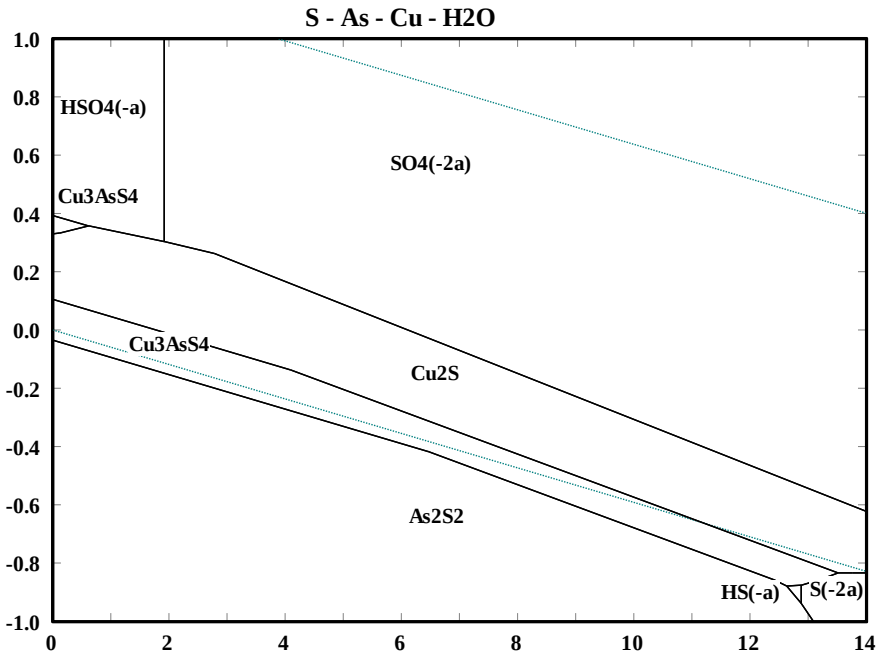

Figure 10. Eh-pH diagrams for the Cu-As-S-H_2O, As-Cu-S-H_2O and S-As-Cu-H_2O systems at 278K. Dissolved copper, arsenic and sulfur activities are assumed to be 3, 1 and $4x10^{-3}$ M, respectively. The vertical and horizontal axes describe the redox potential (Eh) in V (SHE) and the solution pH, respectively, while the dashed lines indicate the upper and lower limits of water stability.

Appendix 4 – XPS comparison of applied potential by element

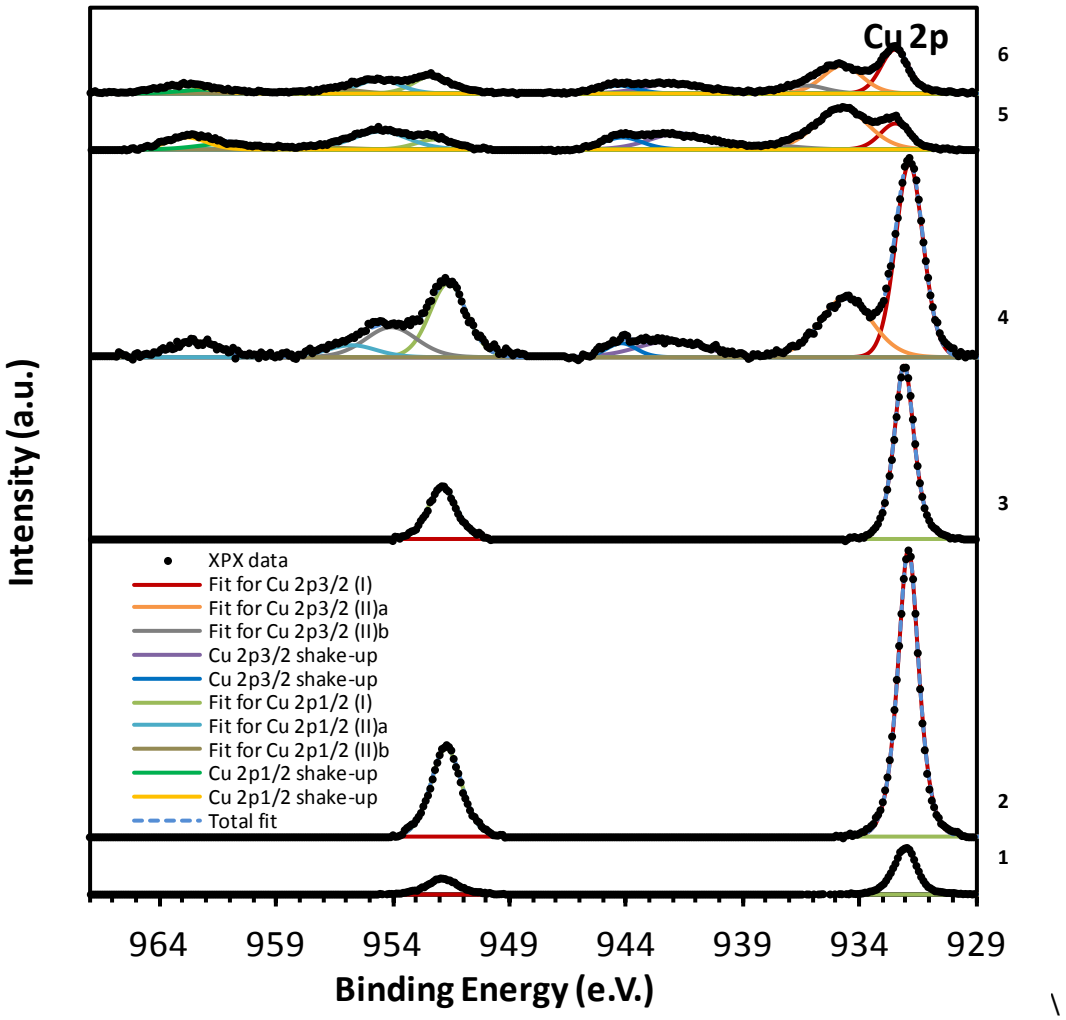

Figure 11. The Cu 2p XPS photoelectron spectra collected from the unoxidised enargite surface and at applied potentials of +347, +516, +705, +869 and +1100 mV (1 to 6 respectively).

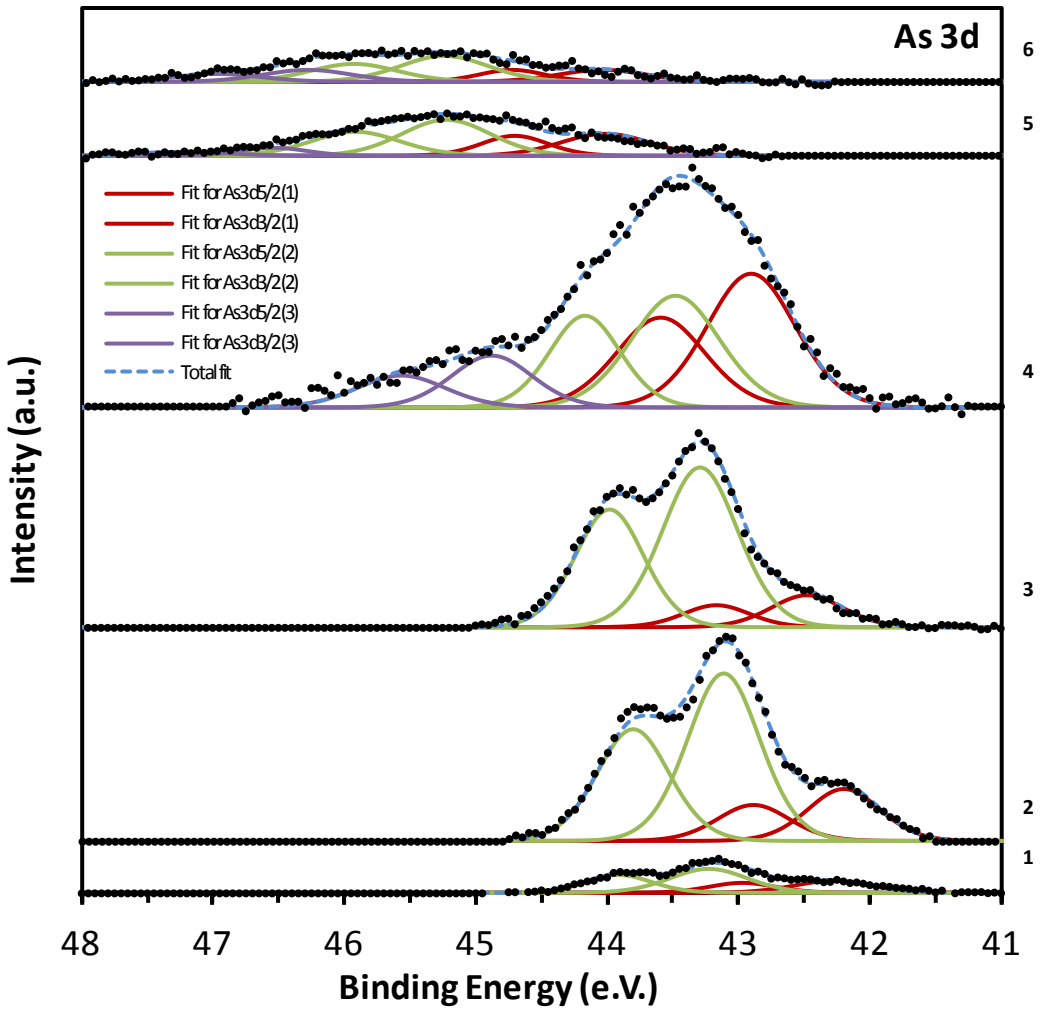

Figure 12. The As 3d XPS photoelectron spectra collected from the unoxidised enargite surface and at applied potentials of +347, +516, +705, +869 and +1100 mV (1 to 6 respectively).

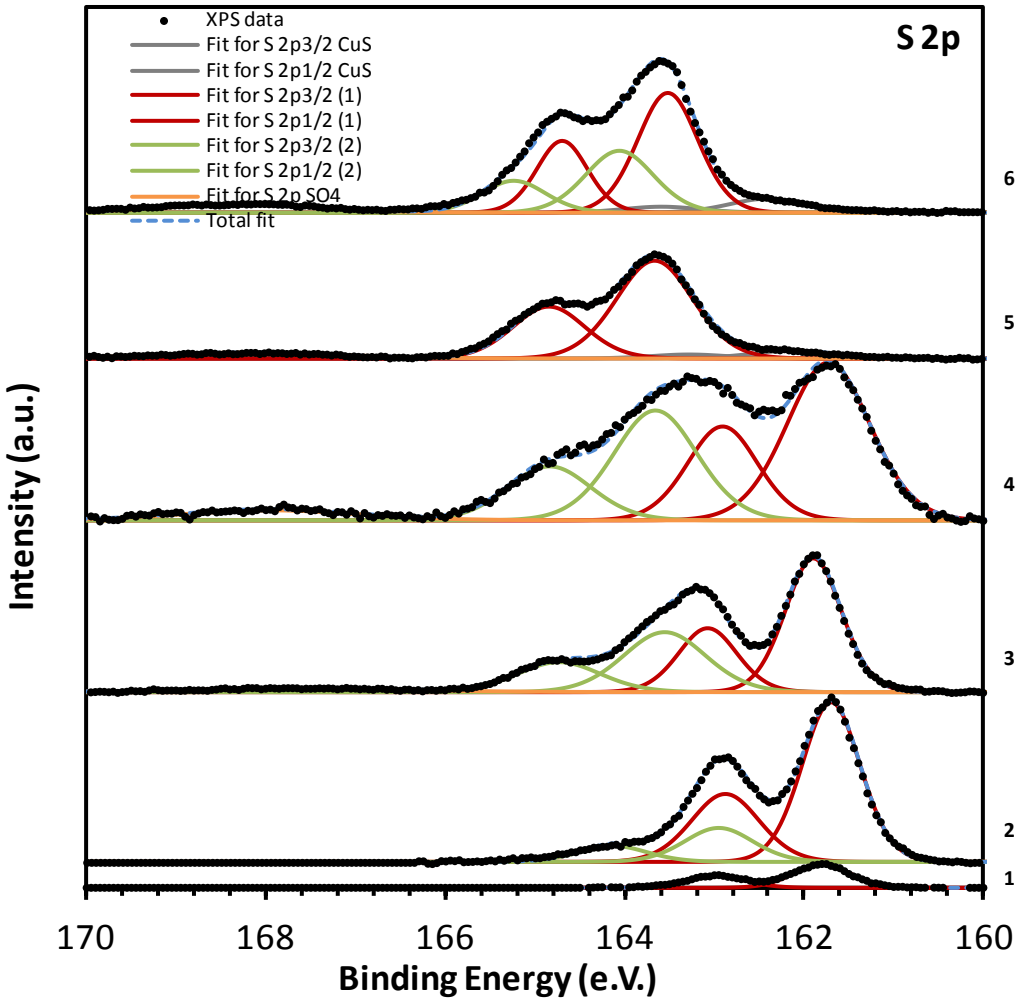

Figure 13. The S 2p XPS photoelectron spectra collected from the unoxidised enargite surface and at applied potentials of +347, +516, +705, +869 and +1100 mV (1 to 6 respectively).

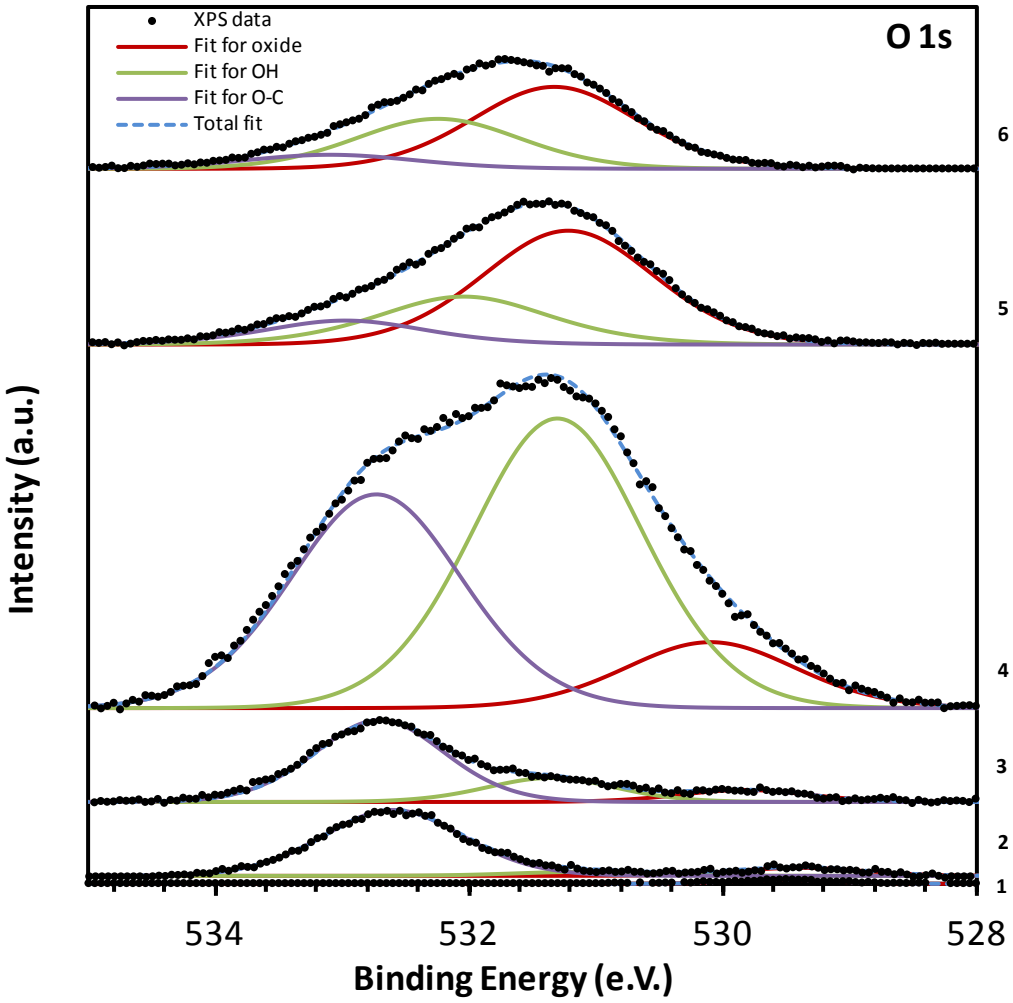

Figure 14. The O 1s XPS photoelectron spectra collected from the unoxidised enargite surface and at applied potentials of +347, +516, +705, +869 and +1100 mV (1 to 6 respectively).

Appendix 5 – HSC7 thermodynamic data (ICP measured molality for total concentrations of dissolved copper, arsenic and sulfur activities being equal to $2.2x10^{-5}$ M, $5.59x10^{-6}$ M and $1.4x10^{-4}$ M, respectively, after treatment at +347 mV for 30 minutes).

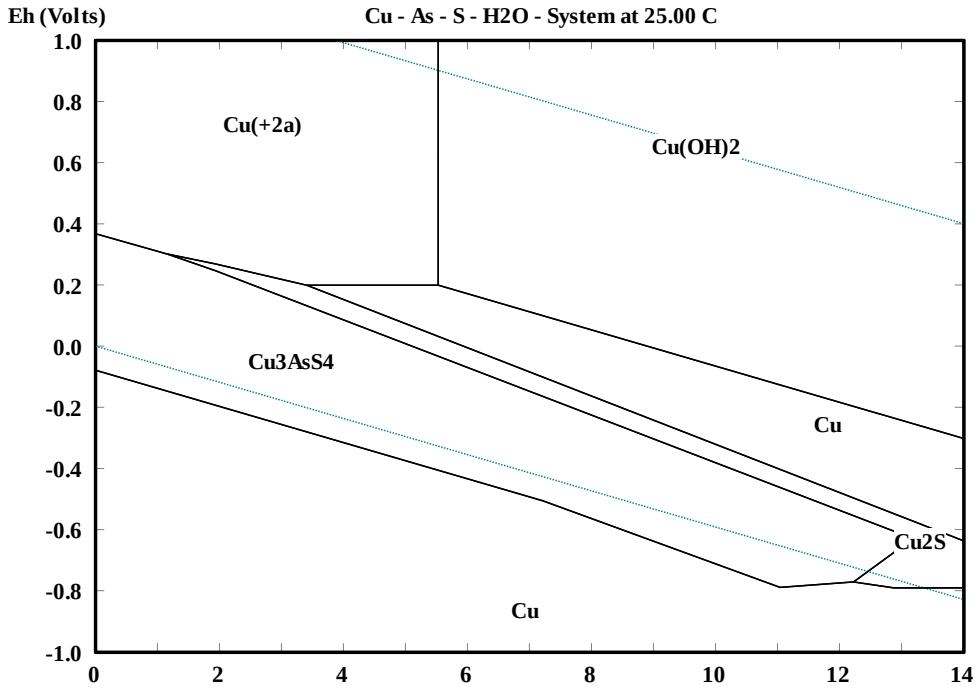

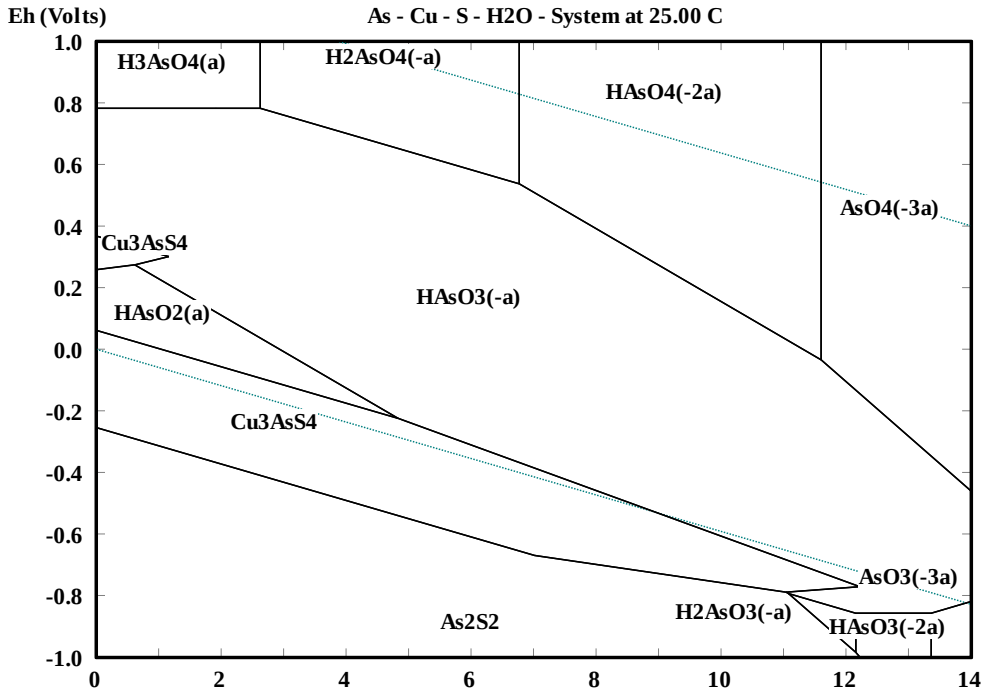

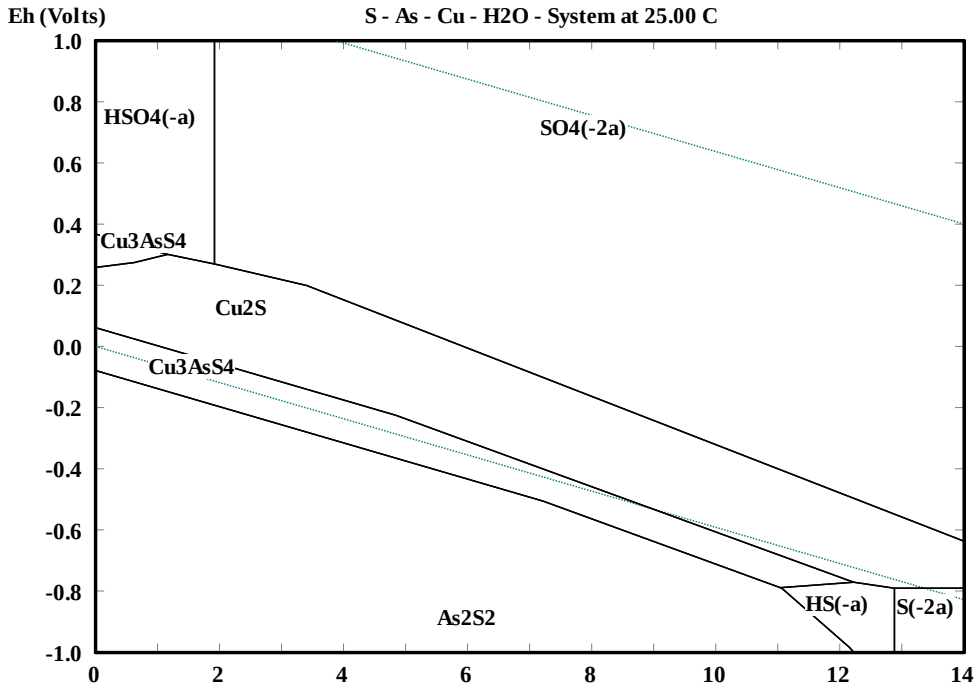

Figure 15. Eh-pH diagrams for the Cu-As-S-H_2O, As-Cu-S-H_2O and S-As-Cu-H_2O systems at 278K. Dissolved copper, arsenic and sulfur activities are determined by ICP measurement to be $2.2x10^{-5}$ M, $5.59x10^{-6}$ M and $1.4x10^{-4}$ M respectively after treatment at +347 mV for 30 minutes. The vertical and horizontal axes describe the redox potential (Eh) in V (SHE) and the solution pH, respectively, while the dashed lines indicate the upper and lower limits of water stability.

Appendix 6 – Solution concentrations of As, Cu and S after surface oxidation at selected anodic potentials expressed in ppm as measured by ICP, and calculated molar concentration

Treatment	As	**Cu**	**S**	**As**	**Cu**	**S**
	(ppm)			**(mole/L)**		
347 mV	0.45	1.40	4.62	5.95E-06	2.20E-05	1.44E-04
516 mV	0.79	1.86	4.69	1.06E-05	2.93E-05	1.46E-04
705 mV	2.13	4.54	7.13	2.84E-05	7.15E-05	2.22E-04
869 mV	3.20	6.19	8.41	4.27E-05	9.74E-05	2.62E-04
1100 mV	3.95	8.94	9.24	5.28E-05	1.41E-04	2.88E-04

Chapter VI

Surface characterisation, collector adsorption and flotation response of enargite in a redox potential controlled environment

Chris Plackowski, Warren J. Bruckard and Anh V. Nguyen

Submitted to Minerals Engineering, Feb. 2014.

1. Abstract

We previously investigated oxidation of the surface of natural enargite (Cu_3AsS_4) under potentiostatic control and the formation of oxidation species at the mineral surface at selected applied potentials in the oxidative range. Here we further extended the research by incorporating flotation collectors into the system. Electrochemical techniques, X-ray photoelectron spectroscopy (XPS) and microflotation in a redox potential controlled environment were applied to examine surface properties, collector adsorption and flotation response of enargite in pH 10 solutions of sodium ethyl xanthate (SEX) and sodium dialkyl dithiophosphinate (3418A). The spectral details of XPS analysis of electrochemically treated enargite surfaces show significant adsorption of SEX and 3418A collectors onto enargite at an applied voltage of +516 mV, but no adsorption of both collectors at -400 mV. The results of XPS analysis agree with the floatability of enargite determined by microflotation, showing that the flotation recovery was highest at high oxidative potential (+516 mV), then decreased at low oxidative potential (+100 mV) and was very poor at -400 mV. These results confirm that enargite floatability can be efficiently controlled electrochemically.

Key words: arsenic, copper, xanthate, dithiophosphinate, XPS, surface electrochemistry

2. Introduction

Enargite (Cu_3AsS_4) is an important mineral in the processing of copper ores due both to its value as a commercial source of copper, and the harmful impact of its arsenic content in terms of health, environmental, economic and final product quality issues associated with its processing (Biswas and Davenport, 1994; Chatterjee et al., 1995; Cordova et al., 1997). A number of previous studies have investigated methods of separating arsenic and copper during the flotation stage of mineral processing operations (Bruckard et al., 2010; Bruckard et al., 2007; Senior et al., 2006; Smith and Bruckard, 2007). The motivation for this work is the growing importance of finding an economic and effective means of reducing the arsenic levels in flotation concentrates to acceptable levels. However, to date no effective flotation method capable of selectivity for arsenic minerals in industrial applications has been developed. A recent review of the literature found that although some progress has been made in understanding the flotation response of copper arsenic sulphides, fundamental knowledge of enargite surface chemistry must be further developed before the mechanisms that enable a successful separation by flotation can be fully understood (Plackowski et al., 2012).

Electrochemical techniques combined with surface analysis are useful methods to characterize a mineral surface and provide valuable information about its surface reactivity. Using this approach electrochemically induced surface oxidation of enargite by applied potentials of +869 mV at pH 10

and + 610 mV at pH 4 has been investigated in a previous study (Plackowski et al., 2013b) (All voltages reported in this paper are relative to SHE if not stated otherwise). Changes in surface morphology (roughness and distribution of surface products), hydrophobicity and surface speciation were found. Surface layer formations consisting of metal deficient sulphide and elemental sulphur were identified, and a mechanism of Cu dissolution and diffusion-limited surface layer deposition was proposed. In this study only one applied potential of +869 mV at pH 10 was considered. In order to quantify surface chemical changes over a broad potential range, further work was completed (Plackowski et al., 2014). Five anodic potentials representing current peaks identified using cyclic voltammetry (+347, +516, +705, +869 and +1100 mV) were investigated to identify the chemical changes induced at the enargite surface in the oxidative range. These data can be used to identify potentials at which electrochemical reactions occur and, in combination with thermodynamic data, reaction mechanisms proposed to be responsible for the chemical changes at the surface have been derived (Guo and Yen, 2008). Characterisation of the electrochemically oxidized surface using XPS provided partial confirmation of these mechanisms but also revealed significant differences in speciation, allowing alternative mechanisms to be formulated in combination with thermodynamic data (Plackowski et al., 2014).

These previous studies considered a simple system where enargite is electrochemically oxidized in buffer solution with no other reagents present. To further develop our understanding of the flotation response of enargite as a function of pulp potential additional complexity is required. In this paper XPS is used to examine the enargite surface and identify the surface chemical species present after treatment at oxidizing and reducing potentials (+516 and -400 mV, respectively) in the presence of flotation collector. Two commonly used collectors for sulphide minerals, namely sodium ethyl xanthate (SEX) and sodium dialkyl dithiophosphinate (DTPI), were chosen for this study.

The flotation response was investigated using the UCT microflotation cell as described by Bradshaw and O'Connor (1996). This was done to determine if there would be a difference in the flotation response of enargite after conditioning in the presence of flotation collector at pulp potentials equivalent to the electrochemically applied oxidizing and reducing potentials used for the XPS work. The aim of this research work was to determine what differences exist in collector adsorption after treatment at these applied potentials, and if there is a correlation with the flotation recovery of enargite in a simple single mineral microflotation system.

3. Experimental

3.1. Materials

A high purity sample of natural enargite (Cu_3AsS_4) sourced from Wright's Rock Shop (USA) was used for the experimental work. Initial characterisation was carried out by X-ray diffraction for determining its crystal structure and identifying the mineral phases present. Enargite was the predominant phase determined with no other significant phases detected. Its chemical composition was confirmed by XPS. A resin mounted thin polished section with the mineral exposed on both sides was prepared for the electrochemical work, and mounted on a fabricated PVC sample holder to facilitate preparation, handling and the experimental techniques.

A pH 10.0 buffer solution (0.05M) was prepared for the electrochemical work using di-sodium tetraborate decahydrate (Scharlau Chemie S.A., Spain, AR grade) and sodium hydroxide (Sigma-Aldrich, Australia, technical grade). Water freshly purified using a reverse osmosis RIO's unit and an Ultrapure Academic Milli-Q system (Millipore, USA) was used in the experiments. The Milli-Q water had a specific resistance of 18.2 $M\Omega cm^{-1}$.

Collector solutions were prepared using pH 10 buffer as the base solution, to which SEX (Flottec, USA, commercial grade) and DTPI (Aerophine 3418A promoter, Cytec, USA) solutions were added to give the final concentration of collector in solution required for the CV (cyclic voltammetry) and XPS studies. SEX was supplied in solid crystalline form, while DTPI was supplied as a 50 vol % solution made up with water.

For the microflotation tests 0.1 M sodium hydroxide solution (Chem Supply, Australia, analytical reagent) and 0.1 M nitric acid solution (Ajax Finechem Pty Ltd, analytical reagent) were used for pH control, while sodium dithionite ($Na_2S_2O_4$, Sigma Aldrich, technical grade) and sodium hypochlorite (NaOCl, APS Finechem, Australia, technical grade) solutions (2.5% w/v) were used to set and control the pulp potential.

3.2. Sample Preparation

The freshly polished mineral surface was prepared for XPS by electrochemical conditioning in a pH 10.0 buffer solution at selected potentials using an Asylum AFM electrochemical cell (Asylum, Santa Barbara, USA) and a Gamry Reference 600 potentiostat (Gamry, Warminster, USA). The solution consisted of either buffer alone or buffer containing selected concentrations of flotation collector, depending on the test requirements.

The potentiostat working electrode cable was connected to the enargite working electrode (resin mounted polished sample) by an insulated copper wire attached to its lower surface using

silver epoxy (ITW Chemtronics, USA) to ensure good electrical contact, while a platinum wire was used as the counter electrode. A Ag/AgCl 3M KCl microelectrode (Microelectrodes Inc., USA) was used as the reference electrode.

Prior to each measurement any pre-existing surface oxidation was removed by machine polishing with 9, 3 and 1 micron diamond suspensions (Dia-duo, Struers Australia) in sequence to ensure a fresh surface was exposed. The surface was then washed with ethanol (AR grade) and dried with high purity compressed nitrogen, and immediately transferred to the electrochemical cell. The reference and counter electrodes were then attached to the cell, the enargite surface covered with buffer solution and the oxidizing potential initiated.

To ensure all collector residue was removed from the mineral surface after each test, CV measurements were conducted after polishing to check that the response of the surface was the same as for a known clean enargite surface. Where the voltammogram did not match the clean surface, polishing and the CV measurement was repeated until no evidence of variation from the clean surface due to the presence of collector was found.

Surface conditioning was performed as a single-step experiment using the chronoamperometry (CA) technique where the desired potential was applied for 10 min at room temperature (25 ^{o}C). The conditioning potentials were chosen based on the work of Senior et al. (2006) and Guo and Yen (2005) which investigated the effects of pulp potential on the flotation response of enargite. These studies revealed the existence of a threshold potential range over which enargite undergoes a transition from non-floating to floating as the potential increases. Guo and Yen (2005) found this range to be about -150 to +200 mV for synthetic enargite at pH 10 in potassium amyl xanthate (PAX) solution, while Senior et al., (2006) found the transition occurred over the range -100 to +100 mV for natural enargite at pH 11 in the presence of potassium ethyl xanthate (KEX).

To ensure conditioning was performed outside the transition potential range, potentials of -400 and +516 mV were selected. These potentials were chosen with reference to previous CV results which identified an oxidative current peak at +516 mV and a reductive peak at -400 mV (Plackowski et al., 2014). In addition these values were also considered sufficiently distant from the transition potential range identified by Senior et al., (2006) as between about -150 and -50 mV, below which enargite was found to be non-floatable and above which it was strongly floatable. Comparative testing was also carried out at approximately +100 mV to evaluate recovery within the transition potential range.

3.3. Electrochemistry

To provide a baseline reference curve for enargite without collector, CV was performed with a freshly polished enargite sample in a pH 10.0 buffer solution using the Asylum AFM electrochemical cell and the Gamry Reference 600 potentiostat. The connections and electrodes are described in the Sample Preparation section. All voltages have been converted and reported relative to SHE (standard hydrogen electrode) as noted earlier.

In preparation for a measurement, the sample was polished, washed with ethanol, dried with high purity N_2 and quickly transferred to the electrochemical cell. The reference and counter electrodes were attached to the cell, the enargite surface covered with the required buffer solution (with or without collector) and the measurement initiated. All measurements were initiated in the positive potential direction and conducted at a scan rate of 1 mV/s: all CV curves were started from a potential of 0 mV at a sweep rate of 1 mV/s in the positive sweep direction, switched to the cathodic scan direction at 1100 mV, then switched back to the anodic direction at -690 mV and terminated at 0 mV. Deoxygenation of the buffer solution and electrochemical cell was not necessary (Plackowski et al., 2014).

Surface preparation for XPS was carried out using the CA technique performed as a single-step experiment at the selected conditioning potentials of either -400 or +516 mV. Using this method the selected potential is applied to the enargite working electrode and the resulting current measured over a pre-determined period of time. In the present work the conditioning potential was applied for 600 s to a freshly polished enargite surface immersed in a quiescent pH 10 buffer solution with or without collector as required. The conditioning potentials were selected based on the proposed threshold potential for enargite flotation as discussed earlier.

3.4. X-ray photoelectron spectroscopy

XPS measurements of the enargite surface after treatment using the experimental procedures described above were carried out to identify the chemical species formed at oxidising or reducing potentials of +516 and -400 mV, respectively.

Data was acquired using a Kratos Axis ULTRA X-ray Photoelectron Spectrometer incorporating a 165 mm hemispherical electron energy analyzer. The incident radiation was monochromatic Al Kα X-rays (1486.6 eV) at 150 W (15 kV, 15 mA). The instrument work function was calibrated to give a binding energy (BE) of 83.96 eV for the Au $4f_{7/2}$ line for metallic gold and the spectrometer dispersion was adjusted to give a BE of 932.62 eV for the Cu $2p_{3/2}$ line of metallic copper. Detection limits ranged from 0.1 to 0.5 atomic percent depending on the element. The Kratos charge neutralizer system was used on all specimens. Survey (wide) scans were taken with

an analysis area of 300 x 700 microns at an analyzer pass energy of 160 eV. Multiplex (narrow) high resolution scans were carried out with an analysis area of 300 x 700 microns and an analyzer pass energy of 20 eV. Survey scans were carried out over a 1200-0 eV binding energy range with 1.0 eV steps and a dwell time of 100 ms. Narrow high-resolution scans were run with 0.05 eV steps and 250 ms dwell time. Base pressure in the sample analysis chamber (SAC) was $1.0x10^{-9}$ torr and during sample analysis it was $1.0x10^{-8}$ torr. Spectra have been charge corrected using the main line of the carbon 1s spectrum photoelectron peak (adventitious carbon) as an internal reference to account for sample charging, with an assigned BE of 284.8 eV, and were analysed using the CasaXPS software (version 2.3.14).

The oxidised enargite specimen was secured to a metal stub with conductive tape in preparation for the measurement, which was then attached to the sample holder and inserted into the loading chamber. Sample cooling was used for all measurements. The sample holder was pre-cooled to liquid nitrogen temperatures by a cold probe before evacuation of the XPS instrument loading chamber. This procedure is designed to preserve volatile species on the specimen surface, which have been demonstrated to be unstable without cooling (Plackowski et al., 2013a). During initial cooling the chamber was continuously flushed with high purity dry nitrogen to remove moisture and oxygen. Once a temperature of -100 °C was reached the chamber was sealed and evacuation commenced. Once the required vacuum was reached the specimen was then transferred to the SAC and attached to the pre-cooled sample stage, where it was maintained at -135 °C throughout the measurement.

A single survey scan was first completed to identify surface elemental composition and then multiplex high resolution scans of each elemental region were completed. From these spectral distributions, the relative elemental concentrations, oxidation state and chemical bonding associations were determined. Relative elemental atomic concentrations were determined by peak fitting using the CASA XPS software package and the Kratos library of sensitivity factors. XPS data for the Cu 2p, O 1s, C 1s, S 2p and As 3d regions was fitted using Shirley background subtraction and Gaussian-Lorenztian peak profiles.

The XPS analysis of oxidized enargite has been shown to be dependent on the temperature at which it is carried out (Fantauzzi et al., 2006), as is the general case for other sulphides (Hampton et al., 2011; Wittstock et al., 1996). At ambient temperature, the ultrahigh vacuum required during analysis ($1.0x10^{-8}$ torr) creates an environment where elemental sulphur formed on the surface is unstable and evaporates. In addition, it has been reported that Cu(II) species, in particular $Cu(OH)_2$, undergo a combination of vacuum and thermal dehydration and decomposition to CuO at ambient temperature (Skinner et al., 1996), typically found to be about 30 °C in the XPS sample analysis

chamber. This effect can be controlled by pre-cooling (below -130 °C) the sample before evacuation thereby limiting evaporation of sulphur and decomposition of $Cu(OH)_2$ and other unstable compounds on the surface. When cooling is not used, elemental sulphur present on the surface quickly evaporates and so is lost and not detected, while other compounds undergo degradation. The effects of XPS analysis on the surface species present on oxidised enargite was investigated in a previous study (Plackowski et al., 2013a), and similar behaviour as seen for other sulphides was demonstrated. For this reason the sample was cooled in the loading chamber using a liquid nitrogen system to below -130 °C prior to evacuation. After transfer it was maintained at that temperature in the SAC.

3.5. Microflotation

Microflotation tests were conducted to confirm the effects of conditioning at different redox potentials in the presence of collector on the flotation recovery of enargite. The UCT microflotation cell as described by Bradshaw and O'Connor (1996) was used for this purpose and is shown diagrammatically in Figure 1. The mineral used was natural enargite as described in Section 3.1, in the size range of 53-106 μm. Following the method described by Bradshaw and O'Connor (1996), for each test 2 g of enargite was added to 50 mL of de-ionised water and treated in an ultrasonic bath for 10 min to remove any fine particles and oxidised surface material, then washed and filtered.

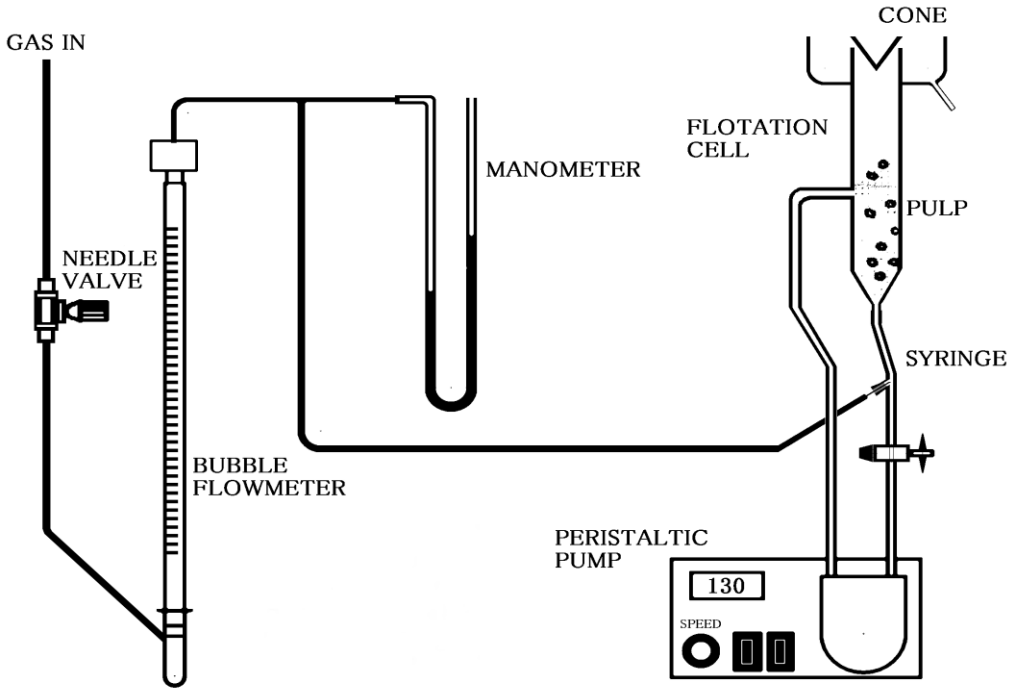

Figure 1. Schematic of the UCT microflotation apparatus (after Bradshaw and O'Connor, 1996) used in this study.

The flotation solution was prepared separately with de-ionised water, the pH was set as required using sodium hydroxide and nitric acid solutions as needed, while Eh was set using sodium hypochlorite solution or sodium dithionite solution. Once the desired values were reached the solution was transferred to the flotation cell, and the pH and Eh checked and adjusted as required. The mineral was then placed in the flotation cell and the peristaltic pump set to 130 rpm (flow rate 1.8 L/min), and the pH and Eh checked and adjusted again if required. The desired flotation collector was then added and the pulp conditioned for 5 min. Throughout conditioning pH and Eh were monitored and adjusted if needed. The positive and transition potentials (+500 and +100 mV, respectively) were found to be stable throughout conditioning. However, reagent addition was required to maintain the cathodic potential (-400 mV).

Nitrogen was used as the flotation gas, and at the commencement of flotation the syringe was inserted at the base of the cell with a pre-set flowrate of 8 mL/min. After a flotation time of 1 min, the syringe was removed and the recovered enargite filtered and weighed. Recovery was determined as the mass fraction of enargite reporting to the concentrate.

4. Results and Discussion

4.1. Cyclic voltammetry

Previous investigations (Plackowski et al., 2013b) have examined the current response to applied potential of natural enargite in pH 10 buffer solution alone and the resulting CV curve for a freshly polished natural enargite surface is shown in Figure 2. These results support the work of Guo and Yen (2006, 2008) who compared natural and synthetic enargite at pH 10, and Velasquez et al. (2000) and Cordova et al. (1997), who investigated natural enargite at pH 9.2. Those differences that can be seen between the present work and the published data were considered the result of variations in mineral composition, such as the type and concentrations of impurities present, sample preparation, and experimental method.

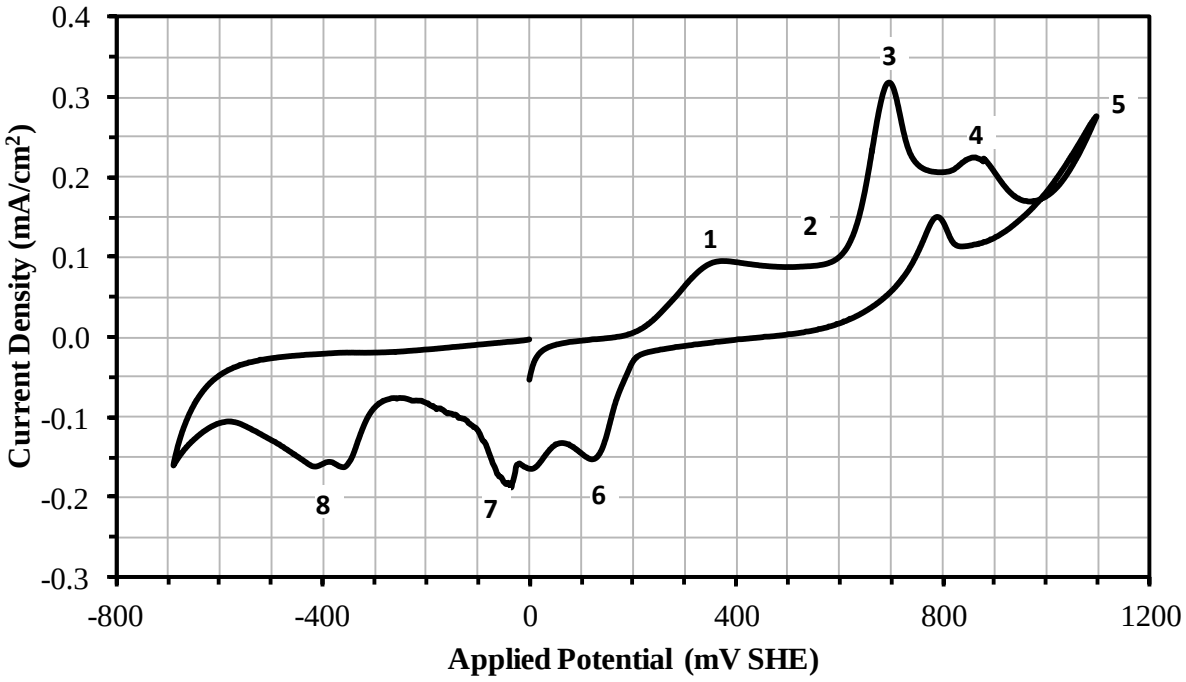

Figure 2. Typical cyclic polarization curve for natural enargite at pH 10 obtained using a scan rate of 1 mV/s (Plackowski et al., 2013b).

In the anodic portion of the scan five current peaks were observed at potentials of +347, +516, +705, +869 and +1100 mV, labelled as peaks 1-5 in Figure 1, respectively. The peak at +516 mV is not clearly evident in the figure, but a local current maximum can be seen at this potential in the numerical data. These potentials are similar to those found by Guo and Yen (2008), who reported five anodic CV peaks at +228, +548, +728, +826 and +1074 mV.

In the cathodic sweep current peaks are seen at 100 mV, -100 mV and -400 mV (numbered 6 to 8, respectively). In addition a peak is present at about 790 mV in the oxidative range on the return sweep from 1100 mV. Such a peak was not present in the data of Guo and Yen (2008). One possible explanation for its presence is that it represents the continuation of a reaction process first occurring at about 800 mV during the anodic scan in the forward sweep direction. Peak 3 represents the highest current density observed, the enargite surface has greater reactivity at this potential and this reaction does not reach equilibrium, even at the low sweep rate of 1 mV/sec used.

Changes in the surface reactivity were also investigated using CV, where enargite was immersed in the same pH 10 buffer solution, containing different concentrations of flotation collectors. Shown in Figure 3 are the cyclic voltammograms for enargite in the presence of SEX at different concentrations.

The effect of surface potential on the contact angle of the mineral surface in a 7 x 10^{-4} M PAX solution at pH 7 and 10 was investigate by Guo and Yen (2002). The relatively high concentration

was chosen to ensure a constant xanthate concentration during the measurement. The oxidation of xanthate to form dixanthogen during anodic polarisation was observed as an emulsion surrounding the mineral surface. Hexane extracts of this solution were identified as dixanthogen using UV spectroscopy. The effect of PAX on the cyclic polarisation of enargite was also investigated by Guo and Yen (2006), where the effects of PAX concentrations of 0 and 10^{-4} M on the current density of enargite polarisation at pH 10 were compared. It was concluded that the PAX passivated the enargite surface at about 80 mV as a result of dixanthogen formation.

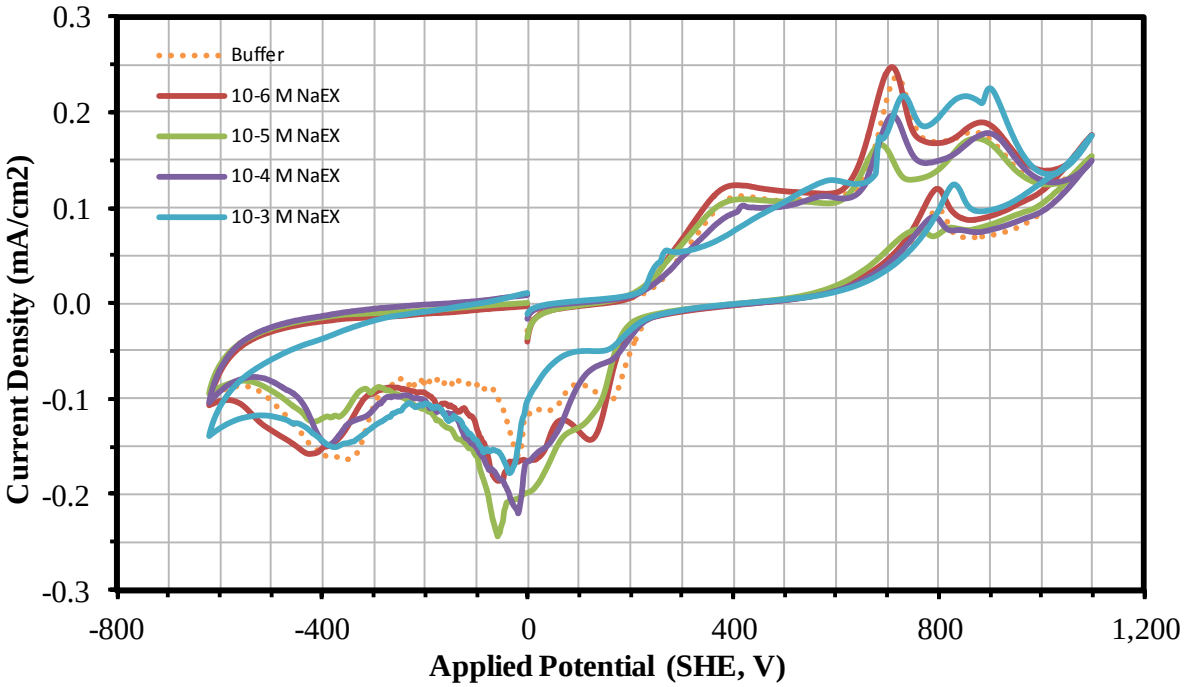

Figure 3. Reactivity of the enargite surface in the presence of 10^{-6}, 10^{-5}, 10^{-4} and 10^{-3} M SEX in pH 10 buffer solutions.

Surface passivation during anodic polarisation in the presence of increasing concentrations of xanthate is supported by Guo (2004) who investigated the effects of increasing PAX concentration. In addition, cyclic polarisation of natural enargite in pH 10 buffer solution revealed five anodic current peaks at similar potentials to those shown in Figure 2. Guo (2004) reported that increasing PAX concentration from 10^{-5} to 10^{-4} M caused the shift of peaks 1 and 3 to a higher potential while the current density of peaks 1 and 2 decreased. At 10^{-3} M xanthate concentration, peaks 1 and 2 were no longer present, and a new peak appeared in their place, representing the oxidation of xanthate to dixanthogen. Bagci et al. (2007) attribute a similar peak observed in a chalcopyrite and sodium isopropyl xanthate system to the adsorption of xanthate as CuX. Comparing the voltammograms of different xanthate concentrations in Figure 3 it can be seen that the current density of peak 1 diminishes with increasing `concentration and a peak at low positive potential is

present at a concentration of 10^{-3} M, suggestive of dixanthogen formation. Peak 3 is also shifted to a higher potential as a consequence of surface passivation by a hydrophobic dixanthogen layer, which prevents oxidation of the surface at lower anodic potentials.

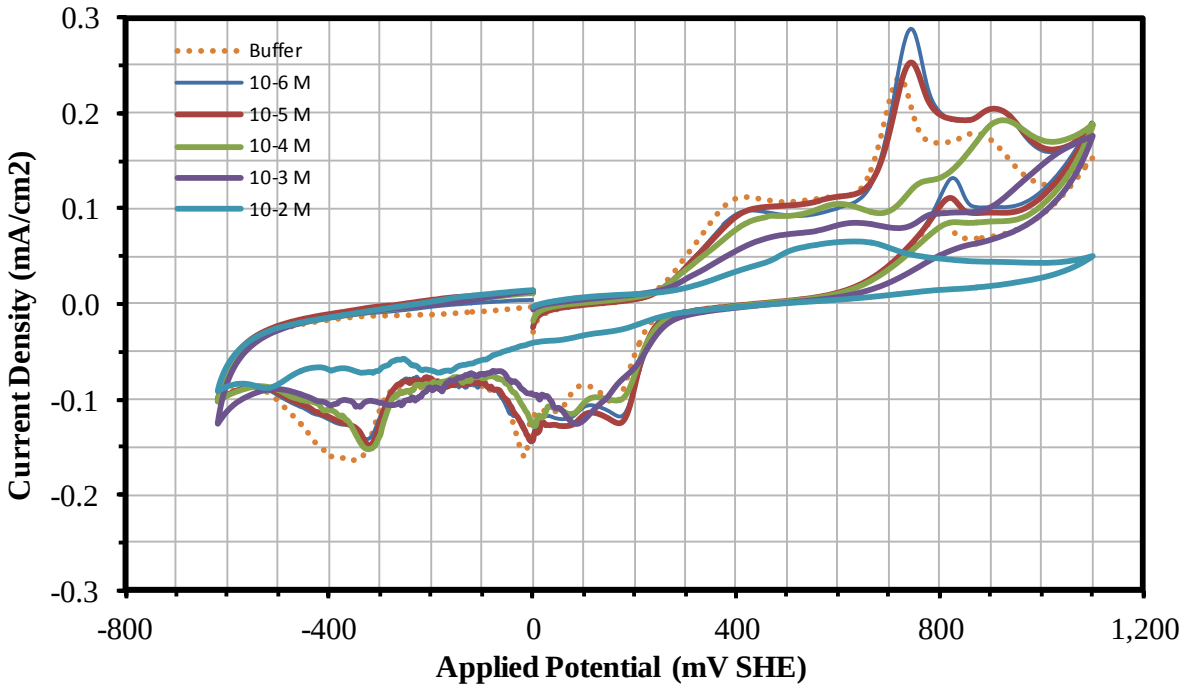

Figure 4. Reactivity of the enargite surface in the presence of 10^{-6}, 10^{-5}, 10^{-4}, 10^{-3} and 10^{-2} M DTPI in pH 10 buffer solutions.

Although the interaction of DTPI collectors with sulphide minerals has been well studied in the literature (Bagci et al., 2007; Güler et al., 2006; Pecina et al., 2006), these works have focussed on the more common base metal and iron sulphides such as chalcopyrite, pyrite and galena. Limited information is available about the interaction of DTPIs with arsenic-bearing sulphides, of which enargite and tennantite ($Cu_{12}As_4S_{13}$) are the most significant in copper ore bodies (Petrus et al., 2011a). Of these two minerals, the adsorption of the related dithiophosphate (DTP) collector onto tennantite has been investigated (Petrus et al., 2011a; Petrus et al., 2011b), and the flotation response of enargite with several collectors, including isopropyl xanthate and diisobutyl dithiophosphate, at pH 10.5, has been studied using a modified Halimond tube (Castro et al., 2003). Fornasiero and co-workers (Fornasiero et al., 2001) studied the effects of selective oxidation or dissolution on the separation of enargite and tennantite from non-arsenic copper sulphides using diethyl dithiophosphate collector. Smith and Bruckard (2007) used sodium isobutyl xanthate and a dithiophosphate (AP 208) in their study of tennantite separation, while Senior et al. (2006) conducted single mineral studies of enargite using KEX collector. However apart from pulp

potential measurements these studies did not involve any investigation of the specific effects of these collectors on the electrochemical response of these systems.

In this study sodium dialkyl dithiophosphinate (Aerophine 3418A promoter) was chosen for investigation as it is reported to be a strong collector for sulphides and selective against iron sulphide minerals. Electrochemical investigations show the effect of DTPI concentration on the cyclic polarisation of natural enargite at pH 10, as shown in Figure 4.

This outcome is similar to that seen with chalcopyrite (Güler et al., 2004) over a range of DTPI concentrations, although the voltammograms in this work are first cycle, rather than fifth cycle as used by Güler et al., (2004) hence the current peaks are more pronounced. Current density decreases proportionally with increasing DTPI concentration, which can be interpreted as indicative of the formation of a passivating layer on the mineral surface. This layer inhibits access of the surrounding solution to the surface, limiting redox activity and the formation of current density peaks in the cyclic voltammogram.

4.2. Surface composition of unoxidised (natural) enargite

The composition of the natural enargite used for this study was characterized using XPS to analyse a crushed fragment of freshly-cleaved natural enargite, which was transferred to the loading chamber as a fine powder immediately after preparation, to minimise oxidation. Analysis was carried out at room temperature throughout the measurements. Characteristic photoelectron peaks were detected for copper, arsenic and sulphur, as well as for oxygen and carbon. The relative atomic concentrations of all elements show small deviations with respect to the stoichiometric formula of enargite, i.e. Cu_3AsS_4, with concentrations of Cu 2p 27.1%, As 3d 12.3% and S 2p 35.9% detected.

Normalizing with respect to copper gives a Cu:As:S ratio of 3:1.4:4 which indicates that the content of arsenic contained in the mineral sample is slightly higher than the stoichiometric content. Other elements detected include O 1s (3.2%) and C 1s (21.6%), where C 1s is used as the internal reference for charge correction.

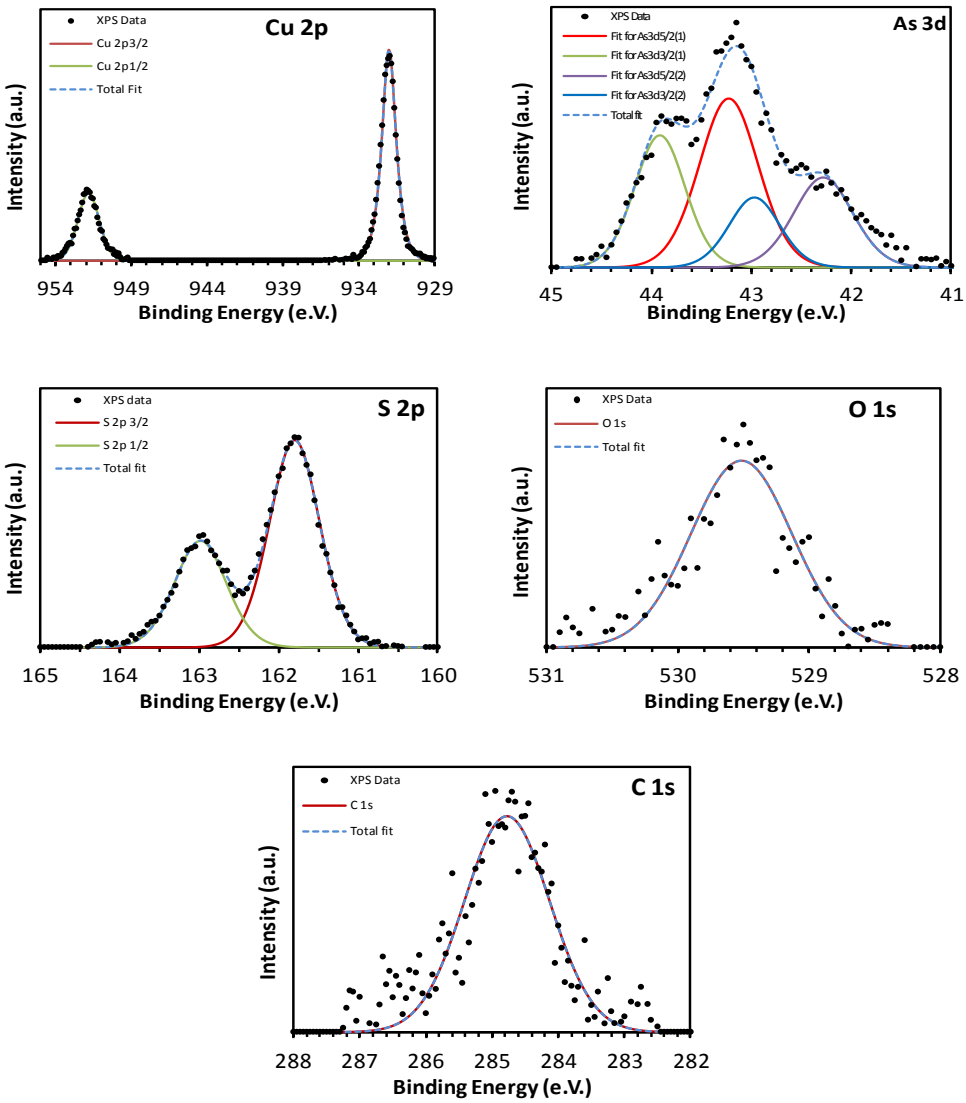

Figure 5. Cu 2p, As 3d, S 2p, O 1s and C 1s high resolution photoelectron spectra recorded from the fractured surface of natural enargite prepared by crushing an unoxidised crystalline sample and immediately transferring it to the XPS instrument.

Shown in Figure 5 are the high resolution photoelectron spectra for Cu 2p, S 2p, As 3d, O 1s and C 1s. The Cu $2p_{3/2}$ spectrum peak occurs at a binding energy of 932.0 eV. The S 2p spectrum is fit with one spin-orbit doublet at binding energies of 161.8 and 163.0 eV for the S $2p_{3/2}$ and S $2p_{1/2}$ peaks, respectively.

The As 3d spectrum for the bulk enargite matrix is fit with a spin-orbit doublet, the 5/2 component located at 43.2 eV, and the low binding energy shoulder is fit with another doublet with the 5/2 component at 42.2 eV. A single O 1s spectrum is located at 529.5 eV while the position of each peak has been corrected to account for charging effects by reference to the C 1s spectrum, which has been fixed at 284.8 eV. The complete XPS data is contained in Table 1.

Table 1. Binding energies, full width half-maxima (FWHM) and atomic concentrations (Atom %) of the elements identified on the freshly fractured enargite surface.

	BE	FWHM	Atom %
Cu $2p_{3/2}$	932.0	1.1	18.9
Cu $2p_{1/2}$	951.9	1.7	8.2
O 1s	529.5	0.9	3.2
C 1s C-C ref	284.8	1.5	21.6
S $2p_{3/2}$	161.8	0.7	23.4
S $2p_{1/2}$	163.0	0.8	12.5
As $3d_{5/2}$ (surface)	42.2	0.8	2.6
As $3d_{3/2}$ (surface)	42.9	0.8	1.7
As $3d_{5/2}$ (bulk)	43.2	0.6	4.8
As $3d_{3/2}$ (bulk)	43.9	0.6	3.2

In previous work (Plackowski et al., 2014) thermodynamic data, XPS results, and published work (Guo and Yen, 2008), were used as the basis for formulating new reaction mechanisms for each of the applied anodic, or oxidative, potentials investigated as treatment conditions. The reaction mechanism corresponding to an applied potential of +516 mV using natural enargite at pH 10 without collector is presented as follows (Plackowski et al., 2014):

$$Cu_{3-x}AsS_4 + (14-2x)OH^- = (3-x)Cu^{2+} + (6-2x)OH^- + AsO_4^{3-} + 4S_n^{2-} + 4H_2O + (3-2x)e^- \quad [1]$$

Plackowski et al. (2013b) also considered the cathodic scan returning from high applied potential (peaks 6, 7 and 8 in Figure 2), where the current peaks result from the reduction of copper hydroxide (peak 7 in Figure 2) and elemental sulphur and polysulfide ions (peak 8, -400 mV). The reduction reactions can be presented as follows:

$$2Cu(OH)_2 + 2e^- = Cu_2O + 2OH^- + 2H_2O \quad E(SHE) = -95\,mV \quad [2]$$

$$2S^0 + 2e^- = S_2^{2-} \quad E(SHE) = -670\,mV \quad [3]$$

$$S_2^{2-} + 2e^- = 2S^{2-} \quad E(SHE) = -720\,mV \quad [4]$$

At low potential the reduction decomposition of enargite must also be considered, and includes arsenic sulphide and copper sulphide among its products as shown below:

$$2Cu_3AsS_4 + 6H_2O + 6e^- = As_2S_2 + 3Cu_2S + 2H_2S + 6OH^- \quad [5]$$

These mechanisms are useful to give an indication of the nature of the chemical species which may be present on the enargite surface as a result of electrochemical oxidation, thus providing a baseline reference for further studies. In this work XPS was used to investigate the enargite surface after application of an oxidising or reducing potential in the presence of a flotation collector. The

principal purpose was to identify whether the collector was present on the surface or not, and secondary to this, to identify the chemical species present. This information may then be useful to suggest the type of adsorption mechanism responsible for any surface layer formation.

4.3. Enargite in the presence of xanthate collector

Changes in the elemental species detected on the surface of enargite at oxidising and reducing potentials in the presence of sodium ethyl xanthate were investigated by XPS to identify which species are present after treatment and to compare with untreated enargite.

Analysis of the crystalline xanthate used to prepare the experimental solutions revealed the presence of Na 1s, O 1s, C 1s and S 2p species in accord with the chemical formula of sodium ethyl xanthate, $CH_3CH_2OCS_2Na$, and the binding energies for each species are shown in Table 2.

Table 2. Binding energies, full width half-maxima and atomic concentrations of the elements identified in crystalline SEX at -130 °C.

	BE	**FWHM**	**Atom %**
Na 1s	1071.6	1.3	15.9
O 1s	531.5	1.4	6.5
O 1s O*-C-S	533.2	1.3	9.2
C 1s C-C ref	284.8	1.0	20.4
C 1s C-COO	285.4	0.9	1.8
C-O	286.2	1.0	11.0
C-S	287.5	0.9	9.4
COO	288.5	1.0	1.8
S $2p_{3/2}$ CS_2	162.0	0.9	10.8
S $2p_{1/2}$ CS_2	163.2	0.9	5.4
S $2p_{3/2}$ SO_4	168.2	0.9	0.4
S $2p_{1/2}$ SO_4	169.4	0.9	0.2

Figure 6 shows the XPS photoelectron spectra recorded from enargite after conditioning for 10 minutes at +516 mV in SEX solution, while the binding energies are included in Table 3. In this enargite sample the O 1s spectrum shows the presence of an additional species at about 529.6 eV which was identified as antimony (Sb $3d_{5/2}$) and confirmed by the presence of a corresponding Sb $3d_{3/2}$ peak at the correct area ratio and peak separation of 9.34 eV. It represents a minor contaminant at a concentration of about 0.3 atom%, and is present in other results shown below although for clarity has been omitted from the tables.

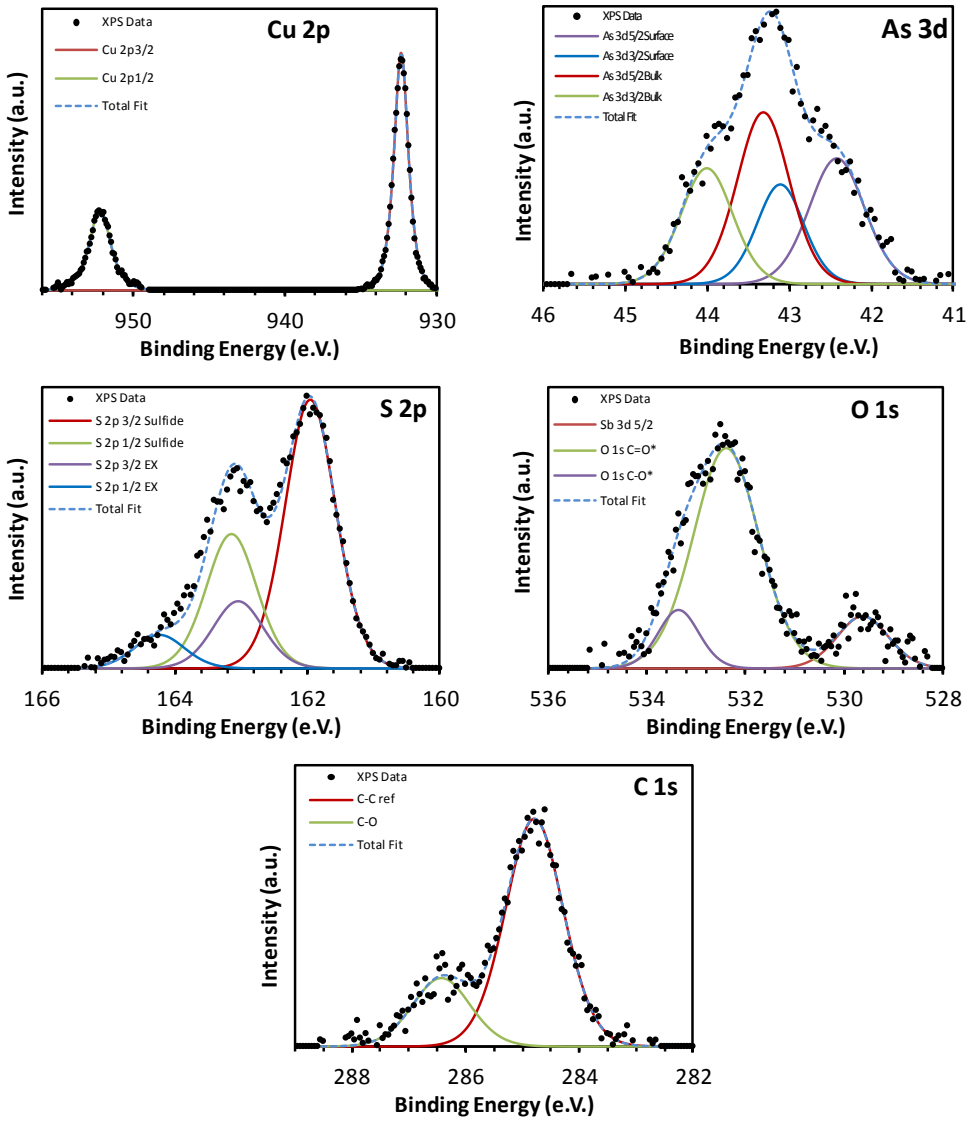

Figure 6. Cu 2p, As 3d, S 2p, O 1s and C 1s high resolution photoelectron spectra recorded from the enargite electrode surface at -130 °C after application of +516 mV at pH 10 in a 10^{-3} M SEX solution.

Adsorption of xanthate on sulphide surfaces was investigated by Ranta et al. (1981) using XPS to determine the binding energies of C, O and S of KEX on synthetic thin sulphide layers. They report a S 2p BE of 163.7 eV for bulk KEX, although it appears insufficient resolution was obtained to isolate the S $2p_{3/2}$ component, which makes comparison with the present results difficult. In our work S $2p_{3/2, 1/2}$ BEs of 162.0 and 163.2 eV were found for crystalline sodium ethyl xanthate.

A BE range between 162.1 and 162.6 eV was reported by Ranta et al. (1981) for adsorbed xanthate, which is significantly lower than the S $2p_{3/2}$ BE of 163.1 eV in this work. Such a comparison is useful to show the expected BE shift of the S 2p component between the bulk and adsorbed xanthate. Differences in S 2p BEs between SEX and KEX are shown to exist and,

combined with the different substrates onto which they were adsorbed (Ranta et al., 1981 used a copper sheet with a thin layer of copper sulphide), direct comparison of these different systems is difficult.

Table 3. Binding energies, full width half-maxima and atomic concentrations of the elements identified on the enargite surface at -130 °C after application of +516 mV at pH 10 in a 10^{-3} M SEX solution.

	BE	**FWHM**	**Atom %**
Cu $2p_{3/2}$	932.3	1.1	10.6
Cu $2p_{1/2}$	952.2	1.6	5.2
O 1s	532.4	1.6	8.6
O 1s O*-C-S	533.4	1.0	1.4
C 1s C-C ref	284.8	1.2	30.1
C 1s C-O-C	286.4	1.2	9.1
S $2p_{3/2}$ sulphide	161.9	0.9	15.3
S $2p_{1/2}$ sulphide	163.2	0.9	7.7
S $2p_{3/2}$ EX	163.1	0.9	3.8
S $2p_{1/2}$ EX	164.2	0.9	1.9
As $3d_{5/2}$ surface	42.4	0.8	1.6
As $3d_{3/2}$ surface	43.1	0.7	1.1
As $3d_{5/2}$ bulk	43.3	0.7	2.0
As $3d_{3/2}$ bulk	44.0	0.7	1.4

According to Ranta et al. (1981), the C 1s spectra can be used to determine ethyl xanthate adsorption by the presence of a peak additional to the adventitious carbon peak (284.8 eV in the present work) between 286.3 – 286.5 eV, which compares well with the present work where a second peak exists at 286.4 eV. Mielczarski (1987) also found a C 1s peak at about 286.5 eV after treatment of chalcocite with KEX, attributed to the C-O-C group in xanthate. The carbon atom in the CH_3 group is characterised by a peak at about 284.9 eV and cannot be distinguished from hydrocarbon contamination, although it accounts for the significant increase in this component compared to the fresh enargite surface (21.6 to 30.1 %).

Considering the O 1s spectra, Ranta et al. (1981) report the presence of a new component at 532.9 eV after xanthate adsorption which they conclude indicates the presence of collector. Mielczarski (1987) reports an increase in the contribution of the O 1s component at 533.0 eV, which is due to oxygen from the xanthate. This is in good agreement with the O 1s peak detected at 533.4 eV in this work.

Thus a comparison of the results from enargite conditioned at +516 mV to the fresh enargite surface reveals that clear differences in the S 2p, C 1s and O 1s spectra exist, which can be attributed to the presence of xanthate on the surface after conditioning.

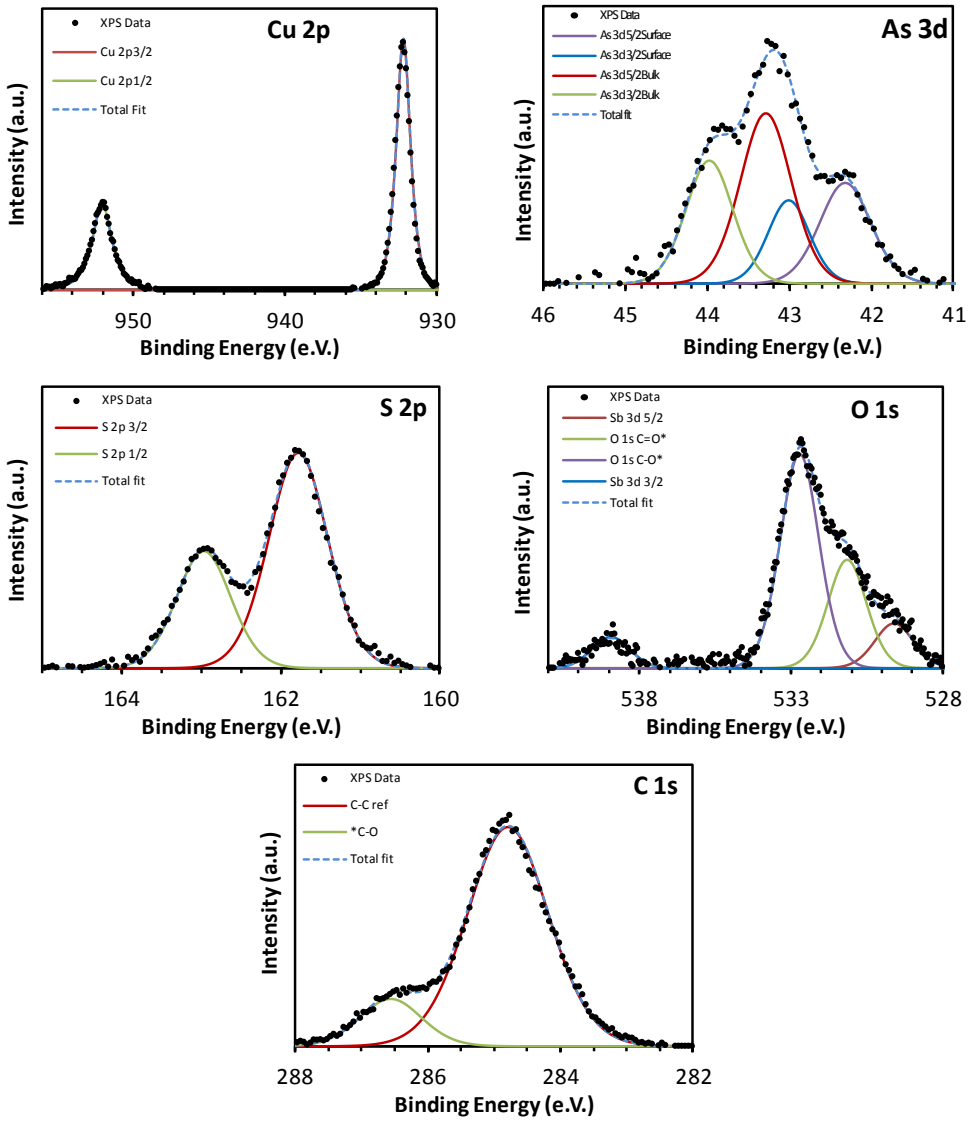

Figure 7. Cu 2p, As 3d, S 2p, O 1s and C 1s high resolution photoelectron spectra recorded from the enargite electrode surface at -130 °C after application of -400 mV at pH 10 in a 10^{-3} M SEX solution.

Regarding the nature of the surface xanthate species, the XPS results suggest the adsorption products detected on the enargite surface are more likely to be in the form of dixanthogen rather than copper xanthate, which in another study has been reported as the only adsorption product (Valli and Persson, 1994). Evidence for this contention is provided by the absence of any change in the Cu 2p spectrum, both in terms of BE and number of Cu species present, while the decrease in relative proportion of Cu can be interpreted as partial passivation of the surface by the formation of an incomplete xanthate surface layer. According to Mielczarski et al. (1996) while dixanthogen is

often assumed to be the surface product, no consensus exists as to whether it and copper xanthate are formed concurrently or sequentially, and if so which is the first to form.

The resulting XPS photoelectron spectra obtained after conditioning at -400 mV are shown in Figure 7 and the associated binding energies in Table 4. After conditioning of enargite at -400 mV in the presence of sodium ethyl xanthate, XPS analysis shows the surface has undergone some changes, with additional O 13 and C 1s species present (Figure 7) when compared to a clean surface, as shown in Figure 5. However only one S 2p species exists, and along with Cu 2p and As 3d peaks their BE's remain unchanged compared to the fresh enargite surface.

The presence of Cu $2p_{3/2}$ at 932.2 eV and S $2p_{3/2}$ at 161.8 eV corresponds to enargite but according to Mielczarski (1987) is also characteristic of cuprous sulphide (Cu_2S). The fact that the relative proportions of both these elements are decreased to about one third of that found for fresh enargite suggests the presence of a partial surface layer, possibly composed in part of cuprous sulphide, occluding the mineral surface. However the ratio of Cu:As:S is approximately 9:3:12 which corresponds well to the stoichiometric ratio for enargite and does not support the presence of additional copper-containing compounds.

Table 4. Binding energies, full width half-maxima and atomic concentrations of the elements identified on the enargite surface at -130 °C after application of -400 mV at pH 10 in a 10^{-3} M SEX solution.

	BE	**FWHM**	**Atom %**
Na 1s	1071.3	1.5	1.2
Cu $2p_{3/2}$	932.2	1.1	6.2
Cu $2p_{1/2}$	952.1	1.5	3.1
O 1s	531.2	1.5	3.8
O 1s C=O*	532.7	1.5	7.6
C 1s C-C ref	284.8	1.4	53.8
C 1s C*-O	286.6	1.1	8.8
S $2p_{3/2}$ sulphide	161.8	0.9	8.1
S $2p_{1/2}$ sulphide	163.0	0.8	4.1
As 3d $_{5/2}$ surface	42.3	0.7	0.7
As 3d $_{3/2}$ surface	43.0	0.5	0.5
As 3d $_{5/2}$ bulk	43.3	1.2	1.2
As 3d $_{3/2}$ bulk	44.0	0.8	0.8

The presence of an O 1s peak at 531.2 eV is suggestive of $Cu(OH)_2$ or possibly CuO, as a reduction product of the hydroxide form, according to Mielczarski (1987) and McIntyre and Cook (1975), although there is no evidence of any corresponding Cu (II) species. It therefore seems

reasonable to conclude that the additional O 1s and C 1s species may represent residual decomposition products of xanthate remaining on the surface. Although only one S 2p species was detected, the BEs of S in enargite (Table 1) and S in xanthate (Table 2) vary by only about 0.2 eV, so it is possible a second species is present but cannot be resolved. This can be confirmed by examining the atomic ratio of Cu:As:S which, at 9.3:3.2:12.2 (Table 4), is very close to that of enargite (3:1:4). As there is no excess of sulphur, this is a strong indication the S 2p peak is from enargite alone.

4.4. Enargite in the presence of dithiophosphinate collector

Adsorption of DTPI on chalcopyrite has been studied by Güler et al. (2006) using Diffuse Reflectance Fourier Transformation spectroscopy to determine the form of adsorbed collector species. They found that formation of cuprous-(DTPI) and dithiolate (a dimer of thiol, $(DTPI)_2$) takes place as the predominant collector species on the surface, while adsorbed DTPI and a dithiophosphinate radical ($(DTPI)^0$) was also detected in minor amounts on the mineral surface.

The XPS results for enargite conditioned at +516 mV in the presence of DTPI are shown in Figure 8 and the associated BEs are contained in Table 6, while the BE data for the bulk DTPI solution are presented in Table 5. It is evident from the XPS data that additional species are present on the enargite surface and that an incomplete surface layer exists, the former demonstrated by the presence of additional Cu, S and O species. The detection of Cu, As and S peaks at BEs corresponding to those seen for a fresh enargite surface, at significantly reduced atomic concentrations, provide the evidence for the existence of a partially exposed mineral surface. In an atomic force microscopy (AFM) study of chalcopyrite and tennantite surfaces after treatment with the related DTP collector (Petrus et al., 2011a) the formation of so-called islands, composed of reaction products such as metal hydroxide species under alkaline conditions, was observed, indicating incomplete mineral surface coverage. Adhesion force measurement using AFM showed a decreasing trend after DTP treatment, and this increase in hydrophobicity was explained as a result of DTP adsorption.

The adsorption of DTPI is considered to take place by a chemisorption mechanism (Pecina-Treviño et al., 2003) and this mechanism has been further elaborated as consisting of a combination of chemical and electrochemical processes (Pecina et al., 2006) depending on the potential of the system.

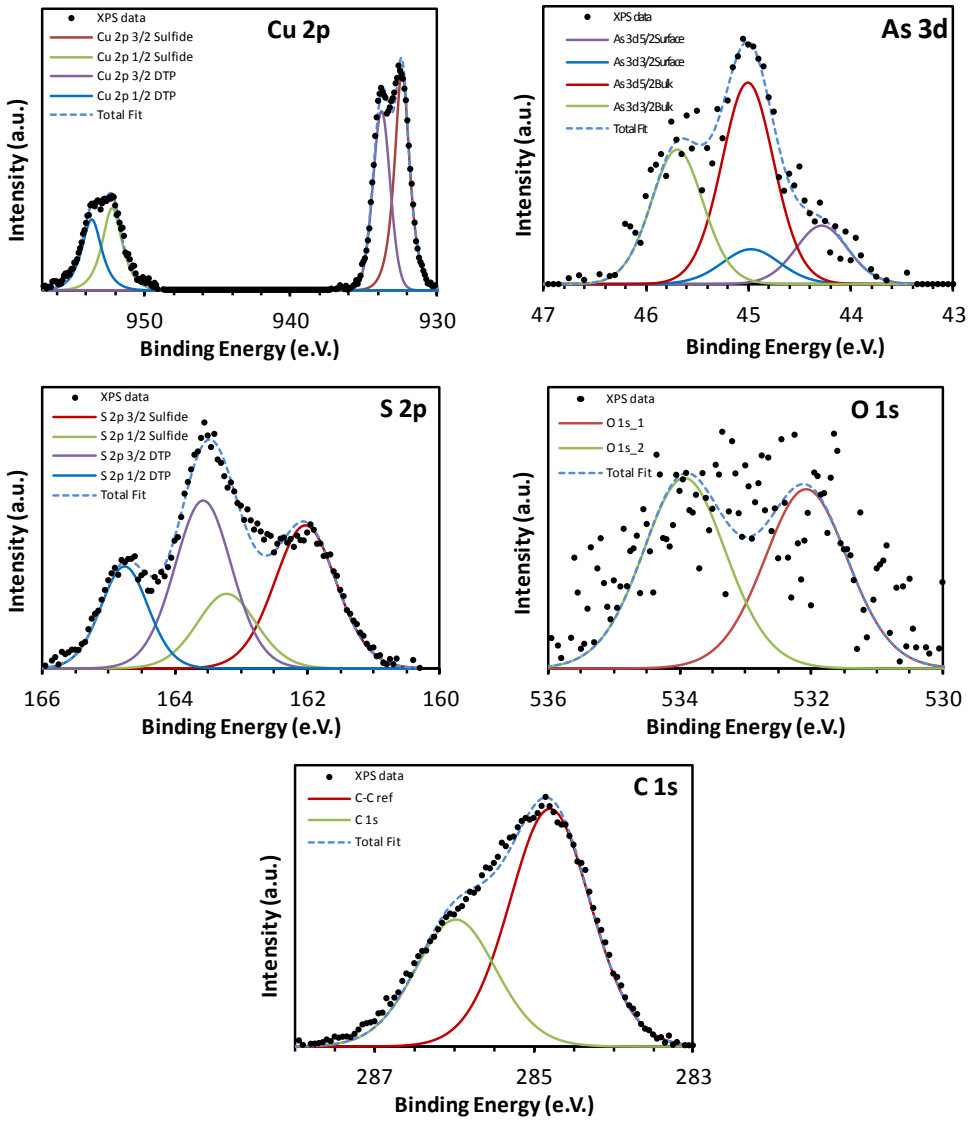

Figure 8. Cu 2p, As 3d, S 2p, O 1s and C 1s high resolution photoelectron spectra recorded from the enargite electrode surface at -130 °C after application of +516 mV at pH 10 in a 10^{-3} M DTPI solution.

Where such a mechanism exists, reaction between the $DTPI^-$ anion and the metal atoms exposed at the surface of the mineral lattice results in the formation of a metal-collector compound such as $Pb(DTPI)_2$ in the case of galena (Pecina et al., 2006), and of Cu(DTPI) where chalcopyrite is involved (Güler et al., 2006). That such a mechanism also exists in the enargite-DTPI system is supported by the presence of the second Cu species (Cu $2p_{3/2}$ 933.8 eV), in addition to the Cu in enargite (Cu $2p_{3/2}$ 932.4 eV), detected by XPS and shown in Figure 8. The presence of a second S 2p species in addition to that from the enargite, and a P 2p doublet, and to a lesser extent a C 1s peak at 286.0 eV, attributable to C-O-C bonding, based on the previous discussion, provide additional evidence for the presence of what is likely to be a Cu(DTPI) species.

Table 5. Binding energies, full width half-maxima and atomic concentrations of the elements identified in DTPI (Aerophine 3418A Promoter) at -130 °C.

	B.E.	FWHM	Atom %
Na 1s	1072.0	1.2	8.8
O 1s	531.5	1.1	0.4
O 1s O*-C-S	532.4	1.2	0.8
O 1s ex H_2O	533.5	1.2	0.5
C 1s C-C ref	284.8	1.0	53.2
C 1s C-P	285.3	1.1	13.9
S $2p_{3/2}$	162.0	1.0	8.6
S $2p_{1/2}$	163.2	0.9	4.3
P $2p_{3/2}$	168.2	0.8	4.5
P $2p_{1/2}$	169.4	0.8	2.2

Further analysis of the surface after conditioning at -400 mV was necessary to confirm the effects of treatment under conditions regarded as within the non-floating potential range for enargite, that is, at a potential below about -25 mV depending on system pH (Senior et al., 2006). The XPS spectra obtained from this surface are shown in Figure 9 while the respective elemental binding energies are given in Table 7.

Table 6. Binding energies, full width half-maxima and atomic concentrations of the elements identified on the enargite surface at -130 °C after application of +516 mV at pH 10 in a 10^{-3} M DTPI solution

	B.E.	FWHM	Atom %
Cu $2p_{3/2}$ I	932.4	1.2	2.7
Cu $2p_{1/2}$ I	952.2	1.6	1.4
Cu $2p_{3/2}$ II	933.8	1.4	2.3
Cu $2p_{1/2}$ II	953.7	1.6	1.2
O 1s	532.1	1.5	0.8
O 1s	533.9	1.5	0.9
C 1s C-C ref	284.8	1.2	45.9
C 1s C-O-C	286.0	1.2	24.5
S $2p_{3/2}$	162.0	1.1	4.5
S $2p_{1/2}$	163.2	1.1	2.2
S $2p_{3/2}$	163.6	1.0	4.9
S $2p_{1/2}$	164.7	0.8	2.4
As $3d_{5/2}$ (1)	44.3	0.6	0.2
As $3d_{3/2}$ (1)	44.9	0.7	0.1
As $3d_{5/2}$ (2)	45.0	0.6	0.6
As $3d_{3/2}$ (2)	45.7	0.6	0.4

The Cu, As and S species detected correspond in their binding energies to those found in enargite, and no additional Cu species are present. No phosphorus was found on the surface and although a small amount of Na was found (about 3 atom %) this may be attributed to Na^+ ions dissociated from DTPI in solution and deposited on the mineral surface. On its own it is not sufficient evidence for the adsorption of collector on the surface. Additionally only one S 2p component is detected and with a S $2p_{3/2}$ BE of 161.5 eV, this corresponds to sulphur in unaltered enargite where a BE of 161.8 eV was found.

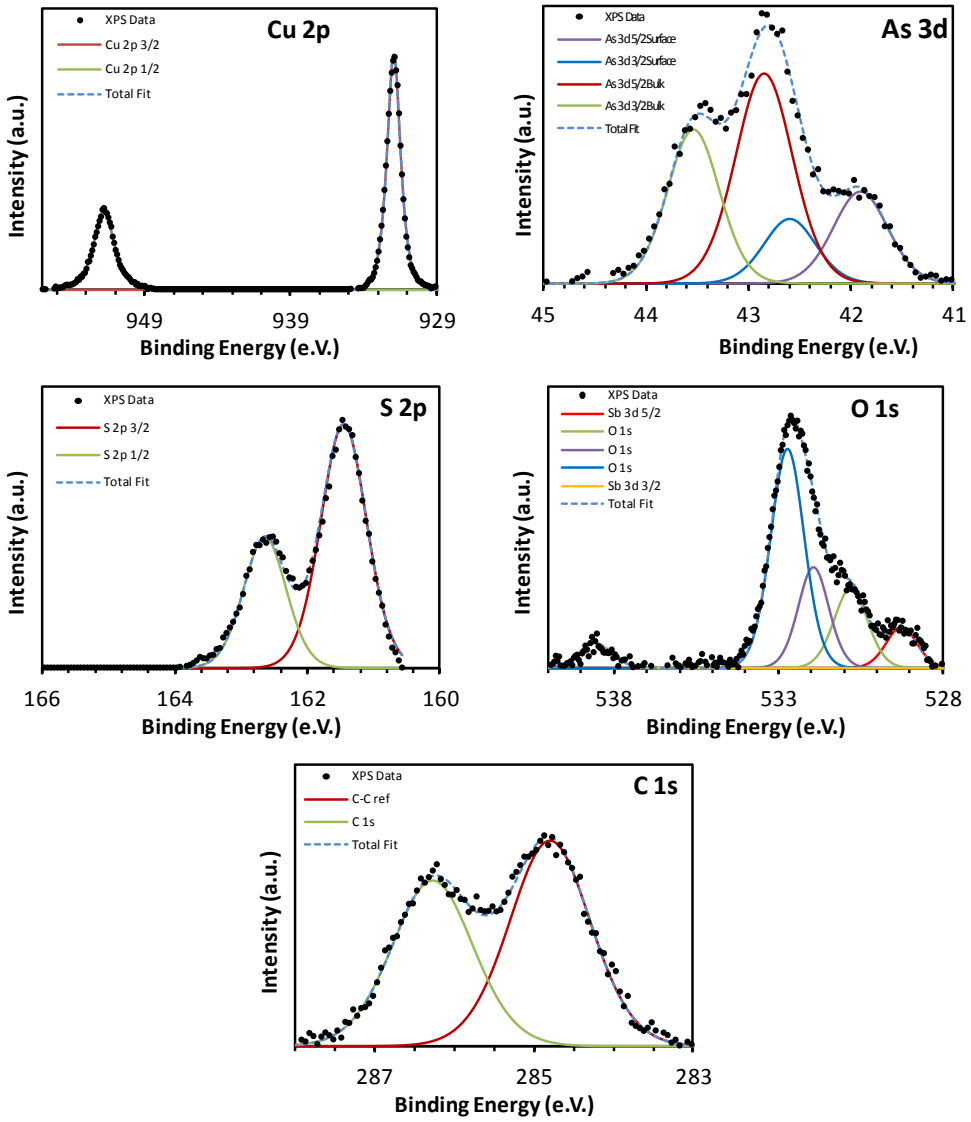

Figure 9. Cu 2p, As 3d, S 2p, O 1s and C 1s high resolution photoelectron spectra recorded from the enargite electrode surface at -130 °C after application of -400 mV at pH 10 in a 10^{-3} M DTPI solution.

That collector adsorption is demonstrated at +516 but not at -400 mV suggests that in the case of the DTPI-enargite system an electrochemical-chemical mechanism as proposed by Pecina et al.

(2006) is responsible for the interaction. Such a mechanism involves electrochemical oxidation of the mineral, followed by chemical formation of the metal-collector compound.

Table 7. Binding energies, full width half-maxima and atomic concentrations of the elements identified on the enargite surface at -130 °C after application of -400 mV at pH 10 in a 10^{-3} M DTPI solution.

	B.E.	**FWHM**	**Atom %**
Na 1s	1071.2	1.4	3.0
Cu $2p_{3/2}$	931.9	1.1	12.2
Cu $2p_{1/2}$	951.8	1.6	6.0
O 1s	530.8	1.2	3.2
O 1s	531.9	1.1	3.7
O 1s C-O*	532.7	1.2	8.7
C 1s C-C ref	284.8	1.2	21.7
C 1s C-O-C	286.3	1.2	17.5
S $2p_{3/2}$ sulphide	161.5	0.8	12.9
S $2p_{1/2}$ sulphide	162.6	0.8	6.4
As $3d_{5/2}$ surface	41.9	0.6	0.8
As $3d_{3/2}$ surface	42.6	0.6	0.5
As $3d_{5/2}$ bulk	42.8	0.6	1.9
As $3d_{3/2}$ bulk	43.5	0.6	1.3

4.5. Micro flotation with pulp potential control

Microflotation tests were conducted to confirm the effects of conditioning at different redox potentials in the presence of collector on the flotation recovery of enargite. Although many different variables have the potential to affect recovery, including collector dosage, flotation time, gas rate, pH and others, the purpose of these tests was to confirm the effects of conditioning at oxidising and reducing potentials in the presence of collector on hydrophobicity, therefore only the effects of varying Eh were investigated.

Potentials of +500 and -400 mV were selected to correspond to anodic and cathodic peaks respectively identified in the CV studies, and also to ensure the test values were sufficiently separated from the transition potential range of approximately -100 to +100 mV to ensure the results were representative of flotation in the floating or non-floating potential regions. An additional test was carried out at approximately +100 mV to evaluate flotation performance in the region of the transition range, using SEX as the collector. However since automatic titrators were not used, maintaining precise control of Eh over a wide range of values was found to be impractical and no attempt was made to characterise flotation recovery at closely spaced Eh values.

Flotation recovery (as determined by mass recovery of enargite to the concentrate) using xanthate as the collector was found to be 82%, at +500 mV, at +100 mV 52% reported to the concentrate, and at -400 mV about 11% of the total sample mass was recovered. Using 3418A, a recovery of 69% was found at +500 mV, while at -400 mV this figure dropped to 31%. These results support the XPS findings where collector adsorption was confirmed after conditioning at +516 mV but not -400 mV, and are also in agreement with published results, such as Smith and Bruckard (2007) and Bruckard et al., (2010), showing similar trends to these results.

4.6. General Discussion

Although this work demonstrates differences in collector adsorption according to potential, further study including investigation of whether collector adsorption at positive potentials is electrochemically reversible by subsequent application of cathodic potentials, is recommended to better characterize the nature of the adsorption mechanism. Development of a means of precise automatic pulp potential control in the UCT Micro Cell is also required to enable accurate determination of the transition potential range of enargite under different treatment conditions, particularly for different collectors. Investigation of alternative flotation collectors with a high selectivity and strong affinity for the arsenic sites in the enargite crystal structure is an essential step to facilitate an efficient separation of arsenic-bearing sulphides from non-arsenic copper sulphides while minimizing copper losses.

Although reliance on pulp potential control has demonstrated that it is possible to achieve a crude separation of enargite from non-arsenic sulphides under idealized conditions, usually involving single mineral systems, typically separation efficiency is low and copper losses are high in more complex systems that attempt to replicate multi-mineral systems or conditions in an industrial flotation plant. In addition, the flowsheet for such a process is complex, for example as proposed by Senior et al., (2006), likely to be difficult to operate and require significant operational expenditure. However, these factors must also be balanced against the increasing costs of treating high arsenic ores and the necessity of finding alternative treatment routes to enable processing of these less favourable ores.

5. Conclusions

Consideration has been given to the adsorption of SEX and DTPI onto the surface of natural enargite at pH 10 at applied potentials of -400 and +516 mV. Analysis of the results presented in this paper shows there is a significant difference in the chemical composition on the surface of enargite after conditioning with the flotation collectors at these potentials.

XPS analysis shows that conditioning with xanthate at +516 mV results in the presence of C 1s and O 1s spectra diagnostic of xanthate adsorption, as well as BE differences in the S 2p combined with the presence of an additional S 2p spectrum after conditioning. Together these findings demonstrate the presence of xanthate on the enargite surface as a result of electrochemical treatment. After conditioning at -400 mV no evidence was found for xanthate adsorption with no additional S 2p species identified, and C 1s and O 1s species corresponding to adventitious hydrocarbon deposition detected. In addition, the Cu:As:S atom% ratio was in good agreement with the stoichiometrically correct ratio for enargite, showing no excess of sulphur or copper depletion.

Investigation of the enargite/DTPI system also shows significant differences in the surface speciation when the effects of these two different conditioning potentials are compared. After treatment at +516 mV additional Cu, S and O species to those in enargite alone exist on the surface and form an incomplete surface layer. While Cu, As and S peaks at BE's corresponding to enargite are found, their significantly reduced atomic concentrations support the argument for a mineral surface partially occluded by adsorbed collector. Similar to conditioning in the presence of xanthate at -400 mV, no evidence was found to confirm the presence of DTPI species adsorbed on the enargite surface under these conditions.

Floatability measurements using the UCT microflotation cell were used to assess the hydrophobicity of enargite mineral particles after conditioning at pulp potentials equivalent to the applied potentials used in the conditioning treatments for the XPS studies. The selected collectors were SEX and DTPI. Mass recovery of enargite was measured at potentials of +500, +100 and -400 mV. Using xanthate recovery, and therefore hydrophobicity, was greatest at high potential (82%), then decreased to 52% at +100 mV, while a poor flotation response was observed at -400 mV with 11% mass recovery to concentrate. When DTPI was the collector, recoveries of 69% at high potential and 31% at low potential were recorded. These results were consistent with those of the XPS measurements of surface species present after conditioning at equivalent applied electrochemical potentials.

Acknowledgments

The authors gratefully acknowledge The University of Queensland (UQ) for an APA Scholarship (C.P.), CSIRO for the top-up scholarship (C.P.) and research expenses support, Prof Dee Bradshaw from UQ for use of her UCT microflotation cell, and the CMM (Centre for Microscopy and Microanalysis, UQ) for the facilities and assistance.

References

Bagci, E., Ekmekci, Z., Bradshaw, D., Adsorption behaviour of xanthate and dithiophosphinate from their mixtures on chalcopyrite. Minerals Engineering, 2007, **20(10)**, 1047-1053.

Biswas, A.K., Davenport, W.G., *Extractive metallurgy of copper*. 3rd edn. 1994, Pergamon, Oxford.

Bradshaw, D.J., O'Connor, C.T., Measurement of the sub-process of bubble loading in flotation. Minerals Engineering, 1996, **9(4)**, 443-448.

Bruckard, W.J., Davey, K.J., Jorgensen, F.R.A., Wright, S., Brew, D.R.M., Haque, N., Vance, E.R., Development and evaluation of an early removal process for the beneficiation of arsenic-bearing copper ores. Minerals Engineering, 2010, **23(15)**, 1167-1173.

Bruckard, W.J., Kyriakidis, I., Woodcock, J.T., The flotation of metallic arsenic as a function of pH and pulp potential - A single mineral study. International Journal of Mineral Processing, 2007, **84(1-4)**, 25-32.

Castro, S.H., Baltierra, L., Hernandez, C., 2003. Redox conditions in the selective flotation of enargite, In *Electrochemistry in Mineral and Metal Processing VI*, ed. Fiona M. Doyle, R. Woods. The Electrochemical Society Inc., New Jersey, 2003-18, pp. 27-36.

Chatterjee, A., Das, D., Mandal, B.K., Chowdhury, T.R., Samanta, G., Chakraborti, D., Arsenic in Ground-Water in 6 Districts of West-Bengal, India - The Biggest Arsenic Calamity in the World .1. Arsenic Species in Drinking-Water and Urine of the Affected People. Analyst, 1995, **120(3)**, 643-650.

Cordova, R., Gomez, H., Real, S.G., Schrebler, R., Vilche, J.R., Characterization of natural enargite/aqueous solution systems by electrochemical techniques. Journal of the Electrochemical Society, 1997, **144(8)**, 2628-2636.

Fantauzzi, M., Atzei, D., Elsener, B., Lattanzi, P., Rossi, A., XPS and XAES analysis of copper, arsenic and sulfur chemical state in enargites. Surface and Interface Analysis, 2006, **38(5)**, 922-930.

Fornasiero, D., Fullston, D., Li, C., Ralston, J., Separation of enargite and tennantite from non-arsenic copper sulfide minerals by selective oxidation or dissolution. International Journal of Mineral Processing, 2001, **61(2)**, 109-119.

Güler, T., Hiçyilmaz, C., Gökag˘aç, G., Ekmeçi, Z., Adsorption of dithiophosphate and dithiophosphinate on chalcopyrite. Minerals Engineering, 2006, **19(1)**, 62-71.

Güler, T., Hiçyilmaz, C., Gökağaç, G., Ekmekçi, Z., Voltammetric and drift spectroscopy investigation in dithiophosphinate–chalcopyrite system. Journal of Colloid and Interface Science, 2004, **279(1)**, 46-54.

Guo, H., 2004. Electrochemistry and flotation of enargite and chalcopyrite, In *Department of Mining Engineering*. Queen's University, Ontario, p. 270.

Guo, H., Yen, W.T., Surface potential and wettability of enargite in potassium amyl xanthate solution. Minerals Engineering, 2002, **15(6)**, 405-414.

Guo, H., Yen, W.T., Selective flotation of enargite from chalcopyrite by electrochemical control. Minerals Engineering, 2005, **18(6)**, 605-612.

Guo, H., Yen, W.T., 2006. Electrochemical floatability of enargite and effects of depressants, In *Proceedings of the XXIII International Mineral Processing Conference*, eds. Önal, Güven, Acarkan, Neşet, Çelik, Mehmet S., Arslan, Fatma, Ateşok, Gündüz, Güney, Ali, Sirkeci, Ayhan A., Yüce, A. Ekrem, Perek, K. Tahsin. Promed, Istanbul, Turkey, pp. 504-509.

Guo, H., Yen, W.T., Electrochemical study of synthetic and natural enargites. Proceedings of [the] 24th International Mineral Processing Congress, Beijing, China, Sept. 24-28, 2008, 2008, **1**, 1138-1145.

Hampton, M.A., Plackowski, C., Nguyen, A.V., Physical and Chemical Analysis of Elemental Sulfur Formation during Galena Surface Oxidation. Langmuir, 2011, **27(7)**, 4190-4201.

McIntyre, N.S., Cook, M.G., X-ray photoelectron studies on some oxides and hydroxides of cobalt, nickel, and copper. Analytical Chemistry, 1975, **47(13)**, 2208-2213.

Mielczarski, J., XPS study of ethyl xanthate adsorption on oxidized surface of cuprous sulfide. Journal of Colloid and Interface Science, 1987, **120(1)**, 201-209.

Mielczarski, J.A., Cases, J.M., Alnot, M., Ehrhardt, J.J., XPS characterization of chalcopyrite, tetrahedrite, and tennantite surface products after different conditioning .2. Amyl xanthate solution at pH 10. Langmuir, 1996, **12(10)**, 2531-2543.

Pecina-Treviño, E.T., Uribe-Salas, A., Nava-Alonso, F., Pérez-Garibay, R., On the sodium-diisobutyl dithiophosphinate (Aerophine 3418A) interaction with activated and unactivated galena and pyrite. International Journal of Mineral Processing, 2003, **71(1–4)**, 201-217.

Pecina, E.T., Uribe, A., Finch, J.A., Nava, F., Mechanism of di-isobutyl dithiophosphinate adsorption onto galena and pyrite. Minerals Engineering, 2006, **19(9)**, 904-911.

Petrus, H.T.B.M., Hirajima, T., Sasaki, K., Okamoto, H., Effect of pH and diethyl dithiophosphate (DTP) treatment on chalcopyrite and tennantite surfaces observed using atomic force microscopy (AFM). Colloids and Surfaces A: Physicochemical and Engineering Aspects, 2011a, **389(1–3)**, 266-273.

Petrus, H.T.B.M., Hirajima, T., Sasaki, K., Okamoto, H., Study of diethyl dithiophosphate adsorption on chalcopyrite and tennantite at varied pHs. J Min Sci, 2011b, **47(5)**, 695-702.

Plackowski, C., Hampton, M.A., Bruckard, W.J., Nguyen, A.V., An XPS investigation of surface species formed by electrochemically induced surface oxidation of enargite in the oxidative potential range. Minerals Engineering, 2014, **55(0)**, 60-74.

Plackowski, C., Hampton, M.A., Nguyen, A.V., Bruckard, W.J., The effects of X-ray irradiation and temperature on the formation and stability of chemical species on enargite surfaces during XPS. Minerals Engineering, 2013a, **45(0)**, 59-66.

Plackowski, C., Hampton, M.A., Nguyen, A.V., Bruckard, W.J., Fundamental Studies of Electrochemically Controlled Surface Oxidation and Hydrophobicity of Natural Enargite. Langmuir, 2013b, **29(7)**, 2371-2386.

Plackowski, C., Nguyen, A.V., Bruckard, W.J., A critical review of surface properties and selective flotation of enargite in sulphide systems. Minerals Engineering, 2012, **30**, 1-11.

Ranta, L., Minni, E., Suoninen, E., Heimala, S., Hintikka, V., Saari, M., Rastas, J., XPS studies of adsorption of xanthate on sulfide surfaces. Applications of Surface Science, 1981, **7(4)**, 393-401.

Senior, G.D., Guy, P.J., Bruckard, W.J., The selective flotation of enargite from other copper minerals - a single mineral study in relation to beneficiation of the Tampakan deposit in the Philippines. International Journal of Mineral Processing, 2006, **81(1)**, 15-26.

Skinner, W.M., Prestidge, C.A., Smart, R.S.C., Irradiation effects during XPS studies of Cu(II) activation of zinc sulphide. Surface and Interface Analysis, 1996, **24(9)**, 620-626.

Smith, L.K., Bruckard, W.J., The separation of arsenic from copper in a Northparkes copper-gold ore using controlled-potential flotation. International Journal of Mineral Processing, 2007, **84(1-4)**, 15-24.

Valli, M., Persson, I., Interactions between sulphide minerals and alkylxanthates 8. A vibration and X-ray photoelectron spectroscopic study of the interaction between chalcopyrite, marcasite, pentlandite, pyrrhotite and troilite, and ethylxanthate and decylxanthate ions in aqueous solution. Colloids and Surfaces A: Physicochemical and Engineering Aspects, 1994, **83(3)**, 207-217.

Velasquez, P., Ramos-Barrado, J.R., Cordova, R., Leinen, D., XPS analysis of an electrochemically modified electrode surface of natural enargite. Surface and Interface Analysis, 2000, **30(1)**, 149-153.

Wittstock, G., Kartio, I., Hirsch, D., Kunze, S., Szargan, R., Oxidation of Galena in Acetate Buffer Investigated by Atomic Force Microscopy and Photoelectron Spectroscopy. Langmuir, 1996, **12(23)**, 5709-5721.

Chapter VII

Conclusions and recommendations

1. Research Summary and Conclusions

1.1. Overview

This body of work evolved out of past research at the CSIRO in Australia that took place over a number of years in response to the growing problem of arsenic contamination in copper sulphide ores, with the aim of developing a new approach to address this issue. Their approach involved researching a means of selective flotation of arsenic-bearing minerals, including enargite and tennantite, from copper sulphides using controlled potential flotation. The greatest difficulty in achieving selectivity is that arsenic-bearing copper minerals have very similar flotation behaviour to the valuable minerals they are commonly associated with, and as such they are generally recovered together to the concentrate.

Several recent studies (Bruckard et al. 2007, Smith and Bruckard 2007, Senior et al. 2006, Bruckard et al. 2010) have demonstrated that controlled potential flotation has the potential to separate arsenic from non-arsenic sulphide minerals. However our understanding of the fundamental mechanisms that underlie this process is incomplete. The purpose of this thesis is to develop greater knowledge of these mechanisms, in particular for the mineral enargite, and thus inform further development of selective flotation processes.

Having used single mineral flotation studies to identify that the floatability of copper sulphide minerals is pulp potential dependent, it was possible to identify potential ranges where a window of separation between mineral types exists. By exploiting these differences it was shown that it is possible to use pulp potential control to separate arsenic-bearing and non-arsenic copper sulphides under ideal conditions in laboratory scale batch-flotation.

The fundamental question this thesis set out to address is the nature of chemical and morphological changes taking place at the enargite mineral surface in a flotation environment. By understanding these processes, and how they are affected by pH, cell potential, reducing and oxidising agents, and the presence of other chemicals in solution (such as flotation reagents) our understanding of the mechanisms by which the electrochemical environment affects the floatability of enargite will be enhanced. Ultimately it is hoped this knowledge will contribute to the development of an economically viable method of separating copper arsenic sulphides by selective flotation.

In Chapter 2 three main areas, or research directions, were identified. The first includes studies relating directly to surface properties and floatability of enargite, which can be divided into the topics of surface potential, use of electrochemical and surface analysis techniques, surface oxidation by chemical means, and contact angle measurements. These different methodologies were

used to develop and improve our understanding of mechanisms of surface oxidation and its effects on collector adsorption.

Further investigation of surface products formed by electrochemical oxidation was identified as an area needing study, since it was not clear what the main oxidation products were. Contact angle measurements show that collector adsorption dependends on the formation of an oxide surface layer, and form a link between the fundamental studies of surface oxidation and flotation of enargite.

The second area is concerned with the use of single mineral flotation studies, which have been used to characterise mineral recovery under idealised conditions and make predictions about the feasibility of achieving a separation of arsenic bearing and non-arsenic minerals using pulp potential control methods.

Third, consideration was given to those studies investigation the potential for achieving selective flotation of enargite (and other arsenic bearing minerals) through the use of selective flotation reagents, selective oxidation as a means to influence collector adsorption and the use of pulp potential control.

Of these methods, pulp potential control seems to have the most promise as an effective method of selective flotation, but further work is required to understand the fundamental mechanisms responsible for selectivity. Investigation of the nature of surface changes, and the underlying processes by which they take place at the enargite surface, has formed the basis of the work in this thesis. In combination with a well-developed method of pulp potential control, there is the potential for worthwhile progress towards achieving a robust industrial separation process capable of removing arsenic-bearing minerals using froth flotation.

An experimental method using a novel approach of voltametric techniques combined with in-situ AFM imaging under potentiostatic control was used to study the surface reactivity of natural enargite. This was combined with ex-situ XPS to identify the reaction products formed at the surface under different conditions, and measurement of contact angle as a function of applied potential as a measure of floatability. Changes in surface chemical species (XPS), surface morphology (AFM) and contact angle measurements have been correlated on the basis of applied potential, allowing analysis of the contribution of each of these factors to enargite floatability. Further detailed XPS analyses of the enargite surface after electrochemical treatments over a range of oxidizing potentials followed, while subsequent investigations sought to correlate applied potential with collector adsorption, and the effect of pulp potential on enargite floatability. In the following sections the main findings of the experimental work are summarized.

1.2. Effects of XPS analysis

Since X-ray photoelectron spectroscopy (XPS) is the main surface analysis technique used in this work, and in much of the literature relating to the surface speciation of sulphide minerals, it is essential that its effects on the surface to be analysed are well understood, and the proper technique used, to enable accurate determination of surface chemical species. Other studies have described the photoreduction effects of X-radiation on sulphide minerals, as well as the effects of ultra-high vacuum and elevated temperatures during analysis, but this has not been done before for enargite.

In the case of the oxidised enargite surface, it was demonstrated that a two-stage process of decomposition or dehydration of $Cu(OH)_2$ to CuO due to heating effects of X-ray exposure and/or exposure to ultra-high vacuum effects, followed by photoreduction of CuO to Cu_2O, takes place during XPS analysis. In addition elemental sulphur, if present, is quickly volatilised under these conditions and lost from the surface.

These results have significant implications where the quantitative surface analysis of oxidation species is important, since the XPS measurement process can alter their proportions significantly. The result is likely to be an underestimation of the degree of oxidation and potentially the failure to identify important species affecting the interaction of the mineral surface with other chemicals such as flotation reagents. The use of liquid nitrogen cooling to minimize degradation of surface oxidation products has been demonstrated as an effective means to enable accurate quantification of these chemical species, and permit extended multiple-element analyses to be completed.

1.3. Fundamental investigations of enargite oxidation

Initial investigations used a combination of experimental techniques to study the effects of applied electrochemical potential on the surface of natural enargite at pH 10 and pH 4. Surface oxidation and the formation of surface species were confirmed by electrochemical techniques and XPS. Surface layer formation, and changes in physical characteristics such as roughness and apparent heterogeneous distribution of surface products, was demonstrated by AFM imaging.

At pH 10, initial polarization and fast dissolution of Cu leads to deposition of copper sulphate and hydroxide species, forming a surface layer. AFM demonstrated a significant increase in surface roughness and formation of a discontinuous surface layer in discrete domains, causing partial surface passivation and thereby slowing diffusion.

In contrast, at pH 4 a clear difference between initial fast dissolution followed by diffusion limited surface layer formation was found. AFM imaging showed the formation of a continuous

surface layer interspersed with isolated domains of what is believed to be elemental sulphur. XPS analysis confirmed the presence of elemental sulphur and metal deficient sulphide.

Contact angle measurements demonstrated no significant difference between the freshly polished surface and a surface oxidized at pH 10. A significant difference was found between the polished surface and that oxidized at pH 4, with an increase in contact angle of about 13° (46° to 59°) after oxidation. It is theorized that the competing effects of hydrophilic (copper oxides and hydroxides) and hydrophobic (elemental sulfur) species on the mineral surface under oxidizing conditions, and the change in surface roughness, contribute to the lack of significant difference in contact angle observed for a surface oxidized at pH 10.

1.4. XPS investigation of electrochemically induced surface oxidation of enargite

Following these initial investigations a more detailed study of the effects of oxidising potentials on enargite was carried out. Here the surface was conditioned at five increasingly oxidizing anodic potentials, then analysed by XPS. The aim was to determine the surface changes induced by progressively stronger oxidizing conditions and use these findings in combination with thermodynamic data to predict the reaction mechanisms responsible.

At low potentials (+347 and +516 mV) dissolution of copper predominates, leaving a metal (Cu) deficient surface. No evidence of the formation of Cu(II) species such as hydroxides or sulphates, as predicted by other authors, was found. This was true for applied potentials below +705 mV, and the principal mechanism at these lower potentials was proposed to be dissolution of Cu leaving metal-deficient sulphide species, and possibly the formation of polysulphides.

Sulphates (SO_4^{2-}) appeared after oxidation at +516 mV and above, but no corresponding Cu species were detected to support the presence of $CuSO_4$. Additional S species (polysulphide) first appeared after oxidation at +705 mV, as did Cu(II) species, the latter present at all higher potentials. Both $CuSO_4$ and $Cu(OH)_2$ were confirmed after treatment at +705 mV, however the hydroxide species was not found after treatment at higher potentials. In its place, CuS was confirmed, and the presence of an arsenic oxide, most likely As_2O_3, was also detected.

Thermodynamic data supports the formation of both copper hydroxide and sulphate species at pH 10 above about +100 mV, while $HAsO_4^{2-}(aq)$ is predicted above about +200 mV. The XPS data has been found to support the presence of both these copper species, but although As oxides are found, the precise form they take is not obvious. The presence of both As_2O_3 and As_2O_5 was supported by the XPS data although the former is considered more likely.

Concentrations of Cu, As and S in solution after surface conditioning were measured using ICP. A step-change increase in concentration between +516 and +705 mV was found. Combined

with the XPS findings this shows that enargite is resistant to electrochemically induced oxidation and subsequent precipitation of other species on the mineral surface until a threshold potential, somewhere between +516 and +705 mV, is reached. Reaction mechanisms for each of the applied potentials used for conditioning were devised based on thermodynamic data and the XPS results, and are shown as reactions [1] to [5] in Chapter 5.

1.5. Collector adsorption, surface characterisation and flotation response of enargite in a redox potential controlled environment.

The next stage of experimental work sought to extend the investigation further to better understand the potential for selective recovery of enargite in froth flotation systems. Characterisation of the mineral surface after oxidation on its own is not sufficient. It is necessary to incorporate froth flotation collectors into the system and investigate the effects of applied potential on collector adsorption. Two collector types were selected for study, sodium ethyl xanthate and sodium dialkyl dithiophosphinate (DTPI) in a pH 10 buffer solution, to provide useful information about collector adsorption and enargite surface speciation for a simplistic system. Using electrochemical techniques and x-ray photoelectron spectroscopy it was found that there is a significant difference in the chemical composition on the surface of enargite after conditioning at applied potentials of -400 and +516 mV.

XPS analysis after conditioning with xanthate at +516 mV showed C 1s and O 1s spectra diagnostic of xanthate adsorption, as well as BE differences in the S 2p combined with the presence of an additional S 2p spectrum after conditioning. Together these findings demonstrate the presence of xanthate on the enargite surface as a result of electrochemical treatment. In contrast no evidence was found of xanthate adsorption after conditioning at -400 mV.

Use of DTPI collector also produces significant differences in surface speciation after conditioning. Treatment at +516 mV results in additional Cu, S and O species to those in enargite alone and form an incomplete surface layer. This conclusion is reached based on the XPS data showing the presence of Cu, As and S peaks at BE's corresponding to enargite, but at significantly reduced atomic concentrations, which supports the argument for a mineral surface partially occluded by adsorbed collector. Similar to conditioning in the presence of xanthate at -400 mV, no evidence was found to confirm the presence of DTPI species under these conditions.

Confirmation of the effects of potential on floatability was sought using microflotatiuon tests to assess hydrophobicity of after conditioning at pulp potentials equivalent to the applied potentials used in the XPS studies. The selected collector was sodium ethyl xanthate and mass recovery of enargite was measured at potentials of +500, +100 and -400 mV. Recovery, and therefore

hydrophobicity, was greatest at high potential (82%), then decreased to 52% at +100 mV, while a poor flotation response was observed at -400 mV with 21% mass recovery to concentrate. These results were consistent with those of the XPS measurements of surface species present after conditioning at equivalent applied electrochemical potentials.

1.6. Conclusions

Throughout this thesis we have sought to improve our fundamental understanding of the chemical changes taking place on the enargite surface under controlled conditions that mimic those to which the mineral would be exposed in a controlled potential flotation environment. Moving from simple, idealized systems to the final stage of a more complex microflotation environment, the changes in chemical species on the surface with applied potential, and ultimately the link to the flotation response of enargite, were investigated and described.

In Chapter 1 four hypotheses were proposed for investigation. The question of how well they were addressed must now be considered. These hypotheses are:

i. Electrochemical products on the enargite surface significantly influence the floatability of enargite.

Surface products resulting from electrochemical oxidation depend on the applied potential to which the enargite surface is subjected, and it was found that with increasing anodic potentials, progressive dissolution and precipitation processes occur. Initially the surface becomes copper deficient leaving metal-deficient sulphide and polysulphide. At higher potentials, copper hydroxide and sulphate were found. These findings were linked to floatability through microflotation studies. However further work is needed to better understand the effects of these compounds. In this regard collectorless controlled potential flotation would provide useful direct information about the effects of these species on enargite floatability.

ii. An optimum range of applied potential exists over which enargite demonstrates good floatability.

Various studies have shown that where single mineral flotation is considered, once Eh increases through a transition range (usually around -150 mV) enargite becomes strongly floating. In this thesis, although enargite was shown to be non-floating at -400 mV, in transition at +100 mV and strongly floating at +500 mV, further work is needed to precisely define the Eh range over which this transition takes place. However it was shown that enargite is strongly floating above this range, thus this hypothesis is supported.

iii. Application of an electrical potential changes surface morphology, collector adsorption and contact angle at the mineral surface.

It was shown in Chapter 4 that surface morphology changes but contact angle does not after treatment at pH 10. The latter finding is thought to be a result of competing effects of hydrophilic and hydrophobic species, as well as increased surface roughness. In Chapter 6 the link between collector adsorption and applied potential was shown, where a transition from non-floating to floating around +100 mV was found, and it was demonstrated that collector adsorption is potential dependent. Thus this hypothesis is supported, but further work investigating mechanisms of collector adsorption, and the role surface species play, would be useful.

iv. Flotation selectivity of enargite is influenced by changes in surface properties resulting from an applied electrical potential.

The work in this thesis has shown only that enargite floatability is influenced by applied potential and the resulting surface changes. In order to demonstrate selectivity it is necessary to consider multi-mineral systems, which was not a part of this work. Thus although the inference can be made that this hypothesis is likely to be correct, it has not been demonstrated to be so. An opportunity exists for future work to investigate in detail the effects of mineral interactions in a controlled potential environment on the selectivity of flotation for one species above another.

Thus in terms of the fundamental question this thesis set out to address, which is the nature of chemical and morphological changes taking place at the enargite mineral surface in a flotation environment, it has contributed to the body of knowledge that supports the development of selective flotation under Eh control. The nature of chemical changes at increasingly anodic potentials has been described, and chemical species identified. The link between applied potential and enargite floatability has also been shown. The need for further work has also been identified, particularly in the areas of direct effects of surface species on floatability, mechanisms of collector adsorption in response to applied potential, and flotation response in multi-mineral systems.

2. Future Directions and Recommendations

The series of studies completed in this thesis have attempted to develop a better understanding of fundamental processes that take place at the mineral surface, in particular enargite, under controlled potential conditions. The intention is that this knowledge can be used to inform further research into selective flotation of arsenic bearing copper sulphides with the ultimate aim of

developing an effective full-scale flotation process that is selective for, or against, arsenic-bearing sulphide minerals.

It was shown that at low oxidizing potentials enargite undergoes a process of progressive dissolution of copper leaving a metal deficient surface, with limited evidence of oxidation products on the surface. As oxidizing potential increases formation of a surface layer composed of copper hydroxide and sulphate was found, and at high potential sulphur and arsenic species were found. Thus although the changes in surface species were well characterized the link between these species and collector adsorption was not fully investigated.

Although it has been shown that there are differences in collector adsorption on enargite depending on potential, further study is necessary to better characterize the nature of the adsorption mechanism. Investigation of whether collector adsorption at positive potentials is electrochemically reversible by subsequent application of cathodic potentials, as well as detailed investigation of the mechanisms of collector adsorption, as has been done for other minerals, (Güler et al. 2005, Petrus et al. 2011, Buckley et al. 2003), is also necessary.

Small scale flotation such as that using the UCT Microflotation cell is a useful means of investigating the effects of pulp potential in an idealised system, and can be used to better characterise the floatability of enargite and other copper sulphide minerals, both arsenic and non-arsenic bearing sulphides. To achieve this a means of precise automatic pulp potential control is required to enable accurate determination of the transition potential range of enargite under different treatment conditions. Manual control by reagent addition does not give the necessary level of control, and cannot give the fine resolution needed to accurately determine transition potentials.

This can be done using single mineral systems, and then extended to multi-mineral systems in a synthetic ore. A significant limitation of the work done in this thesis is that it does not consider what effects the presence of other mineral types have on the flotation response of enargite. It is well known that mineral interactions have a significant effect on floatability and these effects mean that, even in simple two-mineral systems, loss of selectivity in the combined system can be significant (Woods 2003). The direct implication is that selectivity for enargite can be lost in the presence of non-arsenic copper sulphides and the separation will not be achieved. It is this difficulty of achieving in real systems the same level of selectivity predicted from single mineral studies that is the key problem in developing a truly effective flotation process that will allow differentiation between sulphide minerals with inherently very similar flotation behavior.

The effects of mineral interactions and mineral-gangue interactions can then be systematically investigated to determine their effects on separation efficiency. Further to this is the study of collector adsorption and surface speciation on mineral particles in a flotation pulp, using surface

analytical tools such as XPS, to better understand the relevant mechanisms and relate the surface chemistry to flotation performance.

Investigation of alternative froth flotation collectors with a high selectivity and strong affinity for the arsenic sites in the enargite crystal structure is an essential step to facilitate an efficient separation of arsenic-bearing sulphides from non-arsenic copper sulphides while minimizing copper losses. At present the focus has been on using existing reagents which, although effective collectors for copper sulphides, do not distinguish between arsenic and non-arsenic bearing minerals as their affinity is for the metal species. This would bring significant benefits in treating the more complex, fine grained deposits containing arsenic which at present are at best difficult and costly to process, and often uneconomic to mine, an important prospect as the copper industry is faced with the challenges of processing these ores.

References

Bruckard, W.J., Kyriakidis, I. and Woodcock, J.T. (2007) The flotation of metallic arsenic as a function of pH and pulp potential - A single mineral study. International Journal of Mineral Processing 84(1-4), 25-32.

Smith, L.K. and Bruckard, W.J. (2007) The separation of arsenic from copper in a Northparkes copper-gold ore using controlled-potential flotation. International Journal of Mineral Processing 84(1-4), 15-24.

Senior, G.D., Guy, P.J. and Bruckard, W.J. (2006) The selective flotation of enargite from other copper minerals - a single mineral study in relation to beneficiation of the Tampakan deposit in the Philippines. International Journal of Mineral Processing 81(1), 15-26.

Bruckard, W.J., Davey, K.J., Jorgensen, F.R.A., Wright, S., Brew, D.R.M., Haque, N. and Vance, E.R. (2010) Development and evaluation of an early removal process for the beneficiation of arsenic-bearing copper ores. Minerals Engineering 23(15), 1167-1173.

Güler, T., Hiçyılmaz, C., Gökağaç, G. and Ekmekçi, Z. (2005) Electrochemical behaviour of chalcopyrite in the absence and presence of dithiophosphate. International Journal of Mineral Processing 75(3–4), 217-228.

Petrus, H.T.B.M., Hirajima, T., Sasaki, K. and Okamoto, H. (2011) Study of diethyl dithiophosphate adsorption on chalcopyrite and tennantite at varied pHs. Journal of Mining Science 47(5), 695-702.

Buckley, A.N., Goh, S.W., Lamb, R.N. and Woods, R. (2003) Interaction of thiol collectors with pre-oxidised sulfide minerals. International Journal of Mineral Processing 72(1-4), 163-174.

Woods, R. (2003) Electrochemical potential controlling flotation. International Journal of Mineral Processing 72(1-4), 151-162.